

Cdk12 Maintains the Size of the Proximal Axon and the Actin Barrier

Louise Townsend

November 2022



This thesis is submitted for the Degree of Doctor of
Philosophy

Acknowledgements

Firstly, I would like to thank each of my supervisors Dr Gaynor Smith and Dr Owen Peters. Thank you, Gaynor, for your endless patience, encouragement, support and impeccable organisation skills and Owen, for your help, support, and advice. I really cannot thank both of you enough, thank you for taking me under your wing(s) and guiding me throughout my PhD. Your continued energy, excitement, and positivity is incredibly inspiring and motivational, and I cannot recommend a better lab group. You both work incredibly hard and are a great team to work for, thank you for letting me be a part of it.

I would like to thank Cardiff University and the School of Biosciences for funding my PhD studentship, thank you for this opportunity. I would also like to thank the members of the Dementia Research Institute (DRI), thank you all for your help during working hours, evenings, and weekends. I would particularly like to thank the DRI Lab manager, Dr Andrew Jefferson, for your help with lab equipment, in particular the microscopes. Thank you for always being there when the Zeiss would break and knowing how to fix it! You always have time to help myself and others no matter how busy you are – a true asset to the DRI!

I would next like to thank the DRI Fly lab, I can't think of a better group of people to work with during a pandemic! To Leo Amadio, our technician, thank for being the most hardworking technician I have ever known, you keep the lab running so smoothly and always brighten everyone's day! To the postdocs, Dr Daniel Maddison and Dr Bilal Malik: to Dan thank you for being Leo's next in command and helping the lab run so smoothly, thank you for answering my many questions! And to Bilal, thank you for your help throughout – I thoroughly enjoyed our many conversations! To the 'new-but-not-so-new' PhD students: Peta Greer, Uroosa Chughtai, and Hannah Clarke. Thank you to Peta for listening to my advice (not sure how helpful it is!), to Hannah, thank you for helping finish up some of my experiments for the paper and to Uroosa, a huge thank you for all the experiments you helped me out with whilst on placement, thank you for also introducing me to climbing! To all three of you, best of luck finishing up your PhDs – you'll smash it! Last but by no means least, to the PhD students who started with me: Freya Storer, Freja Sadler, Eilish MacKinnon, and Andrew Lloyd. To Freya, thank you for working with me during the Covid-19 shift pattern and being so helpful throughout even when you had a load of brain dissections to do; to Freja, for being the best pub organiser and one of my '365 friends'; to Eilish, for the many

hilarious conversations throughout and for being a shoulder to cry on; and to Andrew, for your smart wit and quick jokes that would have me crying of laughter and thank you for letting me talk you to death during tissue culture (we both know you loved it really!).

I would next like to thank my friends in the School of Biosciences, past and present; in particular, Dr Richard Ludlow and Dr Eluned Broom for all those great BBQs, and to Rakhee Dhorajiwala and Nicola Graham for the many coffees at Brodies – I still stand by the beetroot lattes!

To Adam, for the continuous support, patience, and for providing me with tea on tap! Thank you for your help and for making every day brighter.

Lastly, to my parents for your endless love and support, thank you for always believing in me.

Original Publications during the course of this PhD Studentship

- Lin T., Brewer D.M., Sheehan A.E., **Townsend L.N.**, Maddison D.C., Zuchner S., Smith G.A. & Freeman M.R. TSG101 negatively regulates mitochondrial biogenesis in axons. *The Proceedings of the National Academy of Sciences*. 118 (20). May 2021.
- **Townsend L.N.**, Chughtai U., Clarke H., Amadio L., Maddison D.C., Van der Goes van Naters W., Peters O. & Smith G.A. Cdk12 maintains the Size of the Proximal Axon and the Actin Barrier. *In preparation*. 2022.

Summary

Neurons involved in brain functions such as learning, memory, and emotion rely on neuronal polarity to receive information and transmit this unidirectionally to other neuronal cells or tissues. In order to maintain neuronal polarity, the neuron relies on two structurally and functionally different regions, the axonal and somatodendritic domains that are separated by molecular barriers in the proximal axon to selectively sort, transport and deliver axonal and dendritic proteins. One barrier, the axon initial segment (AIS), that functions in action potential initiation has a distinct structure and uses an actin-based filter and microtubule binding to filter cargo.

Recent work suggests that these molecules and structure are conserved in the model organism, *Drosophila melanogaster*. However, how this neuronal sub compartment is maintained and whether other molecules are involved in its function and integrity remains unknown.

This thesis demonstrates that cyclin-dependent kinase 12 (Cdk12), previously identified in an unbiased genetic screen, controls proximal axon width and neuronal survival. Using actin as an AIS marker, it was shown that Cdk12 interferes with actin dynamics and form actin swellings in the proximal axon. These actin changes altered the selectivity filter in the AIS and facilitated peroxisomes (a vesicle marker of the soma) to enter the axon.

Based on the previous findings, this thesis also aimed to investigate the physiological effect the loss of *Cdk12* had on neuronal changes and on other organelles in the neuron. This thesis demonstrated that Cdk12 influences neuronal Ca^{2+} levels, ER distribution and mitochondria morphology in the proximal axon in the stages prior to neurodegeneration.

Therefore, Cdk12 is crucial to maintain the size and function of the AIS and to regulate neuronal physiology. This in turn regulates neuronal polarity which, if disrupted, leads to neurodegeneration, a key characteristic seen in many neurodegenerative diseases.

Table of Contents

1	Introduction	1
1.1	Neuronal development and maintenance throughout life	1
1.1.1	The discovery of neurons and circuitry.....	1
1.1.2	Neuronal polarity.....	3
1.1.3	Neuronal calcium levels.....	4
1.2	Actin and the cytoskeleton in neurons	5
1.2.1	Actin in the axon.....	7
1.3	Organelles and their regulation in neurons	9
1.3.1	Organelles in the neuron	9
1.3.2	Peroxisomes.....	9
1.3.3	Endoplasmic reticulum	10
1.3.4	Golgi apparatus.....	12
1.4	Mitochondrial regulation in the axon in health and disease	12
1.4.1	Mitochondrial regulation in healthy axons.....	12
1.4.2	Mitochondrial regulation in neurodegenerative disease	16
1.5	The pre-axonal exclusion zone.....	18
1.5.1	The importance of the pre-axonal exclusion zone	18
1.6	Function of the axon initial segment	19
1.7	Molecular organisation of the mammalian axon initial segment	20
1.8	The AIS acts as a barrier.....	22
1.8.1	Two barriers in one neuron	23
1.9	Dysfunction of the AIS in neurological disease	23
1.10	The role of Cdk5 in AIS barrier formation	25
1.11	Are there other molecules that can maintain the axon initial segment?.....	26
1.11.1	Cdk12.....	27
1.12	Using <i>Drosophila melanogaster</i> in research.....	28
1.12.1	The importance of <i>Drosophila</i> in neurobiology research.....	29
1.12.2	<i>Drosophila</i> as a model organism to study polarity and the AIS.....	31
1.12.3	Available tools to study organelles, biochemistry, and physiology in <i>Drosophila</i> neurons	
	32	
1.12.3.1	Biochemical sensors.....	32
1.12.3.2	Neuronal physiology	34
1.12.4	The <i>Drosophila</i> wing as a model for neurology.....	36
1.13	Aims of the thesis	39

2	<i>Materials and methods</i>	41
2.1	Maintenance of fly stocks	41
2.2	Fly stocks and genetics	41
2.2.1	Deficiency stock	41
2.2.2	Bacterial artificial chromosome stock	41
2.2.3	RNA interference	42
2.3	Fly food	42
2.4	Gal4-UAS binary system	44
2.5	MARCM	44
2.6	Wing dissections and live wing imaging	47
2.6.1	Wing dissections	47
2.6.2	Live imaging	48
2.7	Microscopy	48
2.8	Analysis of neuronal and organelle morphology and biochemistry	49
2.8.1	Measuring fluorescence intensity in wing neurons	49
2.8.2	Measuring fluorescent intensity in actin patches and endoplasmic reticulum	50
2.8.3	Measuring neuronal morphology and actin patches.....	50
2.8.4	Quantifying mitochondria and peroxisome morphology and number.....	50
2.9	Imaging of <i>in vivo</i> reporters for mitochondrial physiology	51
2.10	Fluorescent recovery after photobleaching	51
2.10.1	Imaging actin in actin patches	51
2.10.2	Analysing actin in actin patches	52
2.11	Statistical analysis	53
3	<i>Cdk12 controls proximal axon width, maintains neuronal number, and is localised to the cell body</i>	54
3.1	Abstract	54
3.2	Introduction	55
3.2.1	Aims and objectives	56
3.3	Experimental Design	57
3.4	Results	62
3.4.1	Sequencing and mapping of the <i>Cdk12</i> mutation	62
3.4.2	<i>Cdk12</i> controls proximal axon width	64
3.4.3	<i>Cdk12</i> maintains neuronal number	64
3.4.4	<i>Cdk12</i> has little effect on neuronal cell body size	64
3.4.5	<i>Cdk12</i> has no effect on the length of the proximal axon.	65
3.4.6	Rescue of the <i>Cdk12</i> ^{-/-} phenotype	66

3.4.7	Cdk12 is localised to the cell body	71
3.5	Discussion	72
3.6	Conclusion	74
4	<i>Cdk12 controls actin redistribution and filtration barrier in the neuron</i>	75
4.1	Abstract	75
4.2	Introduction	75
4.2.1	Aims and objectives	77
4.3	Experimental design	77
4.4	Results	82
4.4.1	Actin as an AIS marker	82
4.4.2	Cdk12 controls β -actin distribution	84
4.4.3	Cdk12 controls F-actin levels	86
4.4.4	Cdk12 regulates β -actin diffusion in the proximal axon swellings.....	88
4.4.5	β -actin swellings were stationary in <i>Cdk12</i> ^{-/-} clones.....	91
4.4.6	Cdk12 regulates peroxisome positioning in the axon and the cell body	93
4.5	Discussion	96
4.6	Conclusion	98
5	<i>Cdk12 controls neuronal physiology and mitochondrial dynamics ...</i>	100
5.1	Abstract	100
5.2	Introduction	100
5.2.1	Aims and objectives	104
5.3	Experimental design	104
5.4	Results	116
5.4.1	Cdk12 regulates neuronal calcium levels in the proximal axon swellings	116
5.4.2	Cdk12 had no effect on glutathione disulfide oxidation levels in the neuron	117
5.4.3	Cdk12 influences endoplasmic reticulum levels in the proximal axon.	118
5.4.4	Cdk12 controls mitochondrial morphology in the axon and cell body which is controlled by Drp1.	119
5.4.5	Cdk12 does not regulate calcium levels in mitochondria	122
5.4.6	Cdk12 had no effect on glutathione and hydrogen peroxide oxidation levels in mitochondria	123
5.4.7	Cdk5 does not genetically interact with Cdk12	124
5.5	Discussion	126
5.6	Conclusion	130

6	<i>Discussion</i>	131
6.1	Summary of findings	131
6.2	Cdk12 regulates the axon initial segment	131
6.3	Actin formation requires actin-binding proteins	134
6.3.1	The importance of actin-binding proteins in mitochondrial fission	134
6.4	The importance of actin-binding proteins in neurodegeneration	137
6.5	The importance of actin-regulating binding proteins in synapse formation	138
6.6	The axon initial segment in neurological disease	139
6.7	Concluding remarks	140
7	<i>Bibliography</i>	141
8	<i>Appendices</i>	180

Abbreviations

20E	20-hydroxyecdysone/ecdysone
AAA	ATPases associated with diverse cellular activities
ACBD5	Acyl-coenzyme A-binding domain protein 5
AD	Alzheimer's disease
ADF	Actin depolymerising factor
ADP	Adenosine diphosphate
AIS	Axon initial segment
ALS	Amyotrophic lateral sclerosis
AMP	Adenosine monophosphate
ANOVA	Analysis of variance
APF	After pupae formation
APP	Amyloid precursor protein
Arp2/3	Actin related protein 2/3
<i>ATM</i>	<i>Ataxia-telangiectasia mutated</i>
ATP	Adenosine triphosphate
<i>ATR</i>	<i>Ataxia telangiectasia and Rad3-related</i>
AUC	Area under curve
A β	Amyloid- β
BAC	Bacterial artificial chromosome
BDSC	Bloomington Drosophila Stock Center
<i>BRCA1</i>	<i>Breast cancer gene 1</i>
<i>BRCA2</i>	<i>Breast cancer gene 2</i>
CaM	Calmodulin
cAMP	Cyclic adenosine monophosphate
Cdk12	Cyclin-dependent kinase 12
Cdk5	Cyclin-dependent kinase 5
cDNA	Complementary DNA
CK2	Casein kinase 2
CNS	Central nervous system
COP	Coat protein complex
cpGFP	Circularly permuted GFP variants
CTF	Corrected total fluorescence
d.p.e.	Days post eclosion
DIOPT	DRSC integrative ortholog prediction tool
DIV	Days <i>in vitro</i>

DRI	Dementia Research Institute
Drp1	Dynamin-related 1
EMS	Ethyl methanesulfonate
Ena/VASP	Enabled/vasodilator-stimulated phosphoprotein
Eps8	Epidermal growth factor receptor pathway substrate 8
ER	Endoplasmic reticulum
ERG	Electroretinogram
F ₀	Start of recovered fluorescence intensity (post-bleach)
F _{1/2}	Half time of fluorescence intensity
F-actin	Filamentous actin
F _E	End of recovered fluorescence intensity (post-bleach)
F _I	Initial (pre-bleach) fluorescence intensity
FP	Fluorescent protein
FRAP	Fluorescent recovery after photobleaching
FRET	Förster resonance energy transfer
FRT	Flippase recognition target
GABA	Gamma aminobutyric acid
G-actin	Globular actin
gDNA	Genomic DNA
GECI	Genetically encoded calcium indicator
GFP	Green fluorescent protein
GFSTF	EGFP-FIAsH-StrepII-TEVcs-3xFlag
Grx	Glutaredoxin
Grx1	Glutathione reductase
GSH	Glutathione (reduced form)
GSSG	Glutathione (oxidised form), glutathione disulfide
GST	Glutathione S-transferase
GTPase	guanosine triphosphatase
HD	Huntington's disease
HDAC6	Histone deacetylase 6
INF2	Inverted formin 2
KA	Kinase dead
KIF5	Kinesin family member 5
L1/2/3/4/5	Longitudinal 1/2/3/4/5 (vein)
LAS	Leica Application Suite
Lis1	Lissencephaly type 1

MAP2	Microtubule-associated protein 2
MARCM	Mosaic analysis with a repressible cell marker
MERCS	Mitochondria-endoplasmic reticulum contact sites
MFN1	Mitofusin-1
MFN2	Mitofusin-2
Miro1	Mitochondrial Rho GTPase 1
MMP-1	Matrix metalloproteinase-1
MS	Multiple sclerosis
mt	Mitochondrial
NAD ⁺	Nicotinamide adenine dinucleotide
NADPH	Nicotinamide adenine dinucleotide phosphate
Ndel1	Nudel 1
NF186	Neurofascin 186
NFEF2L2	Nuclear factor-erythroid factor 2-like 2
NrCAM	Neuron-glia related cell adhesion molecule
Nrf	Nuclear respiratory factor
<i>ns</i>	Not-significant
ONOO ⁻	Oxidant peroxynitrite
Opa1	Optic atrophy 1
Orp1	Oxidant receptor peroxidase-1
OXPPOS	Oxidative phosphorylation
PAEZ	Pre-axonal exclusion zone
PCT-1	PCTAIRE-motif protein kinase 1
PD	Parkinson's disease
PEX	Peroxin
PGC	Proliferator-activated receptor γ co-activator
PGC-1 α	Peroxisome-proliferator-activated receptor γ co-activator-1 α
PINK1	Phosphatase and tensin homolog-induced putative kinase 1
Plk2	Polo-like kinase 2
PNS	Peripheral nervous system
PTM	Post-translational modifications
RNAi	RNA interference
roGFP	Reduction-oxidation-sensitive green fluorescent protein
ROI	Region of interest
ROS	Reactive oxygen species
SEM	Standard error of the mean

SERCA	Sarcoplasmic/ER calcium ATPase
SKL	Serine-lysine-leucine
SNAP	Synaptosome-associated protein
SNARE	Soluble <i>N</i> -ethylmaleimide-sensitive factor attached protein receptor
SPAR	Spine associated Rap GTPase-activating protein
SPCA	Secretory pathway calcium ATPase
SSG	S-glutathionylation
STED	Stimulated emission depletion
STORM	Stochastic optical reconstruction microscopy
$t_{1/2}$	Half time of recovery
TRAK	Trafficking kinesin protein
TRIM46	Tripartite motif-containing protein 46
Tsg101	Tumour susceptibility gene 101
UAS	Upstream activation sequence
VAPB	Vesicle associated membrane protein associated protein B
VDAC	Voltage-dependent anion channel
VDRC	Vienna Drosophila Resource Center
WASP	Wiskott–Aldrich syndrome protein
WAVE	WASP-family verprolin-homologous protein
WH2	WASP homology 2
WLD ^s	Wallerian degeneration slow
WT	Wild-type

List of Figures

FIGURE 1.1 ACTION POTENTIALS IN A NEURON.....	2
FIGURE 1.2 ACTIN POLYMERISATION.....	6
FIGURE 1.3 ACTIN STRUCTURES IN THE AXON.....	8
FIGURE 1.4 MITOCHONDRIA REGULATION IN NEURONS.....	15
FIGURE 1.5 THE BOUNDARY BETWEEN THE PAEZ AND THE AIS IN HIPPOCAMPAL NEURONS.....	19
FIGURE 1.6 THE STRUCTURE OF THE AIS.....	21
FIGURE 1.7 <i>DROSOPHILA</i> CDK12 IS EXPRESSED UBIQUITOUSLY IN THE BRAIN.....	27
FIGURE 1.8 <i>Cdk12</i> GENE.....	28
FIGURE 1.9 <i>DROSOPHILA</i> FLY WING.....	37
FIGURE 2.1 GAL4-UAS SYSTEM.....	44
FIGURE 2.2 LABELLING CELLS WITH <i>CDK12</i> MUTANT USING MOSAIC ANALYSIS WITH A REPRESSIBLE CELL MARKER.....	46
FIGURE 2.3 A RECOVERY FRAP CURVE.....	53
FIGURE 3.1 FLY CROSSES TO GENERATE WT AND <i>CDK12</i> ^{-/-} MARCM CLONES.....	59
FIGURE 3.2 FLY CROSSES TO GENERATE RESCUE LINES IN MARCM CLONES.....	60
FIGURE 3.3 FLY CROSSES TO GENERATE A CDK12 LOCALISATION IN NEURONAL MARCM CLONES.....	61
FIGURE 3.4 SEQUENCING AND MAPPING OF THE <i>CDK12</i> ^{-/-} MUTATION.....	63
FIGURE 3.5 CDK12 REGULATES PROXIMAL AXON SWELLING AND NEURONAL DEATH.....	65
FIGURE 3.6 CDK12 EXPRESSION RESCUES THE NULL PHENOTYPE.....	68
FIGURE 3.7 REINTRODUCTION OF <i>CDK12</i> BY gDNA PARTIALLY RESCUED THE MUTANT PHENOTYPE.....	69
FIGURE 3.8 EXPRESSION OF <i>5xUAS-CDK12</i> RESCUED THE <i>CDK12</i> ^{-/-} PHENOTYPE.....	70
FIGURE 3.9 CDK12 IS LOCALISED TO THE CELL BODY.....	71
FIGURE 4.1 FLY CROSSES FOR FLIES EXPRESSING GFP-TAGGED AIS MARKERS AND B-ACTIN IN MARCM CLONES.....	80
FIGURE 4.2 FLY CROSSES TO GENERATE MARCM CLONES EXPRESSING GFP TAGGED PEROXISOMES.....	81
FIGURE 4.3 ACTIN AS A MARKER FOR SOMADENDRITIC REGIONS.....	83
FIGURE 4.4 CDK12 CONTROLS B-ACTIN LOCALISATION.....	85
FIGURE 4.5 CDK12 CONTROLS F-ACTIN LEVELS.....	87
FIGURE 4.6 CDK12 REGULATES B-ACTIN DIFFUSION AFTER PHOTBLEACHING.....	89
FIGURE 4.7 CDK12 CONTROLS B-ACTIN DIFFUSION IN THE PROXIMAL AXON.....	90
FIGURE 4.8 CDK12 HAD NO EFFECT ON B-ACTIN SWELLING MIGRATION.....	92
FIGURE 4.9 CDK12 RESTRICTS PEROXISOME TRAFFICKING INTO THE AXON.....	94
FIGURE 4.10 CDK12 CONTROLS PEROXISOME MORPHOLOGY IN THE CELL BODY.....	95
FIGURE 5.1 GCAMP SCHEMATIC.....	105
FIGURE 5.2 FLY CROSSES TO GENERATE GFP-TAGGED GCAMP EXPRESSING MARCM CLONES.....	106
FIGURE 5.3 SCHEMATIC OF THE MECHANISM BEHIND ORP1 AND Grx1 roGFP OXIDATION.....	107
FIGURE 5.4 FLY CROSSES TO GENERATE GFP-TAGGED GLUTATHIONE AND HYDROGEN PEROXIDE REDOX STATES IN MARCM CLONES IN NEURONS AND MITOCHONDRIA.....	108

FIGURE 5.5 FLY CROSSES TO GENERATE GFP-TAGGED ER EXPRESSING MARCM CLONES.....	109
FIGURE 5.6 CROSSING SCHEME FOR MARCM CLONES EXPRESSING GFP-TAGGED MITOCHONDRIA.....	111
FIGURE 5.7 FLY CROSSES TO GENERATE <i>Drp1</i> KNOCK DOWN EXPRESSING MARCM CLONES.....	112
FIGURE 5.8 CROSSING SCHEME TO GENERATE GFP-TAGGED MITOGCAMP EXPRESSION IN NEURONAL MARCM CLONES.	113
FIGURE 5.9 FLY CROSSES FOR OVEREXPRESSION OF <i>Cdk5</i> IN MARCM CLONES.	115
FIGURE 5.10 CDK12 INCREASES CALCIUM LEVELS IN THE PROXIMAL AXON SWELLINGS.	116
FIGURE 5.11 CDK12 HAD NO EFFECT ON GLUTATHIONE LEVELS IN THE NEURON.	117
FIGURE 5.12 CDK12 INFLUENCES ER DISTRIBUTION IN THE PROXIMAL AXON SWELLINGS.....	118
FIGURE 5.13 CDK12 AND DRP1 CONTROL MITOCHONDRIAL MORPHOLOGY IN THE AXON.	120
FIGURE 5.14 CDK12 CONTROLS MITOCHONDRIAL MORPHOLOGY IN THE CELL BODY.	121
FIGURE 5.15 CDK12 HAD NO EFFECT ON MITOCHONDRIAL CALCIUM LEVELS.	122
FIGURE 5.16 CDK12 HAD NO EFFECT ON GLUTATHIONE DISULFIDE AND HYDROGEN PEROXIDE OXIDATION IN MITOCHONDRIA.....	123
FIGURE 5.17. CDK5 DOES NOT GENETICALLY INTERACT WITH CDK12.	125
FIGURE 5.18 CDK5 DOES NOT GENETICALLY INTERACT WITH CDK12.	126
FIGURE 6.1 A SUMMARY OF CDK12 POTENTIAL PATHWAYS.....	132
FIGURE 6.2 CALCIUM-INDUCED MITOCHONDRIAL FISSION.	136

List of Tables

TABLE 2.1 INGREDIENTS FOR FLY FOOD.....	43
---	----

1 Introduction

1.1 Neuronal development and maintenance throughout life

1.1.1 The discovery of neurons and circuitry

The neuron theory or doctrine was first described at the end of the 19th century by Cajal and Sherrington and states that the nervous system is made up of individual neurons supported by astrocytes and other glial cells (Cajal 1888; Sherrington 1906). It is worth noting that several other scientists (namely Jan Purkinje, Gabriel Valentin, Robert Remak, Robert Bentley, Wilhelm His, Fridtjof Nansen, and Auguste Forel) laid the groundwork but none directly articulated the neuron theory (Mayr 1982; Shepherd 1991; Mazzarello 1999; López-Muñoz et al. 2006).

Cajal also concluded that, in an individual neuron, information is transmitted from dendrites to cell bodies and through to axons (Cajal 1995). An individual neuron is a morphologically distinct cell with elaborate dendrites and axons spanning long distances. Neurons require electrical impulses and chemicals to transmit information that is crucial to the function of all complex organisms. The transmission of information is in the form of an action potential that propagates unidirectionally along the axon and terminates at axonal terminals.

At the start of an action potential, voltage-gated sodium ion channels open and sodium ions enter the neuron (depolarisation), depolarising the membrane. If the threshold potential is met, an action potential is generated triggering sodium ion channels to close and voltage-gated potassium channels to open and an influx on K⁺ enters the neuron. The movement of positive K⁺ ions causes the membrane potential to become repolarised but this overshoots past the resting membrane potential (hyperpolarisation) and the neuron enters a refractory period (crucial for the unidirectional flow of information), before returning back to its resting potential (Kandel et al. 2012).

Action potentials terminate at axonal terminals and trigger voltage-gated calcium channels to open which causes an influx of Ca²⁺ into the presynaptic terminal. This causes synaptic vesicles, consisting of neurotransmitters, to fuse with the plasma membrane and release their contents into the synaptic cleft ready for the following neuron/tissue to engulf them (**Figure 1.1**).

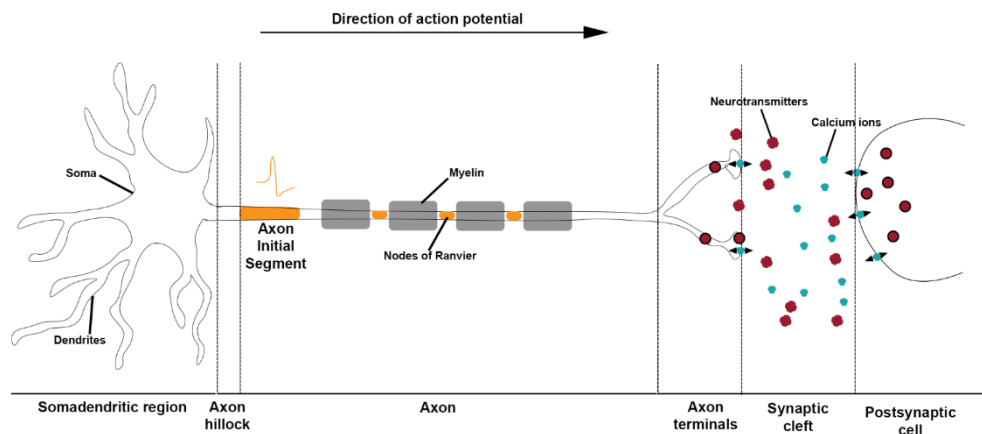


Figure 1.1 Action potentials in a neuron. Neurons are divided into several key regions: somadendritic, axon hillock, axon initial segment (AIS), axon, and axonal terminals. In the somadendritic region, dendrites receive extracellular information from other cells, which is passed to the soma/cell body that consists of the nucleus and other organelles important for cellular function. The next region is the axon hillock (where the axon originates) which leads to the AIS, the region for action potential initiation. Information in the form of action potentials then travels along the axons, facilitated by myelin sheaths and Nodes of Ranvier. At the axon terminals, action potentials trigger a calcium influx which causes neurotransmitters to be released from the presynaptic cell, entering their contents into the synaptic cleft where they are engulfed by the postsynaptic cell. Binding of neurotransmitters to ligand-gated ion channels on the postsynaptic cell causing sodium ions to enter the cell. If enough sodium ions enter the cell, a new action potential is produced (not shown).

Neurons function, not as individual cells, but as neuronal circuits to process information. Neuronal circuits comprise of many neuronal populations, interconnected with inhibitory and excitatory synapses that once activated, results in different behaviours. Glia cells are also important in neuronal circuits as they provide physical and metabolic support to neurons. Astrocytes, major glial cells, function in ion homeostasis, neurotransmitter clearance at synapses and provide an energy supply to neurons. The basis behind neuronal circuits is to form functional units, transmitting information to and from the brain in order to serve a specific function. An example of a circuit is the 'knee-jerk' myotatic reflex that helps to keep an upright posture. Peripheral sensors are stimulated (muscle stretch receptor) which, through synaptic contacts, excites spinal motor neurons and triggers peripheral motor neurons to cause the leg extensor muscle fibres to contract (Purves et al. 2001).

Neuronal circuits are formed from a balance of excitatory and inhibitory neurons that together control neuronal activity. Excitatory neurons activate their targets whilst

inhibitory neurons repress them. Excitatory neurons are important in, for example, the visual system where signals are transmitted from photoreceptors in the eye to visual cortex neurons in the brain via bipolar cells and retinal ganglion cells, an important process for an individual to successfully process a visual image (Gilbert and Wiesel 1979; Felleman and Van Essen 1991; Cajal 1995). Inhibitory neurons on the other hand function in balancing excitation and inhibition and control pathological excitatory activity, such as seizures (Van Vreeswijk and Sompolinsky 1996; Schevon et al. 2012). Therefore, demonstrating the importance of inhibitory and excitatory interneurons in neuronal circuits.

1.1.2 Neuronal polarity

The function of a neuron is to receive information from other neurons and transmit this to other neuronal cells or tissues, which is necessary for brain functions such as learning, memory and emotion. These processes occur across two important regions, the axonal and somadendritic domains, that both differ in morphology, function and molecular composition. These distinct regional arrangements and functions are known as neuronal polarity and hence neuronal polarity is essential for the unidirectional flow of information. Maintaining neuronal polarity relies on selective sorting, transport and delivery of axonal and dendritic proteins (Jones and Svitkina 2016; Letierrier 2016; Huang and Rasband 2018).

Axonal and dendritic proteins are both processed and synthesised in the same region, the cell body, by the rough endoplasmic reticulum (ER) and the Golgi apparatus. Proteins are synthesised by the rough ER and then undergo post translational modifications in the Golgi. Vesicles carrying these proteins arise from the Golgi and have to be delivered to the correct domains (Peters et al. 1991). After leaving the Golgi, vesicles undergo either budding (from the Golgi), transport (long-range via binding to dynein or kinesin on microtubules) or fusion (fusing with target membranes) events (Jahn and Scheller 2006; Hirokawa et al. 2009; Sztul and Lupashin 2009; Akhmanova and Hammer 2010; Vallee et al. 2012; Chia and Gleeson 2014; Guo et al. 2014; Bhabha et al. 2016).

Vesicles with axonal and somatodendritic cargo are sorted at the axonal entry point. Here, vesicles bind to the unipolar microtubules of plus-end orientation and axonal cargo bound to kinesin-1 is accepted and moves through the pre-axonal exclusion zone (PAEZ) whilst somatodendritic cargo is rejected and reverses back to the soma

(Nakata and Hirokawa 2003; Song et al. 2009; Baas and Lin 2011; Al-Bassam et al. 2012; Farías et al. 2015; Kuijpers et al. 2016; Yau et al. 2016)

Neuronal polarity is also important in axon and dendrite specification during development through the involvement of positive and negative feedback loops. Positive signals, such as amplification of neurotrophins, induce elongation and axon specification whilst negative signals, such as Ca^{2+} waves, inhibit the formation of new axons, leading to dendrite specification and therefore maintaining neuronal polarity (Arimura and Kaibuchi 2007; Inagaki et al. 2011; Takano et al. 2015; Schelski and Bradke 2017).

In development, neuronal polarity of different neuronal regions forms in *in vitro* cortical rat neurons, derived from 18-day fetuses, at embryonic stage 14, 4-15 days *in vitro* (DIV). *In vitro*, the lamellipodial and filopodial protusions initially develop, followed by neurite extension, axon specification and dendrite and axon branching and emergence of the axon initial segment (AIS) and lastly, refinement (synapse formation and spine morphogenesis) of the neuron (Polleux 2020).

1.1.3 Neuronal calcium levels

The function of an axon is to transmit information in the form of action potentials, see **Section 1.1.1** above. When an action potential reaches the axon terminals, a calcium influx occurs which causes neurotransmitters to be released into the synaptic cleft and information is passed from one neuron to another neuron or tissue (**Figure 1.1**).

Presynaptic neurotransmitter release is controlled by Ca^{2+} and soluble *N*-ethylmaleimide-sensitive factor attached protein receptor (SNARE) proteins. SNARE proteins consist of synaptobrevin, synaptosome-associated protein-25 (SNAP-25), and syntaxin (Bajjalieh and Scheller 1995; Südhof 1995). With the addition of calcium sensor synaptotagmin, SNARE proteins mediate fusion of vesicles to the plasma membrane. Synaptobrevin is localised to vesicles, whilst SNAP-25 and syntaxin are located on the plasma membrane. Interaction of these proteins forms a tight complex that is separated by adenosine triphosphate (ATP) hydrolysis. Ca^{2+} bind to synaptotagmin, a Ca^{2+} -sensor protein, and promote its interaction with other SNARE proteins, facilitating the fusion of the trafficking vesicles to the plasma membrane and hence the release of neurotransmitters into the synaptic cleft (Südhof 2004; Chapman 2008).

In addition to neurotransmitter release in neurons, the signalling function of Ca^{2+} are also important in learning and memory, gene regulation, long-term potentiation, depression of synaptic transmission and in the direct coupling between membrane depolarisation and increase in Ca^{2+} . Further to this, Ca^{2+} autoregulate and act as first and secondary messengers in several essential cellular processes such as metabolism, transport of cellular components, gene transcription and cell death (Carafoli 2007; Mellström et al. 2008).

Ca^{2+} is able to promote release of more Ca^{2+} from intracellular calcium stores, such as the ER and sarcoplasmic reticulum. Known as 'calcium induced calcium release', this process is important in skeletal muscle contraction as the arrival of an action potential causes a Ca^{2+} influx, activating ryanodine receptors on the sarcoplasmic reticulum and triggering Ca^{2+} release and muscle contraction (Endo 1977; Fabiato 1983; Näbauer et al. 1989; Tanabe et al. 1990; Fill and Copello 2002).

1.2 Actin and the cytoskeleton in neurons

Proteins within the cytoskeleton are crucial in maintaining and developing the function of the nervous system. In adult life, the cytoskeletal proteins also function in maintaining neuronal homeostasis, neuronal plasticity and lastly in nerve regeneration after damage (Sekino et al. 2017; Basu and Lamprecht 2018; Blanquie and Bradke 2018; Borovac et al. 2018; Filous and Schwab 2018).

If the proteins are abnormally mutated (due to chemical, physical, or biological damaging agents) cytoskeletal proteins can become destabilised leading to several neurodegenerative diseases. This can either be as a direct cause such as, but not limited to, hereditary sensory autonomic neuropathy type VI, amyotrophic lateral sclerosis (ALS) (familial and sporadic) and Charcot-Marie-Tooth disease type 1F (Edvardson et al. 2012; Wu et al. 2012; Chen et al. 2013; Tiloca et al. 2013; Horga et al. 2017; Manganelli et al. 2017; Wu et al. 2017a; Fortugno et al. 2019) or as a contributing factor as in, but not limited to, Alzheimer's disease (AD), Lowe syndrome and Friedreich's ataxia (Willers et al. 1993; Pastore et al. 2003; Maloney et al. 2005; Maloney and Bamburg 2007; Iqbal et al. 2009; Sparaco et al. 2009; Zhang et al. 2015; Bamburg and Bernstein 2016; Piermarini et al. 2016; Kovacs et al. 2017; Zafar et al. 2018).

The cytoskeleton is composed of three main classes of filaments: intermediate filaments, which are protein-based neurofilaments (10 nm in diameter), tubulin-based microtubules (24 nm diameter) and actin-based microfilaments (6 nm diameter). Actin-based microfilaments or filamentous actin (F-actin) are composed of individual globular actin (G-actin) proteins that polymerise and form F-actin (Hanson and Lowy 1963; Huxley 1963) (**Figure 1.2**). Together, F- and G-actin comprise of 4-7% of protein expression in neurons (Clark et al. 1983). In mammals, three isoforms of actin are present: α -, β - and γ -actin but α - and β -actin isoforms are more common in neurons (Cajigas et al. 2012).

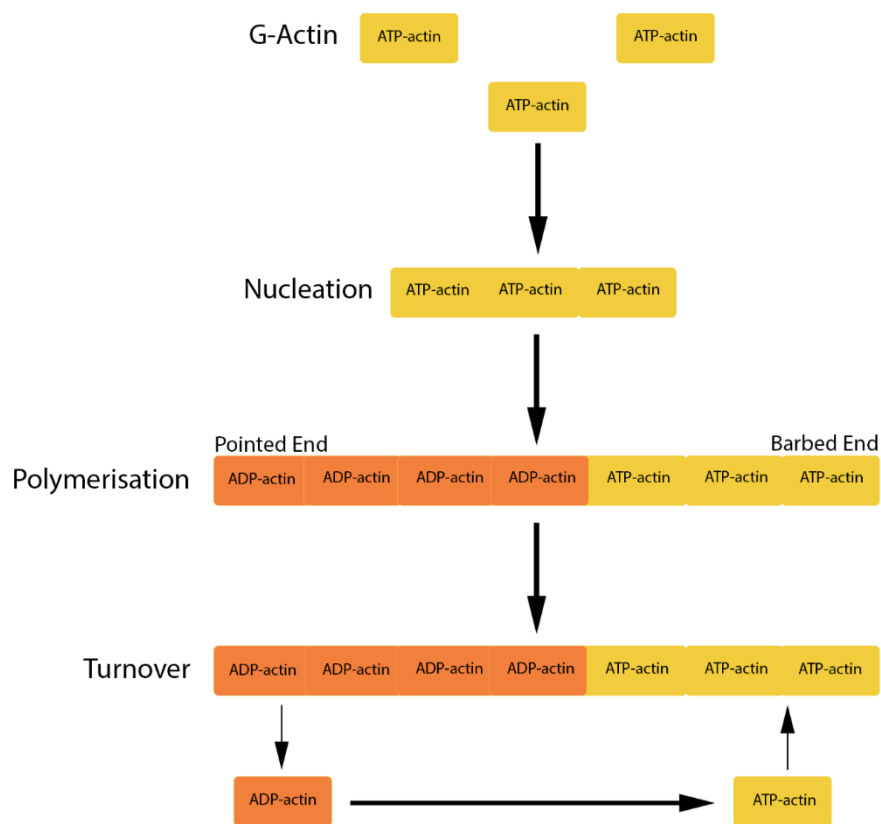


Figure 1.2 Actin polymerisation. Actin monomers (G-Actin) with ATP form a seed filament, consisting of three G-actin subunits, this process is known as nucleation. The seed filament expands, and additional G-actin subunits are added to the barbed (+) end of the filament (polymerisation). The filament becomes depolymerised at the pointed (-) end, losing a phosphate group to form ADP, whilst elongating occurs at the barbed end leading to a continuous turnover of the actin filament. Capping proteins and Arp2/3 can be added to the barbed and pointed ends, respectively, to terminate the polymerisation and depolymerisation reactions (Mullins et al. 1998; DiNubile et al. 2017). Image adapted from Muñoz et al. (2020) (Muñoz-Lasso et al. 2020).

Actin polymerisation and depolymerisation occur at the barbed and pointed ends, respectively. Some proteins such as formins accelerate actin polymerisation by removing capping proteins at the barbed (+) end whereas other proteins like gelsolin and actin depolymerising factor (ADF)/cofilin encourage depolymerisation by severing and capping actin filaments. (Kinosian et al. 1998; Kovar and Pollard 2004; De La Cruz et al. 2015). Capping proteins regulate actin polymerisation at the barbed end by binding directly to actin filaments to prevent the addition of new G-actin molecules. Other mechanisms to regulate actin polymerisation are through the nucleation of actin monomers. Actin related protein 2/3 (Arp2/3) complex is located at the pointed ends of actin filament to protect against depolymerisation and, together with Wiskott–Aldrich syndrome protein (WASP) family verprolin-homologous protein (WAVE)s, prepares the nucleation of actin filaments (Machesky et al. 1999; Rohatgi et al. 1999). In addition, Arp2/3 and WAVE both promote nucleation and elongation of actin filament by binding with profilin, a protein important in maintaining adenosine diphosphate (ADP)/ATP exchange on actin monomers (Pollard 2016; Goldschmidt-Clermont et al. 2017).

In neurons, F-actin is important to stabilise organelles such as the nuclei and dynamic organelles such as mitochondria and ER. Actin filaments are also important in maintaining and stabilising the axolemma (plasma membrane of the cell body and axon) (Wang et al. 2002; Pfisterer et al. 2017; Antoku and Gundersen 2018; Chakrabarti et al. 2018). They also facilitate axonal transport and enable myosins (actin-based motor proteins) to transport organelles along the axon across short distances (Kendrick-Jones and Buss 2016). Actin filaments in the cytoskeleton have also been reported to play a role in axon regeneration after injury (Wang et al. 2018b).

1.2.1 Actin in the axon

Most neuroscience research has focused on the dynamics of actin in growth cones, the protrusions from the axon that occur in axonal growth. However, more recently, actin dynamics within the mature axon has been closely researched and several structures of actin have been identified. The first are actin rings that form a cylindrical shape and give rise to the shape of the axon membrane skeleton. Each ring is comprised of actin filaments that is stabilised by adducin, a capping protein. The rings are separated and also held in place by α/β heterodimeric spectrins (Xu et al. 2013; Han et al. 2017). The next actin structure are actin waves that are composed of actin and microtubule filaments. The actin waves emerge from the base of neurites and protrude out on the plasma membrane, they appear slowly and irregularly with

approximately 1-2 waves appearing every hour. The waves function in anterograde microtubule and kinesin-based transport during neurite outgrowth just before an axon is specified (the multi-polar state) (Ruthel and Banker 1998; Ruthel and Banker G 1999; Flynn et al. 2009; Katsuno et al. 2015; Winans et al. 2016). The last actin structure, actin trails are actin hotspots that are specific locations along the axons that bidirectionally generate actin filaments (Ganguly et al. 2015). Therefore, this determines that actin has several structures in the form of rings, waves, and trails (Figure 1.3).

Another function of actin in the cytoskeleton is to constrict the circumferential size of the axon and disrupting microtubules, caused by actin rings (Fan et al. 2017). This is important in axonal processes such as synaptic plasticity, growth and vesicle transport and release (Bray 1984; Chen and Grinnell 1995; Pfister et al. 2006; Siechen et al. 2009; Lamoureux et al. 2010; Ahmed et al. 2012; Fan et al. 2015; Koser et al. 2016).

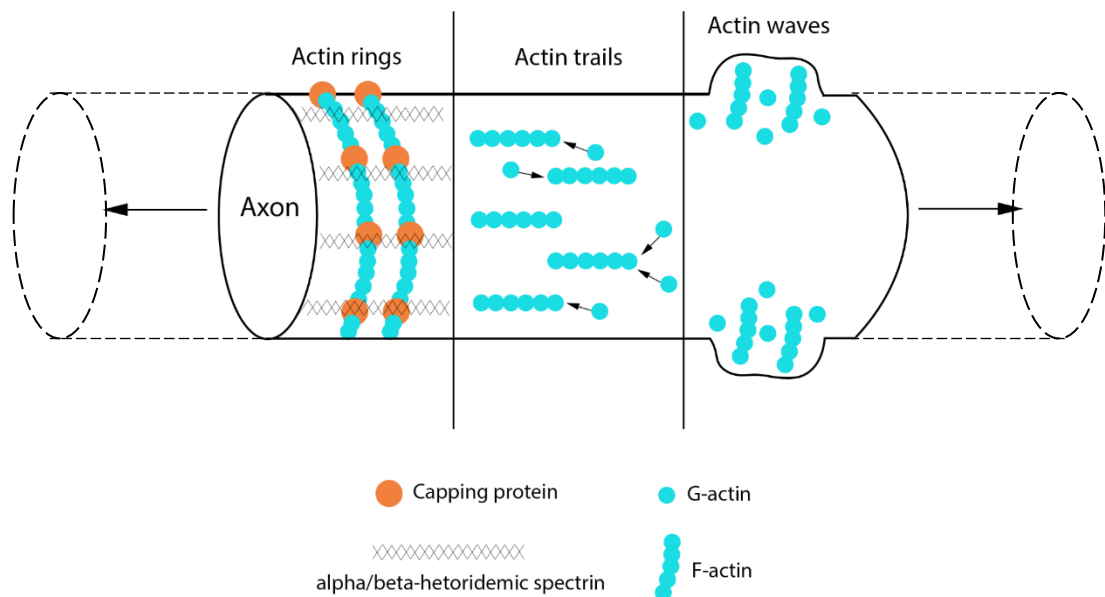


Figure 1.3 Actin structures in the axon. Actin rings are present on the outside of the axon and actin filaments separated by capping proteins (actin rings, left). G-actin binds to actin filaments at focal points in the axon (actin trails, centre) and actin filaments separated by capping proteins (actin rings, left). G-actin binds to actin filaments at focal points in the axon (actin trails, centre) and actin filaments form protrusions from the axon (actin waves, right). Image adapted from Muñoz et al. (2020) (Muñoz-Lasso et al. 2020).

1.3 Organelles and their regulation in neurons

1.3.1 Organelles in the neuron

As described in **Section 1.1.1**, neurons are divided into two distinguished subdomains: the somatodendritic and axonal domains. The function of the somatodendritic domain is to receive and process information whilst the function of axons is to transmit electrical and chemical signals to other cells. In neurons, organelles are distributed based on demand and neuronal function. In addition to the refractory period, it is thought that the structural polarity, that forms different regions, causes unidirectional neurotransmission of information in and between neurons, and this was termed dynamic polarisation by Cajal, (Cajal 1906).

Lysosomes, peroxisomes, mitochondria, and the smooth ER are non-polarised and are located in both somatodendritic and axonal regions (Krijnse-Locker et al. 1995; Ligon and Steward 2000; Farías et al. 2015; Lipka et al. 2016). The Golgi complex, rough ER and somatodendritic vesicles are present in the somatodendritic region only and prohibited from entering the axon (Palay et al. 1968; Farías et al. 2015). These organelles and vesicles are prevented from entering the axon at the PAEZ, located within the axon hillock (Braun et al. 1993; Farías et al. 2015; Britt et al. 2016). Organelles are able to either bind to axonally-plus-end-directed kinesins and cross the PAEZ or bind to dynein or dendritically-directed kinesins and travel to the cell body and dendrites (because they are excluded). If there are any organelles that are missorted at the PAEZ, they are picked up and sorted accordingly at the AIS (Gurel et al. 2014). Distribution of organelles via kinesins and dyneins is important for neuronal function as mislocation can contribute to neurological disease (Sleigh et al. 2019). This section will focus on three organelles in the neuron, ER (that synthesises new protein), the Golgi apparatus that transports, sorts and modifies new proteins and peroxisomes, vesicles produced from the Golgi. Together, this section will explore regulation of these organelles in neurons. Mitochondria are discussed in **Section 1.4** of this chapter.

1.3.2 Peroxisomes

Peroxisomes are present throughout the cell and are important in the metabolism of reactive oxygen species (ROS) and β -oxidation of fatty acids and lipid synthesis (Islinger et al. 2012). Peroxisomes attach to the cytoskeleton enabling them to travel long-distances within the neuron (Stamer et al. 2002; Van Bergeijk et al. 2015), when studied *in vitro*. They bind to either kinesin or dynein, regulated by mitochondrial Rho

GTPase 1 (Miro1), via several adaptor proteins, such as peroxin 1 (PEX1) or PEX14 and move in either an anterograde or a retrograde direction along the microtubules, respectively (Covill-Cooke et al. 2020). The binding of peroxisomes to kinesin or dynein is regulated by Miro1, a GTPase tail-anchored protein, that functions similarly with mitochondria (Birsa et al. 2013; Castro et al. 2018; Okumoto et al. 2018).

There is evidence to suggest that peroxisomes may contribute to calcium signalling. In cardiomyocytes, peroxisomes function in calcium handling and take in Ca^{2+} when peroxisomal calcium levels are low suggesting peroxisomes may have a cardioprotective effect (Sargsyan et al. 2021). In neurons, however, little is known about the regulation of Ca^{2+} in neuronal peroxisomes.

Peroxisomes also function in maintaining ROS homeostasis in neurons and breakdown ROS after oxidative reactions (Fransen et al. 2012; Trompier et al. 2014). Anti-cancer treatment such as doxorubicin causes cognitive impairment in the majority of cancer patients. Doxorubicin promotes oxidative stress which contributes to cell damage. In neurons, peroxisomes produce ROS, promoting cell aging and exposure of doxorubicin increases peroxisome number and increases the amount of ROS produced in these organelles, leading to pexophagy, and therefore neurotoxicity (Tannock et al. 2004; Vardy and Tannock 2007; Soussain et al. 2009; Ahles et al. 2012; Schagen and Wefel 2013).

The ER and peroxisomes also physically interact via Acyl-coenzyme A-binding domain protein 5 (ACBD5) (peroxisomal protein) and vesicle associated membrane protein associated protein B (VAPB) (ER membrane protein) two tail-anchored molecular tether proteins (Costello et al. 2017; Hua et al. 2017; Wang et al. 2018a). The association of peroxisomes to the ER suggests that the ER is important in peroxisome elongation and division which requires lipids, most likely supplied by the ER.

1.3.3 Endoplasmic reticulum

The function of the ER is to synthesise and assemble proteins for the neuron. They are then delivered into coat protein complex (COP) II-coated vesicles that bud off the ER. The vesicles then uncoat and the protein content is delivered to the Golgi apparatus where proteins are transported, sorted, and modified, see **Section 1.3.4**. The ER is differentiated into two regions, rough and smooth, depending on their binding to ribosomes (Baumann and Walz 2001).

The ER also functions as a calcium store for the cell and hence functions in calcium ion homeostasis. Protein chaperones (calreticulin, calnexin and protein disulphide isomerase) bind to many Ca^{2+} at once and regulate calcium levels to $\sim 100\text{-}200\ \mu\text{M}$ (in metazoan cells) (Görlach et al. 2006; Prins and Michalak 2011).

Like mitochondria and peroxisomes, the ER produces hydrogen peroxide and ROS, and it is here that redox enzymes chemically modify ROS to act as an intercompartmental signal. Without this, an abundance of ROS can build affecting the functions of several processes such as oxidative phosphorylation (OXPHOS), ER oxidative protein folding and calcium exchange between organelles (De vos et al. 2012; Fan et al. 2016; Costello et al. 2017; Hua et al. 2017).

In the ER, calcium levels are unusually high as opposed to other organelles in the cell. Calcium levels are controlled by calcium leak and calcium uptake and uptake is maintained by sarcoplasmic/ER calcium ATPase (SERCA)-type calcium pumps (Carafoli and Brini 2000). Calcium in the ER regulates chaperone complexes and loss of calcium inhibits the production of folding and maturation of new proteins (H F Lodish et al. 1992; Wetmore and Hardman 1996; Kuznetsov et al. 1997; Stevens and Argon 1999).

The ER forms contact sites with the plasma membrane and here are platforms for signalling molecules such as lipids and ions (Gallo et al. 2016; Saheki and De Camilli 2017; Stefan 2020). The ER also forms mitochondria-ER sites which are Ca^{2+} hotspots, locations of metabolite exchange, autophagosomes biogenesis, mitochondrial DNA (mtDNA) replication and mitochondrial fusion and division (Vance 1990; Giacomello et al. 2010; Hailey et al. 2010; Friedman et al. 2011; Hamasaki et al. 2013; Murley et al. 2013; Böckler and Westermann 2014; Garofalo et al. 2016; Lewis et al. 2016; Wu et al. 2016; Gomez-Suaga et al. 2017; Valm et al. 2017; Guo et al. 2018; Petrungraro and Kornmann 2019; Abrisch et al. 2020). Many of these functions are dysfunctional in neurodegenerative diseases (Zampese et al. 2011; Area-Gomez et al. 2012; Cali et al. 2012; Cali et al. 2013; Ottolini et al. 2013; Guardia-Laguarta et al. 2014; Sepulveda-Falla et al. 2014), suggesting mitochondria-ER sites as a potential therapeutic target site.

1.3.4 Golgi apparatus

The Golgi apparatus is located in the cell body of neurons and functions in transporting, sorting, and modifying lipids and newly synthesised protein by adding or removing molecular groups. The Golgi consists of several interconnected stacks of cisternae and is located near the centrosome and maintains this position due to the microtubule network (Hay et al. 1994). However some Golgi outposts may exist in dendrites and important for microtubule nucleation and establishment of polarity (Ori-McKenney et al. 2012). Calcium levels are important for the function of the Golgi apparatus because they facilitate in protein sorting and the trafficking of vesicles (Lissandron et al. 2010; Micaroni et al. 2010). Levels are maintained in the lumen via secretory pathway calcium ATPases (SPCAs) (Missiaen et al. 2007).

Vesicles can also be trafficked from the ER to the Golgi and back via COPI and COPII proteins. COPI-coated vesicles move in a retrograde direction, from the Golgi to the ER and around the Golgi compartments and COPII-coated vesicles move from the ER to the Golgi complex (Hara-Kuge et al. 1994; Tabb et al. 1998). This is important for protein sorting in vesicle biogenesis in the cell.

The Golgi apparatus also undergoes irreversible fragmentation during apoptosis and this has been observed in several diseases including, but not limited to, AD, ALS, and Parkinson's disease (PD) (Fariás et al. 2015; Britt et al. 2016; Sleight et al. 2019). The reason why is unknown, but Golgi fragmentation may contribute to neurotoxicity in disease.

1.4 Mitochondrial regulation in the axon in health and disease

1.4.1 Mitochondrial regulation in healthy axons

Another important organelle to neuronal function is the mitochondrion, and when damaged can contribute significantly to disease. Mitochondria are essential organelles in maintaining neuronal survival as they function in calcium buffering, metabolite synthesis and ATP production and maintaining low levels of ROS. Mitochondria tend to be more abundant at synaptic terminals and also at neuronal growth cones, the distal tip of developing axons, as ATP production is essential for the growth of new axons (Morris and Hollenbeck 1993). Therefore, in order for neurons to remain healthy, functional mitochondria need to be well distributed and this is coordinated by microtubule-based transport machinery (Werth and Thayer 1994; Misgeld and Schwarz 2017).

Mitochondria are important organelles that produce ATP during glucose metabolism. The process that produces ATP is respiration which involves three steps: glycolysis, the Krebs cycle, and OXPHOS. The majority of ATP is produced from the electron transport chain, powered by the proton gradient, of OXPHOS, occurring across the mitochondrial inner membrane (Bertram et al. 2006).

Mitochondria undergo constant fission and fusion events. Fission is important in the production of growth and new mitochondria and in separating healthy and damaged mitochondria, whilst fusion mitigates stress by mixing contents of damaged and healthy mitochondria. Both of these processes have to be carefully regulated and are mediated by GTPases (Hoppins et al. 2007). Fission is controlled by dynamin-related 1 (Drp1) whereas fusion is regulated by mitofusin-1 (MFN1) and mitofusin-2 (MFN2) (for mitochondria outer membrane fusion) and optic atrophy 1 (Opa1) (for inner membrane fusion) (Taguchi et al. 2007) (**Figure 1.4A**). The fine balance of mitochondrial fission and fusion events are important in the maintenance of energetic homeostasis in neurons. Fusion is important in spatial distribution of mitochondria as mutations of fusion proteins (MFN1, MFN2 and Opa1) caused alterations in morphology and distribution of mitochondria in the axon (Spinazzi et al. 2008; Misko et al. 2012; Bertholet et al. 2013). Fission is important in regulating mitochondria size and distribution as only small mitochondria can enter the axon and hence facilitate the even distribution of mitochondria along the neuron (Lewis et al. 2018) (**Figure 1.4A**). Both fission and fusion are affected by calcium and ROS levels which will be discussed below.

In mitochondria, the activity of Drp1 and Opa1, mitochondria fission/fusion protein, are affected upon an increase of Ca^{2+} levels. Calcium and calmodulin (CaM) regulate the activity of a serine/threonine protein phosphatase called calcineurin to phosphorylate Drp1 and recruit it to the outer mitochondrial membrane to initiate fission. (Cribbs and Strack 2007; Hom et al. 2007; Cereghetti et al. 2008; Jahani-Asl et al. 2011; Martorell-Riera et al. 2014; Wang et al. 2015). ROS levels also contribute to fission and fusion events in mitochondria. In fission, an increase in ROS causes Drp1-mediated mitochondria fragmentation. This loss in Drp1 prevents mitochondria fission and mitochondria are unable to be distributed down the axon, leading to neuronal damage (Kageyama et al. 2012). Increased ROS levels also contribute to Opa1 deactivation which leads to mitochondrial fragmentation and degradation (Gray et al. 2013).

In addition to fission and fusion events, mitochondria are constantly moving around the neuron. Mitochondrial transportation along the axon involves interaction with the actin cytoskeleton and microtubules. Mitochondria use kinesin-1 to travel in the anterograde direction, and dynein, to travel in the retrograde direction (Pilling et al. 2006; Drerup et al. 2017) (**Figure 1.4B**) similar to peroxisomes (Tanaka et al. 1998; MacAskill and Kittler 2010). Mitochondria mobility can be halted in high intracellular calcium levels enabling mitochondria to buffer calcium levels and provide ATP energy for ion pumps (Saotome et al. 2008; MacAskill et al. 2009; Wang and Schwarz 2009; Vaccaro et al. 2017). In addition, mitochondria mobility can also be restricted by Myosin VI, syntaphilin (an anchoring protein) and GlcNAcylation of Milton (Kang et al. 2008; Pathak et al. 2010; Chen and Sheng 2013; Pekkurnaz et al. 2014). Adapter molecules, Miro-1 and Milton (trafficking kinesin protein (TRAK) 1 and TRAK2 in mammals), are important in facilitating anterograde mitochondrial transport along the axon (Russo et al. 2009) as mutations in these genes terminate anterograde transport.

Mitochondria consist of a mitochondrial matrix surrounded by an inner and outer membrane, which is important in calcium buffering in the cell. The outer membrane of mitochondria is freely permeable to Ca^{2+} whilst the inner membrane controls Ca^{2+} entering and leaving the mitochondria matrix via the Ca^{2+} uniporter and the Na-Ca exchanger, respectively. If Ca^{2+} levels are high in the matrix, then Ca^{2+} exits through the permeability transition pore (Babcock and Hille 1998; Simpson and Russell 1998; Duchen 1999). Calcium uptake into mitochondria is important for energy production, buffering cytosolic calcium levels, and also in cell fate determination as Ca^{2+} can influence apoptosis (Kroemer et al. 2007; Rasola and Bernardi 2007; Satrústegui et al. 2007; Gellerich et al. 2009). In addition, calcium uptake into mitochondria can be influenced based on mitochondrial size as larger mitochondria demonstrate quicker and larger Ca^{2+} uptake as MFN2 knockdown promotes fission and decreases mitochondria retention and uptake of Ca^{2+} (Kowaltowski et al. 2019). This demonstrates the importance calcium buffering of mitochondria has on cell and mitochondrial dynamics.

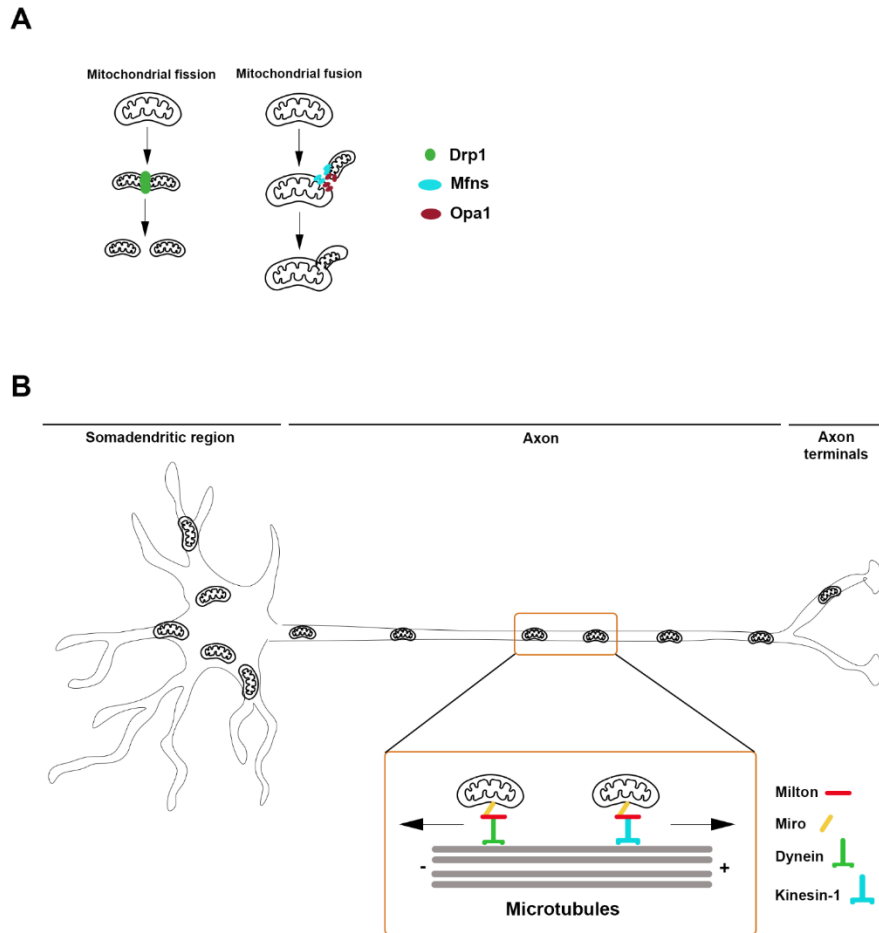


Figure 1.4 Mitochondria regulation in neurons. Mitochondria are regulated by fission events through Drp1, and fusions events through MFNs and Opa1 (A). Mitochondria trafficking is also regulated and require kinesin-1 (anterograde direction, plus end) and dynein (retrograde direction, minus end). Mitochondria are larger in the somadendritic region but are smaller in the axon (B). Image adapted from the review Ren et al. (2020) (Ren et al. 2020).

Mitochondria function in important processes such as fatty acid oxidation and ATP production. These processes are crucial for cell survival but they produce toxic by-products such as hydrogen peroxide, ROS, hydroxyl radical and superoxide anion that can damage cells (Saraste 1999; Wallace 2005), which can be released into the cell if mitochondria are aged or damaged. In addition, damaged mitochondria release high levels of cytochrome *c* and Ca^{2+} into the cytosol triggering apoptosis (Melissa J. Parsons and Green 2010) which leads to neurodegenerative diseases (Wallace 2005). Therefore, to maintain healthy mitochondria in the cell, any misfolded mitochondrial membrane proteins are either degraded by lysosomes and form a vesicle entrapping the misfolded proteins or are degraded by ATPases associated with diverse cellular activities (AAA) protease complexes within mitochondria. If

damage is severe, the entire mitochondrion fuses with lysosomes and the mitochondrion is degraded (Langer et al. 2001; Karbowski and Youle 2011; Soubannier et al. 2012). To maintain healthy mitochondria and to replenish mitochondria stocks, the organelle undergoes biogenesis. Mitochondria biogenesis is initiated by peroxisome-proliferator-activated receptor γ co-activator-1 α (PGC-1 α) to activate several transcription factors, nuclear related factor 1 and 2 (Nrf1 and Nrf2), leading to mitochondrial transcription factor 1 activation and mitochondrial DNA replication (Virbasius and Scarpulla 1994). Together, this therefore demonstrates that mitochondria number is maintained by a combination of biogenesis and mitophagy.

Free radicals are oxygen radicals and ROS, generated from damaged mitochondria (Chaturvedi and Beal 2013). In addition to ROS, mitochondria also produce reactive nitrogen species and together generate oxidant peroxynitrite (ONOO $^-$) which inactivates several mitochondrial proteins. This therefore contributes to mitochondria dysfunction leading to cell death and organ damage (Navarro and Boveris 2008; Franco et al. 2013; Song et al. 2013; Abdelmegeed and Song 2014; Akbar et al. 2016) which, together, are both also considered major factors in neurodegenerative diseases such as AD, PD, and Huntington's disease (HD) (Navarro and Boveris 2008; Johri and Beal 2012).

Redox homeostasis carefully balances between the removal and production of free radicals (Carocho et al. 2018). Even though there are systems in place to prevent radical-induced oxidative damage, they may not be functional due to lack of antioxidants or are simply insufficient to counteract the damage. Therefore, dietary supplementation can be effective to suppress oxidative stress (Ko et al. 2005; Chen et al. 2018; Bayliak et al. 2019; Tang et al. 2019).

Mitochondria function in calcium buffering, metabolite synthesis and ATP production and controlling ROS levels. They are carefully regulated and undergo several roles in neurons, these include fission, fusion, and axonal transport to travel long distances, in order to achieve their function.

1.4.2 Mitochondrial regulation in neurodegenerative disease

The importance of mitochondria to neuronal health is apparent because of the vast number of neurological disorders caused by mutations that affect mitochondria proteins (Misko et al. 2010; Bertholet et al. 2016). One example is mutations in the fusion proteins, MFN1 and MFN2, that cause Charcot-Marie Tooth disease type 2A,

an inherited disease causing axonal degeneration, that affects axonal mitochondrial movement (Misko et al. 2010). However, it is still unclear on the exact mechanisms behind axonal degeneration (Hales and Fuller 1997; Hermann et al. 1998; Rapaport et al. 1998; Rojo et al. 2002).

Axonal degeneration is also seen in aging, a phenomenon relating to neurological diseases (such as AD and PD) and glaucoma. In glaucoma, ganglion cells and their respective axons degenerate and axonopathy (axoplasm disorganisation and neurofilaments hyperphosphorylation accumulation) is present. In addition, decreased mitochondria transport was seen in degenerative axons as was increased MFN2 levels (Misko et al. 2010). The increase in MFN2 levels in murine glaucoma models suggests the need for increased mitochondrial transport and fusion and explains the elongated and fused mitochondria in glaucoma neurons (Cooper et al. 2016; Nivison et al. 2017). Therefore, this indicates that mitochondria transport is altered in aged neurons.

Phosphatase and tensin homolog -induced putative kinase 1 (PINK1) and Parkin both work together to facilitate the quality control (biogenesis and mitophagy) of mitochondria (Greene et al. 2003; Clark et al. 2006; Park et al. 2006). *PINK1* binds to damaged mitochondria and enables translocation of *Parkin* which leads to the removal of damaged depolarised mitochondria, by mitophagy. Mutations in these genes are linked to the recessive form of PD, suggesting that damaged mitochondria are unable to be removed by mitophagy causing neuronal damage and cell death (Kitada et al. 1998; Shimura et al. 2000; Rogaeva et al. 2004; Valente et al. 2004). Therefore, this implicates an important role of *PINK1*- and *Parkin*-mediated mitochondria maintenance in PD.

In familial ALS, an inherited neurodegenerative disease characterised by a loss of motor neurons, mitochondrial dysfunction occurs which increases the production of ROS in cells (Federico et al. 2012). In addition, ER-mitochondrial contacts are disrupted, increasing cytosolic calcium levels and disrupting axonal transport, ATP generation and protein homeostasis. The reduction in ATP generation may have a negative impact on the transport of mitochondrial, vesicles and cargo along axons (Barber and Shaw 2010; De Vos and Hafezparast 2017). Therefore, this limits molecular motors of ATP energy and disrupts axonal transport by interacting with Miro1 (Mórotz et al. 2012; Webster et al. 2017).

Therefore, mitochondria are important organelles in neuronal survival and can have a big impact on neurons if dysfunctional, such as altered axonal transport and ROS which can ultimately lead to neurodegeneration.

1.5 The pre-axonal exclusion zone

1.5.1 The importance of the pre-axonal exclusion zone

The PAEZ was first noticed in the late 1900s by N. Braun. Cytochemical staining of rough ER RNA was not seen in the axon and axon hillock (Braun et al. 1993) and therefore this region was predicted to be a cytoplasmic region consisting of Nissl bodies or trigroid substance. The PAEZ is located in the axon hillock at the start of the axon before the AIS. The PAEZ prevents large organelles from the soma such as Golgi complex and rough ER and somadendritic vesicles from entering the axon, acting as the end of the cytoplasmic boundary (Braun et al. 1993). Farías and colleges were able to show that somadendritic vesicles are able to pass the PAEZ (and AIS) if they are fused with a kinesin light chain binding sequence and migrate along the microtubules into the axon (Farías et al. 2015). This suggests that the PAEZ is dependent on motor proteins. It has also recently been reported that at the PAEZ, kinesin-1 controls and regulates ER and lysosome transport into the axon. P180 (an ER protein) binds to microtubules in the cytoskeleton, enabling lysosome fission and facilitating lysosome entry into the axon (Özkan et al. 2021).

The PAEZ is abundant in cytoskeletal components (microtubules and neurofilaments) (Palay et al. 1968). After the PAEZ, ankyrin G is found in abundance, corresponding to the AIS (Kordeli et al. 1995; Berghs et al. 2000) and is typically used to separate these regions at the start of the axon. It is suggested that the PAEZ takes on the role of somadendritic vesicle and organelle sorting and that the AIS complements the PAEZ by supporting it and rejecting any somadendritic cargo or organelles that have escaped the PAEZ. The AIS uses dynein and the actin structures to redirect cargo back to the somadendritic region and it is predicted that the PAEZ does too (Lewis et al. 2009; Al-Bassam et al. 2012; Watanabe et al. 2012; Kuijpers et al. 2016). There have been reports that the PAEZ uses the tripartite motif-containing protein 46 (TRIM46) / microtubule-associated protein 2 (MAP2) based mechanism to sort axonal cargo (Gumy et al. 2017) (**Figure 1.5**). Cargo bound to MAP2-inhibited motors are prohibited from entering the axon, but cargo bound to motors not inhibited by MAP2 are able to enter the axon.

Therefore, proposing that the PAEZ excludes somadendritic cargo and organelles without the use of a physical filter such as actin but with dynamic sorting (movement along microtubules). These data suggest PAEZ is a specialised region in the neuron that emerges immediately after the soma, to commence the initiation of the axon and coordinates with the AIS for sorting.

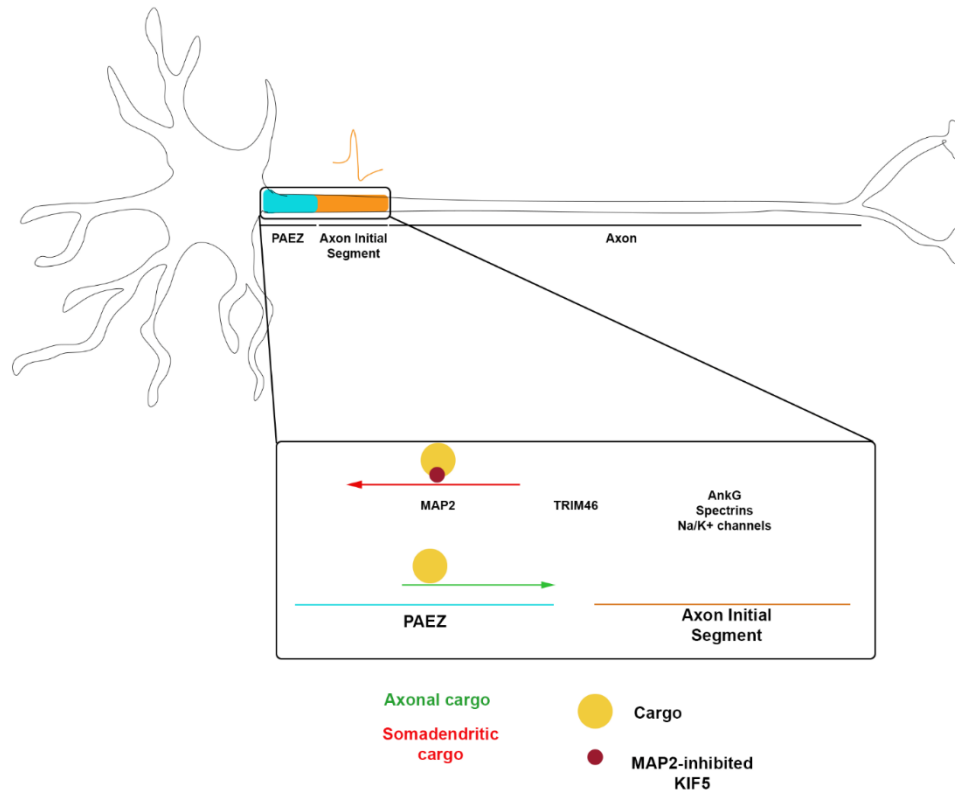


Figure 1.5 The boundary between the PAEZ and the AIS in hippocampal neurons. The PAEZ is located upstream of the AIS and uses the MAP2 / TRIM46 mechanism to filter cargo. MAP2 defines the PAEZ whilst TRIM46 is located between the two, regulating MAP2 localisation, and the AIS has AIS-specific components such as ankyrin G, spectrins and an abundance of sodium and potassium channels. Cargo, bound to MAP2-inhibited KIF5 motor protein of kinesin, are unable to enter the axon because they cannot bind to microtubules. Cargo bound to motors not inhibited by MAP2 can enter the axon. Image adapted from Gumy et al. (2018) (Gumy et al. 2018).

1.6 Function of the axon initial segment

The AIS is found within the first 20-60 μm of the proximal axon and is located between the cell body and the axon. The AIS functions in initiating action potentials and ensuring neuronal polarity (Palay et al. 1968). The AIS has a specialised structure that functions in cargo transport filter and diffusion barrier (Winckler et al. 1999; Nakada et al. 2003; Song et al. 2009; Sun et al. 2014). Several different molecules

are located within the AIS, these include ankyrin G, spectrins, neurofascin, and specific sodium and potassium channels, discussed below.

1.7 Molecular organisation of the mammalian axon initial segment

The AIS is densely packed with many voltage-gated ion channels, much more than the rest of the neuron. The high density voltage-gated sodium channels are responsible for the initial depolarisation, which then leads to the initiation of the action potential (Rasband 2010). The sodium ion channels density is approximately 40-50 times more than that in the soma or proximal dendrites (Kole et al. 2008; Lorincz and Nusser 2010). The AIS also has high densities of unique extracellular matrix molecules (neurofascin), cytoskeletal scaffold (ankyrin G and spectrins) and cell adhesion molecules (neurofascin) (Hedstrom et al. 2007; Kriebel et al. 2011) (**Figure 1.6**). Kinases, such as casein kinase 2 (CK2), are also present which control AIS formation. CK2 phosphorylates sodium channels, increasing their binding affinity for ankyrin G (Bréchet et al. 2008).

An important cytoskeletal AIS scaffold protein is ankyrin G; a plasma bound protein linking the spectrin-actin cytoskeleton to the integral components. Acting as a key organiser of the AIS, ankyrin G is required to maintain neuronal polarity. Loss of ankyrin G in hippocampal cells resulted in no detection of Na⁺ channels, β IV spectrin and the AIS cell adhesion molecules: neurofascin 186 (NF186) and neuron-glia related cell adhesion molecule (NrCAM) at the site at which the AIS was formerly located (John et al. 2006; Hedstrom et al. 2008). Two independent epigenetic-wide association studies identified methylation changes in the *ANK1* gene, which codes for a specific ankyrin repeat domain-containing protein, associated with AD (De Jager et al. 2014; Lunnon et al. 2014), suggesting that loss of neuronal polarity may be a pathogenic mechanism in dementia.

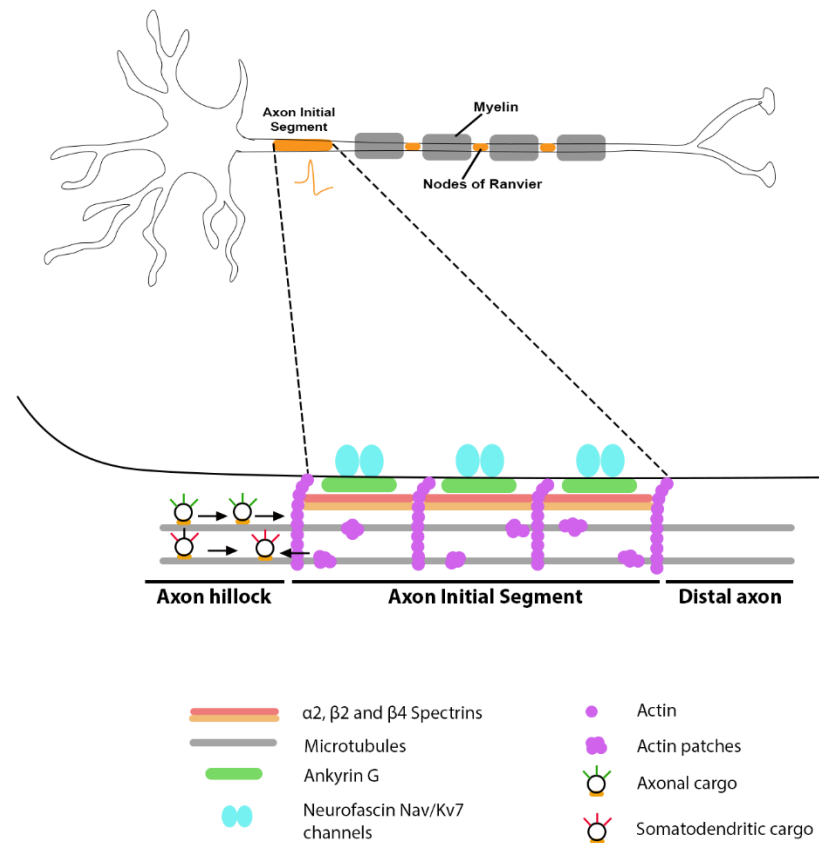


Figure 1.6 The structure of the AIS. The AIS surface is composed of an abundance of voltage-gated channels (sodium (Nav) and potassium (Kv7)). These are supported and bound by neurofascin, a cell adhesion molecule. Further anchoring occurs due to the interaction of these molecules with ankyrin G. Each ankyrin G molecule is also bound directly to BIV-spectrin and microtubules and indirectly to actin bands. Actin patches are also present throughout the AIS compartment. Cargo from the somatodendritic and axonal compartments is transported through the AIS at PTMs/GTP islands (Grubb and Burrone 2010; Bennett and Lorenzo 2013; Leterrier and Dargent 2014; Normand and Rasband 2015). Image adapted from Leterrier et al. (2015) (Leterrier et al. 2015) and Huang and Rasband (2018): (Huang and Rasband 2018).

1.8 The AIS acts as a barrier

Another important AIS cytoskeletal protein is actin, present in different forms such as actin bands, filaments, and patches. Like ankyrin G, the actin cytoskeleton is also a key regulator of sodium ion channel stability (Colbert and Johnston 1996; Colbert and Pan 2002). Actin filaments may also act as a barrier to filter the movement of transmembrane proteins such as sodium channels on the cell surface and large intracellular stains such as the unsaturated phospholipid L- α -dioleoylphosphatidylethanolamine (Nakada et al. 2003), between the somadendritic and axonal compartments (Winckler et al. 1999; Song et al. 2009).

Axonal vesicles have kinesin motors on their surface that recognise sites on microtubules as they enter the AIS. Kinesin family member 5 (KIF5), a motor protein of kinesin-1 family, is able to bind to microtubules that enter the axon, perhaps recognising post-translational modifications (PTMs) (Nakata and Hirokawa 2003; Konishi and Setou 2009; Hammond et al. 2010; Tapia et al. 2010; Huang and Banker 2012; Lipka et al. 2016). As kinesin motors migrate along microtubules, tubulin monomers can be eradicated and must be replaced by GTP-tubulin. GTP-tubulin leaves behind GTP islands that recruit KIF5, perhaps suggesting a pathway behind the axonal specificity of KIF5-mediated vesicle transport and pathway behind microtubule damage (Dimitrov et al. 2008; Nakata et al. 2011; Dumont et al. 2015; Schaedel et al. 2015; Aumeier et al. 2016).

Cargo destined for the somadendritic region enter the AIS but are stopped by actin patches that recognise myosin on the surface of the vesicles. Cargo is then guided back to the soma (Burack et al. 2000; Al-Bassam et al. 2012; Petersen et al. 2014) by Nudel 1 (Ndel1)-based dynein activation that's bound to ankyrin G (Kuijpers et al. 2016). In addition, cyclin-dependent kinase 5 (Cdk5) has been reported in the Ndel1-dynein pathway as it functions in the phosphorylation and activation of Ndel1, demonstrating the importance of Cdk5 in the sorting of somadendritic cargo (Klinman et al. 2017).

Together, the AIS therefore functions as a barrier to filter axonal and somadendritic cargo. The mechanism behind this uses both actin and motor proteins, such as kinesin and dynein, to carefully control the sorting of cargo.

1.8.1 Two barriers in one neuron

Filtering cargo between the somadendritic and axonal regions is important to maintain neuronal polarity. Several studies indicate that the AIS filters cargo from the somadendritic to the axonal regions (Winckler et al. 1999; Nakada et al. 2003; Song et al. 2009; Leterrier and Dargent 2014; Leterrier 2018). In contrast, other reports suggest that axonal vesicles and somadendritic cargo sorting occurs at the PAEZ, a region within the axon hillock at the AIS entrance (Fariás et al. 2015). It remains unclear why both specialised regions exist and if they are both required to maintain neuronal polarity. The PAEZ can exist without the AIS as adult dorsal root ganglia neurons, that normally lack the AIS, can still selectively filter cargo and vesicles into the axon (Gumy et al. 2017). This suggests that the AIS may be dispensable for cargo sorting and the PAEZ may be most important for this process.

However, since both regions sort cargo by different means they may both be required in the majority of neurons. It appears that cargo at the PAEZ is filtered based on its interaction with the microtubule cytoskeleton (MAP2/TRIM46 mechanism) whilst cargo at the AIS is selectively transported using both an actin-based filter and microtubule binding and together both regions maintain and regulate neuronal polarity between the somadendritic and axonal regions.

1.9 Dysfunction of the AIS in neurological disease

Up until relatively recently, very little was known about the AIS in relation to age-developmental disorders and age-dependent neurodegenerative diseases (Buffington and Rasband, 2011). New evidence has shown that reduction in AIS number and length may be a common feature across diseases (Marin et al. 2016).

There are several mutations in genes related to the AIS that are associated with other neurological diseases and neuropsychiatric disorders, including epilepsy, schizophrenia, bipolar disorder, and also (AIS disassembly caused after) stroke injury. Loss of function of $Na_v1.1$ channels, abundant in the AIS of gamma aminobutyric acid (GABA) -ergic hippocampal interneurons, is associated with early-onset Dravet syndrome (a form of epilepsy) or severe myoclonic epilepsy, in infants (Oakley et al. 2011). This was also observed, in infancy, in severe myoclonic epilepsy modelled mice (Yu et al. 2006; Kalume et al. 2007). They also showed an increase in action potential firing failures in the AIS in GABAergic interneurons, revealing a potential loss of inhibitory control by the GABAergic interneurons (Oakley et al. 2011).

ANK3, the gene that encodes ankyrin G has been identified as a genetic risk factor in schizophrenia and bipolar disorder, however little is known about how the molecular organisation of the AIS changes in these disorders (Ferreira et al. 2008; Schulze et al. 2009; Athanasiu et al. 2010). Pathophysiology from stroke causes damage, which is partly caused by excitotoxicity. A large influx of Ca^{2+} following injury, activates calpains (calcium-dependent proteases), which break down the ankyrin/spectrin cytoskeleton in the AIS (Siman et al. 1984; Schafer et al. 2009). Cytoskeleton loss in the AIS causes a loss in sodium channels which in turn, compromises action potential initiation function.

In some cases, AIS dysfunction may not stem directly from ion channel loss in this region but through organelle dysfunction. Interestingly, the mitochondrial population in the AIS can be functionally separated from dendrite population based on mitochondrial membrane potential and morphology after neuronal silencing (Bülow et al. 2021). With AIS mitochondria more resistant to morphology changes yet more susceptible to mitochondrial membrane potential loss. In a cell model of Fragile X Syndrome, this AIS specific mitochondrial membrane potential loss failed to occur (Bülow et al. 2021), suggesting that mitochondrial plasticity in the AIS may uniquely regulate neuronal plasticity in disease.

AIS dysfunction may also play a role in the most common of age-dependent neurological diseases. There are currently three pathological characteristics of AD: tau neurofibrillary tangles, amyloid plaques, and neurodegeneration (Price et al. 1995). In mice, it has been reported that AIS length and number are significantly reduced when proximate to amyloid- β ($A\beta$) plaques (the key component of amyloid plaques) (Palop and Mucke 2009). Several mechanisms for reduction in AIS length and number have been suggested, such examples are unspecified neuronal death, neuronal displacement ($A\beta$ plaques causing the physical displacement of neurons) or AIS barrier disruption, caused by $A\beta$ triggering calpain-mediated proteolysis of the cytoskeleton in the AIS (Marin et al. 2016). Therefore, this indicates that changes/loss of the AIS could contribute to impaired brain function, seen in patients with dementia (León-Espinosa et al. 2012; Marin et al. 2016).

One function of the AIS is to filter cargo between the somatodendritic and axonal regions (Winckler et al. 1999; Song et al. 2009; Rasband 2010). In AD, this selective filter is disrupted and tau, originally in the axon, once pathologically modified (acetylated) is seen in the somatodendritic compartment (Sohn et al. 2016). In addition,

AIS proteins (ankyrin G and β IV spectrin (**Figure 1.7**)) have been reported to decrease in human AD brains (Li et al. 2011). This suggests that acetylated tau destabilises the AIS and causes misalignment of neuronal proteins that require polarised distribution, exact mechanisms behind this are unknown (Sohn et al. 2016).

1.10 The role of Cdk5 in AIS barrier formation

The mechanisms that control AIS development and maintenance are currently unknown. Ankyrin G, a key protein that is integral to binding AIS components to the cytoskeleton, was currently the only known organiser behind the AIS structure (Hedstrom and Rasband 2006; Trunova et al. 2011). In recent years it has become apparent that Cdk5 also controls the size and properties of the AIS.

Previous literature states that decreasing Cdk5 activity causes the AIS-like compartment, in *Drosophila* mushroom body neurons, to shorten or become absent and increasing Cdk5 causes the AIS-like compartment to almost double in length, altering only the border between the AIS and the axon and not the AIS/soma border. Actin disorganisation disrupted neuronal polarity by altering Fasciclin 2 polarisation (tagged vesicles normally seen in the soma) suggesting actin reorganisation does not interfere with the effect Cdk5 has on AIS size (Trunova et al. 2011). Mechanisms behind the effect Cdk5 has on AIS size could be calpain proteolysis of AIS components as calpain is known to target and convert p35, Cdk5 regulatory subunit, to p25 leading to hyperphosphorylation of Cdk5 and an increase in Cdk5 activity (Schafer et al. 2009; Von Reyn et al. 2009). In addition, Cdk5 involvement in homeostatic synaptic plasticity by acting as a priming kinase for polo-like kinase 2 (Plk2) and spine associated Rap GTPase activating protein (SPAR) binding (Seeburg et al. 2008). Therefore, this suggests that calpain activity increases Cdk5 activity disrupting homeostatic regulation of AIS structure and altering AIS size.

Cdk5 is important in action potential firing at the AIS. Increased Kv1 channels are present on the AIS to facilitate action potential firing. Kv1 channels in the axon are regulated by Cdk5 as Cdk5 phosphorylates Kv β 2 (Kv1 subunit) in hippocampal neurons (*in vitro*) and sciatic nerves (*in vivo*). Inhibition of Cdk5 leads to an increase in intracellular Kv1 channels but has no effect on cell surface Kv1 channels (Vacher et al. 2011). This therefore suggests that Cdk5 specifically regulates Kv1 populations at the AIS and therefore influences the function of the AIS in action potential firing.

In addition, Cdk5 has previously been shown to be important in vesicle trafficking in dorsal A9 motor neurons (in *Caenorhabditis elegans*) as vesicle-associated synaptic proteins (synaptobrevin, synaptogyrin, ras-associated binding-3 and active zone component leukocyte antigen-related interacting protein related protein- α) were mislocalised in neurons defective in Cdk5 and cyclin-dependent PCTAIRE-motif protein kinase 1 (PCT-1), a kinase essential to target axonal presynaptic components (Ou et al. 2010). Vesicle-associated synaptic proteins were instead localised to the dendrites suggesting that Cdk5, in conjunction with PCT-1, is important in the trafficking of synaptic vesicles. It has been suggested that cargo mislocalisation is a result of Cdk5-dependent phosphorylation of Ndel1, a factor important in interacting with lissencephaly type 1 (Lis1), a regulator of the retrograde motor dynein (Niethammer et al. 2000; Sasaki et al. 2000). Therefore, this demonstrates the importance of Cdk5 in dynein-mediated retrograde transport of synaptic vesicles in neurons. In addition, elevated Cdk5 also leads to the mislocation of cargo and mutations preventing Cdk5 phosphorylating Ndel1 in dorsal root ganglia neurons block the activity of Cdk5 suggesting Cdk5 functions via the Lis1/Ndel1/dynein pathway to transport cargo (Klinman et al. 2017).

Cdk5 has recently been reported to be dysregulated in AD brains. Dysregulated Cdk5 caused Tau to become hyperphosphorylated leading to microtubule collapse and neurodegeneration (Patrick et al. 1999). However, specific dysregulation of Cdk5 in AIS in neurological states has not yet been determined.

1.11 Are there other molecules that can maintain the axon initial segment?

The mechanisms that control AIS development and maintenance are currently unknown. In the Smith lab, an unbiased forward genetic screen was previously performed that uncovered other molecules that may maintain the AIS (Smith 2019). To summarise briefly: flies were fed ethyl methanesulfonate (EMS), a chemical mutagen that caused random mutagenesis throughout the genome. Several hundred flies were screened for deficits in AIS size or morphology and a candidate-of-interest identified, mutant 6757. This was identified as predicted deleterious mutation in cyclin-dependent kinase 12 (Cdk12) through whole genome sequencing approaches. Loss of Cdk12 caused an age-dependent swelling specifically in the proximal axon. This thesis demonstrates that *Cdk12* was our gene-of-interest and investigate how this molecule controls AIS morphology.

1.11.1 Cdk12

Cdk12 is known to bind to the C-terminal domain of RNA Polymerase 2 and regulates transcription and pre-mRNA processing (Egloff and Murphy 2008). Cdk12 also binds with CyclinK and controls transcription in both humans and *Drosophila* (Bartkowiak et al. 2010). Cdk12 in the *Drosophila* brain is expressed ubiquitously (**Figure 1.7**).

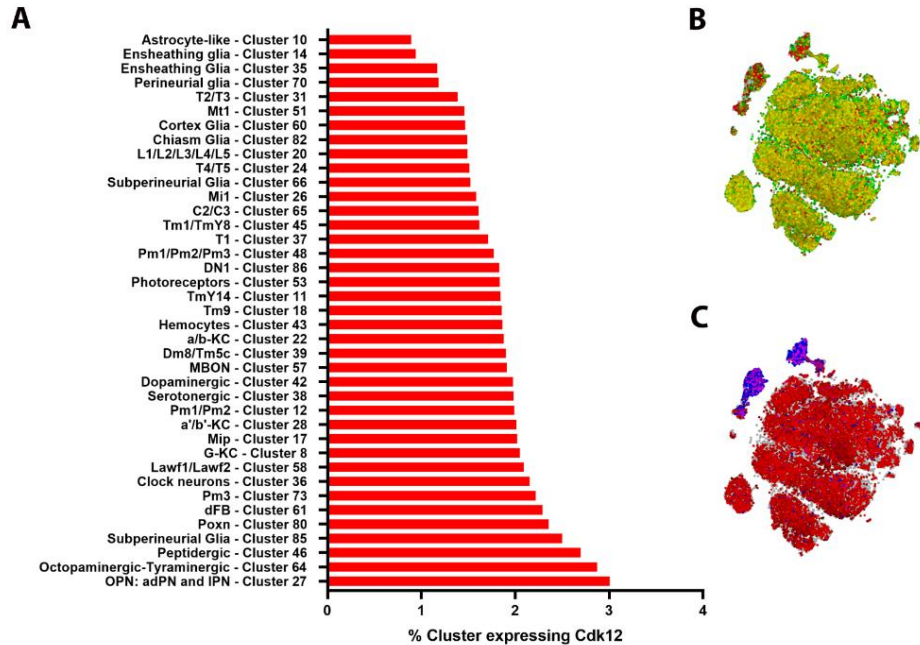


Figure 1.7 *Drosophila* Cdk12 is expressed ubiquitously in the brain. Percentage of cells in the brain within a cluster expressing Cdk12, graph ordered in ascending order (A). SCoPe output demonstrating *Cdk12* (red) is co-expressed with *embryonic lethal abnormal vision* (green) (B) and *reversed polarity* (blue) (C) throughout the brain (Davie et al. 2018).

In *Drosophila*, Cdk12 has three transcripts: RA, RB, and RC isoforms that are 5498, 5851 and 4970 bp in length. The transcripts are flanked by SAK kinase (3747 bp) and an unknown *Drosophila* gene CG7611 (4978 bp) (Larkin et al. 2021). Cdk12 has one key domain, the protein kinase domain, located towards the C-terminal domain of the protein sequence, (**Figure 1.8**).



Figure 1.8 *Cdk12* gene. *Cdk12* is located between 21516322 bp and 21522693 bp position along the 3L *Drosophila* chromosome. *Cdk12* consists of one key domain, the protein kinase domain located at position 21520294-21524 bp, towards the C-terminal domain. Image adapted from Flybase (Larkin et al. 2021).

In addition to regulating transcription of several long DNA repair genes, such as breast cancer genes 1 and 2 (*BRCA1* and *BRCA2*), *Ataxia-telangiectasia- and Rad3-related (ATR)*, and *ataxia-telangiectasia-mutated (ATM)*, *Cdk12* also regulates transcription in genes involved in the homologous recombination repair pathway (Blazek et al. 2011; Bajrami et al. 2014; Ekumi et al. 2015; Popova et al. 2016; Zhang et al. 2016b; Tien et al. 2017; Chirackal Manavalan et al. 2019). Depletion/inhibition of *Cdk12* therefore leads to DNA damage, genome instability, DNA replication defects and alterations in G1/S progression and also generates a non-functional homologous recombination pathway (Joshi et al. 2014; Lei et al. 2018).

Cdk12 has not yet been linked to the maintenance of the AIS or PAEZ so understanding this mechanism may be important new knowledge. In addition to its canonical role in transcription, it is possible that there is a yet undiscovered function of this protein in the cytoplasm analogous to *Cdk5*. Importantly, *Cdk12* is highly conserved from humans to *Drosophila* and we can use the genetic tractability of this system to discover new insights into its role in proximal axon maintenance.

1.12 Using *Drosophila melanogaster* in research

Drosophila melanogaster belongs to the family Drosophilidae which is derived from Greek: *drosos* = dew and *philos* = loving and are commonly found around rotting fruits. Over the years, *Drosophila* has helped improve our understanding of several key fundamental biological processes (Ashburner and Novitski 1976) and this combined with genome sequencing has highlighted how highly conserved gene sequence and function are between humans and flies and this conservation contributed greatly to our knowledge and understanding of human biology and pathology of human disease (Rubin et al. 2000). It is estimated that approximately 75% of human disease-related genes are functional orthologues in flies (Reiter et al. 2001; Lloyd and Taylor 2010). This is further demonstrated by the winners for the

Nobel Prize in Physiology and Medicine (1995). Christiane Nüsslein-Volhard, Eric Wieschaus, and Ed Lewis won the Nobel Prize for their discoveries in the genetic control of early embryonic development. They identified several genes essential for *Drosophila* development which have since been shown to be important for animal development (including humans).

The genome of the fruit fly can be easily manipulated, and structure/function analysis performed, to help determine essential domains and amino acids of a protein-of-interest. Transgenes can be used to knockdown or overexpress specific molecules in specific cell types, controlled by a genetic binary system, Gal4-upstream activation sequence (UAS) that will be discussed in more detail in **Chapter 2**. Disease variants or human genes can also be expressed in order to study potential phenotypes or rescue phenotypes caused by knockout of the fly orthologue.

As a model organism, the fly is a relatively inexpensive and easy to keep model with a fully sequenced and annotated genome and a plethora of available resources and stocks (for example genome-wide RNA interference (RNAi) library). One female fly can lay up to 100 eggs each day for up to 20 days and it takes ~ 10 days at 25°C for an embryo to develop to a mature adult fly (Stocker and Gallant 2008), therefore demonstrating how easy it is to generate large numbers for experiments use, such as genetic screening. The life cycle of the fly is quick and lasts ~80 days at 21°C. After fertilisation, the embryo takes ~ 1 day to hatch into a first instar larvae. The larvae then undergo three molts (first, second and third instar) with their purpose being growth and feeding (Dubrovsky 2005). At the end of each larvae life cycle, the cuticle molts and is replaced with a larger cuticle. At ~ 5 days the third instar larvae pupates and undergoes metamorphosis to transition from larvae to an adult fly. Cuticle synthesis and metamorphosis are regulated by several hormones, such as 20-hydroxyecdysone (20E or ecdysone) and juvenile hormone (Riddiford et al. 2000; Dubrovsky 2005). The fly stays as a pupae for approximately 4 days and during this process most embryonic and larvae tissue undergoes histolysis through programmed cell death (Baehrecke 1996), and is replaced with imaginal structures such as wings or legs derived from specialised cells (imaginal discs) such as the wing or leg imaginal discs, respectively.

1.12.1 The importance of *Drosophila* in neurobiology research

Initial reports of *Drosophila* research were first documented in 1901 by William Castle (Harvard University) but the first major discovery using fruit flies was with Thomas

Hunt Morgan (1910) to identify the *white* gene mutation (Morgan 1910). *Drosophila* research initially was about hereditary, but gradually more and more tools developed, and the use of *Drosophila* became a model of choice for different fields of science, including more recently neuroscience.

In 1971, Seymour Benzer identified three crucial alleles *arrhythmic*, *shortened period* and *lengthened period* of the gene, *period*. *Period* was initially identified in 1984, by genetic cloning, by Jeffery Hall, Michael Rosbash and Michael Young but was not linked to the circadian cycle at this time. *Period* is important in the circadian rhythm in *Drosophila* eclosion and locomotion as all alleles influenced the length of the circadian rhythm (Konopka and Benzer 1971). Later, *timeless*, another important circadian gene, was discovered in *Drosophila* and with *period*, formed a complex that was regulated by the transcription factors CLOCK and CYCLE (Allada et al. 1998; Darlington et al. 1998; Rutila et al. 1998). The circadian rhythm is highly conserved in humans and flies (Kudo et al. 1991) meaning the discovery of *period* was the landmark to understanding human circadian rhythms. Sleep is regulated by the circadian rhythm and *Drosophila* have been used as a useful tool to determine how reductions in sleep can affect behaviours such as courtship, learning, memory, and aggression.

Several models exist today to study neurodegenerative diseases, these include, but are not exclusive to, mice, rats, yeast, zebrafish, *Caenorhabditis elegans*, and *Drosophila* (Dawson et al. 2018). *Drosophila* are a good model to study neurodegenerative disease because several aspects of the disease can be tested in an *in vivo* system. The first transgenic model for human neurodegenerative disease was for spinocerebellar ataxia 3 in 1998 (Warrick et al. 1998), closely followed by a transgenic model for HD (Jackson et al. 1998). Since then, further transgenic flies have been generated to study other neurodegenerative diseases.

Drosophila can be used to model complex behavioural traits associated with disease. One example are disturbances in the sleep/wake rhythm which are common in neurodegenerative diseases and are present in up to 60% of patients (Malhotra 2018). *Drosophila* have a circadian rhythm similar to humans, can undergo jet lag, like humans, when moving between different time zones (Rothenfluh et al. 2000) or showing that having a rhythm out-of-sync with the environment (like that of shift workers) has a negative impact on *Drosophila* fitness (Konopka and Benzer 1971; Klarsfeld and Rouyer 1998). In familial advanced sleep phase syndrome, mutations

in people suffering from sleep disturbances have been mapped to the same genes initially isolated from *Drosophila*. This therefore demonstrates how highly conserved the genome is between *Drosophila* and humans (Toh et al. 2001).

Drosophila models can also be used to study pathological changes and protein aggregation associated with neurological disease. For example in AD research, investigators can express human A β 42 in the fly to help understand its function and pathogenesis in AD (Fernandez-Funez et al. 2015). In addition, these A β 42 models have been used to study amyloid deposits, learning and memory deficiencies and premature death, as seen in AD patients. These studies therefore demonstrate the importance of *Drosophila* as a model organism in neurobiology, particularly in modelling neurodegenerative diseases. Models such as this as therefore viable candidates to examine potential therapeutic targets.

1.12.2 *Drosophila* as a model organism to study polarity and the AIS

In order to maintain distinct axonal and somadendritic regions in neurons, a diffusion barrier exists at the start of the axon that selectively filters cargo from one region to another (Winckler et al. 1999). Most studies show that the diffusion barrier is present in mammalian neurons (the AIS), but emerging research is showing this region is also present in *Drosophila* neurons.

An accumulation of sodium channels has been reported in the AIS region in neurons of the *Drosophila* central nervous system. A compartment similar to the mammalian AIS within *Drosophila* mushroom bodies was identified that expressed an abundance of sodium and potassium channels important for action potential initiation (Trunova et al. 2011; Ravenscroft et al. 2020), ankyrin G accumulation necessary for structural support in the AIS (Trunova et al. 2011; Jegla et al. 2016) and a selective barrier that functions to filter cargo between the axon and the somadendritic compartments, essential to maintain neuronal polarity (Winckler et al. 1999; Trunova et al. 2011). Together, this demonstrates that *Drosophila* are good models to study polarity and the AIS.

Another study focused on mushroom body and olfactory projection neurons of third instar larvae brains and identified ribosomes localised to the soma indicating the high levels of protein synthesis in the soma and microtubules orientated with the minus ends facing distal to the cell body, like that of mammalian neurons, indicating the presence of a selectivity filter to maintain polarity (Rolls et al. 2007). These studies

therefore demonstrate that *Drosophila* is an extremely useful model to study polarity and neuronal compartmentation organisation.

1.12.3 Available tools to study organelles, biochemistry, and physiology in *Drosophila* neurons

In order to study neurobiology and neurodegenerative diseases, several genetically encoded tools are utilised to study biochemical changes in *Drosophila* neurons. Genetically encoded fluorescent markers are UAS controlled and are important because they provide an alternative to immunohistochemistry and facilitate the ability to image *in vivo* and *in vitro* if tissues, such as the fly wing, are too thick to fix and stain. They can be used to fluorescently tag, with green fluorescent protein (GFP), an organelle-of-interest such as mitochondria (*UAS-mitoGFP*), peroxisomes (*UAS-SKL::GFP*) or a protein-of-interest (*UAS-actin-GFP*) and enable measurements in different regions of the neuron in different genetic backgrounds. This can also help to identify any deficits in trafficking, localisation or organelle changes in morphology (Vagnoni et al. 2016; Vagnoni and Bullock 2016; Vagnoni and Bullock 2018; Mattedi et al. 2022). Other genetically encoded tools tagged to fluorescent markers can be used to measure physiology e.g., redox states (*UAS-roGFP*) and calcium levels (*UAS-GCaMP*) in organelles and neurons in both *in vivo* and *in vitro*.

1.12.3.1 Biochemical sensors

Oxidative stress can be measured through genetically coded redox sensors and are probably the most common biochemical sensor used. These sensors measure ROS over a range of ages in various tissues. They are generated in such a way that cysteine residues, either end of the fluorophore (e.g., GFP barrel structure) are excited by ROS, and form disulphide linkages. This results in an excitation peak at 400 nm at the expense of the 480 nm and this ratio determining the redox status (Dooley et al. 2004; Hanson et al. 2004). Different reduction-oxidation-sensitive green fluorescent protein (roGFPs) can be fused to different target signals and expressed in different organelles e.g., mitoroGFP. To quantify cytosolic and mitochondria ROS and measure redox levels in *Drosophila* roGFPs have been used, giving an indication of mitochondria dysfunction (Liu et al. 2012). Together, this therefore shows that oxidative stress can be measured in *Drosophila* by a combination of not only physiological but biochemical assays too.

In addition to ROS measurements other genetically modified GFPs can be used to study mitochondrial physiology and dynamics, these include measuring ATP production by ATPSnFR, mitoQC and kimera and mitoTimer.

ATP is produced by mitochondria during electron transfer during OXPHOS and measuring ATP levels gives an indication of mitochondrial function. Levels of intracellular energy source, ATP, can be imaged using a genetically encoded fluorescent sensor (ATPSnFR). Binding of ATP causes a conformational change of the epsilon subunit of ATP synthase in cpSFGFP and an increase in fluorescence, emitting a single wavelength (Yagi et al. 2007; Lobas et al. 2019). Under UAS control, ATPSnFR can also measure ATP levels in *Drosophila* glutamatergic neurons (Lin et al. 2021). Therefore, ATP sensors are efficient to measure mitochondrial function.

To measure neuronal damage, nicotinamide adenine dinucleotide (NAD⁺) sensors are used to measure NAD⁺ metabolite levels. NAD⁺ levels decrease with aging (Zhu et al. 2015) and increasing NAD⁺ precursor levels (nicotinamide riboside and nicotinamide mononucleotide) can increase lifespan and health span (mitochondrial health, muscle strength and motor functions) in yeast, mice, worms and *Drosophila* (Liu et al. 2013; Menzies et al. 2015; Kerr et al. 2017). NAD⁺ levels upregulate autophagy and mitophagy which can clear A β plaques, improve mitochondrial function and neuronal survival (Belenky et al. 2007; Balan et al. 2008; Yoshino et al. 2011; Gomes et al. 2013; Fang et al. 2016; Zhang et al. 2016a). Therefore, demonstrating NAD⁺ is a good indicator of neuronal damage.

Mitochondria undergo mitophagy as a quality control mechanism to recycle or eliminate mitochondria (Boya et al. 2018; Pickles et al. 2018; Evans and Holzbaur 2020). Mitophagy can be studied using several tools. The first, mitoQC is a construct that expresses a mCherry-GFP tag that is bound to the outer mitochondrial membrane resulting in healthy mitochondria expressing red and green fluorescence. Mitochondria undergoing mitophagy migrate to the lysosomes to form autophagosomes and here, the GFP signal is quenched by low pH and only red fluorescent is expressed (Allen et al. 2013; McWilliams et al. 2016; McWilliams et al. 2019). Another pH-sensitive tool that measures mitophagy is Keima, a fluorescent reporter that targets mitochondria and is bound to a mitochondrial localised signal, is resistant to lysosome degradation. In alkaline conditions e.g. mitochondria (pH 8.0), Keima expresses GFP fluorescence (the shorter wavelength) but in acidic environments (e.g. pH 4.5), such as at lysosomes, where mitochondria undergo

mitophagy, the protein undergoes a shift towards the longer wavelength and expresses red fluorescence (Katayama et al. 2011; Sun et al. 2015). This therefore gives an indication of mitophagy level.

Another tool is mitoTimer that measures mitochondrial age and dynamics. This tool uses a fluorescent Timer, a mutant dsRed, shifting from green to red fluorescence at 48 hours. Timer consists of two amino acid substitutions: V105A and S197T which induces the colour change over time. This change is unaffected by changes in temperature, pH, protein concentration and ionic strength (Terskikh et al. 2000; Terskikh et al. 2002). mitoTimer is a useful tool and gives an indication of mitochondrial age, turnover and dynamic.

1.12.3.2 Neuronal physiology

Ca²⁺ control cell excitability, neurotransmitter release or gene transcription (Hagiwara and Naka 1964). The pattern of intracellular Ca²⁺ is coupled to neuronal activity and hence monitoring Ca²⁺ levels can determine the timing of synaptic input (Yuste and Denk 1995; Denk et al. 1996; Yuste et al. 1999; Yasuda et al. 2004).

Originally, to visualise Ca²⁺ in cells, cells were impaled on calcium-sensitive microelectrodes by microinjecting bioluminescence proteins and non-fluorescent dyes. (Johnson and Shimomura 1972; Rink et al. 1980). From there, fluorescent dyes were made enabling calcium levels to be quantified but the dyes are unable to be targeted to specific cells types and populations (Yasuda et al. 2004; Tour et al. 2007). A solution to this was the design of genetically encoded calcium indicators (GECIs) as they can easily be delivered to different cell types and populations (Miyawaki et al. 1997). They, however, can interfere with other signalling molecules and fluorescent properties and protein stability can suffer at different physiological temperatures (Nakai et al. 2001; Hasan et al. 2004; Palmer and Tsien 2006).

GECIs consist of a calcium-binding element such as CaM or troponin-C (Miyawaki et al. 1997; Nakai et al. 2001; Heim et al. 2007). CaM uses a binding peptide (M13 peptide) to enhance the Ca²⁺-dependent conformational change (Miyawaki et al. 1997).

There are two separate strategies behind GECIs, Förster resonance energy transfer (FRET)-based GECIs and single fluorescent protein (FP), both methods relying on variants of GFP. For FRET-based GECIs, two GFP variants are required, normally

the yellow and cyan variants. The yellow variant is the donor chromophore and cyan the acceptor chromophore, both connected via a calcium binding element (in this case CaM and M13 peptide). When calcium binds to CaM, a conformational change occurs enhancing FRET from the donor to the acceptor chromophore. If the donor chromophore (cyan) is excited at 440 nm, an increase in calcium can be detected by a decrease in emission intensity from the donor chromophore at 485 nm and an increase in intensity from the acceptor chromophore (yellow) at 535 nm. Therefore, determining the presence of intracellular calcium levels (Miyawaki et al. 1997; Heim et al. 2007). GECIs that use only one GFP variant, circularly permuted GFP variants (cpGFP), such as GCaMP sensors, undergo a conformational change of cpGFP due to calcium binding to its binding element (e.g. CaM), changing the structure of GFP and enhancing fluorescence emissions (Nakai et al. 2001).

FRET-based sensors have been used to measure calcium levels in several different neurons in the *Drosophila* brain, these include olfactory sensory neurons (Fiala et al. 2002; Pelz et al. 2006; Niewalda et al. 2011); dopaminergic neurons (Riemensperger et al. 2005); mushroom bodies (Yu et al. 2003; Tsydzik and Wright 2009); and mechanosensory neurons of the Johnston's organ, an organ used to detect sound vibrations (Kamikouchi et al. 2009; Effertz et al. 2011).

In the *Drosophila* brain, GCaMPs have been used to measure calcium levels in several neurons, including in the mushroom bodies (Wang et al. 2004; Wang et al. 2008b) thermosensory neurons (Hamada et al. 2008; Gallio et al. 2011), GABAergic neurons (mushroom bodies) (Liu and Davis 2008) and gustatory sensory neurons (Marella et al. 2006; Fischler et al. 2007; Cameron et al. 2010). Together, FRET-based and single chromophore (GCaMPs) sensors are a good way of measuring calcium levels in *Drosophila*.

Genetically encoded voltage indicators measure voltage dynamics as an indication of neuronal activity. Fluorescent molecules are coupled to voltage sensing domains such as voltage-sensitive phosphatases, potassium, and sodium or proton channels. A conformational change occurs after a voltage influx and enhances fluorescent emissions (Siegel and Isacoff 1997; Ataka and Pieribone 2002; Dimitrov et al. 2007; Jin et al. 2012; Kang and Baker 2016), therefore measuring the level of voltage.

1.12.4 The *Drosophila* wing as a model for neurology

The *Drosophila* wing develops from a ball of cuboidal cells, originating from invagination of the embryonic ectoderm (Bate and Martinez Arias 1991; Fristrom and Fristrom 1993). These cells flatten to form the larval imaginal wing disc and during the larvae stage, as the animal feeds and grows, the wing disc expands (Garcia-Bellido and Merriam 1971; Mandaravally Madhavan and Schneiderman 1977). From 7 hours after pupae formation (APF) (during metamorphosis) the wing disc divides into two sections, the wing blade, hinge and part of the notum, undergoes expansion, elongation, separation and re-apposition of both epithelial sheets (Taylor and Adler 2008; Kanca et al. 2014). At 40 hours APF, cell division and rearrangement has occurred to reshape the wing to its final shape (Aigouy et al. 2010; Sugimura and Ishihara 2013). At this stage, bristles and veins have also developed and the fly ecloses (O'Keefe et al. 2012). The wings emerge folded but gradually spread out due to haemolymph fluid filling the veins.

The glutamatergic sensory neurons project axons from cell bodies into the thoracic ganglion. Glutamatergic neurons in the wing are excellent to study axonal biology and are among the largest in the *Drosophila*. The semitransparency nature of the wing allows for the direct visualisation and imaging of fluorescently labelled organelles/proteins and biochemical sensors and tools (as defined in **Chapter 2, Section 2.6**). Genetically encoded tools can be driven specifically in these sensory neurons using specific drivers (Fang et al. 2012; Fang et al. 2013; Neukomm et al. 2014; Smith et al. 2019; Lin et al. 2021), as defined in the Methods Chapter. As the wing is made from a waxy cuticle, only intragenous fluorescent markers can be used rather than antibody stains. In the *Drosophila* wing, neurons are located in the costal and longitudinal veins 1 (L1) and 3 (L3), see **Figure 1.9** for fly wing schematic (Whitlock and Palka 1995; Nakamura et al. 2002; Fang and Bonini 2015). There are ~250 neurons in the veins, each one terminating at one dendrite and dispatching into bristles in order to sense environmental stimuli. Wings can be dissected for imaging (Fang et al. 2012; Fang et al. 2013; Neukomm et al. 2014; Smith et al. 2019; Lin et al. 2021), or the whole fly is fixed down between a microscope slide and cover slip for live cell imaging (Vagnoni et al. 2016).

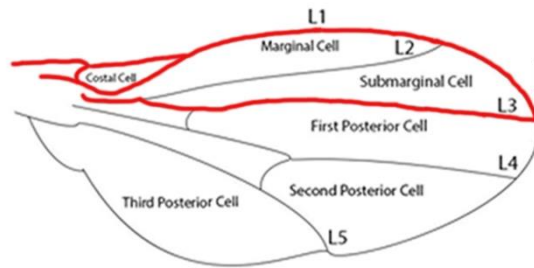


Figure 1.9 *Drosophila* fly wing. The fly wing consists of five longitudinal veins (L1-5) and is divided up into cells: marginal; submarginal; first, second, and third posterior cells; and costal cells, as annotated. Sensory neurons (red) in the fly wing project from the body of the fly, down the costal, L1 and L3 veins, terminating at the distal tip (see black arrow), each glutamatergic sensory neuron terminates at one dendrite. Fly wing image adapted from Yanahawa et al. (2014) (Yanagawa et al. 2014) and created on Adobe Photoshop 2022.

The wing system has been partially useful to study mitochondrial biology and can be combined with unbiased genetic screening to find new modulators of mitochondrial dynamics in neurons *in vivo* (Smith et al. 2019; Lin et al. 2021). Unbiased genetic screening can be achieved through random mutagenesis of the genome and combined with a clonal approach to bypass any potentially lethality relating to the mutations and to screen progenies in the F1 generation. A clonal approach, called mosaic analysis with a repressible cell marker (MARCM) (Lee and Luo 1999), also allows for the visualisation of individual neurons and the mitochondria they contain. Only the sparse fluorescently labelled cells will be null for the gene, the rest of the animal will be wild-type (WT). The clonal approach to study neurons is discussed in more detail in the Methods Chapter.

MARCM clones have been used to study mitochondria biogenesis in neurons deficient in tumour susceptibility gene 101 (*tsg101*) and identified TSG101 to be important in maintaining mitochondrial number and size in axons (Lin et al. 2021). In addition, the use of MARCM clones also identified glutathione-S-transferase (GST) to be important in maintaining redox balance between glutathione (GSH) and glutathione disulfide (GSSG). GST is also important to promote mitochondrial fusion and loss of GST in neurons altered mitochondrial trafficking and neuronal physiology (Smith et al. 2019).

In addition, the *Drosophila* wing is a useful tool to study organelle transport in axons, as discussed in (Vagnoni and Bullock 2016). Mitochondrial transport declines in aging neurons and mitochondrial transport deficits have been implicated in the disease

pathology in neurodegenerative disease (Hinckelmann et al. 2013; De Vos and Hafezparast 2017). The wing system recently identified Lis1, a dynein cofactor, to negatively regulate mitochondrial transport in aging neurons (Vagnoni et al. 2016). This suggests that Lis-1 may be an important target to maintain axonal survival. In addition, the wing model also identified the cyclic adenosine monophosphate (cAMP)/protein kinase A pathway to upregulate kinesin-1 motor, a protein that normally declines with age (Vagnoni and Bullock 2018). This increases mitochondrial transport in neurons and may propose a therapeutic target to disease.

The wing and the MARCM machinery can also be used to study axonal degeneration following injury. To mimic neuronal injury, the wing can be cut using scissors at various points or ablated with lasers, normally using 5-6 laser pulses to sever the nerve bundle, and able to sever individual neurons (Soares et al. 2014). Mammalian and vertebrate models have characterised pathology and cellular responses to neural injury but in recent times invertebrates have uncovered new pathways regulating axon degeneration and regeneration (Bejjani and Hammarlund 2012; Fang and Bonini 2012). One example is the discovery that *With no K 1* contributes to axonal maintenance in developing and aging neurons in *Drosophila*, as the loss of *With no K 1* caused axonal retraction and branch destruction (Izadifar et al. 2021).

In addition to mechanical injury, the wing system can be used to study neurodegeneration associated with genetic manipulations (Fang et al. 2012). For example, depletion of Milton by RNAi caused progressive axonal degeneration and this phenotype could be rescued by expressing Wallerian degeneration slow (WLD^s) (an axon preserving nicotinamide mononucleotide adenylyltransferase fusion protein). Milton is important in the transport of mitochondria in axons and a reduction in mitochondria was seen in axons with a Milton knockdown in injured wings. Axons expressing Milton knockdown and overexpression of WLD^s had healthy axons, suggesting that WLD^s plays a role in preserving mitochondria and in delaying axon degeneration (Fang et al. 2012).

The wing system also contains a number of different glial subtypes which can be independently targeted using specific glial drivers (Neukomm et al. 2014). Glial membrane responses can be seen in the dissected ventral nerve cord following wing injury (Purice et al. 2017), and this system used to discover that matrix metalloproteinase-1 (MMP-1) was a crucial component required for glial clearance of severed axons (Purice et al. 2017). The wing system has also recently been used to

show that glial cells may also spread injury signals between neurons to temporarily suppress vesicle trafficking in non-injured neurons (Hsu et al. 2021).

The fly wing is therefore a valuable system to study neural function and neurodegeneration, providing an ease of imaging, within a highly genetically trackable system. It is partially useful to study axon morphology, organelle distribution, biochemistry, and axon specific mechanisms *in vivo*.

1.13 Aims of the thesis

The overall aim of this project is to determine how Cdk12 contributes to axonal maintenance, and we address this question through the following objectives:

1) To determine if Cdk12 controls proximal axon width and neuronal maintenance (Chapter 3).

An unbiased genetic screen recently performed in the Smith lab group identified mutant 6757 as a key player behind maintaining the size of the axon proximal to the cell body (Smith 2019). Phenotypes in mutant 6757 were predicated to be caused by a predicted deleterious mutation in *Cdk12* through whole genome sequencing analysis. To address this aim, I first used deficiency mapping, together with a rescue experiment, to confirm that my gene-of-interest was *Cdk12*. Next, I used the *Drosophila* wing model to quantify neuronal number and proximal axon size. Single neuron analysis was achieved in homozygous null mutant clones, using the MARCM machinery. Clones were labelled with fluorescently encoded genetic markers, to give single axon resolution under the confocal microscope. Age-dependent analysis of axon size and maintenance was carried out to show how *Cdk12* is essential for neuronal integrity.

2) To determine whether Cdk12 controls actin dynamics in the AIS and barrier formation (Chapter 4).

The AIS is a region in the neuron located between the cell body and the axon and has a distinct structure. This specialised compartment functions in neuronal polarity and action potential initiation (Palay et al. 1968). The mammalian AIS structure is composed of several molecules including ankyrinG, the key scaffold, and actin,

important in the selective barrier of protein trafficking (Winckler et al. 1999; Nakada et al. 2003; Song et al. 2009; Sun et al. 2014).

In *Drosophila*, little is known about the AIS structure but an AIS-like compartment has been identified in mushroom bodies in the *Drosophila* brain (Trunova et al. 2011). High expression of ankyrinG and a decrease in actin was present in the AIS-like compartment, similar to the mammalian structure.

To address this aim, I tested several markers for their ability to localise to the AIS (to act as an AIS label) in wing neurons. While most markers investigated did not consistently label this region, actin was notably absent from the axon and AIS allowing us to visualize the separation with the soma compartment. Therefore, suggesting that in glutamatergic neurons, actin is not a marker for the AIS. We showed that ablation of *Cdk12* caused the formation of actin swellings and altered actin dynamics specifically in this region where actin is usually lost. We further found that actin changes in the AIS altered the vesicle barrier (selectively filter) and allowed peroxisomes (a vesicle marker of the soma) to enter the axon.

3) To investigate physiological changes to neurons and mitochondria occur through loss of Cdk12 (Chapter 5).

To answer this aim, I showed that loss of *Cdk12* leads to an increase in neuronal Ca^{2+} and caused excessive mitochondrial fusion, but has no effect redox balance, in stages prior to cell death. These findings suggest that actin redistribution may contribute to neuronal and mitochondrial dysfunction, which may in turn cause neurodegeneration at later stages.

2 Materials and methods

2.1 Maintenance of fly stocks

Fly stocks were maintained in large plastic vials or bottles on standard culture medium (see **Table 2.1** for recipe) at 21°C in a 12-hour dark 12-hour light cycle. Stocks were flipped every four weeks for maintenance.

To set up a cross, virgin female and male flies were collected and anaesthetised on a pad emitting carbon dioxide. Flies were visualised under a Zeiss Stemi 508 dissecting microscope with CL4500 LED fibre optic cold light source. An approximate ratio of 1:3 male to female flies were used per cross with roughly 30 virgins used for crosses in bottles and 10 and 20 virgins used for crosses in medium and large vials, respectively. After 4-6 days and at 10-12 days at 25°C, parent flies were flipped into new vials. Progenies emerge after 10 days at 25°C and were collected in new vials. For aging experiments, progenies were flipped every 5 days into new vials until the correct age. Specific crosses for experiments are outlined in experimental Chapters.

2.2 Fly stocks and genetics

All Fly stocks are listed in the **Appendix 1**.

2.2.1 Deficiency stock

In **Chapter 3**, a deficiency line purchased from Bloomington Drosophila Stock Centre (BDSC) was used to confirm my mutant was *Cdk12*. The deficiency line I used, Df (3L)9065, deletes the majority of the *Cdk12* gene, including the functional kinase domain, from position 21,517,021..21,517,021 to 21,523,082..21,523,164 on the 3L arm of the third chromosome. It does not overlap with any other genes in the *Drosophila* genome (Parks et al. 2004).

2.2.2 Bacterial artificial chromosome stock

To confirm my mutant was *Cdk12*, I also performed two rescue experiments (**Chapter 3**). For the first rescue, a genomic DNA (gDNA) bacterial artificial chromosome (BAC) construct purchased from P[acman] Resources was used that is continuously expressed, to potentially rescue *Cdk12*. The construct was purchased in *Escherichia coli* cultures but was streaked out on agar plates (in house) and sent to BestGene Inc. They isolated a colony from the plate, grew the colony containing the BAC construct in culture and then extracted the plasmid DNA, which was microinjected

into fly embryos. The second rescue was performed using a *5xUAS-Cdk12* transgenic lines available in house.

2.2.3 RNA interference

In **Chapter 4** and **Chapter 5**, several fly lines were used under the control of RNAi to reduce expression of certain genes. RNAi is a gene silencing method used to reduce (but not eliminate) expression of a gene. In this project, the RNAis are under the control to UAS and hence expression is derived by the Gal4 driver (Fire et al. 1998). RNAi were either purchased from either BDRC, Vienna Drosophila Resource Center (VDRC) or gifted.

2.3 Fly food

To make a 43 L batch of fly food, 32 L of water was pre-heated overnight in the mixer. The following day, 300 g agar (0.7% final concentration) was sifted into the mixer for 30 minutes and heated to 60°C, stirring continuously. At 60°C, 2.5 L molasses, 1000 g yeast and 2500 g cornmeal (in water) was added, and the mixer heated to 95°C. This takes approximately 2 hours. To dissolve the cornmeal in water, 8 L of boiling water was slowly added to 2500 g of cornmeal, with continuous stirring. At 95°C, the heat is turned off and deionised water was added. Once the temperature drops to 75°C, add the 168 ml acid mix (0.4% final concentration) (250 ml propionic acid, 25 ml phosphoric acid and 325 ml deionised water) and dissolved Tegosept solution (56 g Methyl-p-Hydroxybenzoate in 280 ml ethanol, 0.13% final concentration) was added whilst continually mixing. Fly food was then dispensed into vials and bottles and left overnight to cool and set. Cotton balls were then inserted into large vials and plugs inserted into bottles, see **Table 2.1** for fly food ingredients and origin.

Product	Origin
Water	Dispensed from deionised filter
Agar	MIN GEL 960, BTP DREWITT
Yeast	903312, MP biomedical
Cornmeal	901411, MP biomedical
Molasses	BTP DREWITT
100% ethanol	64-17-5, VWR
Tegosept (anti-fungal agent)	p-hydroxybenzoic acid (102341, MP biomedical)
Propionic acid	220130025, ACROS ORGANIC
Phosphoric acid	201140010, ACROS ORGANIC

Table 2.1 Ingredients for fly food.

2.4 Gal4-UAS binary system

The system is used to activate gene expression in *Drosophila*, in a tissue-specific manner, at a particular point in development (Duffy 2002). The system uses two separate fly lines. One line contains a construct that consists of a cell-specific promoter that drives Gal4 expression and the other line contains a construct that consists of a transgene of interest which is driven by an UAS sequence. Crossing of these lines causes Gal4, which is expressed when the promoter is expressed, to bind to UAS which then drives expression of the gene-of-interest, (**Figure 2.1**) (Brand and Perrimon 1993).

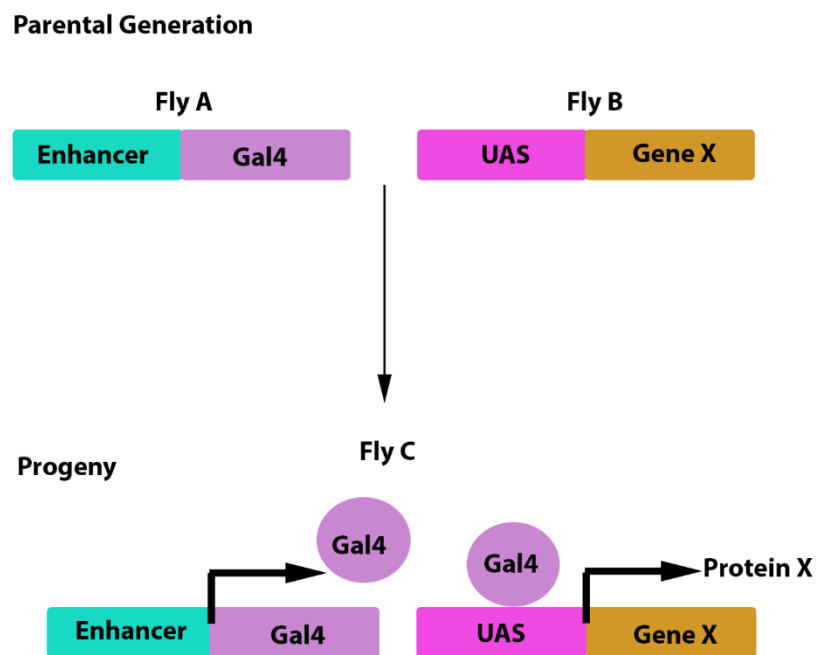


Figure 2.1 Gal4-UAS system. The Gal4-UAS system uses Gal4 (expressed in one parental fly line), which is tissue-specific, to bind to the UAS binding site (expressed in another parental fly line) to activate a target gene-of-interest. Crossing of these two fly lines causes the activation of the Gal4 protein to specifically express the target gene in the F₁ generation, this could be a reporter gene (e.g. GFP) or a gene-of-interest (Gene X) or a knockdown of a gene-of-interest (e.g. Gene X -RNAi) (Brand and Perrimon 1993; Kelly et al. 2017). Image adapted from Kelly et al. (2017) (Kelly et al. 2017).

2.5 MARCM

MARCM produces mosaic flies expressing any transgene including fluorescently labelled fluorophores in only a subset of cells, in a targeted cell population (Wu and Luo 2007). MARCM uses the Gal4-UAS system (**Figure 2.1**) to sparsely label cells containing the fluorescently labelled fluorophore so they can be seen at single cell

resolution (Lai and Lee 2006). In addition to expressing transgenes in a clonal fashion, we can also use the MARCM machinery to analyse homozygous mutations only in the sparsely labelled cells, while unlabelled cells are WT. This allows for the investigator to study homozygous mutant cells in adult flies which would be lethal if present in the whole animal.

Cells with the MARCM machinery start off heterozygous for the Tub-Gal80 gene, which expresses the Gal80 protein. The yeast Gal80 protein inhibits Gal4 (Ma and Ptashne 1987). At the G2 stage in cell division, chromosomal recombination, using Flippase (A sense 2e) and corresponding flippase recognition target (FRT) sites (2A and 82B) (Golic and Lindquist 1989), caused Gal80 to be removed from one of the daughter cells. Therefore, causing a uniquely-labelled Gal80-negative cell containing the homozygous mutation (Lee and Luo 2001). MARCM glutamatergic neurons were visualised in the fly wing (L1 vein) using the, OK371 driven, Tomato transgene (bound to a membrane protein localisation signal) (**Figure 2.2**). Neurons in the L1 wing have long axons and, using MARCM, are easy to visualise.

MARCM clones were produced which fluorescently tagged the *Cdk12* homozygous mutant neurons (a loss-of-function mutation) in an otherwise WT background, (**Figure 2.2**). MARCM fly crosses and progenies were kept at 25°C.

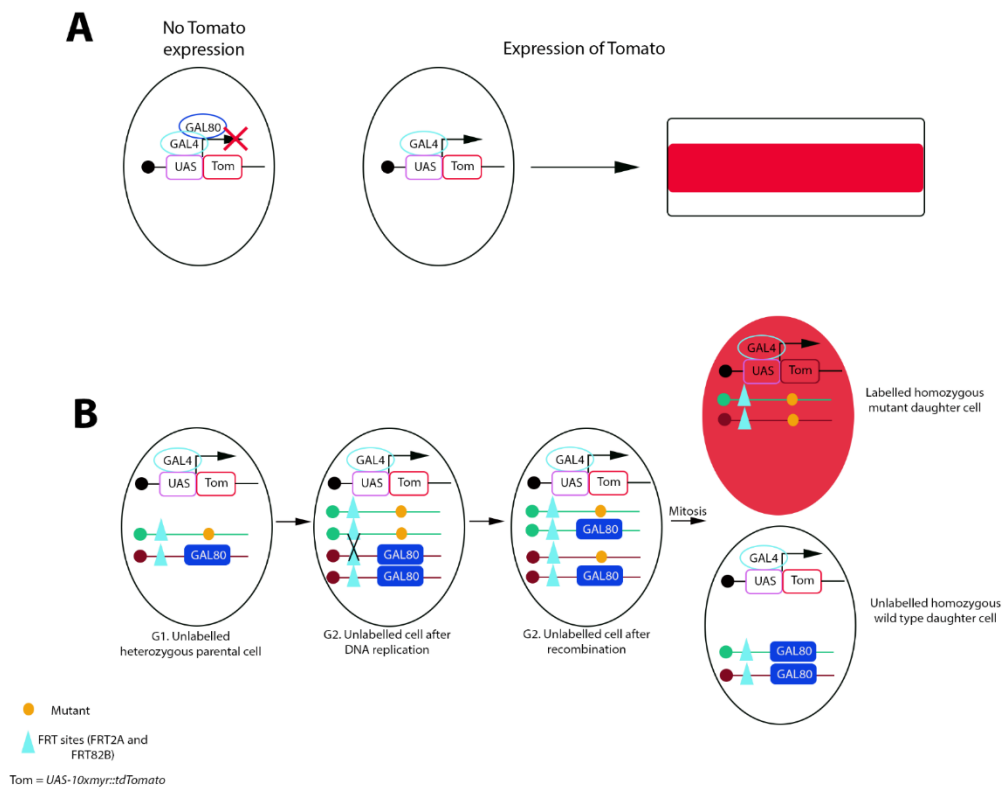


Figure 2.2 Labelling cells with *Cdk12* mutant using mosaic analysis with a repressible cell marker. (A) In the background, neuron cells that express the reporter gene, Tomato, were labelled. In the current project, Tomato expression refers to glutamatergic neurons that expressed Tomato. The reporter gene was under the control of the 'OK371' driver which activated the reporter gene in glutamatergic neurons. Therefore, expression of the OK371 driver activated Gal4, which bound to the UAS binding site. This caused glutamatergic neurons to stain red, hence the cell was labelled. In the presence of Gal80, the Gal4-UAS binary system was inhibited and no Tomato was expressed, resulting in an unlabelled cell. (B) In *Cdk12* mutant (introduced by unbiased screening) and Gal80 cells, the parental cells were unlabelled and the Gal4-UAS system was not activated. The cell divides and recombination was induced by an asense flippase 2E, causing the *Cdk12* mutant and Gal80 to be present on each chromosome set. Mitosis occurred and unlabelled cells with Gal80 and labelled cells (glutamatergic neuron stained with red with Tomato) with the *Cdk12* mutant were produced. It is also possible to generate heterozygous unlabelled cells. Image adapted from Wu and Luo (2007) (Wu and Luo 2007).

2.6 Wing dissections and live wing imaging

2.6.1 Wing dissections

Progenies of the correct genotype and age were collected and kept at 21°C. A total of ~10 flies were added to each vial to minimise flies fighting and causing damage to their wings and a layer of potato flakes was also added to each vial to prevent flies sticking to the food. Flies were flipped every week to prevent parents and progenies mixing. Once flies were the correct age, each fly was anaesthetised on a CO₂ pad and wings were checked for damage under a Zeiss Stemi 508 dissecting microscope with CL4500 LED fibre optic cold light source. Damaged wings were discarded as the neurons may also be injured and give incorrect readings. In order to dissect each wing, a pair of sharp forceps were used to apply slight pressure to the thorax which caused the wing to become elevated. This facilitated access to cut the wing as close to the thorax as possible. Whilst applying slight pressure to the thorax, each wing was dissected in one cut using micro scissors. In most cases, both wings per fly were dissected but sometimes one wing was left, and the fly was further aged. Flies with one wing were unaffected and able to mate and survive as normal. Dissected wings were placed in the centre of a pre-prepared microscope slide on 10S halocarbon oil. Each slide was orientated lengthways, and a line of oil painted in the centre. Each wing was transferred using forceps covered slightly in oil to increase adherence of the wing to the forceps. Approximately 15 wings per genotype was mounted on each slide. Once all wings were transferred on the slide, they were carefully orientated in the same direction with the distal tip facing upwards (towards the edge of the slide, not the ceiling), making sure not to damage the wings. A cover slip was then placed over the wings, ready for imaging. All wings in this project expressed the MARCM machinery and therefore fluorescent neurons were visualised. To achieve good images, mounted wings were only imaged up to 40 minutes post dissection as after this time, fluorescent levels significantly reduced and neurons were difficult to visualise (Vagnoni et al. 2016; Vagnoni and Bullock 2016; Vagnoni and Bullock 2018; Mattedi et al. 2022).

The wings were imaged using the Zeiss Cell Observer spinning disc confocal microscope, starting at the 10x objective to locate the wings on the slide, before moving to the 63x for imaging of the neurons. Neurons were initially located at the costal vein and checked for expression of fluorescent markers. On the imaging software, acquisition mode was selected, and the correct lasers selected depending on the fluorescent reporters expressed. Laser intensity and exposure time was

adjusted accordingly, and settings kept the same for all wing images. The costal vein, locating all axons and the most distal cell body along the distal tip of the L1 vein was imaged. Total axon number in the costal vein and total cell body number in each neuron was recorded for each wing.

2.6.2 Live imaging

The flies were anesthetised on a CO₂ pad and the legs carefully dissected using micro scissors (and discarded) to prevent the fly from moving once mounted. In the meantime, all coverslips were prepared.

Three strips of tape were placed, in layers, on both short ends of the coverslip, followed by a strip of double-sided tape. A strip of double-sided tape was also added directly to the coverslip, at one end, next to one stack of tape. A small layer of 10S halocarbon oil was applied next to the tape (Vagnoni et al. 2016; Vagnoni and Bullock 2016; Vagnoni and Bullock 2018; Mattedi et al. 2022)

To mount the fly on the coverslip, pick each fly up from the pad by the body and place directly on the oil with the wings outwards, head pressed against the double sided tape and ventral side up. Forceps were carefully used to orient the wings outwards and remove any air bubbles from under the wings. A microscope slide was then placed on top of the fly, sealing the fly between the slide and the coverslip. Once sealed, each fly was imaged immediately (Vagnoni et al. 2016; Vagnoni and Bullock 2016; Vagnoni and Bullock 2018; Mattedi et al. 2022)

To image the fly, the slide was orientated with the coverslip (and wings) closest to the objectives. The 10x objective was initially used to locate the fly and check for any damage on the wings of body of the fly. If damage was found, the fly was discarded. Acquisition mode was selected on the imaging software to select for the correct lasers needed depending on the fluorescent reporters expressed. Exposure time and laser power was adjusted accordingly.

2.7 Microscopy

The Zeiss Cell Observer spinning disc confocal microscope was used to image all experiments. Maximum disc rotation speed was 5000 rpm and image acquisition done using Zen 3.1 (blue edition), 2019 and image quantification was performed using ImageJ version 1.52p. For quantification, microscope settings were kept the same for

each sample. Exposure time was 200 ms at 30% intensity, laser power was 50% and 86% for green and red, respectively, magnification was 63x. Samples were imaged down the 1.4 Axiocam 503 Zeiss microscope camera and images analysed using ImageJ version 1.53f51 Java 1.8.0_172, brightness intensity was 38 and contrast intensity was 50 for green and red channel but 5 and -8 for the blue channel. A z-stack with 10 slices was used for each image as this incorporated any neurons present on different focal planes.

A time series on the Zeiss confocal microscope was performed to test for actin swelling migration. Time series lasted for 3 minutes, and images taken every 10 seconds. Maximum Disc rotation speed was 5000 rpm and image acquisition done using Zen 3.1 (blue edition), 2019. Image quantification was performed using ImageJ version 1.52p. Microscope settings were kept the same, as discussed above.

2.8 Analysis of neuronal and organelle morphology and biochemistry

2.8.1 Measuring fluorescence intensity in wing neurons

To analyse areas in the neuron in the fly wing, the line tool was selected on ImageJ 1.53f51 to measure the length of the scale bar. To enable all measurements on each image to be set the same (in μm), set scale was selected (*Analyze>Set Scale*, select 'Global' and enter scale bar measurements). To analyse mitochondria, Ca^{2+} levels and redox state in the neuron, regions of interest (ROIs) expressing high GFP levels were traced using the 'Freehand Selections' tool on the navigation menu. These regions were measured (*Analyze>Measure*) and the zoom function (*Image>Zoom>In(+)*) used, if required.

To measure fluorescence intensity 'Area' 'Mean grey value' and 'Integrated Density' parameters were selected (*Analyze>Set Measurements*, selecting 'Area', 'Mean grey value' and 'Integrated Density') and the ROI traced using the 'Freehand Selection' tool. The same area size for each ROI was also recorded that had no fluorescence, this was used to measure background levels. The results were copied to Microsoft Excel and the corrected total fluorescence (CTF) measured using the following formula: $\text{CTF} = \text{Integrated Density} - (\text{Area of selected ROI} \times \text{Mean fluorescence of background readings})$.

To measure fluorescence intensity of redox states, CTF levels were measured in the blue channel (405 nm) and the green channel (488 nm) for each image and the total average for each channel divided (405 nm / 488 nm).

2.8.2 Measuring fluorescent intensity in actin patches and endoplasmic reticulum

To analyse the fluorescence intensity in actin and ER patches, the scale was initially set in ImageJ (as described in **Section 2.8.1**). To analyse the fluorescent levels, an alternate method of analysis was used as there was only one ROI in each wing image. To measure fluorescence intensity, the line tool was used to draw a segmented line from the edge of the cell body to the end of the axon in the red channel image. This line was defined as the ROI (*Analyze>Tools>ROI Manager* and press 'add') for the image. This was added to the green channel image and a background subtraction was performed (*Process>Subtract Background*) using a rolling ball axis of 80 pixels. The line width was adjusted to 30 px (*Image>Adjust>Line width*) and the profiled plotted (*Analyze>Plot Profile*). To calculate maximum fluorescence intensity (normalised to per μm) only, up to and including, the first 50 μm and plotted to create representative images. For actin patches, area under the curve (AUC) was calculated in the same way. A manual count of actin patches greater than 30 μm in length was measured. All data was copied over to Microsoft Excel.

2.8.3 Measuring neuronal morphology and actin patches

For cell body and axon count, these variables were manually counted based on visualising samples under the microscope. Proximal axon width, cell body width and length and the distance of the cell body from proximal axon swellings were measured using the line tool. Instead of freehand selection (as above), the length of the line was recorded for each variable per wing sample.

2.8.4 Quantifying mitochondria and peroxisome morphology and number

To analyse mitochondria and peroxisomes in the wing images, the line tool was selected on ImageJ and, as discussed above, the scale bar was set for μm measurements. All measurements were selected (*Analyze>Set Measurements*, selecting 'Area', 'Feret's Diameter' and 'Shape descriptors'). In each image, all mitochondria were traced and measured using the 'Freehand Selections' tool in the navigation menu, followed by *Analyze>Measure* and the zoom function

(*Image>Zoom>In(+)*), if required. All final measurements in the 'Results' sheet were copied to Microsoft Excel and an average of 'Area', Feret's Diameter' (depicted as 'Feret' on the results sheet) and 'Aspect Ratio' of all mitochondria for each sample was calculated. Feret's diameter is used as a measure of mitochondrial and peroxisome length as morphology may not be the same across all organelles. To measure the number of peroxisomes in each image, a manual count was recorded, and the total number of each organelle visualised in the axon of in each image. Data was plotted on Microsoft Excel.

2.9 Imaging of *in vivo* reporters for mitochondrial physiology

GCaMP specific to mitochondria (mitoGCaMP) can be achieved by fusing with an N-terminal mitochondrial targeting sequence (Smith et al. 2019). Glutathione and H₂O₂ levels can be measured by fusing either glutaredoxin (Grx) or oxidant receptor peroxidase-1 (Orp1), respectively, to mitochondria-specific roGFP2 and measuring the fluorescent ratio change between the blue (405 nm) and green (488 nm) channels, see **Chapter 5, Section 5.3** for more details.

2.10 Fluorescent recovery after photobleaching

2.10.1 Imaging actin in actin patches

Fluorescent recovery after photobleaching (FRAP) is used to measure molecular diffusion in cells and is performed by photobleaching specific proteins in a certain region within the cell and measuring the rate at which the bleached molecules are replaced with unbleached molecules. The recovery rate reflects the rate of movement of the fluorescently-tagged molecule at that specific region in the cell (Jacobson et al. 1976; Schlessinger et al. 1976). For this project MARCM clones were expressed at 21 days post eclosion (d.p.e.) GFP-tagged beta actin region-of-interest was bleached at 5 seconds in my actin swellings at the distal tip of dissected wings. After optimisation, a FRAP cycle of 57 seconds total duration was used; x2 pre-bleached images taken every 1.295 seconds, x5 images during each bleach cycle taken every 1.295 seconds and finally x10 images taken every 5.295 seconds post bleach. Pre- and post-bleached images were imaged at 52% laser intensity at 488 nm and bleached images at 73% laser intensity at 488 nm. FRAP experiments were bleached and imaged on the Leica SP8 Confocal Microscope, Leica Application Suite (LAS)-X Core 3.5.7_23225 2020.

2.10.2 Analysing actin in actin patches

The scale was set, as described in **Section 2.8.1**, and integrated area was selected (*Analyze>Set Measurements*, selecting 'Integrated density'). Pre-bleached and post-bleached images were opened on ImageJ (not bleached images as these were black images) and a ROI within the bleached region was selected and defined (*Analyse>Tools>ROI Manager* and press 'add'). For all images per wing, the defined ROI was kept the same. Starting with the pre-bleached images, the defined ROI was measured (*Analyse>Measure*) for both pre- and post-bleached images in sequential order. The same ROI was measured in an area with no fluorescence to measure background levels and the results sheet plotted on Microsoft Excel.

In order to analyse FRAP data and determine whether the fraction was mobile or immobile, several calculations on Microsoft Excel were made: the half time of recovery ($t_{1/2}$) and the immobile and mobile fractions. $t_{1/2}$ is the time taken for recovery from the bleach timepoint (t_0) to the point where the fluorescence intensity reaches half of the final recovered intensity. The half time of Fluorescence Intensity ($F_{1/2}$) corresponds to $t_{1/2}$, and $F_{1/2} = (F_E - F_0) / 2$ where F_E and F_0 refers to the end and start of recovered intensity (post-bleach) respectively. To calculate the mobile fraction, the total fluorescent intensity levels were taken from the recovery intensity, mobile fraction = $(F_E - F_0) / (F_1 - F_0)$, where F_1 refers to the initial (pre-bleach) fluorescence intensity, and the immobile fraction is the remaining fraction, therefore, immobile fraction = $1 - \text{mobile fraction}$ (**Figure 2.3**).

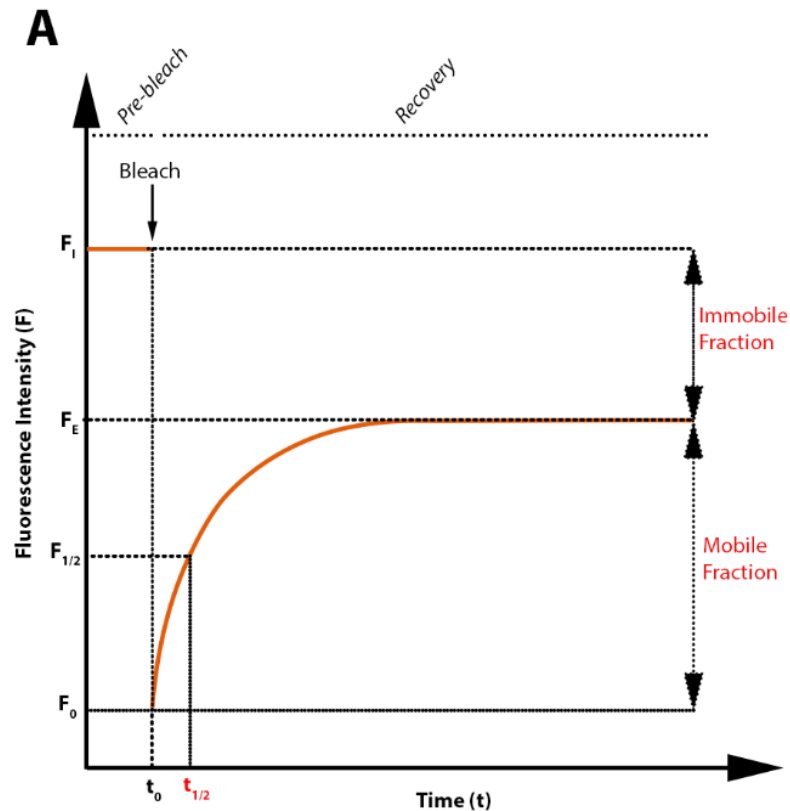


Figure 2.3 A recovery FRAP curve. The FRAP curve was used to measure the mobility of the fraction. Image adapted from Ishikawa-Ankerhold et al. (2012) (Ishikawa-Ankerhold et al. 2012).

2.11 Statistical analysis

All data was analysed, and graphs were produced using GraphPad Prism version 8.0.2 (263). First, data was tested for normality using the D'Agostino-Pearson normality test, to test for discrepancies from a Gaussian distribution. For normal data a 2-way analysis of variance (ANOVA) or unpaired two-tailed t tests statistical analysis were used, and Bonferroni, Šídák and Tukey *post hoc* tests were used to determine significance between groups. For non-parametric data Kruskal-Wallis or Mann-Whitney U tests were used.

3 Cdk12 controls proximal axon width, maintains neuronal number, and is localised to the cell body

3.1 Abstract

The proximal axon is a specifically-ordered region in the neuron, located in close proximity to the cell body and contains the AIS. The AIS is responsible for action potential initiation but also acts as a barrier between the axon and somatodendritic regions and its function is perturbed in several neurodevelopmental and neurodegenerative disorders. The structure of the proximal axon has been found to have a number of unique or differentially expressed molecules such as ankyrinG, actin and an abundance of sodium and potassium channels. However, how this region develops and maintains this specificity remains unclear. It is also unknown as to how the barrier develops and is maintained. Finding new molecules that control the structure and function of this region may aid our understanding of these processes. Therefore, an unbiased genetic screen was previously performed in the Smith lab to find such molecules, and mutant 6757 was uncovered as a novel regulator of proximal axon size (Smith 2019). Through whole genome sequencing it was discovered the causative mutation was likely in *Cdk12*. In this chapter, I have shown that loss of *Cdk12* causes age-dependent proximal axon swelling and caused a reduction in neuronal survival at later time points. The mutant failed to complement a deficiency of the region and re-expression of *Cdk12* rescued this phenotype, confirming *Cdk12* to be the causative gene. In addition, I have shown that Cdk12 is localised to the cell body of neurons. We therefore confirm that Cdk12 is a new molecule involved in the maintenance of the proximal axon which may be implicated in neurodegenerative diseases.

3.2 Introduction

The AIS is a specialised region located between the somatodendritic and axonal regions in the neuron and functions in action potential initiation and neuronal polarity (Palay et al. 1968). In order to maintain neuronal polarity, the AIS consists of a specialised membrane and protein complex that function as a cargo transport filter and diffusion barrier (Winckler et al. 1999; Nakada et al. 2003; Song et al. 2009; Brachet et al. 2010; Sun et al. 2014) The structure of the AIS is comprised of several components including ankyrinG, spectrins, neurofascin and an abundance of sodium and potassium channels (**Chapter 1**). Some molecules are partially important for structural integrity such as ankyrinG which binds directly to spectrin rings, hence ablation of ankyrinG causes a loss in the majority of other AIS residing proteins (Zhou et al. 1998; Jenkins and Bennett 2001; Hedstrom et al. 2008). AnkyrinG is also important to bind components to the cytoskeleton, (Hedstrom and Rasband 2006; Trunova et al. 2011) cytoskeleton architecture is also crucial in this region, serving as vesicle filter and diffusion barrier (Winckler et al. 1999; Nakada et al. 2003; Song et al. 2009; Al-Bassam et al. 2012).

There is very little known about the AIS in age-related neurodegenerative diseases but new evidence has reported that the AIS length and number are significantly reduced when in close proximity to A β plaques (Palop and Mucke 2009). Several mechanisms such as neuronal death, neuronal displacement and AIS barrier disruption have been proposed indicating that that changes/loss of the AIS could contribute to impaired brain function, seen in patients with neurodegenerative diseases (León-Espinosa et al. 2012; Marin et al. 2016). Therefore, a greater understanding of the AIS at a basic level may one-day lead to mechanistic insights in pathological states.

Although we have discovered major proteins that make up the AIS, relatively little is known about the mechanisms that control AIS development and maintenance. Therefore, previous work in the lab sought to find more molecules that function in the AIS. Previously in the Smith lab, an unbiased forward genetic screen uncovered other molecules that may maintain the AIS. Briefly, flies were fed EMS and this caused random mutagenesis throughout the genome. Hundreds of flies were screened for deficits in AIS size or morphology and a candidate-of-interest was revealed, which showed large swellings in the proximal axon. Following whole genome sequencing a mutation was identified in *Cdk12*.

In *Drosophila*, Cdk12 binds to the C-terminal domain of RNA Polymerase 2 and hence controls transcription and pre-mRNA processing (Egloff and Murphy 2008). Cdk12 associates with CyclinK and regulates transcription in both humans and *Drosophila* (Bartkowiak et al. 2010). Cdk12 is known to regulate the transcription of, not only, several long DNA repair genes, including *BRCA1* and *BRCA2*, *ATR*, and *ATM*, but also, genes involved in the homologous recombination repair pathway (Blazek et al. 2011; Bajrami et al. 2014; Ekumi et al. 2015; Juan et al. 2016; Popova et al. 2016; Zhang et al. 2016b; Tien et al. 2017; Chirackal Manavalan et al. 2019). Therefore, the depletion/inhibition of Cdk12 leads to DNA damage, genome instability, DNA replication defects and alterations in G1/S progression and also generates a non-functional homologous recombination pathway (Joshi et al. 2014; Lei et al. 2018). In addition to its canonical role, we suggest that there may be undiscovered function of this protein in AIS maintenance. Interestingly, another Cdk, Cdk5 had been reported to regulate size of the AIS in *Drosophila* (Trunova et al. 2011) and the sorting of axodendritic cargo *in vitro* (Klinman et al. 2017). It remains to be known whether Cdk12 plays a complementary role in this process. In this Chapter we aim to use the fly to examine age-dependent changes of *Cdk12* mutants in proximal axon maintenance.

Most work on the AIS has been carried out in mammals, therefore little is known about the structure of the AIS in *Drosophila*. The AIS has a specific structure compared to the rest of the neuron (**Chapter 1**) The differences and similarities between *Drosophila* AIS to human AIS structure is shown in **Appendix 2**. The specific mammalian and *Drosophila* orthologue for the AIS components (ankyrin G, actin, spectrins, and sodium and potassium channels), DRSC integrative ortholog prediction tool (DIOPT) score and AIS specific information is given for each molecule. Note: the DIOPT score identifies the disease-relevant human gene-to-fly gene relationships (Larkin et al. 2021). In this case, the best homologue score of human proteins is 15, the higher the score the more conserved the sequence is between *Drosophila* and human. We find that the vast majority of AIS components are highly conserved (**Appendix 2**). Therefore, we believe that the fly model would be an appropriate system to study the AIS.

3.2.1 Aims and objectives

The aim of this result chapter is to determine if the loss of Cdk12 contributes to proximal axon maintenance *in vivo*.

- My first objective was to use clonal *Drosophila* genetic approaches to determine the time course of proximal axon swelling and neurodegeneration in a *Cdk12* mutant background. Since this gene is essential, the quantification of neuronal number and AIS size will be achieved in homozygous null mutant MARCM clones, labelled with fluorescently encoded genetic markers, to give single axon resolution under the confocal microscope (**Chapter 2**). Only the sparse fluorescently labelled cells will be null for the gene, the rest of the animal will be WT or heterozygous.
- My second objective will be to confirm that *Cdk12* is in fact our gene-of-interest. Unbiased genetic screening using EMS induces multiple random mutations into the genome. Therefore, it is possible that other mutations of the chromosomal arm could be the causative mutation. To elucidate this I used a deficiency in which *Cdk12* is entirely deleted to test whether the phenotype of the EMS mutant can be complemented when crossed together and perform several rescue experiments to reintroduce *Cdk12* into null clones to see if the phenotype can be rescued.
- Lastly, I aimed to discover where *Cdk12* is localised in the cell by expressing a GFP tagged version of the protein in neuronal MARCM clones.

3.3 Experimental Design

Fly stocks needed to generate MARCM clones were stored at 20°C and maintained under standard conditions with specified media (**Chapter 2, Section 2.1**). MARCM crosses were set up so that clones of the wing could be visualised using a Tomato fluorophore. MARCM clones were labelled using the Gal4/UAS system, see **Chapter 2** for details. MARCM clonal genetics is described in **Chapter 2, Section 2.5**. For transgenes, see **Appendix 3** and for fly stocks used see **Appendix 1**. MARCM crosses were set at 25°C with a 12-hour light-to-dark ratio. Desired progenies with either *Cdk12*^{-/-} clones or WT clones were selected and aged.

For the time course experiment the *Cdk12* null mutant was compared to control at 1, 7, 14, 21, 28 and 35 d.p.e. Genetic crosses are depicted in **Figure 3.1**. N=10 for all samples for day 1, 7 and 21, N=19 and N=26 for control and mutant, at day 14 N=14 for day 35. At each time point both wings were dissected (**Chapter 2, Section 2.6**)

and imaged using the Zeiss Spinning Disc confocal microscope (**Chapter 2, Section 2.7**).

Following initial characterisation rescue experiments were then completed to confirm that *Cdk12* was the causative gene. This first involved rescue using a fly stock carrying gDNA of the region covering *Cdk12*, day 21 and 35 p.e time points were recorded. To produce this fly stock, I acquired a BAC construct (#CH322-59L20, P[acman] Resources), transfected it in *E. coli* culture, plated this onto agar plates with ampicillin antibiotic (100 µg/ml) and selected for resistance. Plates were sent for recombineering into *Drosophila* embryos (BestGene Inc.). Larvae were selected and the chromosome containing the BAC balanced over CyO on the second chromosome. Secondly, we performed a complementary DNA (cDNA) rescue, with the *5xUAS-Cdk12 Drosophila* stock (in house), at both 13 and 21 d.p.e. Genetic crosses for rescue experiments at shown in **Figure 3.2**. For gDNA Rescue, N=10 and N=11 were collected at 21 d.p.e. for control and mutant, respectively and N=8 for 35 d.p.e. for both groups. For *5XUAS-Cdk12* rescue, N=10 were used for control and mutant at 13 d.p.e. and N=13 and N=10 for the 21 d.p.e. time point.

To localise and visualise Cdk12 in glutamatergic sensory neurons, we expressed a GFP-tagged version of Cdk12, *5xUAS-Cdk12::GFP* (in house) in neuronal clones, using an in house *Drosophila* stock and imaged the fly wings at 21 and 35 d.p.e., see **Figure 3.3** for the genetic cross.

Figures were designed on Adobe Photoshop and data analysed on GraphPad Prism, 2way ANOVA statistical analysis and Bonferroni *post hoc* tests were used to determine significance (**Chapter 2, Section 2.11**).

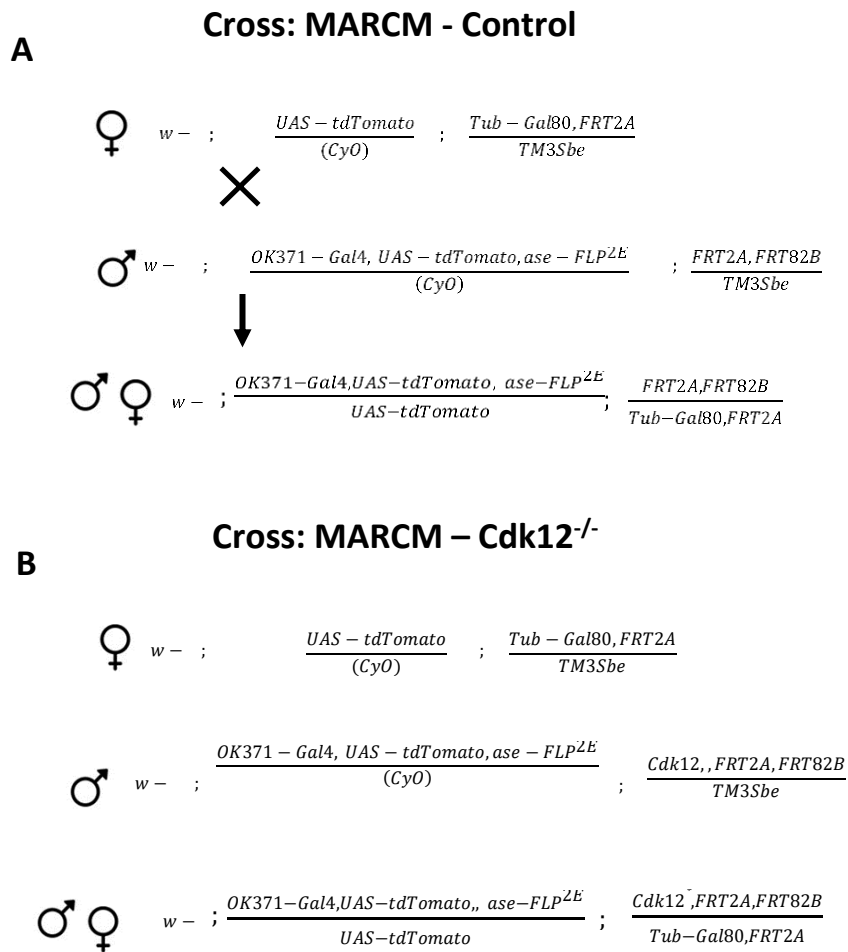
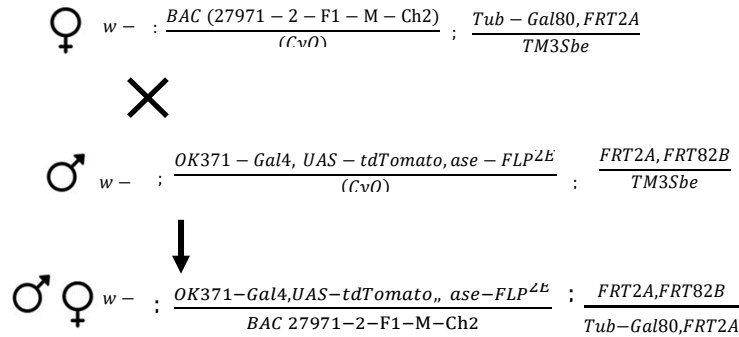
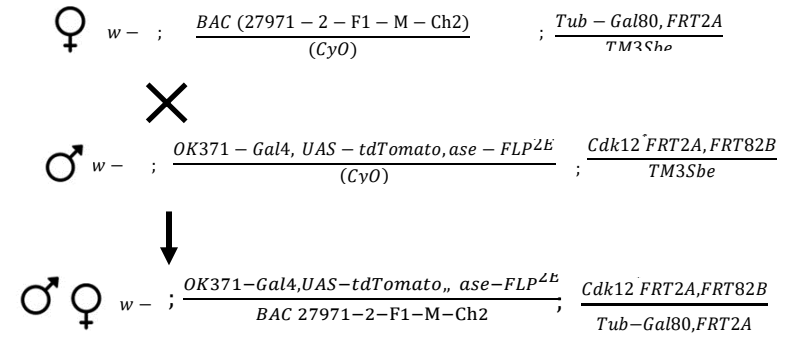


Figure 3.1 Fly crosses to generate WT and *Cdk12^{-/-}* MARCM clones. To generate WT clones for control groups our tester line, including driver, red neuronal marker, flippase and FRT site, and the Gal4 repressor Tub-Gal80 was crossed to flies containing a complementary FRT site (A). The tester line was also crossed to flies containing a mutant FRT chromosome to generate *Cdk12^{-/-}* neuronal clones (B).

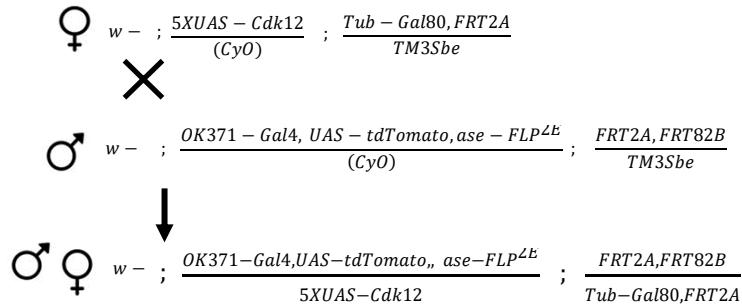
A Cross: BAC (27971-2-F1-M-Ch2) - Control



B Cross: BAC (27971-2-F1-M-Ch2) - *Cdk12*^{-/-}



C Cross: 5xUAS-*Cdk12* - Control



D Cross: 5xUAS-*Cdk12* - *Cdk12*^{-/-}

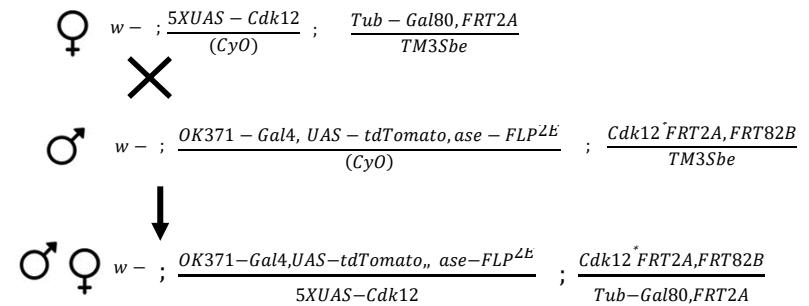


Figure 3.2 Fly crosses to generate rescue lines in MARCM clones. For gDNA rescue crosses, gDNA was integrated onto the chromosome II and a stock made with a repressive element and FRT site on III and crossed to our control (A) and *Cdk12*^{-/-} mutant (B) tester lines. For *UAS* based rescue crosses, *UAS-Cdk12* was integrated onto the chromosome II and a stock made with a repressive element and FRT site on III and crossed to our control (C) and *Cdk12*^{-/-} mutant (D) tester lines. Non rescue control crosses are depicted in **Figure 3.1**.

Cross: GFP-tagged Cdk12 - Control

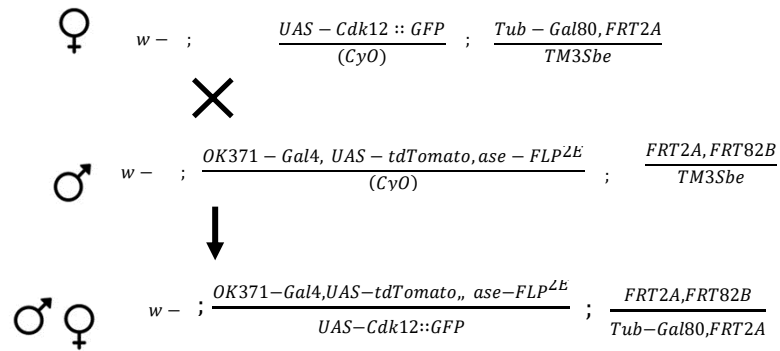


Figure 3.3 Fly crosses to generate a Cdk12 localisation in neuronal MARCM clones. GFP-tagged Cdk12 was integrated on the second chromosome in a MARCM control background.

3.4 Results

3.4.1 Sequencing and mapping of the *Cdk12* mutation

Mutant 6757 was uncovered in a previous unbiased genetic screen using the chemical mutagen EMS (Smith 2019). Whole genome sequencing, done previously in the lab, uncovered a predicted deleterious mutation in *Cdk12* that we believed to be responsible for the axonal swelling phenotype.

EMS induced a nucleotide mutation which lead to a frameshift mutation in the amino acid sequence followed by a premature stop codon (**Figure 3.4A**). The premature stop codon occurs towards the C-terminal domain of the *Cdk12* gene. This may therefore suggest that the protein is expressed but isn't functional or acting as a dominant negative. To test for this reverse transcription-polymerase chain reaction and western blot could be performed to detect mRNA and protein levels. The mutation in the gene was a deletion of ATCACGACTTGATGGGTC nucleotide sequence. See **Appendix 4** for the sequencing data.

In *Drosophila*, The *Cdk12* protein is composed of 1157 amino acids and the gene located at position 21516.5k-21522.5k on the 3L chromosome. *Cdk12* has one key domain, the protein kinase domain, located towards to the C-terminal, between 804 and 1098 amino acids. It is therefore possible that *Cdk12* or specifically the kinase action of *Cdk12* may impact proximal axon size. However, EMS used at our standard doses typically causes many mutations along the chromosome. Although no other random mutations uncovered were as severe as the one found in *Cdk12* it is entirely possible that they may instead cause our phenotype of interest.

I discovered that *Cdk12*^{-/-} was lethal and the mutant chromosome always present over a balancer chromosome in my stocks. Therefore, we first performed complementation analysis as a first experiment to provide genome mapping evidence that *Cdk12* was linked to lethality. I crossed a deficiency line (Df3Lexe19065) (Parks et al. 2004) located at position 21517k-21523k in the genome (to eliminate the majority of the *Cdk12* gene) with our *Cdk12*^{-/-} flies or control. Df3lexe19065 failed to complement *Cdk12*^{-/-} (**Figure 3.4B**), strongly suggesting that *Cdk12* is in fact the causative gene.

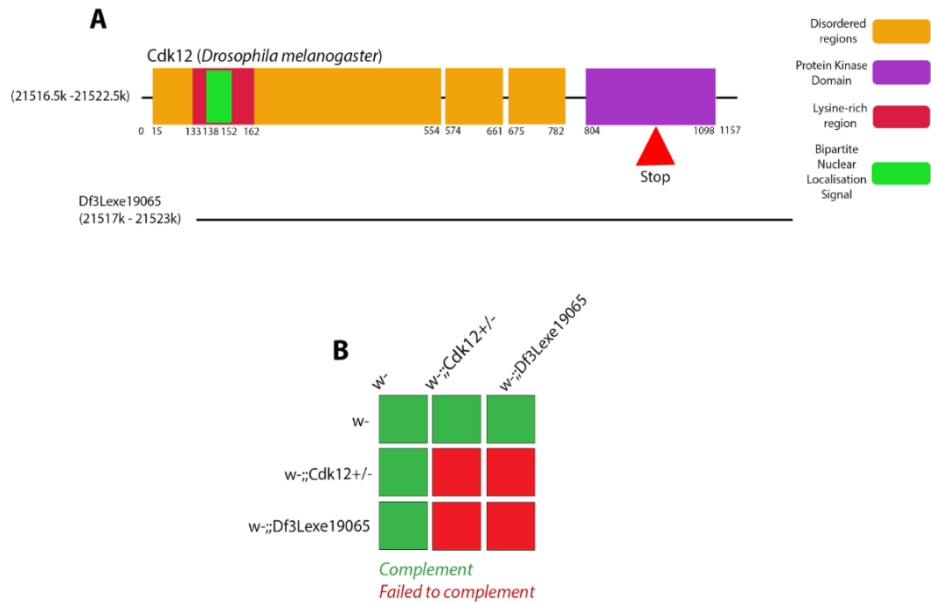


Figure 3.4 Sequencing and mapping of the *Cdk12*^{-/-} mutation. Cdk12 is composed of 1157 amino acids. The disordered regions (orange), the protein kinase domain (purple), lysine-rich region (dark pink) and bipartite nuclear localisation signal (green) and positions on the protein sequence are represented. Position 945 within the protein kinase domain is the frameshift mutation that caused a premature stop codon and resulting null allele (red arrow). The deficiency line, Df3Lexe19065, overlaps with only the *Cdk12* gene and is a 6,378 base deletion (A) (The UniProt Consortium 2021). Complementation showed that the deficiency line crossed with *Cdk12*^{+/-} did not produce viable offspring (failed to complement) (B).

3.4.2 Cdk12 controls proximal axon width

We investigated whether the loss of Cdk12 could affect the morphology of the neurons in the wing at young, intermediate, and old ages. Observation of fluorescent micrographs identified atypical proximal axon swellings from 7-21 d.p.e. in *Cdk12^{-/-}* wings. No proximal axons swellings were present at 28 and 35 d.p.e., but increased swellings were seen throughout the axon (**Figure 3.5A**). Proximal axon width was measured, from 1-35 d.p.e., at the largest point in the axon, closest to the cell body. A 2-way ANOVA showed both a genotype specific difference ($F_{1,131} = 32.86$, $p < 0.0001$) and an age specific difference ($F_{5,131} = 3.67$, $p < 0.01$). Bonferroni *post hoc* tests revealed swellings increased significantly from 1–21 d.p.e. ($p < 0.0001$) in the mutant neurons. In the *Cdk12^{-/-}* null clones, proximal axon width was more than double those of WT neurons at 21 d.p.e. ($p < 0.001$, **Figure 3.5B**) indicating that Cdk12 controls the width of the proximal axon.

3.4.3 Cdk12 maintains neuronal number

To determine neuronal survival during ageing, axons were quantified in the proximal wing, at the costal and L1 vein join. From 7 d.p.e., axon number decreased in the *Cdk12^{-/-}* clones (**Figure 3.5C**) and significant differences between genotypes were observed ($F_{1,137} = 32.43$, $p < 0.0001$). Bonferroni *post hoc* tests revealed a significant decrease, from 1-28 d.p.e. ($p < 0.01$) in axon number in mutant neurons. At 28 d.p.e., axon number decreased significantly by ~2fold in *Cdk12^{-/-}* ($p < 0.05$). To investigate whether cell body death occurs before or after axonal death, cell body number was also recorded from 14-35 d.p.e. (**Figure 3.5D**). A 2-way ANOVA revealed a significant difference between genotypes ($F_{1,74} = 25.55$, $p < 0.0001$) but not age. *Post hoc* tests showed that cell body number significantly decreased by ~2fold at 21 d.p.e. ($p < 0.01$) and 35 d.p.e. ($p < 0.05$). This suggests that cell body and axonal death occurred simultaneously. Reduction in axon and cell body number, in the mutant, thus suggests that Cdk12 is involved in maintaining neuronal survival in the fly.

3.4.4 Cdk12 has little effect on neuronal cell body size

To determine if *Cdk12* ablation had an effect on neuronal cell body morphology, the cell body width and length were measured. A 2-way ANOVA revealed no significant difference between genotype/age in cell body width (**Figure 3.5E**, $p = \text{non-significant}$ (*ns*)) or length (dendrite to axon hillock) (**Figure 3.5F**, $p = \text{ns}$). This suggests that Cdk12 plays a role to limit size specifically in the proximal axon region.

3.4.5 Cdk12 has no effect on the length of the proximal axon.

We investigated whether *Cdk12* ablation had an effect on the distance between the largest part proximal axon and the start of cell body. A 2-way ANOVA showed no significant differences between genotype/age (**Figure 3.5G**, $p=ns$), suggesting that *Cdk12* controls proximal axon width at a specific part of the axon, approximately 8 μm away from the start of the cell body.

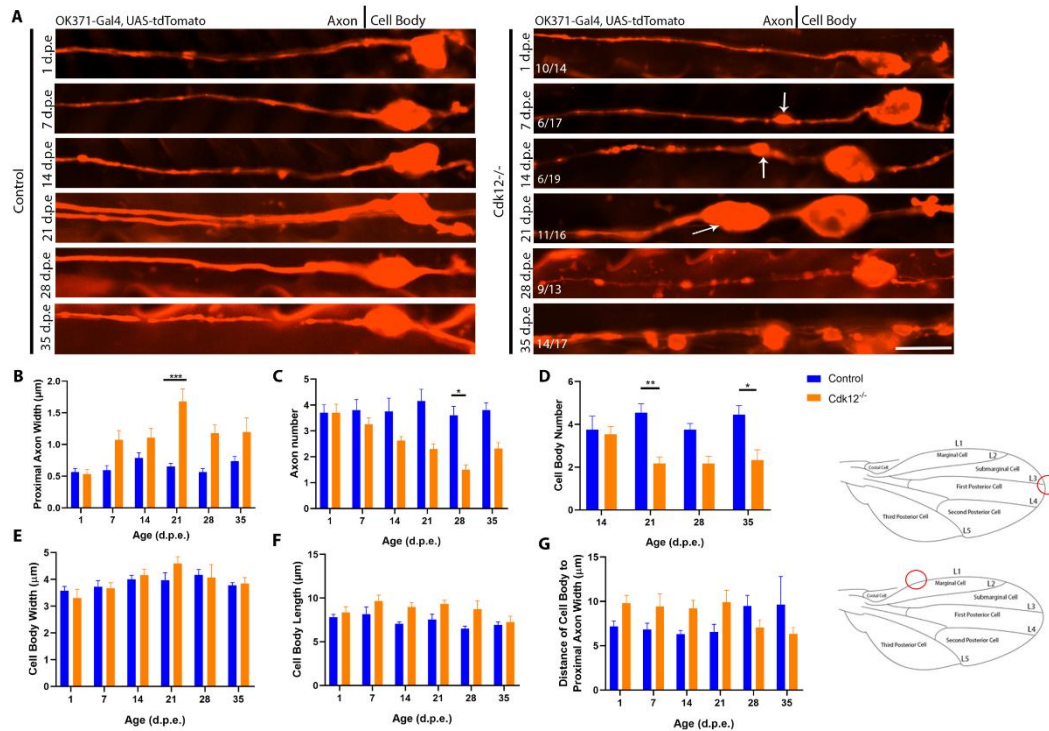


Figure 3.5 *Cdk12* regulates proximal axon swelling and neuronal death. Proximal Axon swelling was seen in the *Cdk12* null clones and peaked at 21 d.p.e. (see white arrows). Neurodegeneration was observed at 35 d.p.e. (A) in the mutant but not in the control. Proximal axon width (B), axon (C), cell body number (D), cell body width (E), length (F), and the distance of the cell body to the proximal axon swelling were recorded (G). Data was analysed using two-way ANOVA and significant differences annotated as $p < 0.05^*$, $p < 0.01^{**}$ and $p < 0.001^{***}$ between genotypes compared to the control. Data was analysed with Bonferroni *post hoc* test. Graphs are expressed as Mean \pm SEM. Scale bar was 10 μm . Axon number was recorded in the L1 vein, but all other variables were recorded at the distal tip, see red circles on wing images.

3.4.6 Rescue of the *Cdk12*^{-/-} phenotype

As previously stated, the *Cdk12*^{-/-} mutant was generated by EMS, a chemical mutagen that induced random mutations along the chromosome arm. To confirm whether *Cdk12* was the causative gene we performed two rescue experiments. We used flies harbouring a genomic BAC construct (20,294bp) to ubiquitously express *Cdk12* and we expressed *Cdk12* cDNA specifically in our mutant clones using the Gal4/UAS system.

Swellings were observed in the proximal axon in both *Cdk12*^{-/-} mutant neurons (**Figure 3.6A**). These swellings were partially rescued by re-expression of *Cdk12* by a genomic approach (**Figure 3.6B**) and were fully rescued by expression of *Cdk12* cDNA (**Figure 3.6C**).

As found previously, a significant difference in the width of the proximal axon was observed between genotypes ($F_{1,79} = 24.24$, $p < 0.0001$) in *Cdk12*^{-/-} mutant neurons ($p < 0.01$) but only partially in mutant neurons expressing *Cdk12* through BAC integration (**Figure 3.7A**, $p = ns$). A 2-way ANOVA revealed no significant differences between genotype or age in axon (**Figure 3.7B**, $p = ns$) and cell body number (**Figure 3.7C**, $p = ns$) at 21 and 35 d.p.e. There were significant increases between genotypes in the width of the cell body ($F_{1,80} = 31.74$, $p < 0.0001$). Bonferroni *post hoc* tests showed a significant increase in cell body width in neurons lacking *Cdk12* ($p < 0.05$) at 21 d.p.e. Cell body width was also significantly increased in gDNA-expressing neurons, but instead at the later time point of 35 d.p.e. (**Figure 3.7D**, $p < 0.01$). There were significant differences between genotypes in cell body length ($F_{1,80} = 90.18$, $p < 0.0001$). *Post hoc* tests showed an increase in cell body length in *Cdk12*^{-/-} mutant neurons at 21 ($p < 0.0001$) and 35 d.p.e. ($p < 0.05$). In gDNA-expressing mutant neurons, the same was also seen at 21 ($p < 0.0001$) and 35 d.p.e. (**Figure 3.7E**, $p < 0.01$). No significant difference was seen in the distance of the cell body to the proximal axon swellings (**Figure 3.7F**, $p = ns$). Taken together, these data show a partial rescue by reintroducing the gene using a genomic approach.

Ubiquitous gDNA expression may not be sufficiently high to rescue in terminal differentiated neuronal clones. We next tested if the *Cdk12*^{-/-} phenotype could be rescued with *Cdk12* cDNA. We expressed 5xUAS-*Cdk12* into *Cdk12*^{-/-} clones and WT control clones in glutamatergic sensory neurons. There were no significant differences between the size of the proximal axon at 13 and 21 d.p.e. in neurons expressing *Cdk12* compared to control (**Figure 3.8A**), indicating a complete rescue.

Axon (**Figure 3.8B**) and cell body number (**Figure 3.8C**) also remained unchanged suggesting neuronal survival was also rescued. Cell body width (**Figure 3.8D**), length (**Figure 3.8E**), and the distance of proximal axon swellings to the cell body (**Figure 3.8F**) were also unaffected, indicating that *Cdk12* is the causative gene controlling proximal axon size and maintaining neuronal survival. Interestingly, the overexpression of *Cdk12* in WT clones did not have the opposite effect and reduce the width of the proximal axon.

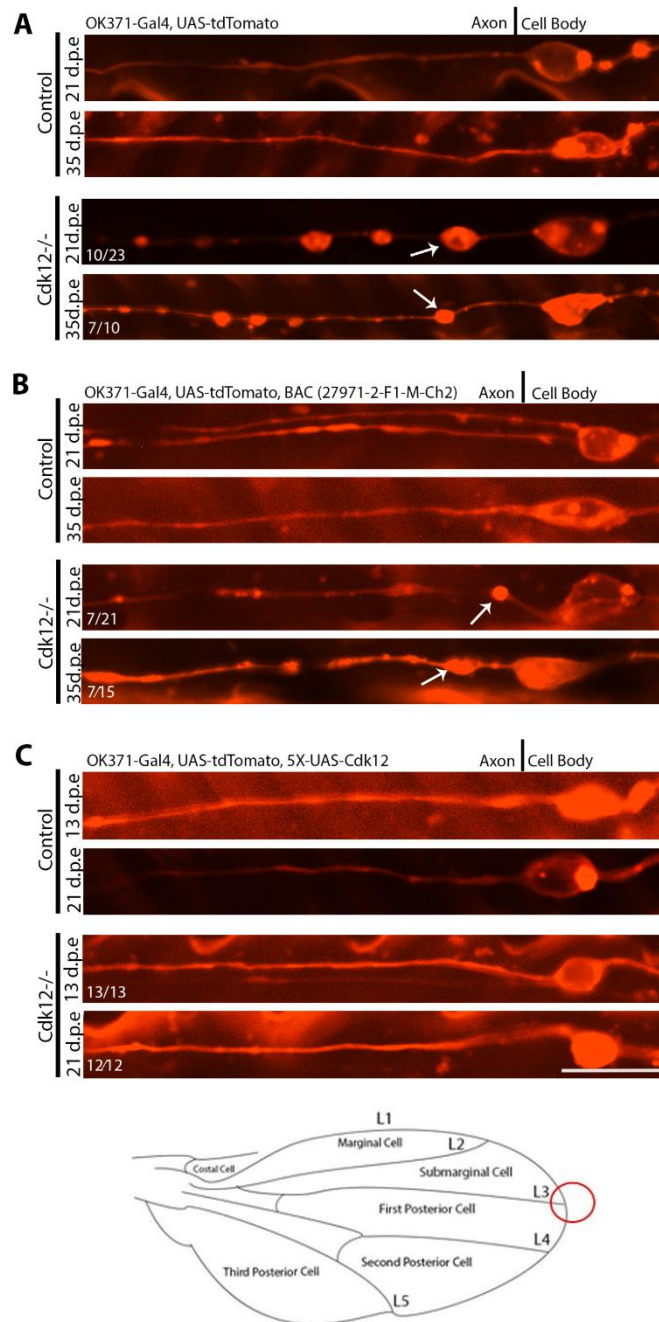


Figure 3.6 Cdk12 expression rescues the null phenotype. Similar to the control (A), swelling and neurodegeneration was seen in the gDNA BAC (27971-2-F1-M-Ch2) rescue flies at 21 and 35 d.p.e., see white arrows (B). However, expression of 5xUAS-Cdk12 rescued the swelling and neurodegeneration at 13 and 21 d.p.e. (C). Scale bar was 10 μ m. Cell bodies were imaged at the distal tip, see red circle in wing image.

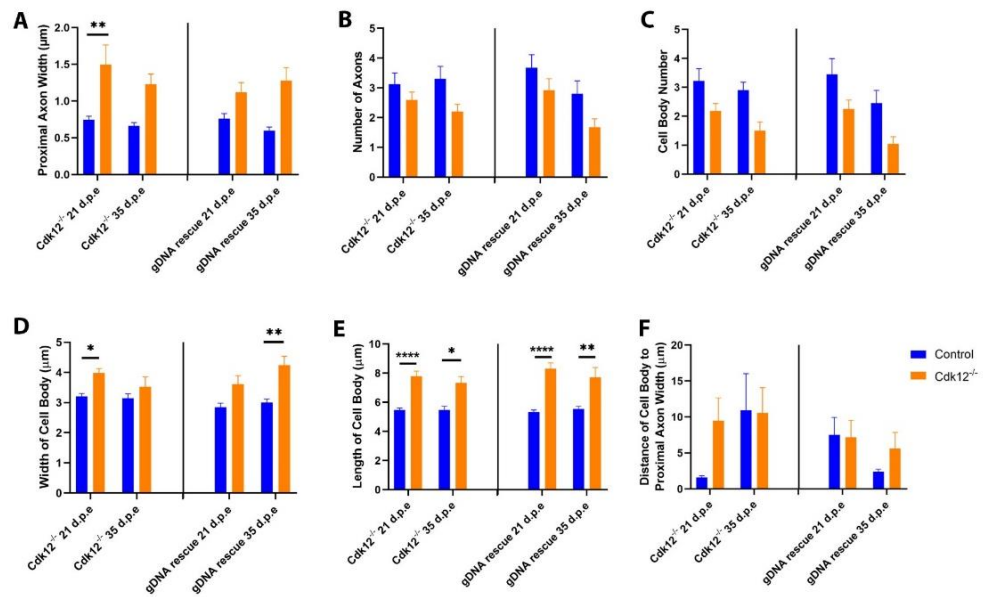


Figure 3.7 Reintroduction of *Cdk12* by gDNA partially rescued the mutant phenotype. Proximal axon width (A), axon (B), cell body number (C), cell body length (D), cell body width (E), and distance of the proximal axon width (F) from the cell body parameters were measured. Data was analysed using two-way ANOVA and significant differences annotated as $p < 0.05^*$, $p < 0.01^{**}$ and $p < 0.0001^{****}$ between genotypes and compared to the control. Data was analysed by Bonferroni *post hoc* test. Graphs are expressed as Mean \pm SEM.

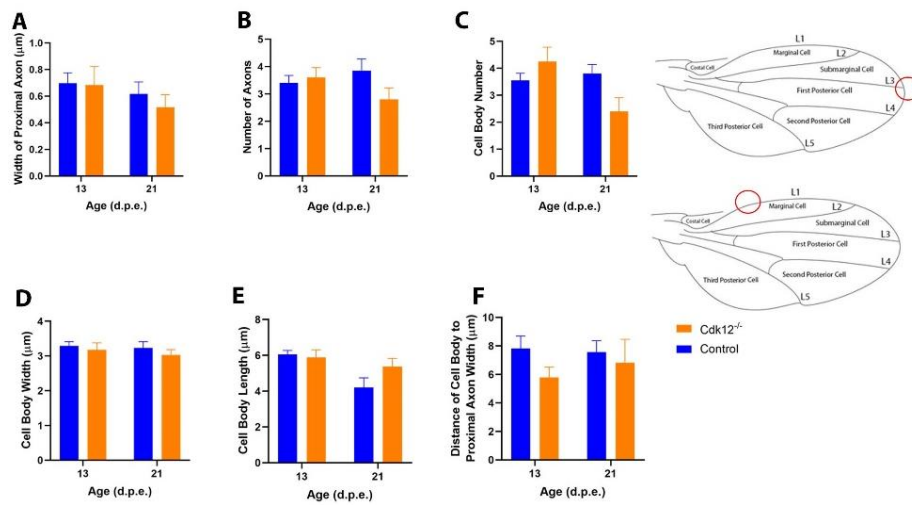


Figure 3.8 Expression of *5xUAS-Cdk12* rescued the *Cdk12*^{-/-} phenotype. Proximal axon width (A), axon (B), cell body number (C), cell body length (D), cell body width (E), and distance of the proximal axon width (F) from the cell body parameters were measured. Graphs are expressed as Mean \pm SEM. Statistical analysis could not be performed as results for Control 21 d.p.e. are pending. Axon number was recorded in the L1 vein, but all other variables were recorded at the distal tip, see red circles on wing images.

3.4.7 Cdk12 is localised to the cell body

To identify the location of Cdk12 in the neuron, the next step was to visualise and localise Cdk12 in the glutamatergic neurons in the control and *Cdk12*^{-/-}, in a MARCM genetic background, (**Figure 3.3**). For this a transgenic fly carrying UAS-*Cdk12::GFP* (made previously) was crossed into our tester lines. Cdk12 is shown to be localised to the cell body in glutamatergic neurons at 21 and 35 d.p.e., with the majority of fluorescent signal in the nuclear compartment, (**Figure 3.9**). This result gives an indication as to the region in which Cdk12 may function to maintain the proximal axon.

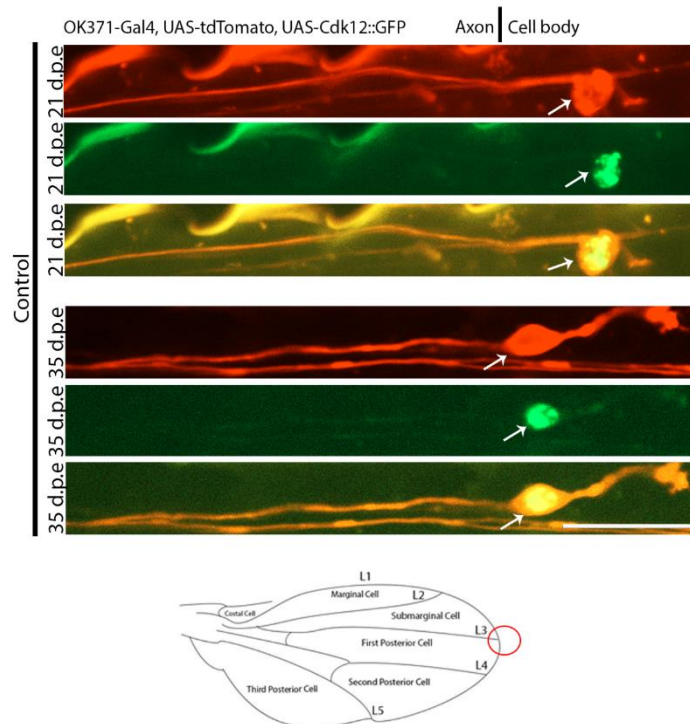


Figure 3.9 Cdk12 is localised to the cell body. Cdk12, tagged to GFP, was seen in the cell body (see white arrows) at both 21 and 35 d.p.e. Scale bar was 10 μ m. N numbers were represented in white. Cell body images were taken at the distal tip, see red circle on wing image.

3.5 Discussion

The unbiased genetic screen uncovered Cdk12 as having potential involvement in proximal axon maintenance (Smith 2019). When analysing the *Cdk12* null mutation in MARCM neuronal clones we found that Cdk12 limited axon width close to the cell body and maintained survival of glutamatergic neurons.

Null mutations in *Cdk12* caused an increase in the proximal axon width, at approximately 8 μm from the start of the cell body, in an age-dependent manner. A gradual increase in width was seen from 1-14 d.p.e. but a sharp rise was seen at 21 d.p.e. Loss of *Cdk12* had little, if any, effect of *Cdk12*^{-/-} on cell body size (width and length) which adds to our evidence that the phenotype is proximal axon specific. The overall difference in proximal axon size, is likely caused by dysregulation of AIS maintenance since the AIS is contained in this region. To address the question, we attempt to look at specific AIS markers in *Cdk12*^{-/-} clones (see the following Chapter). Unusually, loss of *Cdk12* also caused a decrease in the proximal axon width at very late stages. This could be due to a breakdown of the AIS region that occurs with the general degeneration seen. A possible explanation for degeneration could be due to calpain-mediated activation. Calpains are activated with Ca^{2+} influx at the start of neuronal death and cleave p35, a Cdk5 activator, to form p25 and p10, (Patrick et al. 1999). Calpain has also been shown to have a role in the breakdown of the ankyrin G/spectrin cytoskeleton in stroke victims (Siman et al. 1984; Schafer et al. 2009). Perhaps, calpains activate Cdk12 in addition to Cdk5, leading to a breakdown in the AIS region due to ankyrin/spectrin cytoskeleton collapse, as ankyrin is the key organiser in the structure of the AIS (Siman et al. 1984; Schafer et al. 2009). In these specific neurons AIS collapse may manifest through swelling and loss of structure. Interestingly, in mushroom body neurons loss of Cdk5 activity causes an overall decrease in AIS size without gross morphological changes in the neurons (Trunova et al. 2011). Further work could be to study calpain activity, Ca^{2+} dynamics and the interplay with Cdk5.

Proximal axon swelling could result in or manifest through the dysregulation of actin, which has been found to be abundant and disorganised in this region (Watanabe et al. 2012). This could impact on the barrier between somatodendritic and axonal compartments. Aberrant trafficking or reduced trafficking could then eventually cause neurodegeneration. I investigate this in the next chapter.

We observed that loss of *Cdk12* caused age-dependent neurodegeneration which may have triggered calpain activation, however the mechanism of cell death remains unclear. Cell death can generally occur by apoptosis or Wallerian degeneration (death in direction of axons to cell body) and genetic inhibitors could potentially be used to distinguish between the two. We suggest that cell death is likely to be apoptosis since axons and cell bodies die simultaneously and we conclude that *Cdk12* has a role in the maintenance of neurons rather than their development since neurons appeared morphologically like WT at early stages.

To confirm that loss of *Cdk12* caused the phenotype seen in mutant 6757 complementation and rescue experiments were performed. *Cdk12*^{-/-} failed to complement when crossed with a Deficiency of the region and the phenotype rescued when expressing the cDNA of *Cdk12* back into our null allele. This indicates that *Cdk12* is our gene-of-interest. Interestingly, rescue with gDNA only caused a partial rescue of the phenotype, however I predict that this was due to only one copy of the gene being restored. I anticipate that a gDNA duplication may have caused a full rescue, however no duplications for this region are currently existing.

Throughout this chapter, we used the MARCM genetic technique that allows for investigators to bypass lethality and allows for single cell resolution (Wu and Luo 2007). In this project, I focus on glutamatergic sensory neurons, in the L1 vein of the fly wing because the axons span the full length of the wing and can be easily (imaged and) analysed and proximal axon width measured. This technique could potentially be used in future analysis to see if our phenotype manifests in other neuronal sub-type clones within the central brain, through the use of other drivers. Although the variable architecture of neurons in the brain may make analysis difficult.

I also expressed a GFP-tagged version of the *Cdk12* cDNA into neuronal clones to elucidate the sub-cellular localisation of the translated protein. Data shows that *Cdk12* resides largely in the cell body with most in the nuclear compartment. Therefore, *Cdk12* could function as a transcriptional regulator and it is possible that differentially expressed genes may cause proximal axon swelling and neurodegeneration phenotypes. *Cdk12* is known to phosphorylate the C-terminal domain of RNA polymerase 2, contributing to transcriptional elongation (Egloff and Murphy 2008). Co-immunoprecipitation and RNA sequencing data could therefore be used to determine if AIS associated genes are preferentially targeted. On the other hand, we cannot rule out that *Cdk12* may be expressed in lower levels in the proximal axon

region of the cell. Such is that case for Cdk5, previously found to be involved in proximal axon barrier formation (Trunova et al. 2011). To determine this, an antibody would need to be produced to allow for detection of Cdk12 in this region, paired with high resolution microscopy. Antibody detection would also mitigate possible artefacts from overexpressing a tagged version of Cdk12.

3.6 Conclusion

An unbiased forward genetic screen uncovered *Cdk12* as the possible regulator of proximal axon size in adult neurons *in vivo*. Based on complementation analysis and rescue experiments we can confirm that *Cdk12* is our gene-of-interest. We further show *Cdk12* is localised to the cell body, which could indicate that the phenotype observed the null allele background may be caused by transcriptional dysregulation. Loss of this gene causes an age-dependent swelling of the proximal axon and neurodegeneration, and I can conclude that *Cdk12* is a novel limiter of proximal axon size and is essential to maintain neuronal integrity. It is likely that this gene alters the function of the AIS through interaction with specific AIS associated proteins or the actin filament network which is specialized in this region.

4 Cdk12 controls actin redistribution and filtration barrier in the neuron

4.1 Abstract

The AIS is important in action potential initiation and neuronal polarity. As a result, the AIS has a specialised structure consisting of several sodium and potassium channels, actin patches, and key scaffold proteins such as ankyrin G and spectrins strengthening the region. I have previously shown that Cdk12 maintains proximal axon width and controls neuronal survival but exact determination of how this region is maintained is unknown. We hypothesised that Cdk12 could be specifically controlling the AIS region. Therefore, our next goal was to find a reliable marker for the AIS in wing neurons and tested several markers for their ability to localise to that region. However, most markers investigated did not consistently label the AIS. Actin however was notably absent from the axon and AIS allowing us to visualise the separation with the soma compartment. In this chapter, I have shown that loss of *Cdk12* causes F- and β -actin redistribution into swellings within the proximal axon. Interestingly, β -actin molecules with these accumulations were highly diffusible and motile. Based on these observations, we further investigated whether Cdk12 regulates actin barrier formation. Upon *Cdk12* ablation, peroxisomes (used as specific organelle marker of the soma) were no longer restricted to this compartment and entered the axon. Together, these studies show that Cdk12 is likely required for AIS maintenance and actin barrier formation.

4.2 Introduction

The structure of the AIS is comprised of several components including ankyrin G, spectrins, neurofascin, and an abundance of sodium and potassium channels (**Chapter 1, Section 1.8**). Ankyrin G is crucial to the protein complex as it binds to spectrins; loss of ankyrin G causes a loss in all AIS proteins (Zhou et al. 1998; Jenkins and Bennett 2001; Hedstrom et al. 2008). The actin cytoskeleton is also important in this region as it functions as a vesicle filter and diffusion barrier in the AIS (Winckler et al. 1999; Nakada et al. 2003; Song et al. 2009; Al-Bassam et al. 2012).

There has been limited research into the structure and function of the AIS in *Drosophila*. This is in part due to the lack of available markers. 10 years ago it was shown however that mushroom body neurons contain all the hallmark features that

are found in the mammalian AIS, including exclusion of axon specific or somatodendritic molecules, the presence of ankyrin 1, abundance of voltage gated ion channels and notable absence of actin (Trunova et al. 2011). This has allowed fly geneticists for the first time to study how the AIS develops and is maintained *in vivo* (Trunova et al. 2011; Spurrier et al. 2019; Ravenscroft et al. 2020). One major finding of AIS research in the fly has been to show that the actin cytoskeleton is essential for the proper distribution of membrane tethered proteins (Trunova et al. 2011). It remains to be determined whether, in fly neurons, the actin in this region can serve as a barrier for specialized vesicles and organelles bound to the cytoskeleton. Actin in the AIS separates the somadendritic compartment from the axonal region, maintains neuronal polarity, and regulates action potential initiation (Buffington and Rasband, 2011). This barrier acts to selectively filter cargo entering the axon while excluding somatodendritic cargoes (**Chapter 1, Section 1.9**). (Winckler et al. 1999; Song et al. 2009; Rasband 2010).

There are several different isoforms of actin: α -actin isoforms (α -skeletal muscle, α -cardiac muscle, and α -vascular), β -isoform (β -cytoplasmic), and γ -isoforms (γ -cytoplasmic and γ -smooth muscle) (Vandekerckhove and Weber 1978) important for the contractile function of these cells. Actin is also ubiquitously expressed throughout the nervous system and is important for maintaining cell morphology and processes that may require protein association with actin or phase transition (Fifkov 1985). In neurons, actin is required for neuronal development and is partially important for growth cone and synapse formation. In neurons, the actin cytoskeleton is composed of β and γ isoforms. Individual actin monomers are globular (G-actin) and consist of 375 amino acids, they form reversible head-to-tail interactions with two other actin monomers to form filaments (Holmes et al. 1990). Each actin filament is orientated with a plus and minus end enabling them to have a distinct polarity and facilitate cell migration (Pollard and Borisy 2003).

It was originally thought that the AIS barrier was formed by anchorage of transmembrane molecules to the cytoskeleton and restriction of movement caused by the tethering, known as the picket fence model (Fujiwara et al. 2002). More recently however it was discovered that actin, spectrin, and ankyrin form ordered rings in the AIS, 190 nm apart, that were postulated to be important for barrier formation (Xu et al. 2013; He et al. 2016). These rings are conserved between *Drosophila* and mammals. Importantly, Albrecht et al. (2016) demonstrated that membrane protein movement was dependent on these structures (Albrecht et al. 2016).

Specialised actin networks are also important for vesicle transport in the AIS. Actin filaments are orientated with their plus ends closest to the cell body, preventing the passage of vesicles carrying plus-end-directed myosin motors (e.g., Myosin Va) and allowing for minus-end-directed myosins. Therefore, this indicates that actin acts as a semipermeable actin-dependent barrier that filters vesicle transport in the AIS (Korobova and Svitkina 2010). The same is true for vesicles carrying dendritic proteins. In the AIS, almost all vesicles carrying dendritic proteins halt and reverse but those carrying axonal and non-specifically localised proteins move efficiently through the AIS (Watanabe et al. 2012). We aim to determine whether Cdk12 controls AIS formation and actin dynamics.

4.2.1 Aims and objectives

The aim of this result chapter is to determine if the loss of Cdk12 contributes to the structure of the AIS, *in vivo*.

- My first objective was to use *Drosophila* genetic approaches to screen for a valuable marker of specifically the AIS region in the glutamatergic neurons of the wing. I expressed several GFP labelled fluorescently encoded genetic markers in WT MARCM clones, in an attempt to visualize AIS, axon, or somatodendritic compartments at single axon resolution under the confocal microscope.
- My second objective was to investigate the age-dependent role of Cdk12 on β -actin and F-actin distribution and diffusion in the proximal axon.
- I then went on to determine what effect *Cdk12* ablation had on the function of the AIS as a vesicle/organelle barrier. To do this I took advantage of a marker that allowed us to determine the distribution of peroxisomes that usually reside only in somatodendritic regions in fly neurons. We aimed to determine whether soma to axonal transport of this organelle is permitted by loss of *Cdk12*.

4.3 Experimental design

To first identify AIS markers, GFP-tagged proteins-of-interest driven by OK371-Gal4 were expressed in glutamatergic neuronal MARCM clones. All fly stocks were stored at 20°C and expanded. Genetic crosses were set at 25°C with a 12 hour light-to-dark

ratio and flipped to new vials ~every 2 days (see **Appendix 1** for fly stocks used in this chapter). AIS markers of interest were each expressed in WT clones using the Gal4/UAS system: *UAS-Tubulin::GFP*, *UAS-Actin::GFP*, *UAS-Synaptotmin1::GFP*, and *UAS-AnkyrinG::GFP*. See **Figure 4.1A** for the generic genetic crosses. Desired progenies were selected and aged for the required time point. Non-damaged wings were dissected (**Chapter 2, Section 2.6**) and imaged using a confocal microscope (**Chapter 2, Section 2.7**). N=3 flies were used to screen for their ability to indicate the AIS region.

Next, we used two different markers to quantitatively measure the amount and distribution of actin. *UAS- β -Actin::GFP* and *UAS-F-Actin::GFP* were each expressed in neuronal MARCM clones, and wings imaged at 21 and 35 d.p.e., (**Figure 4.1B** and **Figure 4.1C**). For β -actin-GFP analysis N=7 flies were used at 21 d.p.e. for both genotypes and N=5 and N=3 animals used at 35 d.p.e. for control and mutant, respectively. For F-actin-GFP analysis N=9 and N=14 flies were used at 21 d.p.e. for control and mutant respectively and N=10 at 35 d.p.e. for both genotypes.

Following basic quantification of actin, we performed a FRAP experiment to determine β -actin diffusion in the proximal axon swellings. See **Chapter 2, Section 2.10** for more methodological details on FRAP. In brief, GFP-tagged β -actin in the proximal axon was bleached within an ROI with x5 cycles at 72% laser intensity (488 nm) every 1.295 seconds. X2 pre-bleached images were imaged at 72% intensity (488 nm) every 1.295 seconds and post-bleach images every 5.295 seconds (x10 images). See **Figure 4.1B** and **Figure 4.1C** for actin fly crosses. Progenies were aged for 21 days. N=17 and N=14 flies were used to analyse actin diffusion for the control and mutant, respectively.

To determine whether β -actin proximal axon swellings migrated in the glutamatergic neurons of the wing, I performed a time series in MARCM neuronal clones on the Zeiss spinning disc confocal microscope lasting 180 seconds, in both control and *Cdk12^{-/-}* backgrounds at 21 d.p.e., see **Figure 4.1** for actin fly crosses. See **Chapter 2, Section 2.7** for more methodological details. N=3 flies were used for both control and mutant.

To analyse peroxisome positioning, as a proxy for AIS breakdown, we took advantage of a transgenic fly harbouring UAS construct with a peroxisomal targeting sequence, serine-lysine-leucine (SKL), at the C-terminus of GFP (Larkin et al. 2021) (*UAS-*

SKL::GFP). This was expressed in MARCM neuronal clones of the wing in *Cdk12^{-/-}* and control backgrounds at 21 and 24 d.p.e. For genetic crosses for control and mutant see **Figure 4.2A** and **Figure 4.2B**, respectively. N=13 and N=12 flies were used for at 21 d.p.e. and N=4 and N=8 flies used at 24 d.p.e. in the control and mutant, respectively.

Figures were designed on Adobe Photoshop and data analysed on GraphPad Prism, 2-way ANOVA statistical analysis and Bonferroni *post hoc* tests were used to determine significance (**Chapter 2, Section 2.11**).

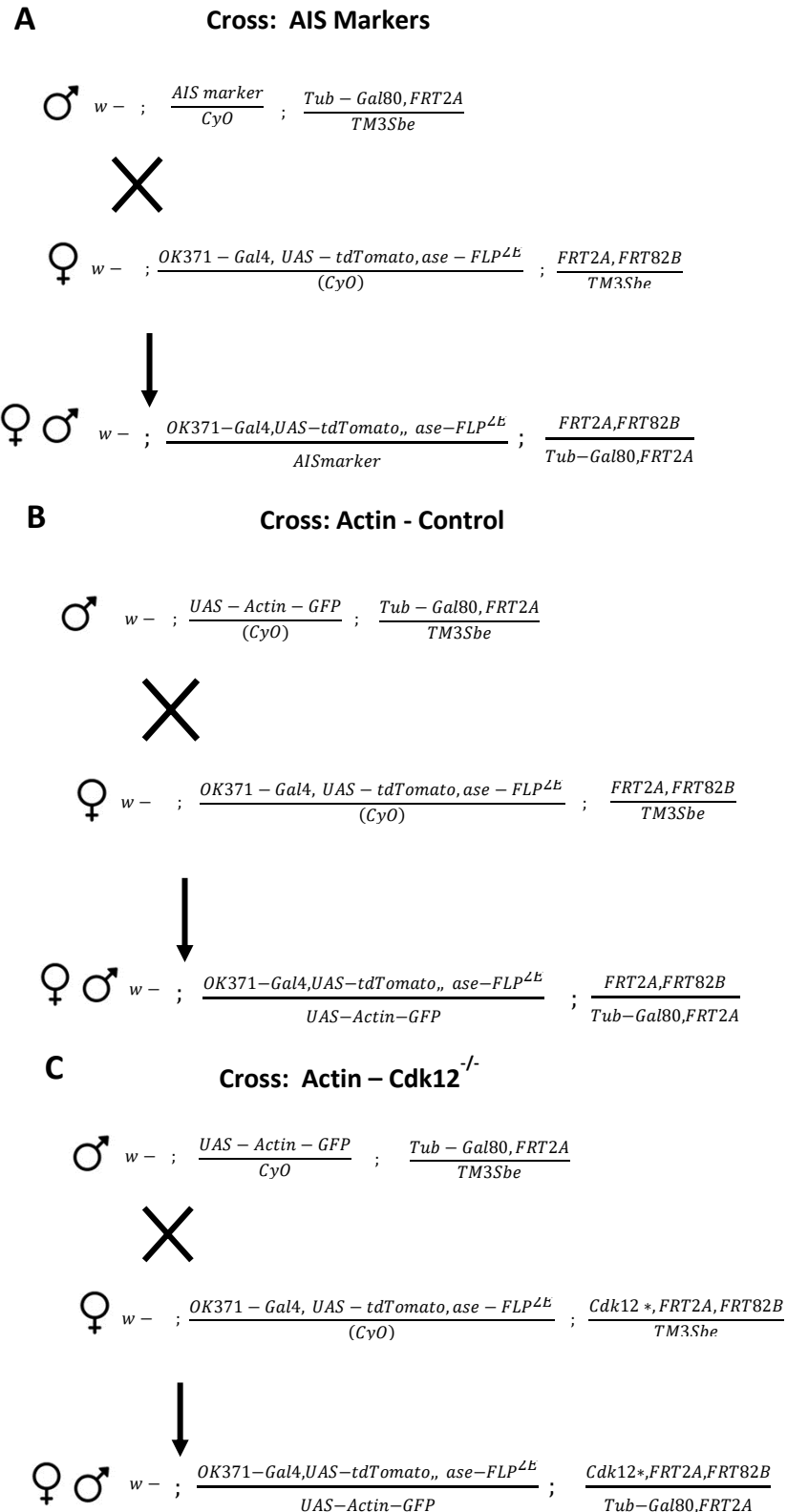


Figure 4.1 Fly crosses for flies expressing GFP-tagged AIS markers and β -Actin in MARCM clones. Generic fly stocks used contained several GFP-tagged AIS UAS markers (**Table 1**) on chromosome II were combined with FRT sites and Gal4 repressor elements on chromosome III and crossed to our control tester line to generate MARCM clones (**A**). Generic crosses are shown to express either tagged β - or F-Actin (*UAS-Actin-GFP*) in control (**B**) and *Cdk12* null clones (**C**).

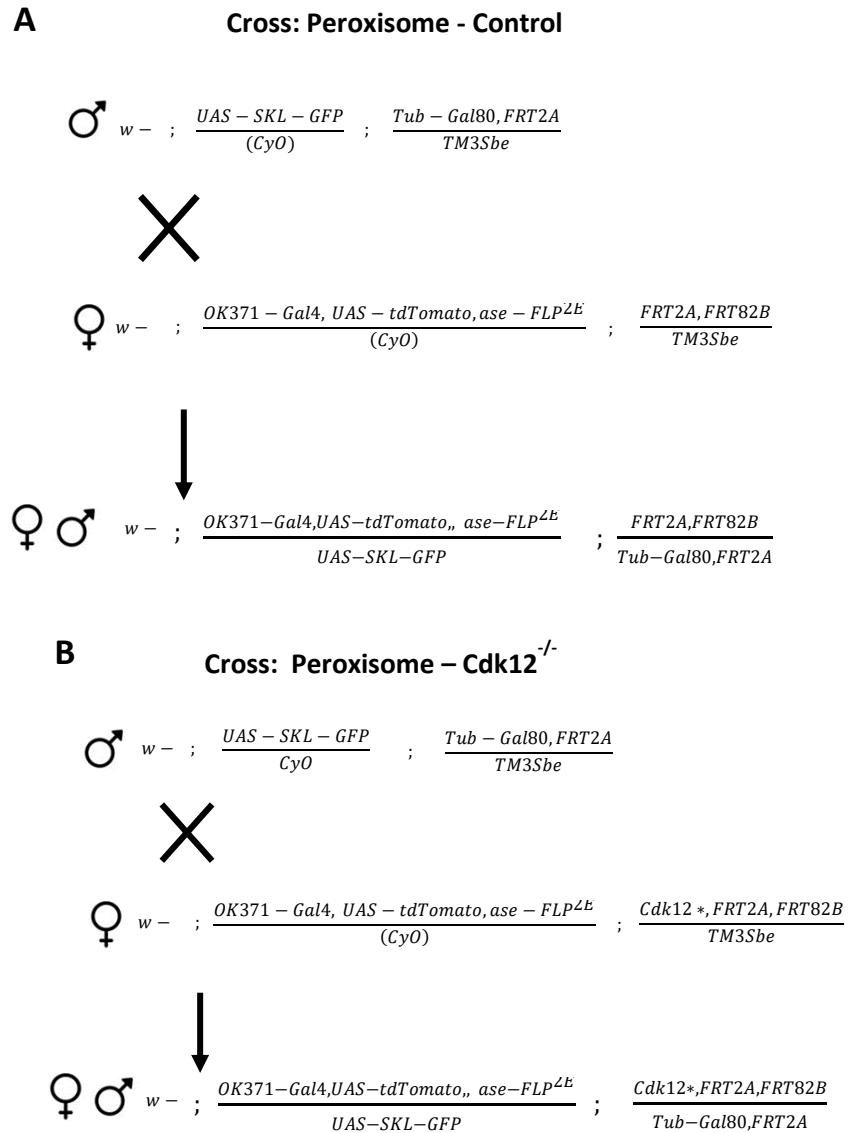


Figure 4.2 Fly crosses to generate MARCM clones expressing GFP tagged peroxisomes. Flies containing *UAS-SKL::GFP* on chromosome II were combined with FRT sites and Gal4 repressor elements on chromosome III and crossed to our control tester line (A) and *Cdk12* mutant tester line (B).

4.4 Results

4.4.1 Actin as an AIS marker

We previously discovered that Cdk12 controls the size of the axon proximal to the cell body (**Chapter 3**) and hypothesised that the swellings observed were within the specialised AIS region. I selected several candidate AIS markers, based on the work in *Drosophila* by Trunova et al. (2011) (Trunova et al. 2011) to determine if we could detect the AIS region in glutamatergic neurons of the *Drosophila* wing. We visualised ankyrin 1 (**Figure 4.3A**), tubulin (**Figure 4.3B** and **Figure 4.3C**), synaptotagmin 1 (**Figure 4.3D**, **Figure 4.3E**, and **Figure 4.3F**), and actin (**Figure 4.3G** and **Figure 4.3H**) in neuronal clones. No cell compartment specific changes were seen in the intensity of ankyrin 1, tubulin, or synaptotagmin 1. Actin however was highly expressed in somatodendritic regions and noticeably reduced in the axon. Although we did not find a specific marker of the AIS in this screen, actin-GFP was found to be a good marker to distinguish the axon and cell body compartments and was used for subsequent experiments.

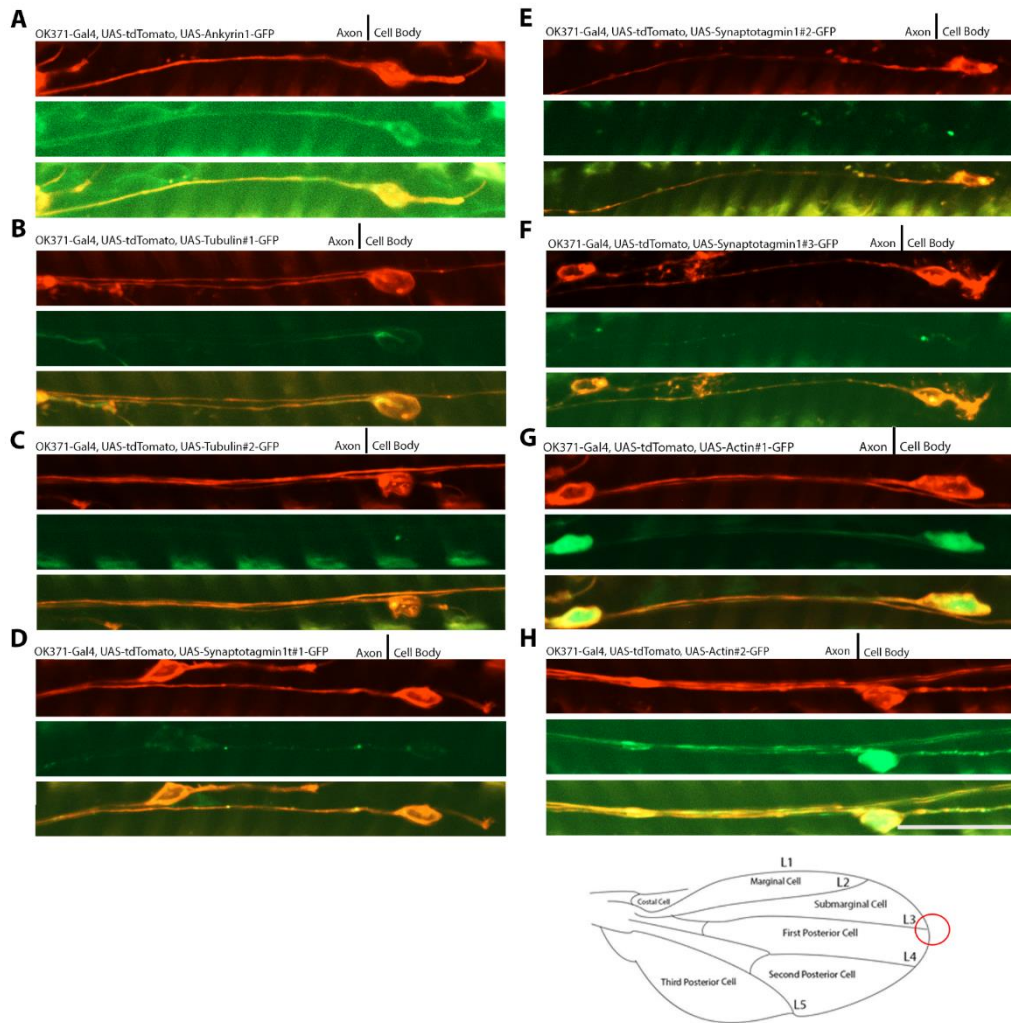


Figure 4.3 Actin as a marker for somadendritic regions. We investigated the cell compartment localisation of GFP tagged ankyrin 1 (A), tubulin #1 (B) and #2 (C), synaptotagmin 1 #1 (D), #2 (E), and #3 (F) and actin #1 (β -actin) (G) and actin #2 (F-actin) (H). We found that *UAS-actin::GFP* was the only construct that could accurately distinguish between somatodendritic and axonal compartments. Scale bar = 10 μ m.

4.4.2 Cdk12 controls β -actin distribution

To investigate the effect of Cdk12 on actin distribution in the neuron, GFP-tagged β -actin (*UAS-Actin8807-GFP*) was expressed in control and *Cdk12^{-/-}* neurons. In control neurons, photomicrographs and fluorescence intensity graphs showed actin was enriched in the cell body but did not mark the AIS in the wing neurons at 21 (**Figure 4.4A**) and 35 d.p.e. (**Figure 4.4B**). In the mutant, actin was enriched in more proximal regions of the axon and accumulated in large proximal axon swellings at 21 d.p.e. (**Figure 4.4C**) and in later stages, actin swellings were more numerous and resided even further down the axon relative to the cell body (**Figure 4.4D**). A Kruskal-Wallis test revealed no significant differences between genotype/age for maximum fluorescent intensity (**Figure 4.4E**, $p=ns$) and the area of total actin fluorescence under the curve (**Figure 4.4F**, $p=ns$) although a strong trend was noted. There was a significant increase between genotypes in the number actin patches $>3 \mu\text{m}$ in the proximal axon ($H_4 = 8.980$, $p<0.01$) and multiple comparisons tests revealed actin patches were increased by ~ 2 fold in the mutant at 35 d.p.e. (**Figure 4.4G**, $p<0.05$). These data indicate that actin has been redistributed within the axon rather than a change in total levels and Cdk12 functions to restrict actin to the somatodendritic regions and the AIS.

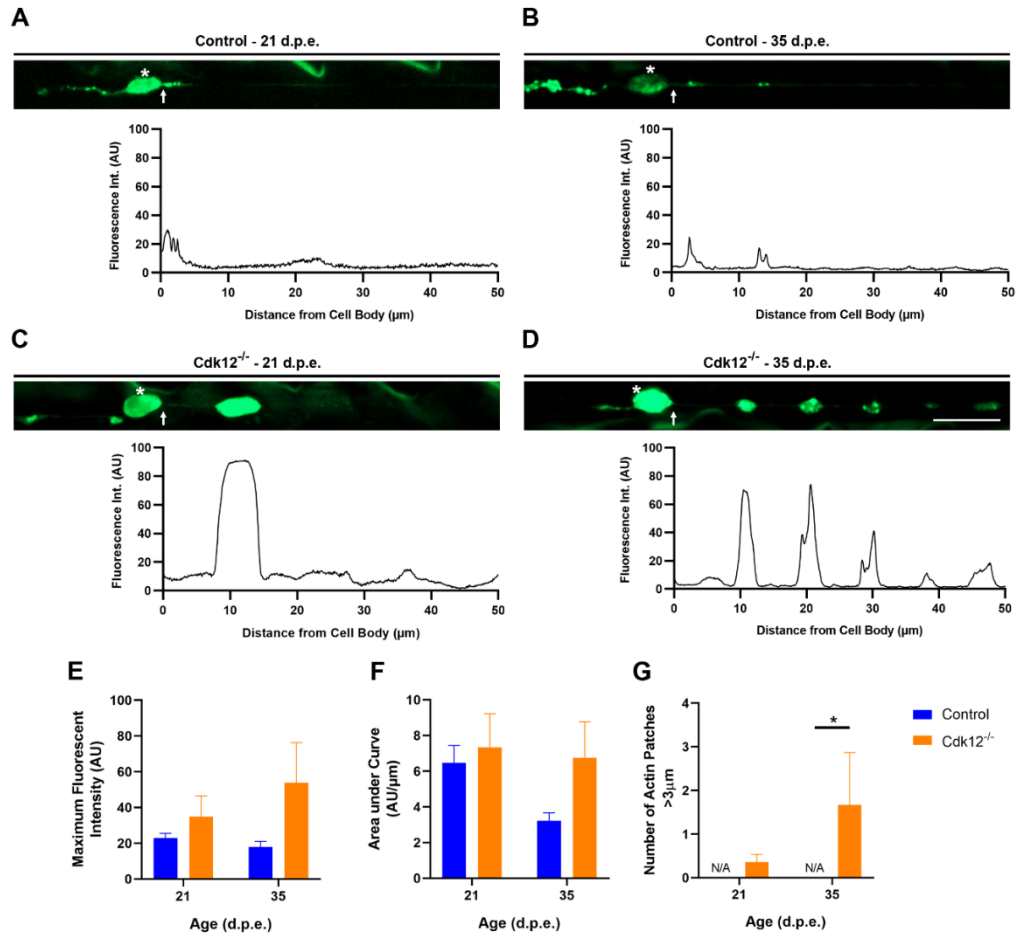


Figure 4.4 Cdk12 controls β -actin localisation. Fluorescent intensity of GFP-tagged β -actin was recorded in the control at 21 (A) and 35 d.p.e. (B) and in the null mutant at 21 (C) and 35 d.p.e. (D) over a 50 μm stretch of axon proximal to the cell body. * indicates the cell body and the arrows represents the start of the axon. Maximum fluorescent intensity (E), area under the curve (F), and number of actin patches $>3 \mu\text{m}$ in length (G) were recorded. Scale bar was 10 μm . Data was analysed using Kruskal-Wallis tests and multiple comparisons. Significant differences annotated as $p < 0.05^*$ compared to the control. Graphs are expressed as Mean \pm SEM.

4.4.3 Cdk12 controls F-actin levels

To investigate the effect of Cdk12 on F-actin distribution in the neuron, GFP-tagged F-actin (*UAS-LifeAct35544-GFP*) was expressed in control and *Cdk12^{-/-}* neurons. In control neurons, photomicrographs and fluorescence intensity graphs showed F-actin was enriched in the cell body and AIS at 21 (**Figure 4.5A**) and 35 d.p.e. (**Figure 4.5B**). In addition to the cell bodies, actin was also present in the proximal axon swellings of *Cdk12^{-/-}* neurons (21 d.p.e., **Figure 4.5C**). At later time points more F-actin signal could be observed throughout the proximal axon including within the axonal swellings (**Figure 4.5D**). A Kruskal-Wallis test revealed significant increases between genotypes for maximum fluorescent intensity ($H_4 = 3.222$, $p < 0.01$) and multiple comparisons revealed max fluorescent intensity levels were more than double in the mutant at 35 d.p.e. ($H_4 = 8.036$, $p < 0.01$, **Figure 4.5E**). There was a significant increase between age ($H_4 = 13.63$, $p < 0.001$) and genotype ($H_4 = 16.83$, $p < 0.0001$, **Figure 4.5F**) for the total area covered by F-actin in the axon under the curve but no significant differences between age and genotype in actin patches $> 3 \mu\text{m}$ in the proximal axon (**Figure 4.5G**, $p = ns$). This suggests that Cdk12 controls the amount of F-actin in the proximal axon region but does not control its distribution in distinct patches.

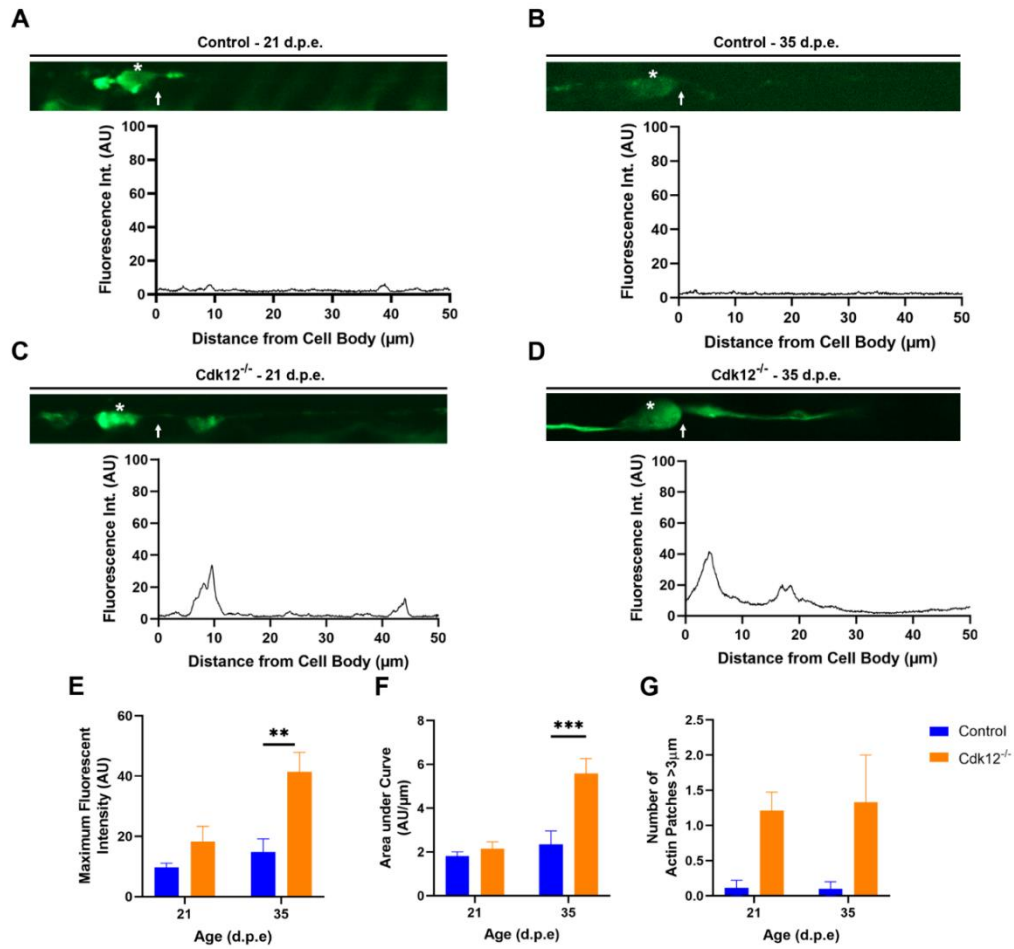


Figure 4.5 Cdk12 controls F-actin levels. Fluorescent intensity of GFP-tagged F-actin was recorded in the control at 21 (A) and 35 d.p.e. (B) and in the null mutant at 21 (C) and 35 d.p.e. (D) over a 50 μm stretch of axon proximal to the cell body. * indicates the cell body and the arrows represents the start of the axon. Maximum fluorescent intensity (E), area under the curve (F), and number of actin patches $>3\ \mu\text{m}$ in length (G) were recorded. Scale bar was 10 μm . Data was analysed using Kruskal-Wallis tests and multiple comparisons. Significant differences between genotypes of the same age annotated as $p < 0.01$ ** & $p < 0.001$ *** compared to the control. Graphs are expressed as Mean \pm SEM.

4.4.4 Cdk12 regulates β -actin diffusion in the proximal axon swellings

To investigate the effect of Cdk12 on β -actin diffusion capacity, FRAP was used (**Figure 4.6A**) to bleach GFP-tagged β -actin in the proximal axon region at 21 d.p.e. A mild recovery of GFP signal was observed in the proximal axon of control neurons but GFP-recovery was seen robustly from 20 seconds in mutant neurons (**Figure 4.6B**). A two-way ANOVA revealed significant differences between GFP recovery levels over time ($F_{11,588} = 29.70$, $p < 0.0001$) between control and mutant groups, and *post hoc* tests show increased levels in mutant neurons at 46 ($p < 0.05$), 51 ($p < 0.01$) and 57 seconds ($p < 0.05$, **Figure 4.7A**). Numerous parameters of GFP recovery were calculated based on our time lapse data (**Figure 4.7B**). There was a significant decrease ($t = 2.42$, $df = 2,48$, $p = 0.0194$) in fluorescence signal calculated to be immobile β -actin fraction present between control and mutant neurons (**Figure 4.7C**), There was also a significant increase ($t = 3.02$, $df = 2,49$, $p = 0.004$) in the mobile fraction in mutant neurons compared to control (**Figure 4.7D**). T-tests revealed no significance differences in the half time of recovery of β -actin in the control and mutant ($p = ns$, **Figure 4.7E**). This experiment suggests that the majority of β -actin residing in the proximal axon was immobile and likely contributed to the low levels of GFP recovery, independent of genotype. However, approximately 10-20% of β -actin was mobile and able to diffuse into our ROI to partially recover GFP signally after the bleach. Based on these genotype specific differences, we suggest that Cdk12 normally functions to limit mobile actin diffusion in this region.

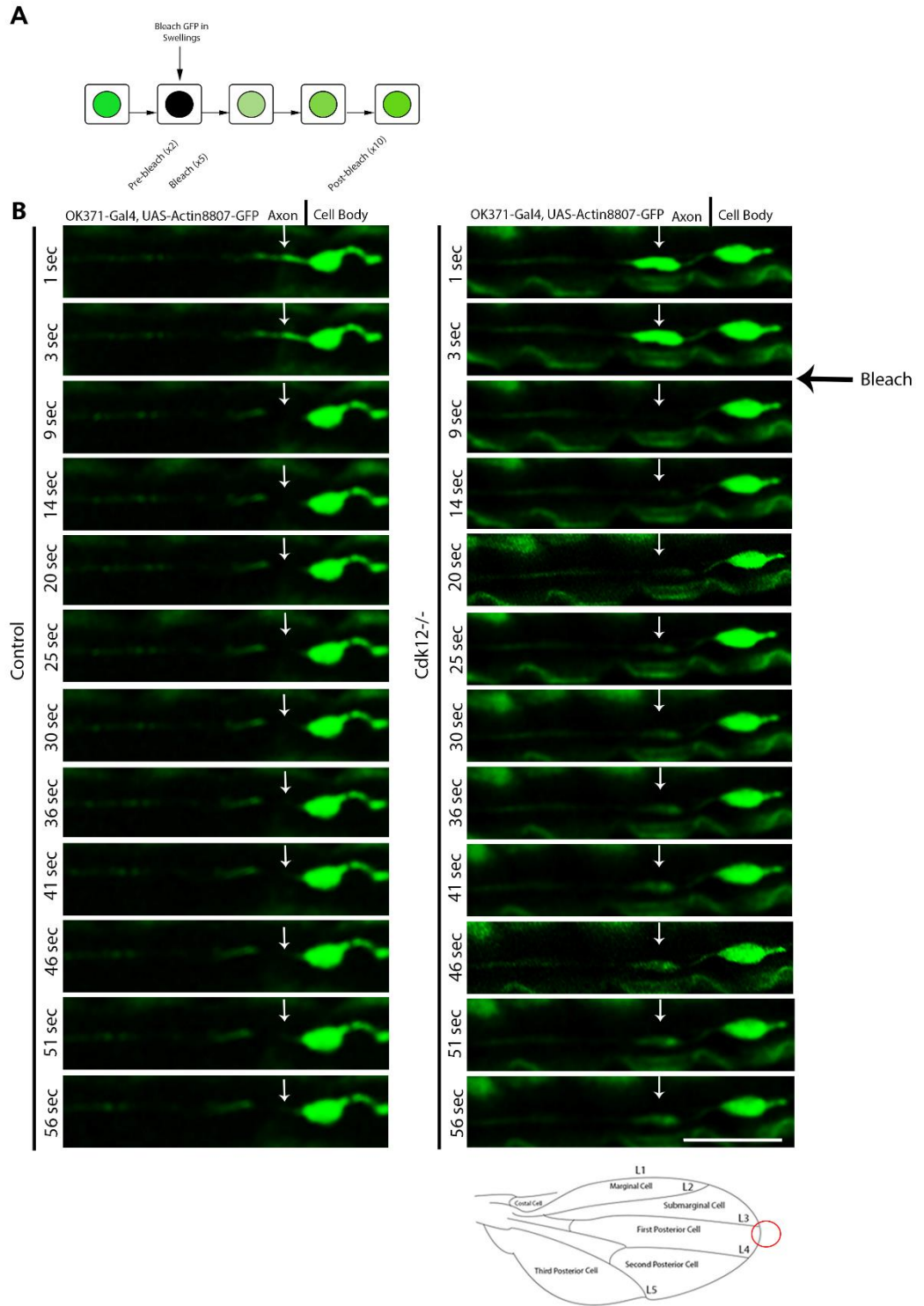


Figure 4.6 Cdk12 regulates β -actin diffusion after photobleaching. A schematic of the FRAP experiment (A). GFP tagged β -actin was bleached at 4 seconds. In the control neurons limited recovery occurred by 56 seconds however fluorescent levels in *Cdk12*^{-/-} neurons gradually recovered from 20 seconds (B). White arrows indicate bleached region. The area of the wing used is shown in the schematic. Scale bar was 10 μ m.

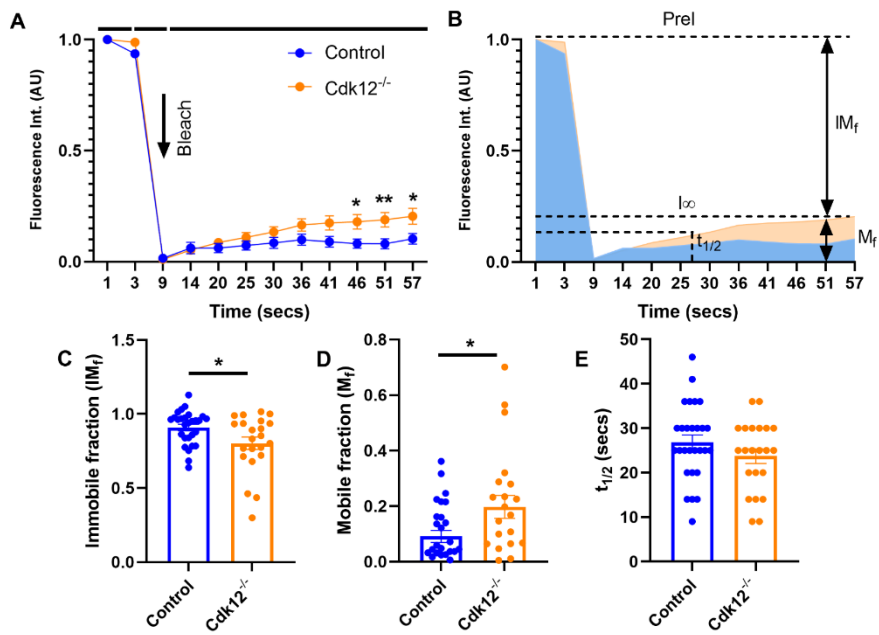


Figure 4.7 Cdk12 controls β -actin diffusion in the proximal axon. β -actin was bleached at 9 seconds in the proximal axon at 21 d.p.e. in control and *Cdk12*^{-/-} clones and plotted overtime (A). Mathematical analysis of fluorescent intensity data (B) was used to determine immobile fractions (C), mobile fractions (D), and $t_{1/2}$ to recovery (E) for control and mutant groups. Data was analysed using multi-way ANOVA with Bonferroni *post hoc* tests and unpaired t-tests at the 57 second time point. Significant differences annotated as $p < 0.05^*$ and $p < 0.01^{**}$ compared to the control. Graphs are expressed as Mean \pm SEM and data points shown.

4.4.5 β -actin swellings were stationary in *Cdk12*^{-/-} clones

To determine whether the β -actin patches observed in our *Cdk12* mutant were able to move, I performed a time series to visualise GFP tagged β -actin in the proximal axon of clonal glutamatergic neurons in the control and *Cdk12*^{-/-} mutant backgrounds, over 180 seconds. At 21 d.p.e., no migration or movement of actin swellings was seen (**Figure 4.8**). No movement of β -actin was seen in the control. This gives an indication that actin patches form and grow in a slow sustained and age-dependent way, but do not migrate or move once formed over short periods of time.

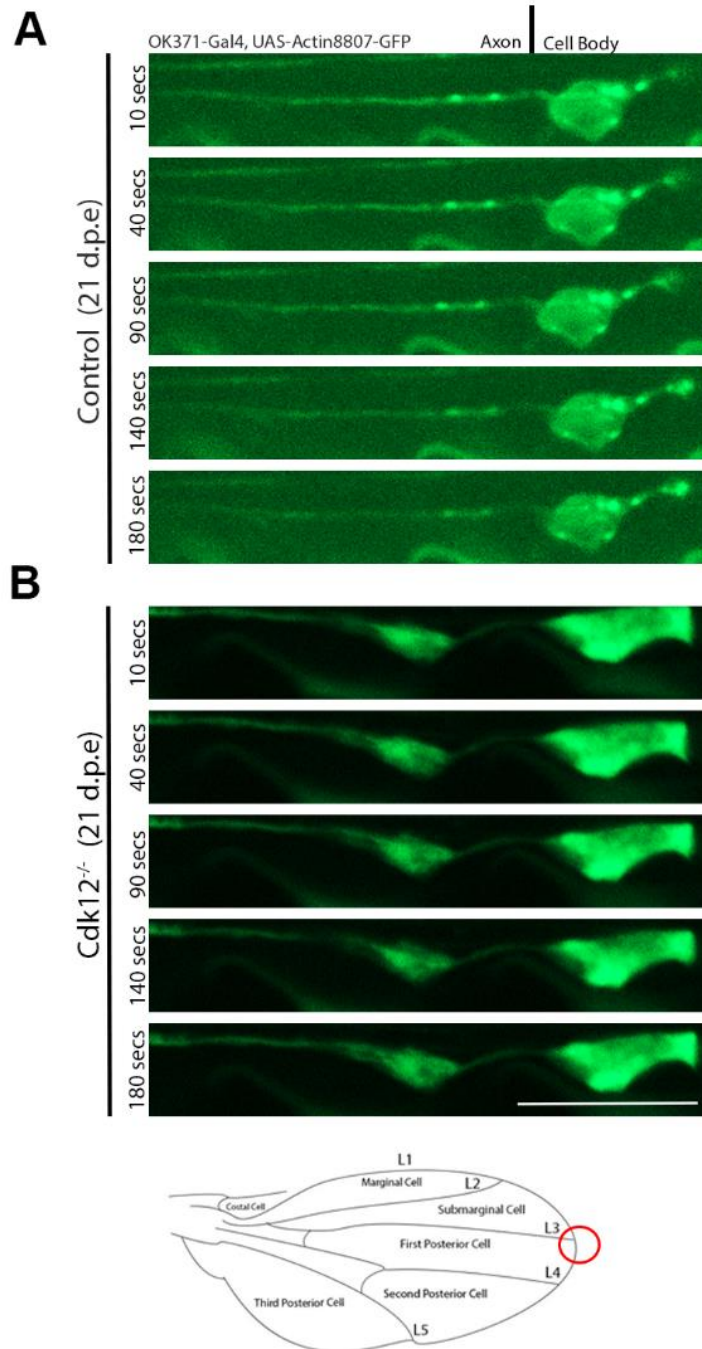


Figure 4.8 Cdk12 had no effect on β -actin swelling migration. A time lapse series was recorded over 180 seconds at 21 d.p.e. using live cell imaging approaches. GFP-tagged β -actin, observed in the control, appeared more diffused within the cell and did not move over time (A) In the mutant, actin swellings were also stationary within the neuron (B). Scale bar = 10 μ m. Images were taken at the distal tip, see red circle on wing schematic.

4.4.6 Cdk12 regulates peroxisome positioning in the axon and the cell body

Since actin in the AIS regulates the barrier of membrane bound proteins and regulates vesicle sorting into neuronal compartment, I decided to investigate the effect Cdk12 had on peroxisome positioning, as this organelle should be restricted to somatodendritic regions. Interestingly, while no peroxisomes were found in control proximal axons at 21 (**Figure 4.9A**) and 24 d.p.e. (**Figure 4.9B**) we did identify peroxisomes in *Cdk12* null clones at 21 (**Figure 4.9C**) and 24 d.p.e. (**Figure 4.9D**), suggesting a barrier breakdown. A 2-way ANOVA revealed significant differences between age ($F_{1,32} = 4.307$, $p < 0.05$) and genotype ($F_{1,32} = 14.74$, $p < 0.001$) in the number of peroxisomes in the proximal axon. *Post hoc* tests revealed that the number of peroxisomes in the proximal axon of *Cdk12* null clones at 24 d.p.e. significantly increased compared to those at 21 d.p.e. ($p < 0.05$) while none were observed in controls at any age (**Figure 4.9E**, $p < 0.01$). In contrast, no significant differences were identified in the total amount of fluorescence AUC (**Figure 4.9F**, $p = ns$). In addition to the proximal axon, I also investigated the effect *Cdk12* ablation on peroxisome morphology and abundance in the cell body and photomicrographs revealed an increase in peroxisomes in *Cdk12* null clones (**Figure 4.10A**). A significant increase between genotypes was identified in aspect ratio ($F_{1,30} = 12$, $p < 0.01$) and *post hoc* tests revealed that this occurred at 21 d.p.e. (**Figure 4.10B**, $p < 0.05$). This suggests that the peroxisome network in the cell body was less spherical. Peroxisome area (**Figure 4.10C**, $p = ns$) and Feret's diameter (**Figure 4.10D**, $p = ns$) were not significantly different although a strong trend was noticed. These data suggest that *Cdk12* functions to restrict peroxisomes to the somatodendritic region of the neuron and may play a role in regulating peroxisome morphology and abundance.

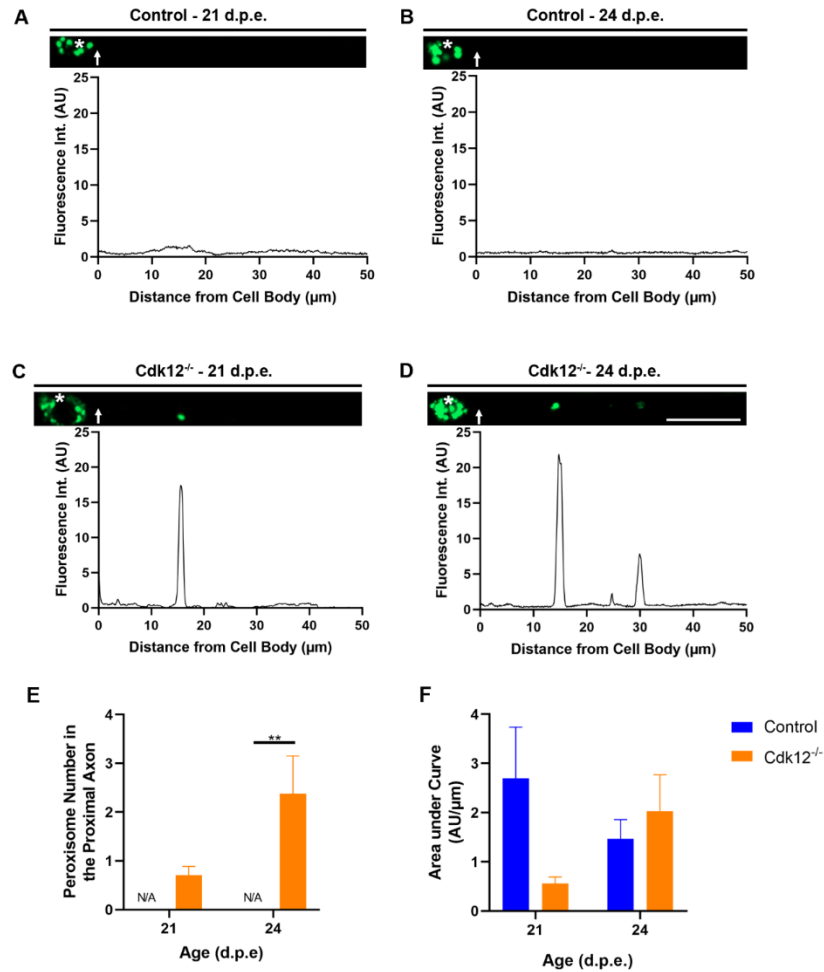


Figure 4.9 Cdk12 restricts peroxisome trafficking into the axon. Plot profiles depicting fluorescent intensity of GFP-tagged peroxisomes along the axon were measured in the control at 21 (A) and 24 d.p.e. (B) and in the null mutant at 21 (C) and 24 (D) d.p.e. * indicates the cell body and arrows correspond to the start of the axon. The number of peroxisomes located in a 50 μm stretch of proximal Axon (E) and the area under the curve (F) were measured. Only *Cdk12*^{-/-} neuronal clones displayed peroxisomes within the axon and more peroxisomes were seen at 24 d.p.e. than 21 d.p.e. Data was analysed using two-way ANOVA and Bonferroni *post hoc* tests. Significant differences annotated as $p < 0.01$ ** between genotypes and $p < 0.05$ # within the *Cdk12*^{-/-} group at different ages. Scale bar = 10 μm Graphs are expressed as Mean ± SEM.

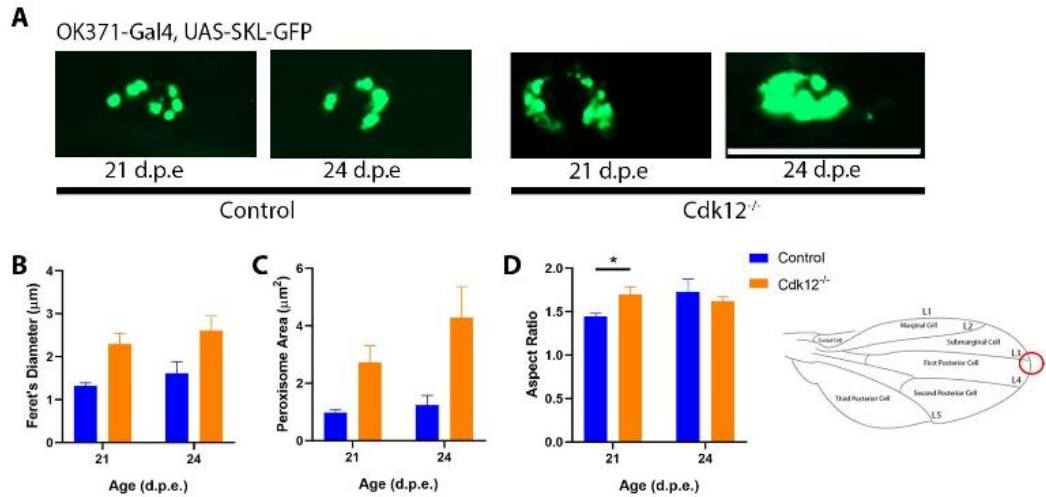


Figure 4.10 *Cdk12* controls peroxisome morphology in the cell body. The peroxisome area was greater in the *Cdk12*^{-/-} neuronal clone cell bodies at 24 d.p.e. compared to control (A). No robust changes in volume were seen at 21 d.p.e. Peroxisome morphology was also recorded through the use of aspect ratio (B), peroxisomal area (C) and feret's diameter (D) calculations. At 21 days peroxisome networks in the *Cdk12*^{-/-} mutant background had a higher aspect ratio. Data was analysed using two-way ANOVA and Bonferroni *post hoc* tests. Significant differences annotated as $p < 0.05^*$ compared to the control. Scale bar was 10 μm . Graphs are expressed as Mean \pm SEM. Peroxisomes were recorded in the cell bodies in the L1 vein, at the distal tip, see red circle on wing schematic.

4.5 Discussion

I previously showed that Cdk12 regulates proximal axon width and maintains neuronal survival in wing glutamatergic neurons (**Chapter 3**). It was hypothesised that the proximal axon swellings, that were most abundant at 21 d.p.e., resided in the AIS, a region between the cell body and axon that regulate neuronal polarity and initiate action potentials (Palay et al. 1968). While I was not able to clearly label the AIS regions using multiple genetically encoded markers for key molecules in the AIS, we found the cell soma could be labelled with a GFP-tagged actin and its immediate absence in the AIS. Using this tool, it was possible to detect large β -actin patches in *Cdk12*^{-/-} ablated neurons, largely absent in WT neurons. These patches were found to be stationary and did not move within the neuron. In contrast, F-actin levels were ubiquitously increased in the proximal axons of *Cdk12*^{-/-} ablated neurons but did not form distinct patches. I further found that β -actin molecules were more diffusible and mobile in *Cdk12*^{-/-} ablated neurons. Actin changes within the neuron were associated with barrier breakdown, since we discovered that peroxisomes, that ordinarily reside in the somatodendritic regions, entered the axon in the absence of *Cdk12*.

In the glutamatergic neurons of the wing we attempted to define the AIS regions using several genetically encoded markers previously used to localise the AIS of mushroom body neurons (Trunova et al. 2011). In mushroom body neurons the AIS could be identified through either the enrichment of ankyrin 1, absence of synaptotagmin, presence of ion channels or reduced actin. In contrast to mushroom body neurons, we find no specific regional differences in ankyrin 1 or synaptotagmin. However, actin was expressed highly in somatodendritic regions of glutamatergic neurons with immediate signal reduction closer to the cell body, indicating the start of the AIS. This suggests that perhaps the AIS composition differs between neuronal subtypes and perhaps these differences in part control the functional properties that different neuronal subtypes have. Actin, spectrin and ankyrin should form ordered rings in the AIS when observed at nanoscale (Xu et al. 2013), so perhaps ankyrin enrichment was not observed due to the limited resolution of the confocal microscope. However, it is also possible that the strength of different Gal4 drivers effects the ability to detect the AIS through UAS based marker methods under confocal microscopy. In future studies, it would be interesting to see if the AIS can be detected in wing neurons through investigations of ion channel distribution. To do this you could take advantage of new tools, that are derived from the Mi(MiC) collections where the stop codon is replaced with an in frame cassette containing GFP (Nagarkar-Jaiswal et al. 2015),

allowing for detection at endogenous levels. These are currently available for the *Shaker*, *Shal*, and *para* ion channels.

We found that ablation of *Cdk12* caused a β -actin redistribution in the wing neurons and an overall increase in F-actin, suggesting a relationship between both actin forms. It has been reported that *in vitro* cells heterozygous for β -actin show a decrease in G-actin and increase in F-actin (Bunnell et al. 2011). Perhaps, the unusual β -actin distribution caused by loss of *Cdk12* may be detected by the cell as a loss of its function and neurons respond by increasing F-actin formation. It would be interesting to see whether γ -actin is also altered in our neurons, since loss of β -actin can also upregulate this isoform in non-neuronal cells *in vitro* (Bunnell et al. 2011). FRAP experiments show that actin in the AIS is more diffusible in a *Cdk12*^{-/-} background than control and this may reflect the highly dynamic capacity of F-actin. Enforced actin polymerization in glial cells by cofilin knockdown or a pharmacological approach caused an increase in the F-actin/G-actin ratio and a faster recovery rate in yellow FP labelled β -actin FRAP experiments (Rasmussen et al. 2010). F-Actin is generated through the activity of Arp2/3 complex and formins, (Mullins et al. 1998; Spence and Soderling 2015) and it is therefore possible that *Cdk12* usually functions to limit their activity in the AIS and would be interesting to investigate molecules like these in future studies. Actin assembly and disassembly has also been linked to mitochondrial fission/fusion (Moore et al. 2016) and the mitochondrial network explored in **Chapter 5**. This suggests that these actin regulatory processes take place in non-dividing and polarised cells and for the first time place *Cdk12* as an upstream regulator of actin dynamics in neurons.

To see if altered actin dynamics influences the selective barrier associated with the AIS, peroxisome localisation was monitored. I found that peroxisomes are usually restricted to somatodendritic regions in fly neurons. It is possible there are cell specific or developmental differences in peroxisome transport mechanisms. Certainly in yeast and other species peroxisomes are associated with the actin cytoskeleton (Neuhaus et al. 2016). Although these organelles are constrained to the cell body in our neurons of interest, *Cdk12* ablation caused a remarkable peroxisome infiltration into the axon. Therefore, suggesting that this is the result of the actin barrier breakdown. In the barrier, actin filaments are orientated with their plus ends closest to the cell body, preventing the passage of vesicles carrying plus-end-directed myosin motors (e.g., myosin Va) (Korobova and Svitkina 2010). We suggest that *Cdk12* controls this actin filament organisation. In this case, loss of *Cdk12* may cause disordered actin

orientation and transport cargos/organelles to the axon via myosin motor proteins. It would be interesting to determine whether knockdown of select myosin motor proteins prevents this mislocalisation in future studies.

Peroxisomes are metabolically linked to mitochondria (Fransen et al. 2017). Very long chain fatty acids are shortened through β -oxidation in peroxisomes and can be transported to mitochondria for further processing. In mitochondria, shortened acyl-CoA is converted into acetyl-CoA and is used to fuel the Krebs cycle. Based on the localisation of peroxisomes in the cell body compartment of our neurons, it is possible that this process is only required in cell body residing mitochondria or intriguingly not needed in axons. We explore whether mitochondria are altered by the loss of *Cdk12* in **Chapter 5**.

I suggest two main hypotheses the first being that *Cdk12* is involved in the transcriptional regulation of genes that code for actin formation and regulation. This would make sense based on its observed localisation in the nucleus (**Chapter 2**). Secondly, it is possible that *Cdk12* has a non-canonical role in regulating actin dynamics modulated through its kinase domain and protein-protein interactions within the proximal axon. Both of these hypothesis will be discussed in detail in **Chapter 5**. It has been shown previously that inhibition of *Cdk5* induces disordered microtubule polarity and loss of AIS cytoskeletal structure (Trunova et al. 2011) leading to changes in synaptic plasticity (Seeburg et al. 2008), phenocopying some of the *Cdk12*^{-/-} changes seen here. Using *Drosophila* it was previously discovered that reducing *Cdk5* activity shortens the AIS and the activity of *Cdk5* is controlled by calpain activation to maintain overall AIS size (Trunova et al. 2011). Calpains are proteases regulated by Ca^{2+} levels, suggesting Ca^{2+} may also be dysregulated in *Cdk12* ablated conditions. This is investigated in **Chapter 5**. It is therefore possible that *Cdk12* functions together with *Cdk5* for to maintain this region and this will be explored further in **Chapter 5**.

4.6 Conclusion

Cdk12 has been shown to regulate proximal axon width in glutamatergic neurons in the fly wing (**Chapter 3**). The swellings were most abundant at 21 d.p.e. and were hypothesised within or near the AIS, a specialised region that regulates neuronal polarity and initiates action potentials (Palay et al. 1968). In this chapter we find a marked change in β -actin distribution with the formation of stationary actin patches in

Cdk12 ablated conditions. We also found a marked upregulation of F-actin. We suggest that Cdk12 functions to constrain β -actin within somatodendritic regions and its mislocalisation may stimulate G-F conversion (polymerisation). This polymerisation may lead to increased actin dynamics and increased actin recovery after bleaching. Actin changes in *Cdk12*^{-/-} conditions were further associated with actin barrier breakdown, that allowed for peroxisomes (usually found exclusively in the cell body) to infiltrate into the axon. Therefore, we place Cdk12 as a regulator of actin dynamics and actin barrier function in neurons.

5 Cdk12 controls neuronal physiology and mitochondrial dynamics

5.1 Abstract

The AIS functions in action potential initiation and maintaining neuronal polarity. The actin cytoskeleton in this region plays a key role in maintaining neuronal morphology. We have previously found that Cdk12 controls actin remodelling in the region of the axon proximal to the cell body (**Chapter 4**). While I found that long-term consequence of this is neurodegeneration, it remains unclear what detrimental biochemical changes occur at initial stages. It remains to be determined whether actin redistribution could impact on redox state, metabolism or even Ca^{2+} dynamics. Metabolism in neurons is controlled by membrane-bound organelles, such as mitochondria and peroxisomes, to maintain energy homeostasis through OXPHOS and I have previously found that Cdk12 plays a role in peroxisome positioning (**Chapter 4**). In this chapter, we therefore investigate whether Cdk12 can control neuronal biochemistry and mitochondrial dynamics which could ultimately impact on neuronal function. We show that loss of Cdk12 leads to an increase in neuronal Ca^{2+} and causes excessive mitochondrial fission but has no effect redox balance suggesting that actin redistribution may contribute to neuronal function.

5.2 Introduction

Ca^{2+} dynamics are important for several processes in the neuron, such as gene transcription, cell death, metabolism and action potentials (Carafoli 2007; Mellström et al. 2008). The function of a neuron is to transmit information from one neuron to another neuron or tissue through action potentials. Once an action potential reaches the axon terminals, a calcium influx is triggered causing neurotransmitters to be released into the synaptic cleft and information is passed on (**Chapter 1, Section 1.1**). Therefore, demonstrating the importance of Ca^{2+} ions in electrophysiological properties.

At the synapse, high Ca^{2+} levels are regulated by mitochondria as excess ions enter the outer and inner membranes through ion channels. Ca^{2+} pass through the outer membrane via voltage dependent anion-selective channels and enter the inner membrane via mitochondrial calcium uniporter, rapid mitochondrial calcium uptake or mitochondrial ryanodine receptor (Israelson et al. 2007; Tan and Colombini 2007;

Perocchi et al. 2010; Baughman et al. 2011; De Stefani et al. 2011; Plovanich et al. 2013). Increased mitochondrial Ca^{2+} levels are essential for ATP production as Ca^{2+} ions trigger the Krebs cycle and electron transport chain in oxidative phosphorylation (Delbaere et al. 1991; Tarasov et al. 2012; Ma et al. 2017). In addition, high levels of cytosolic Ca^{2+} levels contribute to toxicity and excitotoxicity and therefore Ca^{2+} influx into mitochondria prevents (Blaustein 1988; Werth and Thayer 1994; El Idrissi 2006; Bezprozvanny and Mattson 2008). If Ca^{2+} levels are too high, Ca^{2+} is also stored in microdomains that occur at mitochondria-ER contact sites (MERCs) (Marchi and Pinton 2014). In addition, MERCs also function in lipid metabolism, mitochondria quality control (mitochondria fission, fusion and mitophagy), and unfolded protein response (as abundance of unfolded protein causes ER stress). MERCs are also involved in neurodegenerative diseases such as AD, PD, and ALS (Wilson and Metzakopian 2020).

In addition to Ca^{2+} levels, oxidative stress is also regulated in neurons. Oxidative stress is caused by the unregulated production of ROS, such as: nitric oxide, hydrogen peroxide, hydroxyl radicals, and superoxide. At high levels, ROS contributes to cell death and neurodegenerative diseases due to impaired cellular functions and production of toxic species (Ferrari 2000; Tamagno et al. 2003). ROS is produced from several organelles within the cell such as mitochondria, peroxisomes, ER, plasma membrane, cytosol, and extracellular space (Boveris and Chance 1973; Kukreja et al. 1986; O'Donnell and Azzi 1996; McNally et al. 2003; Gross et al. 2006; Wang et al. 2008a). In order to protect from ROS, cells possess several antioxidants such as vitamins C and E, ubiquinol, and glutathione (Jamieson 1998). Glutathione, under normal circumstances, exists in its reduced state (GSH) because glutathione reductase (Grx1), the enzyme that converts glutathione from its oxidised to its reduced state, is continuously active. GSH can be oxidised, via GSH peroxidase, to form GSSG, simultaneously reducing hydrogen peroxide to water. GSSG is reduced back to GSH by GSH reductase and nicotinamide adenine dinucleotide phosphate (NADPH) (Jones 2006). Neuronal dysfunction in disease is often characterised by low GSH:GSSG ratios (Filomeni et al. 2003).

Mitochondria in particular produce high levels of ROS due to OXPHOS in the electron transport chain. If ROS levels increase significantly, oxidative damage occurs to the mitochondrial membrane and causes lipid peroxidation (reaction chain of oxidative degradation of lipids), changes to membrane permeability and damage to mitochondria DNA, proteins, and molecules. This triggers expression of NF- κ B that

triggers inflammasome genes triggering the apoptotic pathway (Ichimura et al. 2003; Wang et al. 2010; Bulua et al. 2011; Naik and Dixit 2011; Próchnicki and Latz 2017; Liu et al. 2018).

Mitochondria provide energy, in the form of ATP to the cell, they buffer cytosolic Ca^{2+} and sequester pro-apoptotic factors. As a result, mitochondria dysfunction causes excitotoxicity, metabolic insufficiency, cell death and oxidative damage (Heales et al. 1999; Kösel et al. 1999; Nicholls et al. 1999; Tatton and Olanow 1999; Sawa 2001; Krieger and Duchen 2002; Swerdlow and Kish 2002; Koch et al. 2003; Nieminen 2003; Rego and Oliveira 2003). The function of mitochondria in neurons is in part dependent on coordination with peroxisomes as β -oxidation produces acetyl-CoA needed for the Krebs cycle. Deficits in peroxisome biogenesis induces mitophagy by increasing mitochondrial oxidative stress (Rahim et al. 2016). Inhibition of peroxisome biogenesis also results in inner mitochondrial membrane alterations, reduced mtDNA and an increase in mitochondrial volume (Dirkx et al. 2005; Peeters et al. 2015; Salpietro et al. 2015), highlighting the importance to maintain peroxisome number and function in energetic cells such as neurons.

Mitochondria are continuously changing shape as they undergo fission and fusion events, controlled by GTPases (Hoppins et al. 2007). Fusion, mediated by Opa1 and the mitofusins, is stimulated by energy demand and stress, allowing damaged mitochondria to share components as the first line of defence. Mitochondria fission, however, is mediated by cytosolic Drp1 and generates new organelles in physiological conditions as the final step in the biogenesis pathway (Hoppins et al. 2007). Fission also occurs as mitochondria become damaged and produce excessive ROS through OXPHOS.

Mitochondria have been directly linked to axonal maintenance as the release of mtROS and pro-apoptotic factors leads to axonal degeneration whilst the function of mitochondria to buffer Ca^{2+} levels protects axons from stress (Lucius and Sievers 1996; Koeberle and Ball 1999; Alvarez et al. 2008; Avery et al. 2012). In the early inflammatory stages of diseases, such as multiple sclerosis (MS), axonal damage is exacerbated by the inflammatory cascade, microglia activation, oxidative stress, and mitochondrial dysfunction (Liu et al. 2001; Smith and Lassmann 2002; Lassmann 2014). At later stages, energy needs are greater due to loss of trophic support provided by myelin. Sodium channels are therefore redistributed, increasing

intracellular calcium levels in axons which leads to axonal fragmentation due to unsatisfied energy demands (Waxman 2006; Nave and Trapp 2008; Simons et al. 2014). Therefore, mitochondria dysfunction is one of the crucial steps in axonal damage.

There have been reports demonstrating that mitochondria, the ER, and the actin cytoskeleton all play a role in mitochondria fission, a process where mitochondria divide into two smaller separate organelles. During fission, mitochondria initially undergo pre-constriction followed by Drp1 binding at this site causing constriction of the mitochondrion to form two mitochondria (**Chapter 1, Section 1.5**) (Hoppins et al. 2007). There are still unknowns in the mitochondria fission process, such as how fission is initiated, what determines the pre-constriction site, and how Drp1 is recruited. Initial understandings that actin plays a role in mitochondria fission was identified when alternations in actin filaments caused changes in mitochondria length and in the recruitment of Drp1 (DuBoff et al. 2012).

It is known that mitochondria fission occurs at ER contact sites, demonstrating that the ER and mitochondria interact (Friedman et al. 2011). Suppression of ER-bound inverted formin 2 (INF2) -isoform CAAX, a formin involved in both actin polymerisation and depolymerisation (Chhabra and Higgs 2006), caused mitochondria length to more than double (Korobova et al. 2013) suggesting the importance of INF2 in mitochondria length and dynamics. Furthermore, actin filaments are needed for INF2-mediated fission. In addition, INF2 increased Drp1-mitochondria association suggesting the importance of INF2 in mitochondria maintenance and its link with the actin cytoskeleton (Korobova et al. 2013). It is suggested that INF2 is activated to polymerise actin between the mitochondria and ER and actin polymerisation drives a force to pre-constrict mitochondria in preparation for Drp1 ring to assemble at the constriction site in order to carry out mitochondria fission. Furthermore, the ability of INF2 to also depolymerise actin may suggest its function to destabilise actin filaments once fission has occurred (Hatch et al. 2014).

In addition to Cdk12, another Cdk, Cdk5, has been identified to be important for cargo trafficking in the AIS (Klinman et al. 2017) and also in maintaining AIS size (Trunova et al. 2011). Importantly, Cdk5 was found to regulate the actin cytoskeleton, where p35 and p39 bind to F-actin to recruit Cdk5 for its stabilisation. G-actin on the other hand binds to Cdk5 and inhibits its function directly (Shah and Rossie 2018). As Cdk12 has previously shown to regulate proximal axon width (**Chapter 3**), it is

important to determine whether Cdk12 and Cdk5 genetically interact in order to maintain AIS size, potentially pointing to a novel biological pathway.

5.2.1 Aims and objectives

I previously showed that loss of *Cdk12* contributes to proximal axon swellings in glutamatergic neurons (**Chapter 3**), which at 21 d.p.e. were most apparent. To determine if this region was the AIS, I screened several AIS markers and identified that Cdk12 regulates actin distribution in the proximal axon and that an abundance of actin was present in the proximal axon swellings (**Chapter 4**) in the *Cdk12* mutant neurons. To further understand the functional consequence of this I decided to investigate the physiological changes in the neuron and mitochondria that take place prior to neurodegeneration, induced by loss of *Cdk12*.

- My first objective will be to determine the biochemical state of the whole neuron in *Cdk12*-deficient *Drosophila* neuronal clones in the wing. I will look at neuronal Ca^{2+} levels and redox states in the neuron using *in vivo* biochemical reporters. I will further determine whether observed actin changes impact the morphology or amount of ER present in the proximal axon.
- The second objective will be to determine if there are any physiological changes to the mitochondrial network. I will specifically investigate changes to mitochondria morphology, calcium levels and redox states in glutamatergic neurons at 21 d.p.e. in MARCM clones using *in vivo* biochemical sensors that are specific to the mitochondrial compartment.
- Lastly, we will determine whether there is an epistatic relationship between Cdk12 and Cdk5 to maintain the size of the proximal axon.

5.3 Experimental design

In order to investigate whether actin redistribution, seen in *Cdk12* null clones (**Chapter 3**), had an impact on the Ca^{2+} levels, MARCM crosses were set to enable wing neurons to be visualised using Tomato fluorophore and Ca^{2+} levels and redox states measured using several modified GFPs. To measure neuronal calcium levels, a Ca^{2+} marker, GCaMP (a GECI), was used which changes conformation depending on cellular levels, see **Figure 5.1** for schematic, under UAS control (*UAS-GCaMP6F*).

MARCM crosses were set for control and *Cdk12*^{-/-} null clones and flies were aged and imaged at 21 d.p.e., see **Figure 5.2A** and **Figure 5.2B** control and *Cdk12*^{-/-} crossing schemes. N=7 for both control and mutant flies.

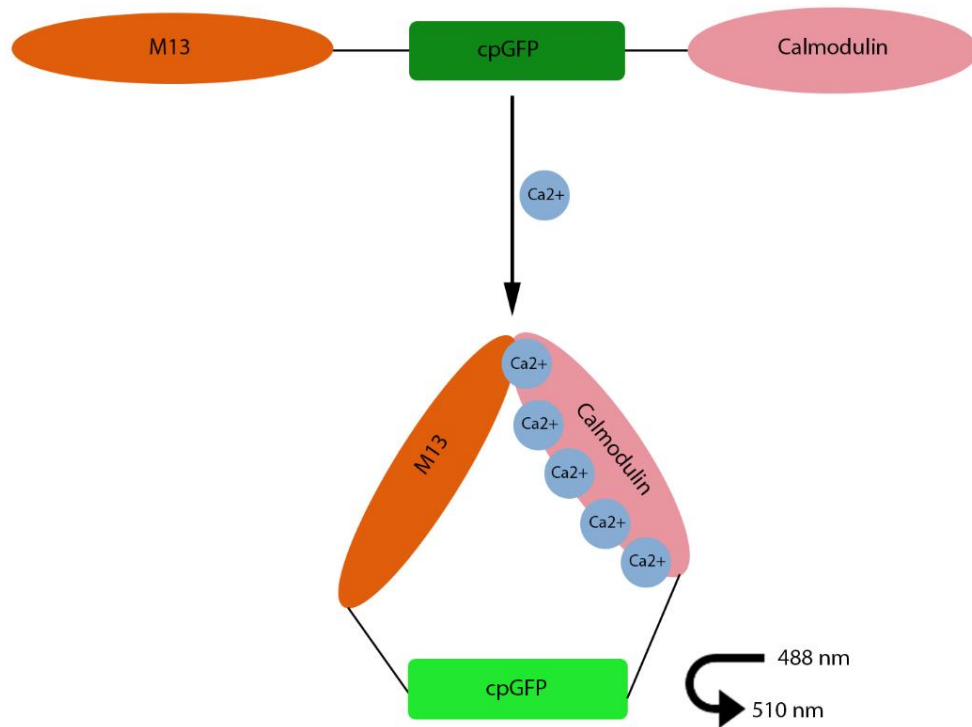


Figure 5.1 GCaMP schematic. GCaMP, consisting of Ca²⁺- binding protein calmodulin, Ca²⁺/calmodulin-binding motif M13 (from myosin light chain kinase) and a cpGFP, undergoes a conformational change of cpGFP when calcium binds to calmodulin and its binding motifs. This change causes cpGFP to switch protonation state and alter spectral properties and emit green light at 488 nm. Image adapted from Zhong and Schleifenbaum (2019) and Pomeroy et al. (2017) (Pomeroy et al. 2017; Zhong and Schleifenbaum 2019).

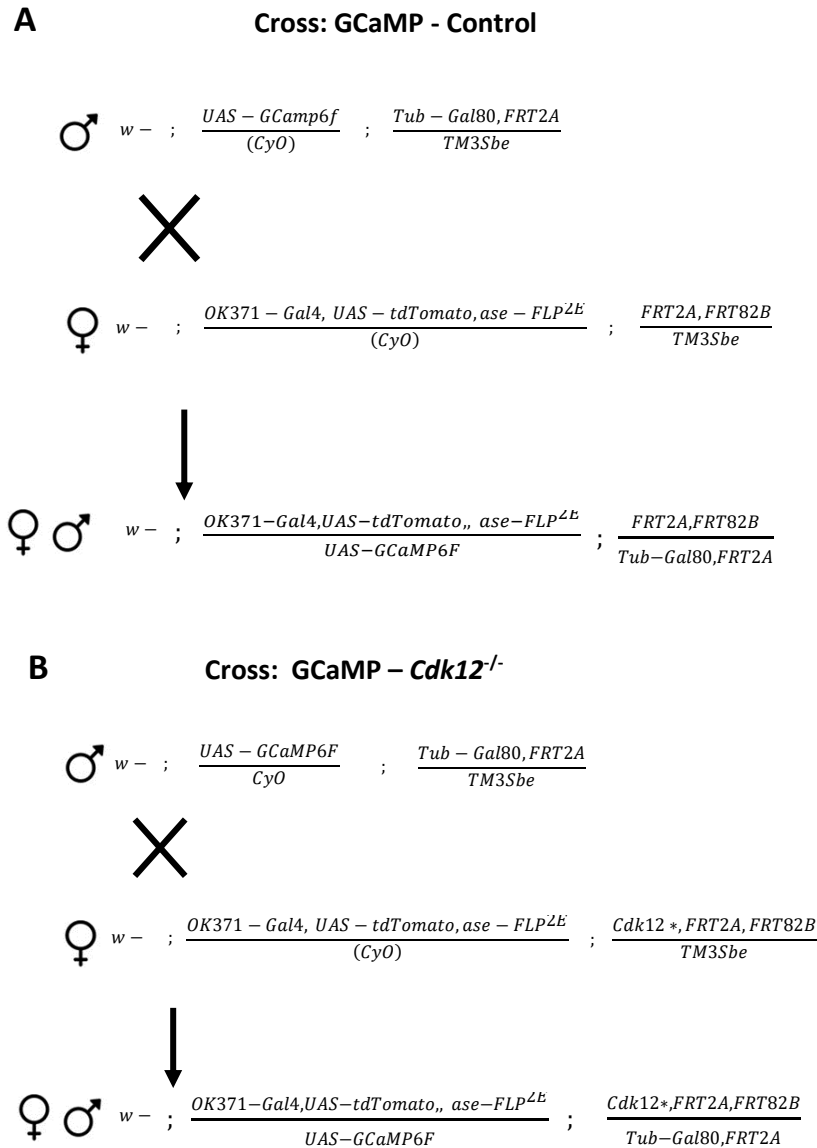


Figure 5.2 Fly crosses to generate GFP-tagged GCaMP expressing MARCM clones. The GFP-tagged GCaMP (*UAS-GCaMP6F*) line was integrated onto chromosome II and the stock was made with a repressive element and FRT site on chromosome III. This line was crossed with the tester line with the glutamatergic driver, Tomato fluorophore and flippase (on chromosome II) and two FRT sites on III for control and *Cdk12* null expressing (on chromosome III) line (B).

To measure the redox state in *Drosophila* neurons, roGFPs were used as a useful tool to measure the change in ratiometric fluorescent changes at 405 nm (blue channel) and 488 nm (green channel), see **Figure 5.3** for schematic. To determine whether actin redistribution had an effect on the redox state, I looked at a Grx-based fluorescent sensor of glutathione oxidation (*UAS-cytoGrx1roGFP*) in neuronal MARCM clones at 21 and 24 d.p.e., see **Figure 5.4** for control and mutant crossing schemes. N=10 and N=3 flies were used for control and *Cdk12*^{-/-}.

roGFPs can be conjugated to different proteins, such as Grx1 or peroxidase 1 (Orp1) that reports roGFP oxidation by glutathione disulfide (GSSG) or hydrogen peroxide (H_2O_2), respectively. In the case of Orp1, H_2O_2 oxidation causes Orp1 to form an SOH bond with its reactive cysteines that later forms a disulfide bridge. Due to dithiol/disulfide interchange, the disulfide bond is transferred to the roGFP molecule attached due to close proximity, causing roGFP to undergo a conformational change and display an emission shift from 488 nm to 405 nm. In order to determine the redox state, the ratio in emission wavelength at 510 nm is measured when the sample is excited at 405 nm and 488 nm. If the sample has been oxidised then the intensity of the emitted light at 510 nm will be higher at 405 nm and lower at 488 nm. (Gutscher et al. 2009). The concept is similar for Grx1, the enzyme that oxidises GSH to GSSG. GSSG oxidation forms an S-glutathionylation (SSG) bond on the Grx1 molecule that is then exchanged to roGFP, releasing two GSH molecules. roGFP then forms a disulfide bond and undergoes a conformational change, displaying an emission shift from 488 nm to 405 nm. (Gutscher et al. 2008).

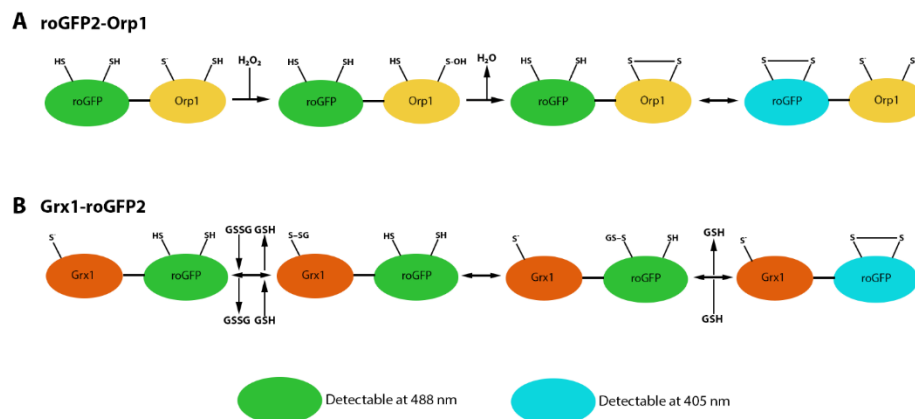


Figure 5.3 Schematic of the mechanism behind Orp1 and Grx1 roGFP oxidation. H_2O_2 triggers oxidation of roGFP attached to Orp1 (A) whilst oxidised GSH (GSSG) triggers roGFP oxidation via Grx1 (B). Image adapted from Fujikawa et al. (2016) (Fujikawa et al. 2016).

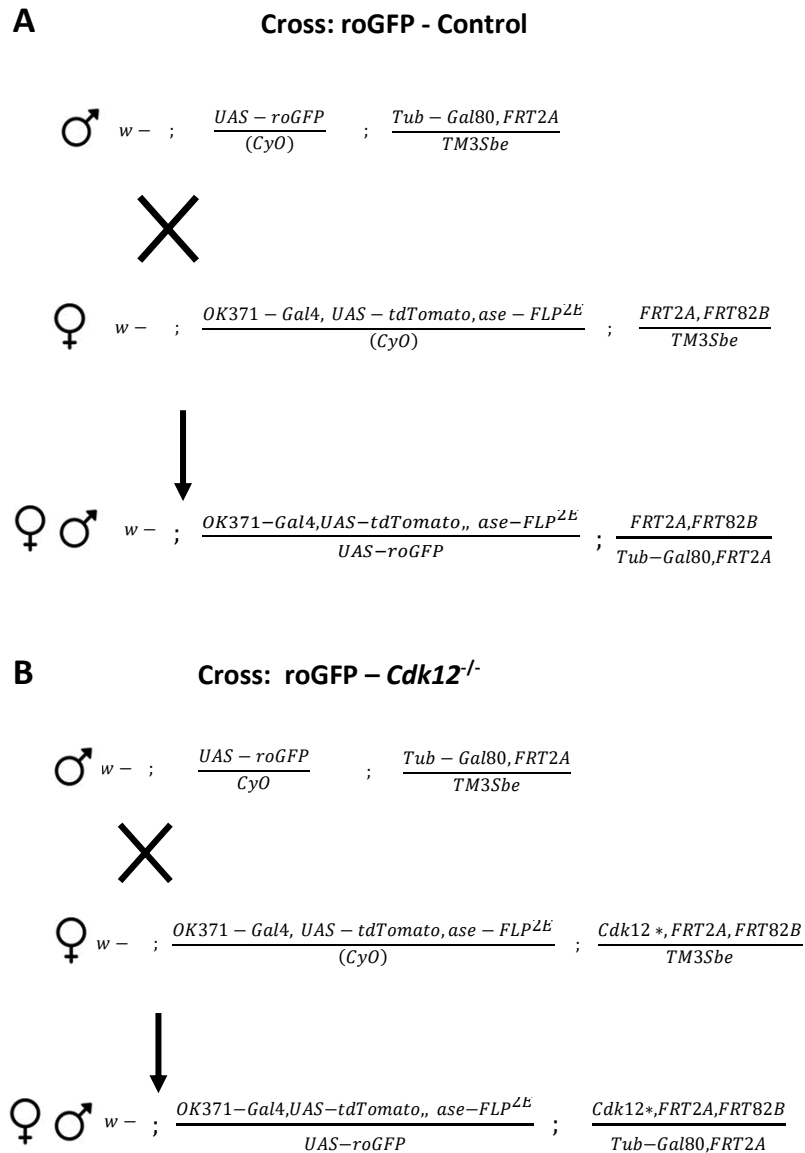
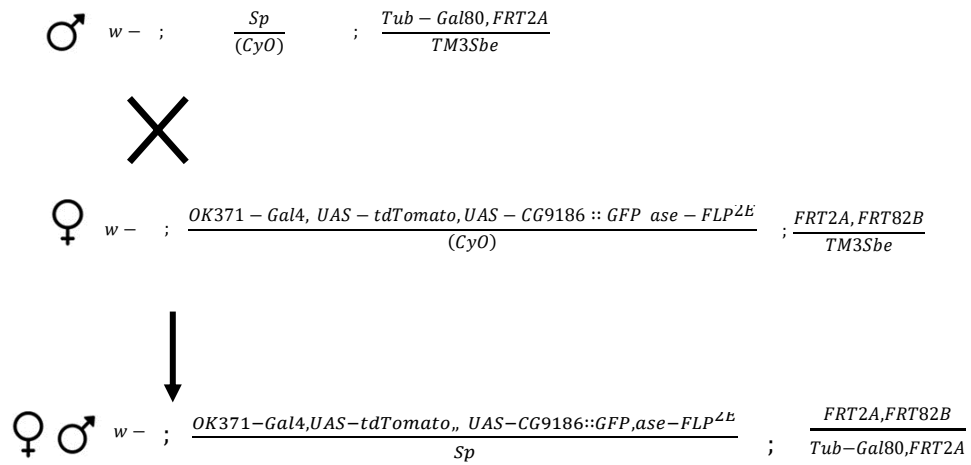


Figure 5.4 Fly crosses to generate GFP-tagged glutathione and hydrogen peroxide redox states in MARCM clones in neurons and mitochondria. GFP-tagged roGFPs inserted on chromosome II and a repressor element and FRT site on III were crossed with control (A) and *Cdk12* null lines (B).

To determine the effect actin redistribution had on the ER distribution in neurons, GFP-tagged ER protein (*UAS-CG9186::GFP*) was expressed in neuronal clones at 21 d.p.e. N=7 and N=11 flies were used for control and mutant, respectively, see genetic crossing schemes in **Figure 5.5**.

A Cross: Endoplasmic reticulum - Control



B Cross: Endoplasmic reticulum - *Cdk12*^{-/-}

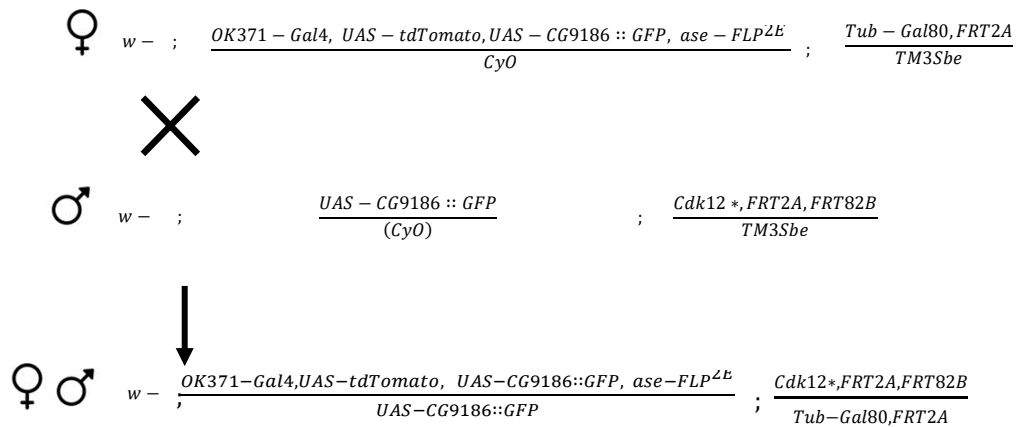


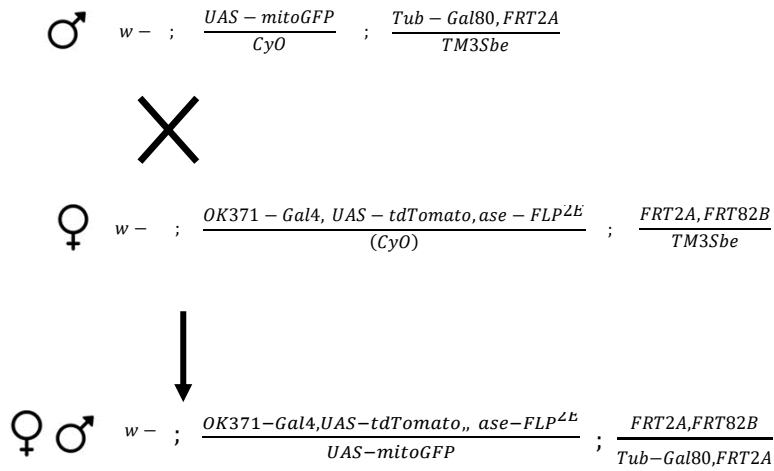
Figure 5.5 Fly crosses to generate GFP-tagged ER expressing MARCM clones. Genetic crosses for GFP-tagged ER was integrated onto chromosome II with a repressor element and FRT site on III and crossed with control (A) and *Cdk12*^{-/-} lines (B).

Next, to investigate whether actin redistribution had an impact on mitochondrial morphology in MARCM clones, I visualised GFP-tagged mitochondria (*UAS-mitoGFP*) in neurons at 21 and 35 d.p.e. GFP is incorporated into mitochondria through conjugation to mitochondrial import sequence derived from hCOX8A. Genetic crosses are represented in **Figure 5.6**. N=7 and N=10 used at 21 d.p.e in control and mutant flies.

In addition to determining the effect the redistribution of actin had on mitochondria morphology, I decided to look at the role of Drp1, a mitochondria fission protein. To investigate whether Drp1 played a role in mitochondria morphology changes, *Drp1* expression was reduced in MARCM clones by RNAi (**Chapter 2, Section 2.2.3**). Genetic crosses are depicted in **Figure 5.7**. N=7 and N=10 flies were used for control and mutant.

I also wanted to determine whether actin redistribution had an effect on the Ca^{2+} dynamics in mitochondria. A calcium-specific indicator, GCaMP, was used (see above, see **Figure 5.1** for schematic) that was directed specifically to mitochondria via conjugation to the mitochondria import sequence and expressed also under UAS control (*UAS-mitoGCaMP*). For control and mutant crossing scheme, see **Figure 5.8**. N=10 flies were used for both genotypes at 21 and 24 d.p.e.

A Cross: Mitochondria - Control



B Cross: Mitochondria - *Cdk12*^{-/-}

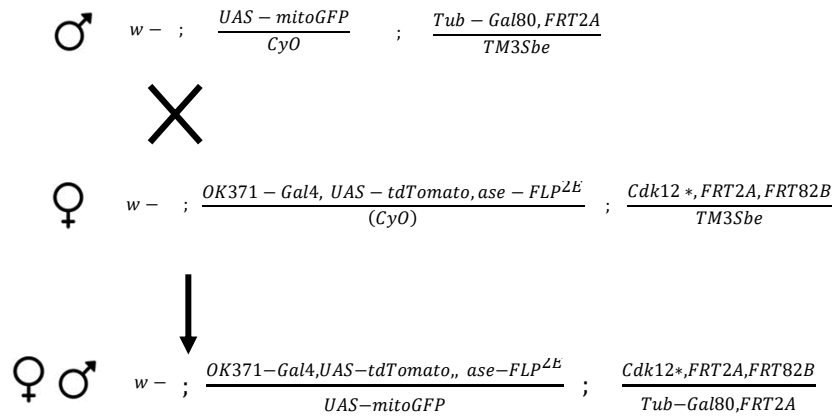


Figure 5.6 Crossing scheme for MARCM clones expressing GFP-tagged mitochondria. Genetic crosses expressing GFP-tagged mitochondria on chromosome II with a repressor and FRT site on III crossed with control (A) and *Cdk12* null line (B).

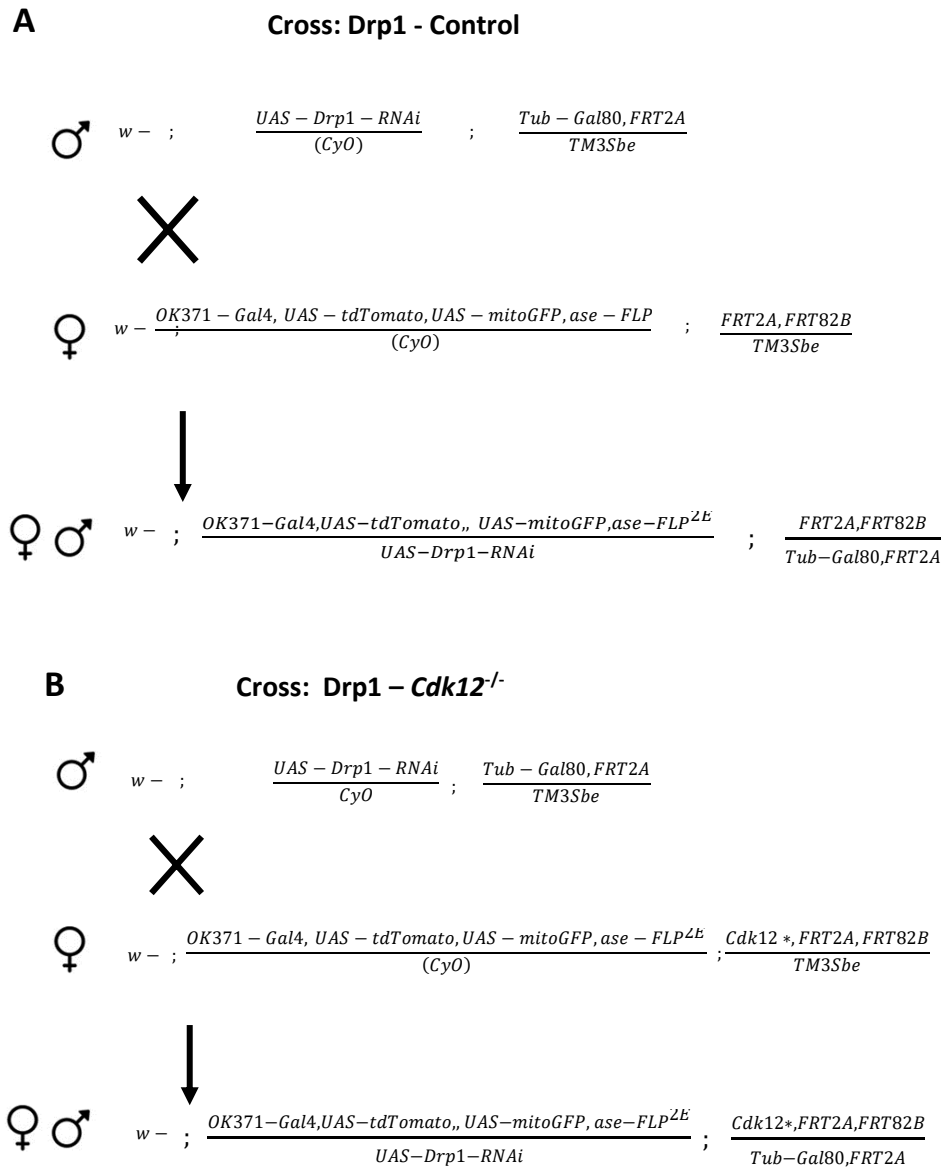


Figure 5.7 Fly crosses to generate *Drp1* knock down expressing MARCM clones. Genetic crosses for *UAS-Drp1-RNAi* expressed on chromosome II and a repressor and FRT site on III, crossed with control (A) and *Cdk12* null lines (B).

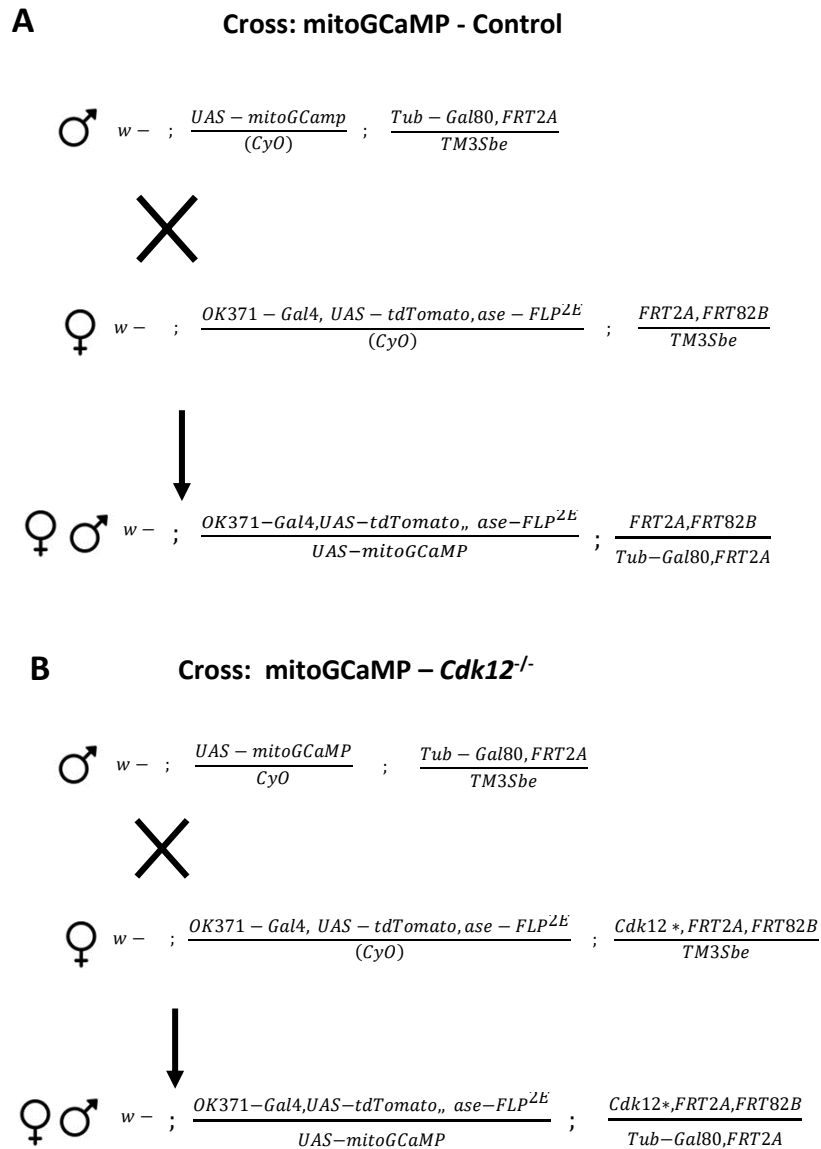


Figure 5.8 Crossing scheme to generate GFP-tagged mitoGCaMP expression in neuronal MARCM clones. Genetic crosses to show GFP-tagged mitochondrial GCaMP integrated on chromosome II with a repressor and FRT site on III and crossed with control (A) and *Cdk12* null lines (B).

Following on from mitochondria morphology and Ca^{2+} levels, I also wanted to investigate if actin redistribution played a role on the mitochondria redox state. I used roGFPs (as mentioned above, see **Figure 5.3** for schematic) specific to mitochondria, to measure fluorescent sensors of glutathione (*UAS-mito-roGFP2-Grx1*) and hydrogen peroxide (*UAS-mito-roGFP-Orp1*) oxidation, both under the control of UAS in MARCM neuronal clones at 21 d.p.e., see crossing schemes in **Figure 5.4**. N=10 to measure glutathione levels and N=10 and N=13 to measure hydrogen peroxide levels for the control and mutant respectively.

An addition protein-of-interest, Cdk5, was previously known to be important in maintaining AIS size (Trunova et al. 2011). To investigate whether Cdk5 acted in the same pathway as Cdk12 and had an effect on actin redistribution, in the proximal axon, a kinase-dead (*UAS-Cdk5KA*) and wild-type (*UAS-Cdk5WT*) versions. These were kindly gifted from the Giniger lab (USA). For 21 d.p.e., N=13 and N=10 for *UAS-Cdk5KA* and N=10 and N=11 for *UAS-Cdk5WT* and at 24 d.p.e., N=8 and N=9 for *UAS-Cdk5KA* and N=10 for *UAS-Cdk5WT* for control and mutant, respectively. In addition, Cdk5 expression was further reduced using RNAi-knock downs (*UAS-Cdk5-RNAi#1* and *UAS-Cdk5-RNAi #2*) of Cdk5 were expressed at 21 and 24 d.p.e. For 21 d.p.e., N=10 and N=14 for *UAS-Cdk5-RNAi#1* and N=11 for *UAS-Cdk5-RNAi #2* and N=8 and N=2 for *UAS-Cdk5-RNAi#1* and N=10 and N=8 for *UAS-Cdk5-RNAi#1* at 24 d.p.e., for control and mutant, respectively. See genetic crosses depicted in **Figure 5.9**.

All stocks used are represented in **Appendix 1** and an explanation of each transgene is described in **Appendix 3**. All figures were designed using Adobe Photoshop 2022 and data analysed on GraphPad Prism using 2-way ANOVA, unpaired and Welch's correction t-test statistical analysis and Bonferroni *post hoc* tests to determine statistical differences (**Chapter 2, Section 2.11**).

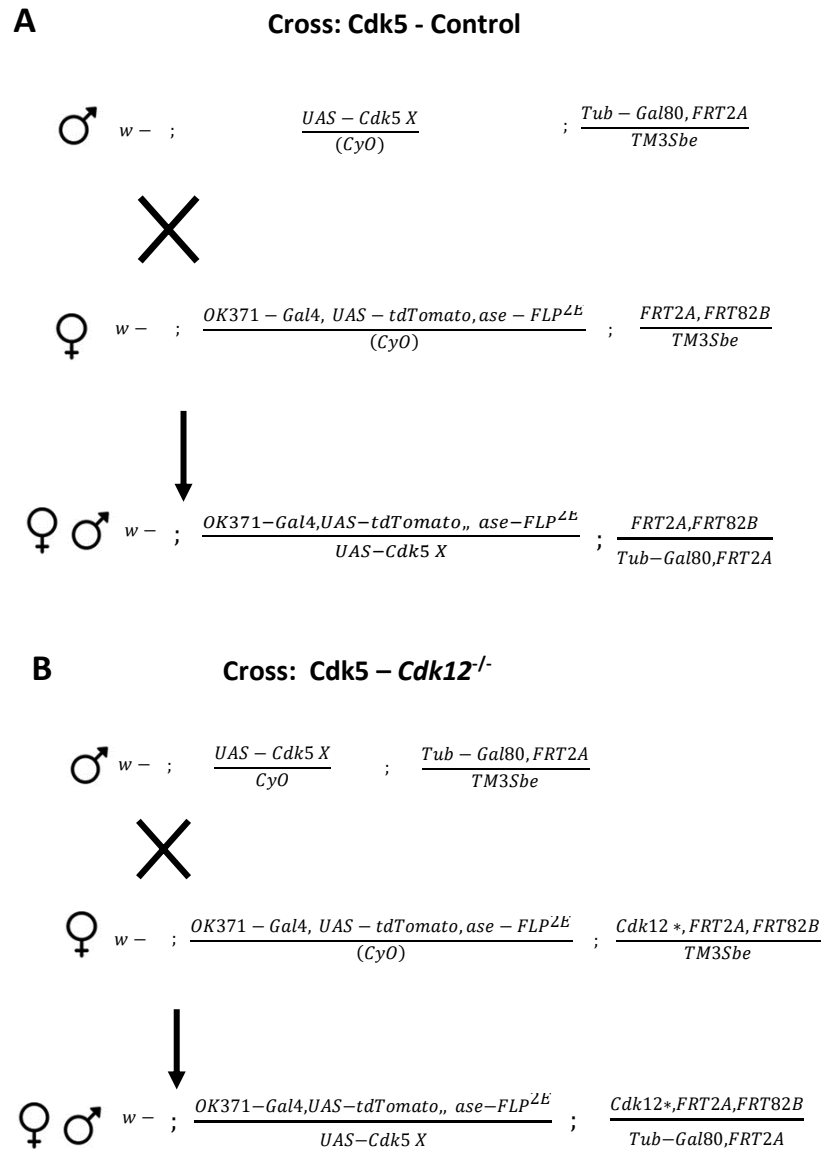


Figure 5.9 Fly crosses for overexpression of *Cdk5* in MARCM clones. Kinase-dead, wild-type, and two individual RNAis (#1 and #2, as denoted by X on figure) were expressed on chromosome II with a repressor element and FRT site on chromosome III. Flies were crossed with control (A) and *Cdk12* null lines (B)

5.4 Results

5.4.1 Cdk12 regulates neuronal calcium levels in the proximal axon swellings

Morphological changes in the ion channel rich section of the axon may alter Ca^{2+} homeostasis and neuronal functionality. To investigate whether the loss of Cdk12 affected Ca^{2+} levels in the neuron of adult wings, I expressed GCaMP6F in neuronal clones and investigated levels at 21 d.p.e. through live cell imaging approaches defined in (Vagnoni and Bullock 2016). Photomicrographs showed increased Ca^{2+} levels in the mutant in the proximal axon swellings as opposed to the control (**Figure 5.10A**). An unpaired t-test revealed a significant increase between genotype in fluorescence intensity of Ca^{2+} in the mutant at 21 d.p.e. (**Figure 5.10B**, $p < 0.05$). This indicates that proximal axon swellings or actin redistribution associated with loss of *Cdk12* may alter Ca^{2+} homeostasis.

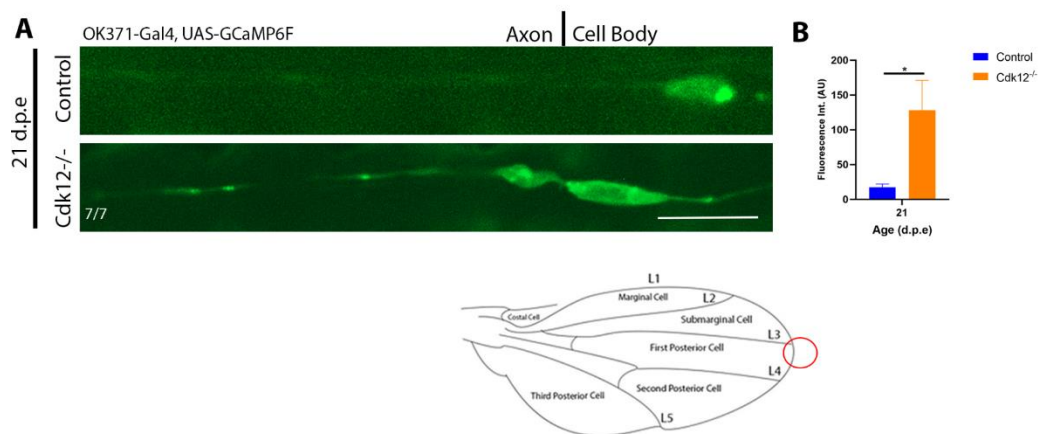


Figure 5.10 Cdk12 increases calcium levels in the proximal axon swellings. Increased calcium levels were greater in the *Cdk12* null mutant (A). Fluorescent intensity was recorded at 21 d.p.e. (B). Data was analysed using Unpaired two-tailed t-tests and significant differences annotated as $p < 0.05^*$ compared to the control. Graphs are expressed as Mean \pm SEM, distal tip neurons were imaged and analysed, see red circle on wing image. Scale bar is 10 μm .

5.4.2 Cdk12 had no effect on glutathione disulfide oxidation levels in the neuron

Oxidation by GSSH is detectable by roGFP-Grx1. To investigate the effect of Cdk12 on GSSH oxidation levels, Grx1-roGFP2 was expressed in the neuron in the proximal axon, and the fluorescent level ratios between 405 nm and 488 nm wavelengths were measured to indicate the degree of GSSG and GSH respectively (**Figure 5.11A**). An unpaired t-test results revealed no significant changes between genotypes ($p=ns$, **Figure 5.11B**) at 21 d.p.e. in the proximal axon. This therefore indicates that Cdk12 ablation had no effect on the antioxidant, glutathione, levels in neurons.

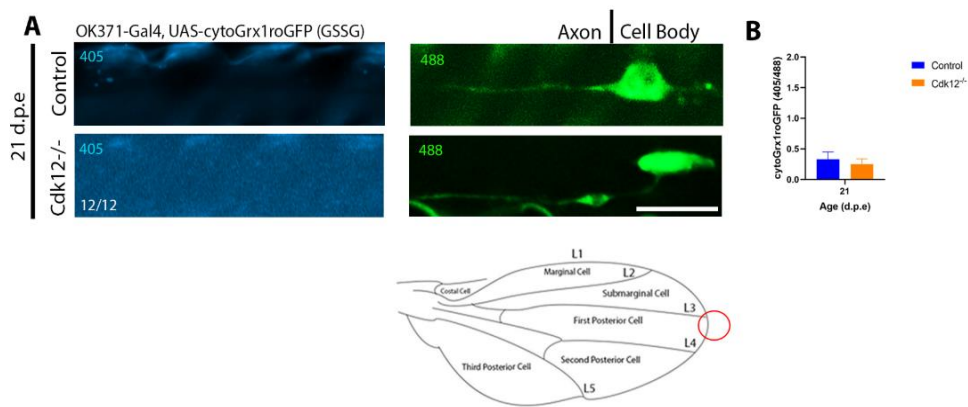


Figure 5.11 Cdk12 had no effect on glutathione levels in the neuron. Glutathione levels were expressed and measured in the neuron (A, B) at 21 d.p.e. No significant changes were seen. Data was analysed using unpaired t-tests. Graphs are expressed as Mean \pm SEM. Scale bar was 10 μ m. Images and analysis were recorded at the distal tip, see red circles on wing images. 405 nm and 488 nm correspond to wavelength.

5.4.3 Cdk12 influences endoplasmic reticulum levels in the proximal axon.

F-actin has been implicated in ER formation in *Xenopus* development (Wöllert et al. 2002) and in the trafficking of ER vesicles in the neuron via myosin V (Tabb et al. 1998). In addition, it has also previously been suggested that actin polymerisation is controlled by INF2 between the ER and mitochondria and it is the actin polymerization that influences pre-constriction force in order for Drp1 to facilitate mitochondrial fission (Korobova et al. 2013; Moore et al. 2016). As Cdk12 influences actin redistribution in the proximal axon (**Chapter 4**), I therefore wanted to investigate whether Cdk12 also affected ER distribution in the proximal axon. To determine the possible effect of *Cdk12* ablation on the ER distribution and quantity, I expressed an ER marker in the neuronal clones at 21 d.p.e. in the proximal axon (**Figure 5.12A**). Welch's correction two-tailed t-tests revealed a significant increase between genotypes at 21 days p.e in the proximal axon swellings (**Figure 5.12B**) suggesting that Cdk12 influences the amount of ER in the proximal axon.

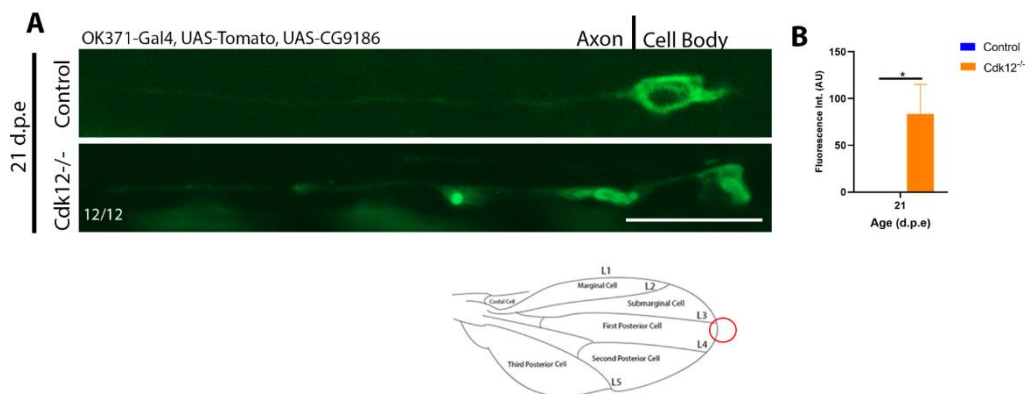


Figure 5.12 Cdk12 influences ER distribution in the proximal axon swellings. The ER marker (*UAS-CG9186-GFP*) was expressed in the proximal axon swelling at 21 d.p.e. in the *Cdk12* null mutant (A) but *post hoc* tests revealed this was not significant. Data was analysed using two-tailed Welch's correction t-tests. Graphs are expressed as Mean \pm SEM. Scale bar was 10 μ m. Axon number was recorded in the L1 vein, but all other variables were recorded at the distal tip, see red circles on wing images.

5.4.4 Cdk12 controls mitochondrial morphology in the axon and cell body which is controlled by Drp1.

It has previously been reported that with the help of INF2, the actin cytoskeleton produces a pre-constriction force to enable Drp1 to perform mitochondrial fission (Korobova et al. 2013; Moore et al. 2016). Therefore, as Cdk12 regulates actin distribution in the proximal axon, (**Chapter 4**), I wanted to firstly determine whether the loss of *Cdk12* could change the morphology of mitochondria in adult neurons in the wing. Photomicrographs identified smaller, rounded mitochondria in the mutant as opposed to elongated mitochondria in the control (**Figure 5.13A**), suggesting that Cdk12 influences mitochondria morphology.

As Drp1 is important in mitochondrial fission, I wanted to determine whether Cdk12 regulates Drp1-mediated fission. Reduction in *Drp1* by RNAi revealed a rescue of mitochondrial morphology in *Cdk12*^{-/-} neuronal clones, where mitochondria were less fragmented and spherical (**Figure 5.13A**). A 2-way ANOVA revealed significant differences between genotype ($F_{1,30} = 17.16$) and *Drp1* knockdown ($F_{1,30} = 9.06$) in the average feret's diameter of mitochondria. *Post hoc* analysis revealed a significant decrease ($p < 0.05$) in feret's diameter in *Cdk12* ablated conditions compared to control, which was not observed when *Drp1* was knocked down (**Figure 5.13B**). A 2-way ANOVA also revealed significant differences between genotype ($F_{1,30} = 9.98$) in the average mitochondria area. *Post hoc* analysis revealed a significant decrease ($p < 0.05$) in area in *Cdk12* ablated conditions, which was not observed when *Drp1* was knocked down (**Figure 5.13C**). Further analysis of mitochondrial aspect ratio by 2-way ANOVA showed significant differences between genotype ($F_{1,30} = 10.59$) and *Drp1* knockdown conditions ($F_{1,30} = 24.86$). *Post hoc* analysis revealed a significant increase in aspect ratio in control neurons following depletion of *Drp1* ($p < 0.05$) and a significant increase in the aspect ratio of axonal mitochondria in *Cdk12*^{-/-} neurons (**Figure 5.13D**). Importantly, the aspect ratio of mitochondria in *Cdk12*^{-/-} neurons was equivalent to WT, indicating a rescue of the mitochondrial phenotype. This suggests that Cdk12 controls mitochondrial morphology through Drp1-dependent mechanisms.

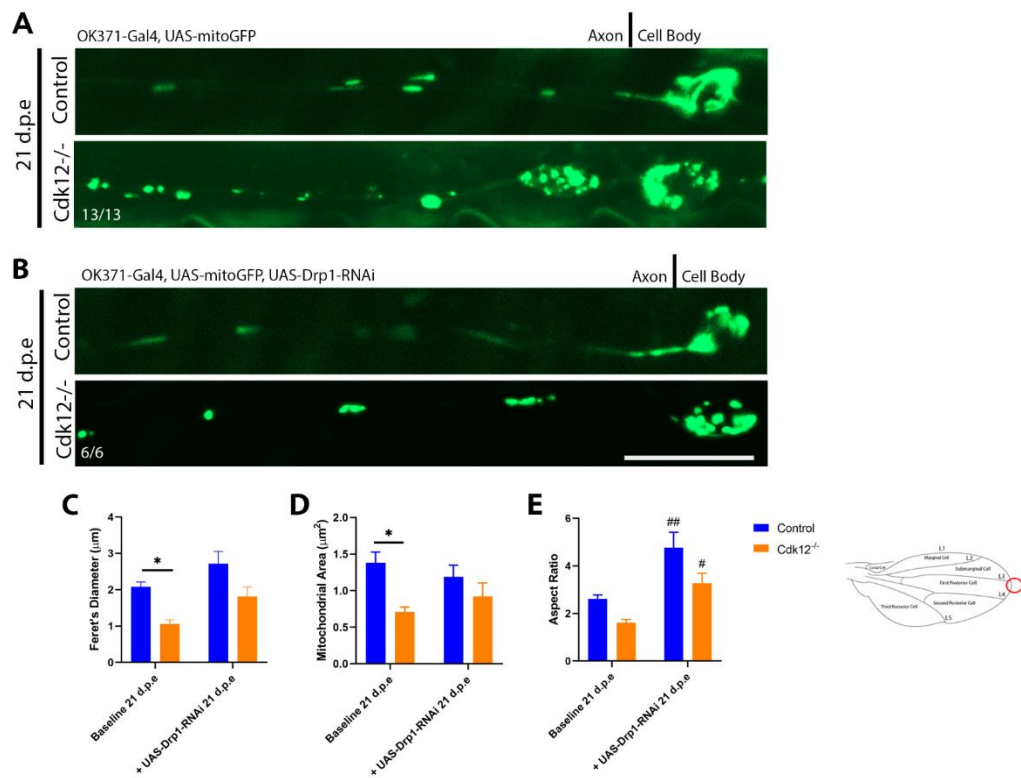


Figure 5.13 Cdk12 and Drp1 control mitochondrial morphology in the axon. Increased mitochondria fission was seen in the mutant compared to the control (A) but was rescued in the *Drp1* null clones (B). Feret's Diameter (C), Aspect Ratio (D) and Mitochondria Area (E) were recorded at 21 d.p.e. for the *Cdk12*^{-/-} mutant and the control in baseline and *Drp1* knockdown wings. Scale bar was 10 µm. Data was analysed using two-way ANOVA and significant differences annotated as $p < 0.05^*$ between genotype and $p < 0.05\#$ and $p < 0.01##$ between baseline and *Drp1* knockdown, compared to their respective genotype controls. Aspect ratio and area were analysed by Tukey *post hoc* tests and feret's diameter by Šidák's *post hoc* test. Graphs are expressed as Mean \pm SEM. 3-30 mitochondria quantified per fly. Mitochondria were recorded at the distal tip, see red circle on wing image.

In addition to the axon, mitochondria in the cell body were also investigated. In the control, mitochondria were elongated, but in the mutant, they were smaller and rounded (**Figure 5.14A**). A 2-way ANOVA revealed significant differences between genotypes in aspect ratio ($F_{1,32} = 12.94$, $p < 0.001$). Bonferroni *post hoc* tests identified no significant differences in Feret's Diameter (**Figure 5.14B**, $p = ns$) and Mitochondrial Area (**Figure 5.14C**, $p = ns$) but a significant decrease was revealed at day 35 p.e in aspect ratio (**Figure 5.14D**, $p < 0.001$). Together, this suggests that Cdk12 controls mitochondrial morphology in the axon and the cell body, which may occur through actin related pathways.

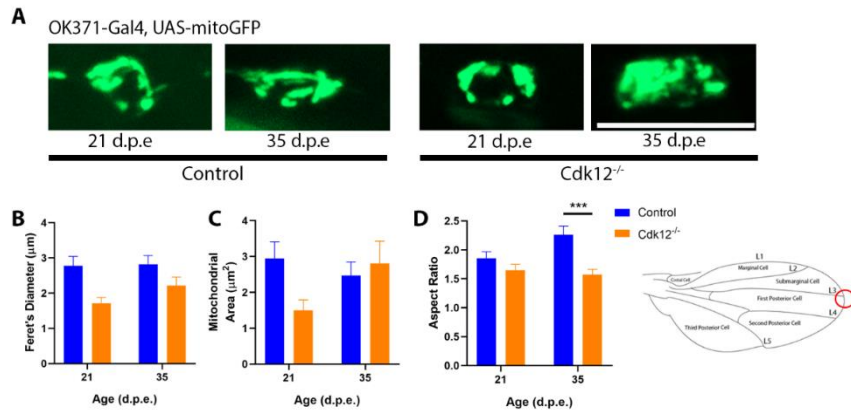


Figure 5.14 Cdk12 controls mitochondrial morphology in the cell body. Increased mitochondrial areas is greater in the null mutant (A). Feret's Diameter (B), Mitochondria Area (C) and Aspect Ratio (D) were recorded at 21 and 35 d.p.e. for the *Cdk12*^{-/-} mutant and the control. Scale bar was 10 μm . Data was analysed using two-way ANOVA and significant differences annotated as $p < 0.001$ *** compared to the control. Data was analysed by Bonferroni *post hoc* test. Graphs are expressed as Mean \pm SEM. Mitochondria were recorded at the distal tip, see red circle on wing image.

5.4.5 Cdk12 does not regulate calcium levels in mitochondria

Cdk12 altered mitochondria morphology and increased fission (Section 5.4.4). To determine whether Cdk12 had an effect on mitochondria Ca^{2+} levels and hence mitochondria dynamics in the proximal axon, the fluorescent levels of mito-GCaMP were measured (Figure 5.15A). A 2-way ANOVA showed no significant changes between genotype/age ($p=ns$, Figure 5.15B) indicating that although Cdk12 altered mitochondria morphology, Cdk12 had no effect on mitochondrial Ca^{2+} buffering.

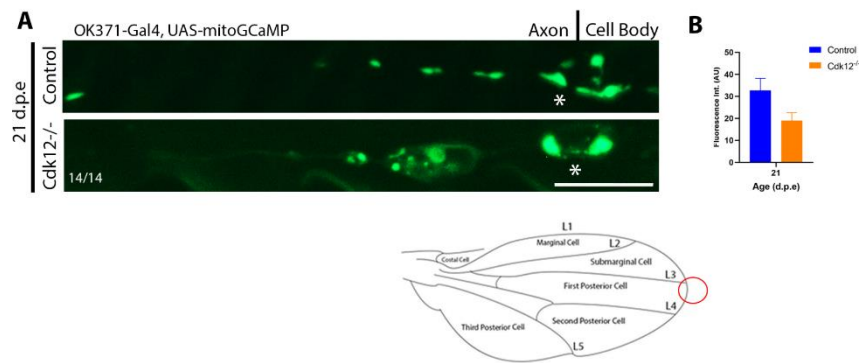


Figure 5.15 Cdk12 had no effect on mitochondrial calcium levels. MitoGCaMP levels were measured at 21 d.p.e. (A) and *post hoc* revealed no significant changes (B). Data was analysed using two-way ANOVA. Data was analysed with Bonferroni *post hoc* test. Graphs are expressed as Mean \pm SEM. Scale bar was 10 μm . Axon number was recorded in the L1 vein, but all other variables were recorded at the distal tip, see red circles on wing images.

5.4.6 Cdk12 had no effect on glutathione and hydrogen peroxide oxidation levels in mitochondria

As mitochondrial morphology was significantly altered in the *Cdk12* null clones, I then decided to determine whether these “balled up” mitochondria produced more ROS. To investigate the effect of *Cdk12* ablation on glutathione redox (using Grx1-roGFP2), and H₂O₂ redox (using roGFP2-Orp1) levels in mitochondria in the proximal axon, the fluorescent ratiometric levels of 405 nm and 488 nm were measured (**Figure 5.16A**). Unpaired t-test results revealed no significant changes in 405/488 ratios between genotype ($p=ns$, **Figure 5.16B**) at 21 d.p.e. in the proximal axon therefore indicating that although *Cdk12* alters mitochondrial morphology it has no effect on mitochondrial ROS.

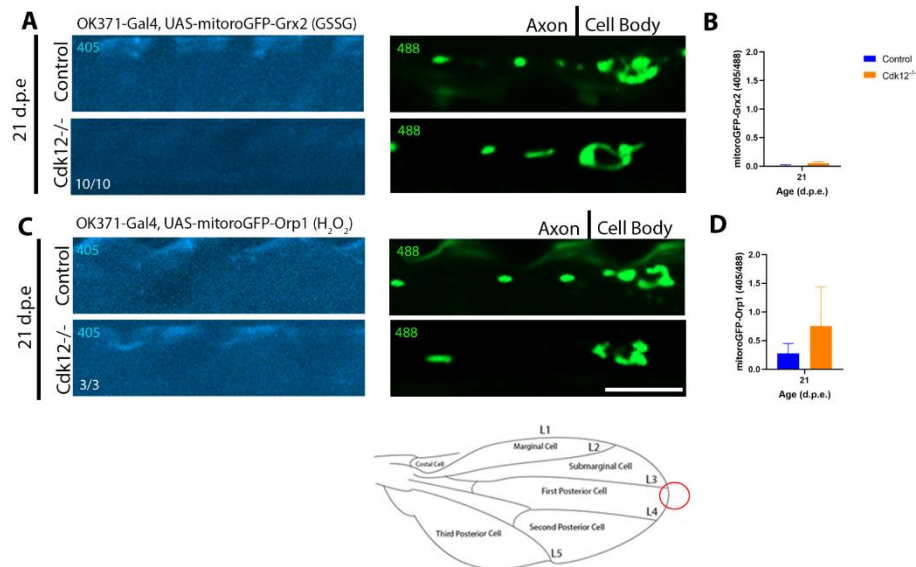


Figure 5.16 *Cdk12* had no effect on glutathione disulfide and hydrogen peroxide oxidation in mitochondria. Glutathione levels were expressed and measured in the mitochondria (A, B) and hydrogen peroxide levels expressed and measured in the mitochondria (C, D), all at 21 d.p.e. No significant changes were seen. Data was analysed using unpaired two-tailed t-tests. Graphs are expressed as Mean \pm SEM. Scale bar was 10 μ m. Images and analysis were recorded at the distal tip, see red circles on wing images. 405 and 488 correspond to wavelength (nm).

5.4.7 Cdk5 does not genetically interact with Cdk12

I have shown that Cdk12 is a regulator of axon size. An additional protein-of-interest Cdk5, was previously known to be important in maintaining AIS size (Trunova et al. 2011). To test whether Cdk5 interacted in the same pathway as Cdk12, I expressed a WT version of Cdk5, a KA version, and two independent Cdk5 RNAs in WT and *Cdk12*^{-/-} MARCM neuronal clones at 21 and 24 d.p.e., all under UAS control. Photomicrographs showed swellings in all *Cdk12* null clones regardless of Cdk5 levels (**Figure 5.17A-E**) at 21 and 24 d.p.e. Bonferroni *post hoc* tests revealed no significant differences between genotype and age of axon number ($p=ns$, **Figure 5.18A**) and cell body number ($p=ns$, **Figure 5.18B**). There was a significant increase in the width of the proximal axon ($p=ns$, **Figure 5.18C**, $F_{4,110} = 43.99$) in neurons lacking *Cdk12* in baseline control ($p<0.01$), *UAS-Cdk5WT* ($p<0.001$) and *UAS-Cdk5-RNAi#2* ($p<0.001$) at both time points. Neither overexpressing nor knocking down Cdk5 was sufficient to induce neurodegeneration, verifying previous results that neurodegeneration occurs at a later stage. This therefore suggests that Cdk5 overexpression or knockdown had no effect on regulating the size of the proximal axon or caused neurodegeneration. This concludes that Cdk12 and Cdk5 are not likely to be in the same genetic pathway.

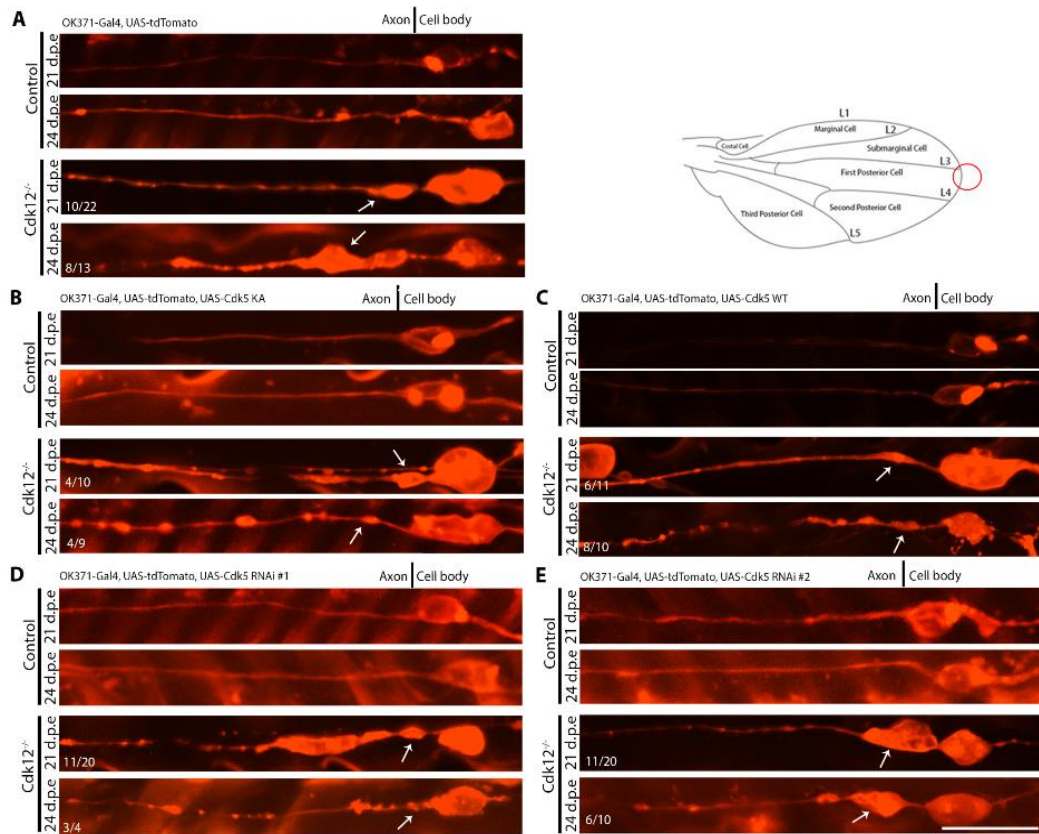


Figure 5.17. Cdk5 does not genetically interact with Cdk12. A *KA Cdk5*, *WT- Cdk5* and two separate *UAS-Cdk5-RNAi* lines (#1 and #2, see **Appendix 1**) were overexpressed under UAS control. N=4-16 flies per time point, 1-2 wings per fly. Axon number was recorded in the L1 vein, but all other variables were recorded at the distal tip, see red circles on wing images. Scale bar was 10 μ m.

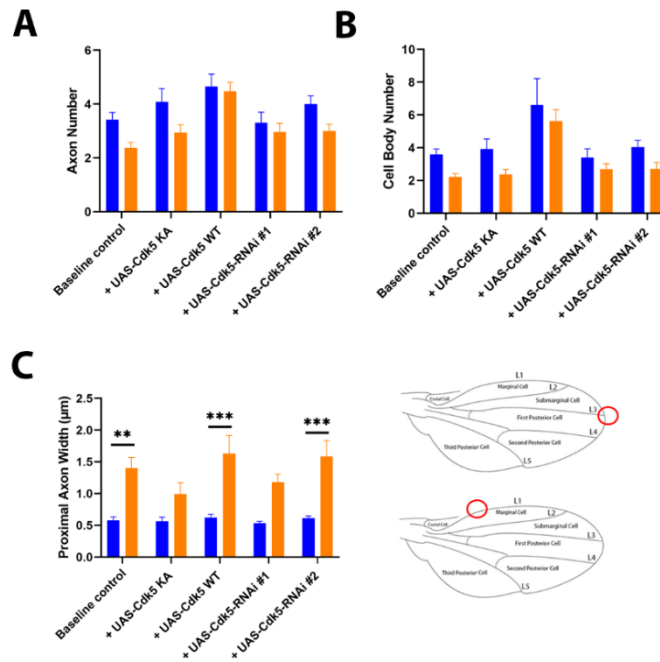


Figure 5.18 Cdk5 does not genetically interact with Cdk12. *KA*- and *WT*- *UAS-Cdk5* and two independent *UAS-Cdk5-RNAi* lines (#1 and #2) were tested. Axon (A) and cell body number (B) were recorded in addition to proximal axon width (C), at 21 and 24 d.p.e. combined time points but denoted as 21 d.p.e. here. Data was analysed using two-way ANOVA and significant differences annotated as $p < 0.001^{***}$ and $p < 0.01^{**}$, compared to the control. Graphs are expressed as Mean \pm SEM. Axon number was measured at the costal vein, but all other variables were measured at the distal tip, see wing schematic.

5.5 Discussion

Data from the previous results chapter (**Chapter 4**) demonstrated that Cdk12 regulates actin distribution in the proximal axon swellings and peroxisome distribution and morphology of glutamatergic neurons. This suggests two things, firstly that the function of the neuron may be compromised prior to cell death and secondly since peroxisomes and mitochondrial coordinate to control metabolism that mitochondrial redox state and dynamics may also be perturbed. Through the use of *in vivo* biochemical sensors and indicators we show that Ca^{2+} are significantly elevated in the *Cdk12*^{-/-} neurons but redox balance is maintained. Conversely, mitochondria display no changes in Ca^{2+} handling and undergo Drp1-mediated fission. This suggests that Cdk12 controls important properties of adult neurons required for adequate function and mitochondrial dynamics.

We discovered that Cdk12 functions to limit Ca²⁺ levels in neurons and overall proximal axon size. It is possible that the actin-rich AIS has been expanded in our mutant and that this has functional consequences to the neuron. The AIS contains numerous sodium and potassium channels to regulate the magnitude and duration of a firing event (Kole and Stuart 2008) which may be controlled through Cdk12-dependent mechanisms. To better understand the consequence of disrupted AIS structure through loss of *Cdk12*, future work may define neuronal electrophysiological function in the form of electroretinograms (ERGs) on mutant and control neurons of the eye to directly measure action potentials in response to light stimulation. It is possible that enlargement of the proximal axon is allowing for a greater number of Ca²⁺ channels, over what is usually seen, which have been found to impact on action potential generation (Bender and Trussell 2009). It has been previously shown that loss of *Cdk12* effects courtship learning in the fly, through heterochromatin remodelling of the X chromosome (Pan et al. 2015). I suggest that these learning deficits may therefore occur through the specific remodelling of the AIS.

Interestingly, we find that neuronal Ca²⁺ levels were not buffered by mitochondria. The voltage-dependent anion channel (VDAC) and mitochondrial Ca²⁺ uniporter are responsible for mitochondrial buffering from the cytoplasm (Tufi et al. 2019). This occurs when cytosolic Ca²⁺ levels between 50 and 500 nM (Imbert et al. 1995; Budd and Nicholls 1996; Hartmann and Verkhratsky 1998), perhaps neuronal Ca²⁺ levels were below 50 nM and hence not buffered by mitochondria. Alternatively Ca²⁺ ions, stored in the ER can be transported at MERCs and enter mitochondria (Chakrabarti et al. 2018). It would be interesting to use an ER specific GCaMP and assess levels within that organelle. Perhaps, increased Ca²⁺ levels in the cytoplasm are not enough to trigger Ca²⁺ induced Ca²⁺ release, which may be needed to prompt mitochondrial uptake.

Loss of *Cdk12* in development and early adulthood may impact neuronal function and in later life induce neurodegeneration. Neurodegeneration may also occur through Ca²⁺ dependent mechanisms. In *Drosophila*, it was previously discovered that reducing Cdk5 activity shortens the AIS (Trunova et al. 2011). Calpains are activated with Ca²⁺ influx and cleave the Cdk5 activator, p35, to form p25 and p10 (Patrick et al. 1999). Calpains also have a role in the breakdown of the ankyrin G/spectrin cytoskeleton (Siman et al. 1984; Schafer et al. 2009) so perhaps the activity of Cdk5 is controlled by calpain activation to maintain the overall AIS size. Therefore, as

calpains are proteases regulated by Ca^{2+} levels, perhaps calpains are also dysregulated in *Cdk12* ablated conditions.

In this chapter, I have shown that Cdk12 and Cdk5 are not likely to genetically interact and may cause proximal axon dysfunction by completely different mechanism, acting in different biological pathways. The experiments suggest that the effect of Cdk12 may be transcriptional since it is localised to the nucleus (**Chapter 3**), whereas Cdk5 functions directly in the cytoplasm. In ALS mouse models, Cdk5 activity causes cargo to accumulate in the cell body and proximal axon in sensory neurons (Cozzolino et al. 2012; Shukla et al. 2012). In addition, even though Cdk5 is not essential for cargo trafficking, high levels of Cdk5 causes misregulation of axonal transport, via the Lis1/Ndel1/dynein pathway (Klinman and Holzbaur 2015). Cdk12 on the other hand may regulate the actin barrier via transcriptional regulation.

I also found that Cdk12 regulates mitochondria morphology in the proximal axon and cell body. Mitochondria fission has been linked to the actin cytoskeleton as actin (F-actin) assembles to the outer membrane of elongated mitochondria to promote fission and prevent fusion (Moore et al. 2016). Actin cycles between different mitochondria populations and assembles for 3-5 minutes before depolarising. As Cdk12 has been shown to redistribute actin (**Chapter 4**) and increase mitochondria fission, perhaps actin is causing the increase in mitochondrial fission. In addition, actin acts as the pre-constriction force behind mitochondrial fission between mitochondria and ER via INF2 (Korobova et al. 2013; Hatch et al. 2014; Moore et al. 2016). The constriction force behind actin facilitates Drp1 recruitment and ability for Drp1 to further constrict mitochondria membranes before fission. In this chapter, I find that Cdk12 normally functions to limit mitochondrial fission and this is controlled by Drp1. It has been previously shown that Drp1 binds to actin filaments (Hatch et al. 2016), which then enhances oligomisation and GTPase activity (Ji et al. 2015), so it is possible that increased actin in this region is therefore recruiting more Drp1 molecules which increases mitochondrial fission. Actin-dependent enhancement of Drp1-mediated fission has been found to be controlled by cofilin (Rehklau et al. 2017). It would therefore be interesting to see whether levels of this depolymerising molecule are altered in the *Cdk12* mutant conditions. In addition, Miro is important in trafficking mitochondria (Glater et al. 2006) and is important in mitochondria morphology as loss of Miro leads to an increase in balled-up mitochondria (Fransson et al. 2003; Frederick et al. 2004; Russo et al. 2009). Perhaps, Miro may also play a role in our observed phenotype.

In addition, Drp1 recruitment also plays a role in peroxisome fission (Kamerkar et al. 2018). A reason for peroxisomes, normally residing in the cell body, to be present in the proximal axon (**Chapter 4**) may be due to increased Drp1-mediated peroxisome fission. As larger organelles such as the rough ER and the golgi complex are restricted to the somatodendritic compartment due to sorting at the PAEZ (Fariás et al. 2015), it may be that smaller peroxisomes are able to avoid and bypass cargo filtering at the PAEZ (and AIS) and hence are present in the proximal axon. It would be therefore interesting to see whether decreasing Drp1 in *Cdk12* ablated conditions is able to restrict peroxisomes to the soma and dendrites in future experiments.

Mitochondrial mobility and morphology have also been linked. Increased fission is linked to anterograde transport demonstrating that morphology and mobility of mitochondria may contribute to the overall cell function (Varadi et al. 2004). In addition, mitochondria trafficking is stalled with increased cytosolic Ca^{2+} (Rintoul et al. 2003). Increased Ca^{2+} destabilises Miro1 binding to kinesin motor proteins to microtubules, preventing mitochondria transport in axons (Wang and Schwarz 2009). In this chapter, no increase in mitochondria Ca^{2+} was seen suggesting mitochondria would still be motile.

Peroxisomes and mitochondria cooperate in several metabolic and signalling pathways and they both communicate through the release of biological messengers such as ROS, lipids and metabolites (Fransen et al. 2017). Mitochondrial fragmentation (fission) is influenced by peroxisome biogenesis as deletion of Pex3 and Pex5 (important for peroxisome assembly and function) in mouse fibroblasts increased mitochondrial fragmentation (Tanaka et al. 2019). As *Cdk12* regulates peroxisome positioning and mitochondrial morphology, perhaps the loss of *Cdk12* could affect mitochondria morphology due to altering peroxisome biogenesis.

In this chapter, I showed that *Cdk12* influences ER levels in the proximal axon. In addition to the cell body, ER distribution was also found in the proximal axon swellings. ER distribution was also found further down the proximal axon and this may be a lipid droplet contact site as overexpression of the ER marker, CG9186, causes an increase in lipid droplet clustering (Thiel et al. 2013). In addition, this may also be a peroxisome that is bound at an ER-peroxisome contact site. Perhaps, *Cdk12* is also regulating and increasing contact sites between ER and peroxisomes or lipid droplets. Electron microscopy is a popular method to study ER contact sites (Csordás et al.

2006; Sood et al. 2014; Wu et al. 2017b) and therefore I propose using this technique to determine whether Cdk12 is increasing ER contact sites.

In this chapter, I also found that Cdk12 did not regulate glutathione and hydrogen peroxide types of ROS. This was surprising since it has previously been shown that Cdk12 regulates nuclear factor-erythroid factor 2-like 2 (NFEF2L2), a transcription factor that targets genes, such as GST and glutamate-cysteine ligases, important in helping protect against oxidative stress (Lee and Johnson 2004). Therefore, this suggests that loss of NFEF2L2 is not sufficient to induce ROS at baseline, and its loss may only be to increase ROS under neuronal damage conditions. In addition, reduction of GSH have previously been linked to the inhibition of several actin-binding proteins which cause changes to the actin cytoskeleton and cell shape *in vitro* (Zepeta-Flores et al. 2018). However, based on my findings changes to actin has no effect on the altered redox state and are likely caused by another mechanism.

5.6 Conclusion

Here, I show that Cdk12 functions to limit Ca^{2+} levels in neurons. Upon ablation of *Cdk12*, Ca^{2+} rises in the cytoplasm which may have physiological consequences. Interestingly, mitochondria did not appear to buffer cytosolic Ca^{2+} rises. I further found that Cdk12 played a role in regulating mitochondrial morphology. Interestingly, this is controlled by Drp1 and ablation of *Cdk12* induced fission without inducing mitochondrial ROS (GSSG or H_2O_2), suggesting mitochondria remain functional. I suggest that AIS expansion, including the ion channels, could be the underlying reason for Ca^{2+} rises seen in this chapter and the increase in actin seen in **Chapter 4**. Increased actin in the proximal axon may also underlie changes in mitochondrial fission. We conclude that Cdk12 is a regulator of actin, Ca^{2+} and mitochondria and in neurons is essential for maintenance during ageing.

6 Discussion

6.1 Summary of findings

This thesis demonstrates that Cdk12, identified in a previous unbiased genetic screen, controls proximal axon width and neuronal survival. Using actin as an approximate AIS marker, I showed Cdk12 to interfere with actin axonal distribution and form actin swellings in the proximal axon. These actin changes altered the putative AIS barrier and facilitated peroxisomes (a soma vesicle marker) to enter the axon. In addition, this thesis also aimed to investigate the physiological effect Cdk12 had on neuronal changes and on other organelles in the neuron. This thesis demonstrates that Cdk12 influenced neuronal Ca^{2+} levels, ER distribution and mitochondria morphology in the proximal axon in the stages prior to neurodegeneration. Therefore, Cdk12 is crucial to maintain the size and function of the putative AIS and to regulate neuronal physiology. This in turn could regulate neuronal polarity which leads to neurodegeneration, a key characteristic seen in many neurodegenerative diseases. We propose a working model (**Figure 6.1**) by which Cdk12 maintains neurons *in vivo*.

6.2 Cdk12 regulates the axon initial segment

In the neuron, the PAEZ and AIS work together to act as a barrier to selectively filter cargo and maintain neuronal polarity. My findings show that Cdk12 regulates the proximal axon width. It is hypothesised that this region is the AIS rather than the PAEZ because Cdk12 has also been shown to regulate β - and F-actin distribution and form large actin swellings in the proximal axon swellings and the actin-based filter is more closely associated with the AIS (Winckler et al. 1999; Nakada et al. 2003; Song et al. 2009; Leterrier and Dargent 2014; Leterrier 2018). The mislocation of peroxisomes is a result of actin redistribution (filament orientation) that interferes with the function of the AIS as a selective filter (**Figure 6.1, Pathway 1**). On the other hand, Cdk12 may regulate both the AIS and the PAEZ. The mislocation of peroxisomes, a somatodendritic marker, located in axons of neurons lacking *Cdk12* could be regulated by the PAEZ, since this region uses dynamic sorting of the cytoskeleton to filter cargo (MAP2/TRIM46 mechanism) (Fariás et al. 2015; Gumy et al. 2017).

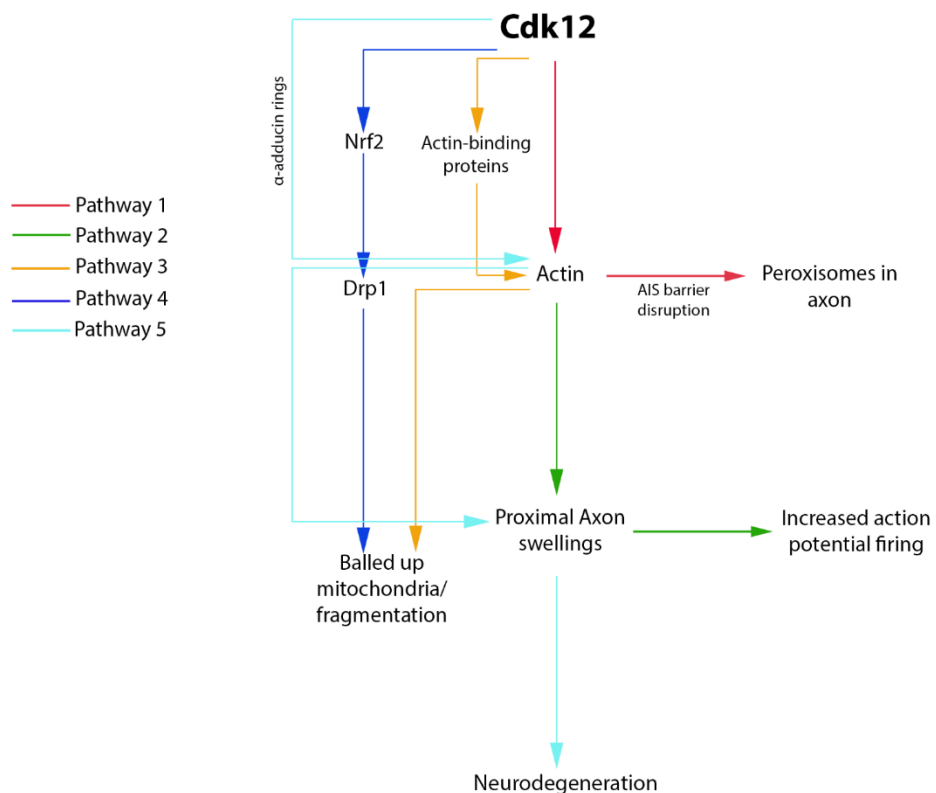


Figure 6.1 A summary of Cdk12 potential pathways. Cdk12 is predicted to have an involvement in several pathways related to several regions in the cell, such as organelle regulation, cytoskeleton, cytosolic ion levels, proximal axon function and neurodegeneration, Pathways 1-5 are labelled accordingly.

To test this hypothesis in *Drosophila*, components in the MAP2/TRIM46 pathway could be overexpressed which may increase cargo sorting in the *Cdk12* null MARCM clones, which may result in detainment of peroxisomes in the soma-dendritic compartment. Conversely, RNAi knockdown in WT clones of these PAEZ may result in barrier breakdown and soma vesicles/ organelles entering the axon. Reasons for this could be due to MAP2 regulation on kinesins, which in turn influences the velocity of cargo transport. In the presence of MAP2, kinesin-1 slows down axonal cargo whilst kinesin-3 increases the velocity of axonal cargo. Inhibition of MAP2, however, inhibits kinesin-1 in the proximal axon but has no effect on kinesin-3 function to transport cargo (Gumy et al. 2017). This would therefore suggest that Cdk12 may also regulate cargo sorting via MAP2/TRIM46 mechanism at the PAEZ.

Two proteins located in the PAEZ are MAP2, located also in the cell body, and TRIM46, which is also found to overlap with the AIS (Gumy et al. 2018). TRIM46 binds to and organises microtubule fascicles (Harterink et al. 2019) whilst MAP2 binds to microtubules and actin (Dehmelt and Halpain 2005). In order to further eliminate if this region is the PAEZ, I could also use an axonal marker, (fluorescently-tagged tau). Tau-misrouting occurs in neurons deficient in TRIM46 (Van Beuningen et al. 2015) and it may be interesting to see if this is also the case for *Cdk12* ablation.

Finding new molecules that can jointly or specifically regulate these two neuronal subdomains of the proximal axon may shed more light on their unique functions. The *Drosophila* wing systems seem to be a good model system to study the proximal axon and could be combined with a targeted or unbiased genetic screen to find more molecules like *Cdk12*. One thing that would enhance the wing system for the study of the AIS is to find/make a panel of markers to robustly visualise the somatodendritic, axonal and AIS subdomains. These tools are beginning to emerge, such as the Para EGFP-FIAsH-StrepII-TEV-3xFlag (GFSTF) (endogenous para with GFP tag that does not impair channel function) line from the Bellen lab (Ravenscroft et al. 2020) which marks a Nav channel found only at the site of action potential initiation. However, we should also consider the complexity and diversity of neurons in the *Drosophila* central nervous system (CNS) and peripheral nervous system (PNS) and the barrier between the axon and soma may be more or less defined depending on neuronal sub-type.

It is interesting that *Cdk12* is the second molecule to be uncovered as a regulator of AIS size and function. *Cdk5* is also reported to maintain AIS size and maintenance, overexpressing it caused the AIS to double in size and knocking it down caused it to disappear altogether (Trunova et al. 2011). *Cdk5* is also involved in axonal transport by phosphorylating Ndel1, a dynein regulator, that operates via the *Cdk5*-Ndel1-Lis1-dynein pathway to selectively transport cargo along the axon at the AIS (Klinman et al. 2017). Our experiments found that *Cdk5* and *Cdk12* do not genetically interact, suggesting that *Cdk5* and *Cdk12* regulate axonal size and axodendritic sorting at the AIS along different pathways. Nevertheless, it would be interesting to see if *Cdk12* plays a role in axonal transport through live cell imaging approaches (Vagnoni et al. 2016; Vagnoni and Bullock 2016; Vagnoni and Bullock 2018; Mattedi et al. 2022), which could be the case based on morphological changes in organelles that we see, such as mitochondria.

Both the PAEZ and AIS regions in the proximal axon function to maintain neuronal polarity but the AIS is also the site of action potential initiation, supported by the abundance of sodium and potassium channels (Rasband 2010). The axon swells at the onset of an action potential and peaks in size as the action potential also peaks (Iwasa and Tasaki 1980; Chéreau et al. 2017). As action potentials initiate in the AIS, it may be that Cdk12 is causing increased neuronal firing that peaks at 21 d.p.e (**Figure 6.1, Pathway 2**). Therefore, suggesting that Cdk12 influences neuronal polarity by regulating neuronal firing. To test this, I would perform electrophysiology in the form of ERGs on mutant and control neurons of the eye to directly measure action potentials in response to light stimulation.

6.3 Actin formation requires actin-binding proteins

Cdk12 regulates actin distribution in the proximal axon. Exactly how Cdk12 regulates actin is unknown but possible mechanisms may be via actin-binding proteins during actin formation steps. The formation of actin requires several processes: actin nucleation, actin polymerisation and actin depolymerisation. Actin nucleation results in the formation of an actin nucleus, composed of three actin monomers and uses several actin nucleators: Arp2/3, Wasp, N-Wasp and Formins (Machesky et al. 1999; Rohatgi et al. 1999; Pollard 2016; Goldschmidt-Clermont et al. 2017). Actin polymerisation and depolymerisation consists of the addition and loss of actin monomers (G-actin) at the barbed and pointed ends, respectively (**Chapter 1, Figure 1.2**) to form F-actin. This process requires several actin-binding proteins: formins, thymosin β 4, gelsolin and ADF/cofilin (Kinosian et al. 1998; Kovar and Pollard 2004; De La Cruz et al. 2015).

6.3.1 The importance of actin-binding proteins in mitochondrial fission

This thesis has highlighted that Cdk12 regulates mitochondrial morphology through fission. I suggest that this could occur via transcriptional mechanisms. Cdk12 positively regulates Nrf2 (Li et al. 2016), which via the Kelch-like ECH-associated protein 1 (Keap1)-Nrf2 stress response pathway, leads to the negative regulation of Drp1 (Sabouny et al. 2017). Drp1 is a crucial mitochondrial fission protein and knockdown of *Drp1* has shown to rescue the increase in mitochondrial fission, seen in *Cdk12* null clones, suggesting that Drp1 occurs along the same pathway as Cdk12 to influence mitochondrial morphology. As Cdk12 regulates Nrf2 which negatively regulates Drp1, perhaps the loss of *Cdk12* in neurons, is causing a decrease in Nrf2 which increases Drp1 and mitochondrial fission. Mitochondrial fission also requires

actin filaments (DuBoff et al. 2012) which I have previously shown are regulated by Cdk12 in the proximal axon. As actin binds to actin-binding proteins to control actin formation, perhaps Cdk12 is regulating actin-binding proteins to influence actin formation and hence mitochondrial fission in the proximal axon (**Figure 6.1, Pathway 3 and Pathway 4**).

Mitochondria fission occurs at ER contact sites (Friedman et al. 2011) and the first step of mitochondrial fission involves the interaction between the ER and mitochondria. Actin filaments are then lengthened at the barbed end via the formin, INF2 (CAAX isoform) (De Vos et al. 2005; Chhabra and Higgs 2006), which results in the tethering of the barbed end of actin to the ER. INF2 is bound to the ER to elongate actin and spire type actin nucleation factor 1C (Spire1C) is bound to the outer membrane of mitochondria to nucleate actin. Spire1C consists of four WASP homology 2 (WH2) domains and each domain binds to an actin monomer (Wellington et al. 1999; Otto et al. 2000). Both INF2 and Spire1C cooperate together in mitochondrial fission to nucleate and elongate actin filaments at ER-mitochondrion contact sites. Myosin II is recruited and together with actin drives a pre-constriction force around the mitochondrion (Korobova et al. 2014). Actomyosin contractility enables Drp1 to form a 100-130 nm ring around the constriction site (Mears et al. 2010) and facilitate mitochondrial fission (Korobova et al. 2013; Hatch et al. 2014) via the GTPase activity of Drp1. Furthermore, INF2 is also able to depolymerise actin, therefore suggesting that INF2 may function in actin filament destabilisation after fission has occurred (Hatch et al. 2014). Actin disassembly may also occur from actin depolymerisation which may be caused by cofilin, an actin-binding protein. Deletion of cofilin increases Drp1 and mitochondrial fragmentation without altering mitochondrial function (Rehklau et al. 2017) suggesting the ability of cofilin to function in actin disassembly. In addition to actin depolymerisation, cofilin1, also functions in polymerisation by binding to ADP-actin and severing the ends of actin filaments to form new barbed and pointed ends. Cofilin and INF2 are able to then bind to the new fragments and induce depolymerisation (**Figure 6.2**) (Bamburg and Bernstein 2010). This therefore demonstrates that several actin-binding proteins (INF2, Spire1C and Cofilin) are important to facilitate mitochondrial fission and may play a role in our observed mitochondrial phenotype.

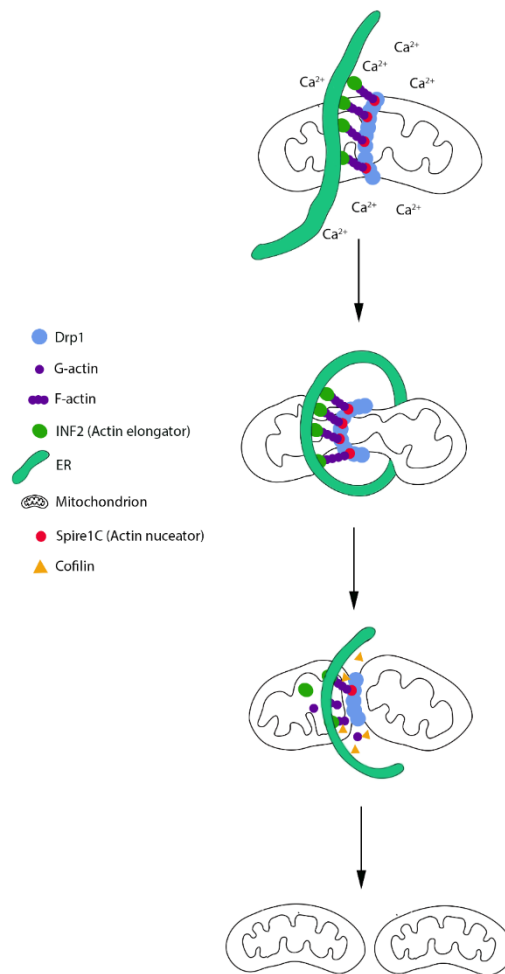


Figure 6.2 Calcium-induced mitochondrial fission. High calcium levels activate ER-bound INF2 which along with, Spire1C, nucleate and elongate actin filaments. Actin, along with myosin II, produces a pre-constriction force which facilitates Drp1 ring assembly at the pre-constriction site which triggers mitochondrial fission. Cofilin and INF2 depolymerise actin filaments which causes the complex to disassemble. Image adapted from Li et al. (2018) (Li et al. 2018).

High levels of calcium activates ER-bound INF2 which in turn leads to actin polymerisation and mitochondrial fission (Wales et al. 2016). In addition to a calcium influx leading to mitochondrial fission, an alternate pathway also leads to fission. Actin clouds (composed of actin polymerisation), dependent on actin-binding proteins: Arp2/3 complex and formin, surround depolarised mitochondria and cause mitochondria to become less elongated and increase mitochondrial fission. Arp2/3 polymerises actin filaments and form branched microfilament arrays but formins form actin bundles. At a later time point, a second actin wave, dependent on myosin VI, surrounds these depolarised mitochondria, preventing fusion of depolarised mitochondria with other mitochondria (Li et al. 2015; Moore et al. 2016; Kruppa et al. 2018). This therefore demonstrates that mitochondrial fission-fusion events are

regulated by actin cycling. I have shown that knockdown of *Cdk12* increases intracellular Ca^{2+} , so it is possible that this is the upstream regulator driving fission.

In addition, calcium-induced actin polymerisation depends on INF2, whereas actin polymerisation dependent on depolarisation is slower and is Arp2/3-dependent but does not depend on INF2 (Fung et al. 2019). Calcium influx activates INF2 via histone deacetylase 6 (HDAC6)-mediated deacetylation of actin. Therefore, genetic manipulation of INF2 or Arp2/3 in our mutant may help define whether fission is Ca^{2+} dependent or independent.

It is possible that morphological changes are also due to decreased mitochondrial fusion. It would be interesting to investigate whether MFNs are changed at the transcriptional or protein level. MFNs oligomerise and induce fusion by glutathione redox fluxes (Shutt et al. 2012; Smith et al. 2019), but since no change in redox was seen in the *Cdk12* depleted axons this is unlikely to be the cause. If MFNs are implicated morphological changes this would be more compelling evidence to investigate mitochondrial transport as mitofusins have been shown to interact with the Miro and Milton complex (Misko et al. 2010).

At this stage we do not know if mitochondrial abnormalities contribute to or are the cause of neurodegeneration that we see at later stages. Although excessive ROS was not observed, mitochondria could still be dysfunctional, and this warrants further investigation through the use of ATP sensors using the wing system or metabolomic analysis.

6.4 The importance of actin-binding proteins in neurodegeneration

As discussed in **Section 6.1** in this chapter, there are several actin-binding proteins that participate in actin formation, and some of these are linked to disease. One protein, cofilin, important in actin depolymerisation, can also bind to ADP-actin in its hyperactive state to produce cofilin-actin rods during low ATP levels or high glutamate and hydrogen peroxide levels to protect neurons from ATP depletion. The formation of cofilin-actin rods in neurons can prevent the transport of vesicles that contain amyloid precursor protein (APP), β - and γ -secretase. These stalled sites provide sites for $\text{A}\beta$ production which causes rod formation in other neurons and hence worsening neurodegeneration and contributing to aging (Maloney et al. 2005; Bernstein et al.

2006; Davis et al. 2011; Cichon et al. 2012). Cofilin-actin rods have also been implicated in disease as huntingtin, the mutated version of this protein that contributes to HD, was localised to cofilin-actin rods under stressful conditions. After cells had recovered from stress, huntingtin remained bound to the rods proposing that huntingtin contributes to actin remodelling (Nishida et al. 1987; Ohta et al. 1989; Munsie et al. 2011). Therefore, perhaps, Cdk12 is increasing the production of rods which are contributing to neurodegeneration.

Another actin-binding protein, α -adducin, binds to the barbed end of F-actin to regulate the growth and size of actin rings, actin structures located around the perimeter of the axon that provide mechanical support to the axon (Hammarlund et al. 2007; Xu et al. 2013). Axon diameter is therefore controlled by α -adducin and an absence of α -adducin leads to axon enlargement and neurodegeneration (Leite et al. 2016). The mislocation of actin in the proximal axon, in *Cdk12* null clones, may be causing an increase in axon diameter and hence axonal swellings which triggers neuron death (**Figure 6.1, Pathway 5**). I have previously shown that Cdk12 regulates actin-dense proximal axon swellings. Perhaps, Cdk12 regulates α -adducin which in turn contributes to the increase in proximal axon swellings. It would be exciting to perform stochastic optical reconstruction microscopy (STORM) or stimulated emission depletion (STED) microscopy in *Cdk12* ablated neurons to see if the actin ring structures are altered.

6.5 The importance of actin-regulating binding proteins in synapse formation

Neuronal growth cones are the site of axon elongation and require the actin cytoskeleton to provide a protrusive force to drive growth cone advancement (Dent et al. 2011). The assembly of actin filaments occurs at the barbed end (Pollard and Cooper 2009). F-actin assembly is promoted by nucleating, bundling and severing but is aborted by actin capping proteins. Synaptic arborisation (terminal branching of nerve fibres) requires Arp2/3 and epidermal growth factor receptor pathway substrate 8 (Eps8) actin-binding proteins.

Arp2/3 nucleates new actin filaments on the side of pre-existing branches. Arp2/3 nucleator protein binds to new actin filaments on the side of pre-existing branches to promote actin polymerisation. Actin capping protein, Eps8, binds to the barbed ends of actin filaments and prevents actin filament extension in long unbranched bundles

hence preventing branch extension. During synaptic arborisation, the presence of enabled/vasodilator-stimulated phosphoprotein (Ena/VASP) increases F-actin extension by inhibiting capping proteins, such as Eps8, to bind to actin (Bear and Gertler 2009; Menna et al. 2011). When bound to actin, Ena/VASP causes microtubules to invade the branch and hence promote neuronal branching. It would be interesting in future work to see if there are any synaptic changes that occur in our *Cdk12* mutant.

6.6 The axon initial segment in neurological disease

In addition to specific actin changes *Cdk12* may be indirectly regulating the properties of the AIS, a region associated with several neurodegenerative diseases. One of the key functions of the AIS is to initiate action potentials and this involves an abundance of ion channels. The abundance of ion channels at the AIS lowers the firing threshold required for action potential initiation (Buffington and Rasband, 2011). Mutations in several sodium (Nav1.1, 1.2, 1.6 and Nav β subunit) and potassium (KCNQ2/3) channels have been linked to epilepsy. Loss of function of Nav1.1 channels, abundant in the AIS of GABA-ergic hippocampal interneurons, is associated with Dravet syndrome or severe myoclonic epilepsy (Yu et al. 2006; Kalume et al. 2007; Oakley et al. 2011). Myoclonic epilepsy mice showed an increase in action potential firing failures in the AIS in GABAergic interneurons, identifying a potential loss of inhibitory control by interneurons (Yu et al. 2006; Kalume et al. 2007; Oakley et al. 2011). Excitotoxicity is associated with AIS disassembly after stroke injury. An influx of Ca^{2+} ions follows injury which activates the breakdown of the ankyrin/spectrin cytoskeleton in the AIS (Siman et al. 1984; Schafer et al. 2009). This loss causes a reduction in sodium channels which compromises action potential initiation function. It would be interesting to investigate specific actin and mitochondrial fission phenotypes in these diseases.

The strict function of the AIS to filter cargo in order to maintain neuronal polarity is also linked to disease when compromised (Rasband 2010). In AD, this delicate filter is disrupted and tau, an axonal marker and key characteristic of AD, localises to the somatodendritic compartment once acetylated (pathologically modified) (Sohn et al. 2016). This suggests that acetylated tau destabilises the AIS and causes misalignment of neuronal proteins that require polarised distribution. In addition to tau mislocalisation at the AIS, other characteristics of AD have also been linked to AIS disruption, this includes AIS reduction in length and number when in close proximity

to A β plaques (Palop and Mucke 2009). Reasons for this could be neuronal displacement due to the size of A β plaques leading to neuronal death or A β plaques triggering calpain-mediated proteolysis of the cytoskeleton in the AIS and causing AIS barrier breakdown (Marin et al. 2016). This demonstrates that a change or a complete loss of the AIS contributes to impaired brain function (León-Espinosa et al. 2012; Marin et al. 2016). It would therefore be interesting to determine whether genetic manipulation of Cdk12 could modulate Tau and other disease associated phenotypes in AD. Together, this demonstrates that the AIS plays a key role in several neurological diseases and disorders. The importance to study the mechanisms controlling AIS maintenance is therefore imperative.

6.7 Concluding remarks

To conclude, Cdk12, previously identified in an unbiased genetic screen, has been shown to regulate proximal axon width and neuronal survival. The proximal axon swellings that occur when Cdk12 is knocked out are likely to be within the AIS, between the neuronal cell body and the axon. Cdk12 has been shown to regulate actin within this region and functions to retain peroxisomes in the somatic dendritic region, suggesting that Cdk12 maintains the AIS filtration barrier. The loss of Cdk12 caused an increase in neuronal Ca²⁺ which may explain the increase in Drp1-mediated mitochondria fission, acting via the Ca²⁺-induced Nrf2/Drp1 pathway or alternatively fission may occur through actin-related mechanisms. This therefore demonstrates the importance of Cdk12 to maintain the size and function of the AIS and to control neuronal physiology. Cdk12 regulates neuronal polarity which, if disrupted, leads to neurodegeneration, a key characteristic seen in many neurodegenerative diseases.

7 Bibliography

- Abdelmegeed, M.A. and Song, B.J. 2014. Functional roles of protein nitration in acute and chronic liver diseases. *Oxidative Medicine and Cellular Longevity* 2014
- Abrisch, R.G., Gumbin, S.C., Wisniewski, B.T., Lackner, L.L., and Voeltz, G.K. 2020. Fission and fusion machineries converge at ER contact sites to regulate mitochondrial morphology. *Journal of Cell Biology* 219(4)
- Ahles, T.A., Root, J.C., and Ryan, E.L. 2012. Cancer- and cancer treatment-associated cognitive change: an update on the state of the science. *Journal of clinical oncology : official journal of the American Society of Clinical Oncology* 30(30), pp. 3675–3686.
- Ahmed, W.W., Li, T.C., Rubakhin, S.S., Chiba, A., Sweedler, J. V., and Saif, T.A. 2012. Mechanical tension modulates local and global vesicle dynamics in neurons. In: *Cellular and Molecular Bioengineering*. Cell Mol Bioeng, pp. 155–164.
- Aigouy, B., Farhadifar, R., Staple, D.B., Sagner, A., Röper, J.C., Jülicher, F., and Eaton, S. 2010. Cell flow reorients the axis of planar polarity in the wing epithelium of *Drosophila*. *Cell* 142(5), pp. 773–786.
- Akbar, M., Essa, M.M., Daradkeh, G., Abdelmegeed, M.A., Choi, Y., Mahmood, L., and Song, B.J. 2016. Mitochondrial dysfunction and cell death in neurodegenerative diseases through nitroxidative stress. *Brain Research* 1637, pp. 34–55.
- Akhmanova, A. and Hammer, J.A. 2010. Linking molecular motors to membrane cargo. *Current Opinion in Cell Biology* 22(4), pp. 479–487.
- Al-Bassam, S., Xu, M., Wandless, T.J., and Arnold, D.B. 2012. Differential trafficking of transport vesicles contributes to the localization of dendritic proteins. *Cell Reports* 2(1), pp. 89–100.
- Albrecht, D., Winterflood, C.M., Sadeghi, M., Tschager, T., Noé, F., and Ewers, H. 2016. Nanoscopic compartmentalization of membrane protein motion at the axon initial segment. *Journal of Cell Biology* 215(1), pp. 37–46.
- Allada, R., White, N.E., So, W.V., Hall, J.C., and Rosbash, M. 1998. A mutant *Drosophila* homolog of mammalian Clock disrupts circadian rhythms and transcription of period and timeless. *Cell* 93(5), pp. 791–804.
- Allen, G.F.G., Toth, R., James, J., and Ganley, I.G. 2013. Loss of iron triggers PINK1/Parkin-independent mitophagy. *EMBO reports* 14(12), pp. 1127–1135.
- Alvarez, S., Moldovan, M., and Krarup, C. 2008. Acute energy restriction triggers Wallerian degeneration in mouse. *Experimental Neurology* 212(1), pp. 166–178.
- Antoku, S. and Gundersen, G.G. 2018. Analysis of Nesprin-2 Interaction with Its Binding Partners and Actin. *Methods in molecular biology (Clifton, N.J.)* 1840, pp. 35–43.
- Area-Gomez, E. et al. 2012. Upregulated function of mitochondria-associated ER membranes in Alzheimer disease. *The EMBO Journal* 31(21), pp. 4106–4123.
- Arimura, N. and Kaibuchi, K. 2007. Neuronal polarity: From extracellular signals to intracellular mechanisms. *Nature Reviews Neuroscience* 8(3), pp. 194–205.
- Ashburner, M. and Novitski, E. 1976. *The Genetics and Biology of Drosophila*.

London Academic Press.

- Ataka, K. and Pieribone, V.A. 2002. A Genetically Targetable Fluorescent Probe of Channel Gating with Rapid Kinetics. *Biophysical Journal* 82(1), pp. 509–516.
- Athanasiu, L. et al. 2010. Gene variants associated with schizophrenia in a Norwegian genome-wide study are replicated in a large European cohort. *Journal of psychiatric research* 44(12), pp. 748–53.
- Aumeier, C., Schaedel, L., Gaillard, J., John, K., Blanchoin, L., and Théry, M. 2016. Self-repair promotes microtubule rescue. *Nature cell biology* 18(10), pp. 1054–1064.
- Avery, M.A. et al. 2012. Wld S prevents axon degeneration through increased mitochondrial flux and enhanced mitochondrial Ca²⁺ buffering. *Current Biology* 22(7), pp. 596–600.
- Baas, P.W. and Lin, S. 2011. Hooks and comets: The story of microtubule polarity orientation in the neuron. *Developmental Neurobiology* 71(6), pp. 403–418.
- Babcock, D.F. and Hille, B. 1998. Mitochondrial oversight of cellular Ca²⁺ signaling. *Current opinion in Neurobiology* 8(3), pp. 398–404.
- Baehrecke, E.H. 1996. Ecdysone Signaling Cascade and Regulation of Drosophila Metamorphosis. *Archives of Insect Biochemistry and Physiology* 33(3–4), pp. 231–244.
- Bajjalieh, S.M. and Scheller, R.H. 1995. The Biochemistry of Neurotransmitter Secretion (*). *Journal of Biological Chemistry* 270(5), pp. 1971–1974.
- Bajrami, I. et al. 2014. Genome-wide profiling of genetic synthetic lethality identifies CDK12 as a novel determinant of PARP1/2 inhibitor sensitivity. *Cancer Research* 74(1), pp. 287–297.
- Balan, V. et al. 2008. Life span extension and neuronal cell protection by Drosophila nicotinamidase. *Journal of Biological Chemistry* 283(41), pp. 27810–27819.
- Bamburg, J.R. and Bernstein, B.W. 2010. Roles of ADF/cofilin in actin polymerization and beyond. *F1000 biology reports* 2(1)
- Bamburg, J.R. and Bernstein, B.W. 2016. Actin dynamics and cofilin-actin rods in alzheimer disease. *Cytoskeleton (Hoboken, N.J.)* 73(9), pp. 477–497.
- Barber, S.C. and Shaw, P.J. 2010. Oxidative stress in ALS: Key role in motor neuron injury and therapeutic target. *Free Radical Biology and Medicine* 48(5), pp. 629–641.
- Bartkowiak, B. et al. 2010. CDK12 is a transcription elongation-associated CTD kinase, the metazoan ortholog of yeast Ctk1. *Genes & development* 24(20), pp. 2303–2316.
- Basu, S. and Lamprecht, R. 2018. The Role of Actin Cytoskeleton in Dendritic Spines in the Maintenance of Long-Term Memory. *Frontiers in molecular neuroscience* 11
- Bate, M. and Martinez Arias, A. 1991. The embryonic origin of imaginal discs in Drosophila. *Development (Cambridge, England)* 112(3), pp. 755–761.
- Baughman, J.M. et al. 2011. Integrative genomics identifies MCU as an essential component of the mitochondrial calcium uniporter. *Nature* 2011 476:7360 476(7360), pp. 341–345.
- Baumann, O. and Walz, B. 2001. Endoplasmic reticulum of animal cells and its

- organization into structural and functional domains. *International Review of Cytology* 205, pp. 149–214.
- Bayliak, M.M., Abrat, O.B., Storey, J.M., Storey, K.B., and Lushchak, V.I. 2019. Interplay between diet-induced obesity and oxidative stress: Comparison between *Drosophila* and mammals. *Comparative Biochemistry and Physiology -Part A: Molecular and Integrative Physiology* 228, pp. 18–28.
- Bear, J.E. and Gertler, F.B. 2009. Ena/VASP: towards resolving a pointed controversy at the barbed end. *Journal of Cell Science* 122(12), pp. 1947–1953.
- Bejjani, R. El and Hammarlund, M. 2012. Neural Regeneration in *Caenorhabditis elegans*. *Annual review of genetics* 46, p. 499.
- Belenky, P., Racette, F.G., Bogan, K.L., McClure, J.M., Smith, J.S., and Brenner, C. 2007. Nicotinamide Riboside Promotes Sir2 Silencing and Extends Lifespan via Nrk and Urh1/Pnp1/Meu1 Pathways to NAD⁺. *Cell* 129(3), pp. 473–484.
- Bender, K.J. and Trussell, L.O. 2009. Axon Initial Segment Ca²⁺ Channels Influence Action Potential Generation and Timing. *Neuron* 61(2), pp. 259–271.
- Bennett, V. and Lorenzo, D.N. 2013. Spectrin- and Ankyrin-Based Membrane Domains and the Evolution of Vertebrates. *Current Topics in Membranes* 72, pp. 1–37.
- Berghs, S. et al. 2000. β iv Spectrin, a New Spectrin Localized at Axon Initial Segments and Nodes of Ranvier in the Central and Peripheral Nervous System. *Journal of Cell Biology* 151(5), pp. 985–1002.
- Bernstein, B.W., Chen, H., Boyle, J.A., and Bamburg, J.R. 2006. Formation of actin-ADF/cofilin rods transiently retards decline of mitochondrial potential and ATP in stressed neurons. *American journal of physiology. Cell physiology* 291(5)
- Bertholet, A.M. et al. 2016. Mitochondrial fusion/fission dynamics in neurodegeneration and neuronal plasticity. *Neurobiology of Disease* 90, pp. 3–19.
- Bertholet, A.M., Millet, A.M.E., Guillermin, O., Daloyau, M., Davezac, N., Miquel, M.C., and Belenguer, P. 2013. OPA1 loss of function affects in vitro neuronal maturation. *Brain* 136(5), pp. 1518–1533.
- Bertram, R., Gram Pedersen, M., Luciani, D.S., and Sherman, A. 2006. A simplified model for mitochondrial ATP production. *Journal of Theoretical Biology* 243(4), pp. 575–586.
- Bezprozvanny, I. and Mattson, M.P. 2008. Neuronal calcium mishandling and the pathogenesis of Alzheimer's disease. *Trends in Neurosciences* 31(9), pp. 454–463.
- Bhabha, G., Johnson, G.T., Schroeder, C.M., and Vale, R.D. 2016. How Dynein Moves Along Microtubules. *Trends in Biochemical Sciences* 41(1), pp. 94–105.
- Birsa, N., Norkett, R., Higgs, N., Lopez-Domenech, G., and Kittler, J.T. 2013. Mitochondrial trafficking in neurons and the role of the Miro family of GTPase proteins. *Biochemical Society Transactions* 41(6), pp. 1525–1531.
- Blanquie, O. and Bradke, F. 2018. Cytoskeleton dynamics in axon regeneration. *Current opinion in Neurobiology* 51, pp. 60–69.
- Blaustein, M.P. 1988. Calcium transport and buffering in neurons. *Trends in*

- Neurosciences* 11(10), pp. 438–443.
- Blazek, D. et al. 2011. The cyclin K/Cdk12 complex maintains genomic stability via regulation of expression of DNA damage response genes. *Genes & development* 25(20), pp. 2158–2172.
- Böckler, S. and Westermann, B. 2014. Mitochondrial ER Contacts Are Crucial for Mitophagy in Yeast. *Developmental Cell* 28(4), pp. 450–458.
- Borovac, J., Bosch, M., and Okamoto, K. 2018. Regulation of actin dynamics during structural plasticity of dendritic spines: Signaling messengers and actin-binding proteins. *Molecular and cellular neurosciences* 91, pp. 122–130.
- Bouley, M., Tian, M.Z., Paisley, K., Shen, Y.C., Malhotra, J.D., and Hortsch, M. 2000. The L1-type cell adhesion molecule neuroglian influences the stability of neural ankyrin in the *Drosophila* embryo but not its axonal localization. *The Journal of neuroscience : the official journal of the Society for Neuroscience* 20(12), pp. 4515–23.
- Boveris, A. and Chance, B. 1973. The mitochondrial generation of hydrogen peroxide. General properties and effect of hyperbaric oxygen. *Biochemical Journal* 134(3), pp. 707–716.
- Boya, P., Codogno, P., and Rodriguez-Muela, N. 2018. Autophagy in stem cells: repair, remodelling and metabolic reprogramming. *Development (Cambridge, England)* 145(4)
- Brachet, A. et al. 2010. Ankyrin G restricts ion channel diffusion at the axonal initial segment before the establishment of the diffusion barrier. *Journal of Cell Biology* 191(2), pp. 383–395.
- Brand, A.H. and Perrimon, N. 1993. Targeted gene expression as a means of altering cell fates and generating dominant phenotypes. *Development (Cambridge, England)* 118(2), pp. 401–15.
- Braun, N., Schikorski, T., and Zimmermann, H. 1993. Cytoplasmic segregation and cytoskeletal organization in the electric catfish giant electromotoneuron with special reference to the axon hillock region. *Neuroscience* 52(3), pp. 745–756.
- Bray, D. 1984. Axonal growth in response to experimentally applied mechanical tension. *Developmental Biology* 102(2), pp. 379–389.
- Bréchet, A. et al. 2008. Protein kinase CK2 contributes to the organization of sodium channels in axonal membranes by regulating their interactions with ankyrin G. *Journal of Cell Biology* 183(6), pp. 1101–1114.
- Britt, D.J., Farías, G.G., Guardia, C.M., and Bonifacino, J.S. 2016. Mechanisms of polarised organelle distribution in neurons. *Frontiers in Cellular Neuroscience* 10(MAR2016), p. 88.
- Budd, S.L. and Nicholls, D.G. 1996. A Reevaluation of the Role of Mitochondria in Neuronal Ca²⁺ Homeostasis. *Journal of Neurochemistry* 66(1), pp. 403–411.
- Buffington, S.A. and Rasband, M.N. 2011. The axon initial segment in nervous system disease and injury. *The European journal of neuroscience* 34(10), pp. 1609–19.
- Bülow, P., Wenner, P.A., Faundez, V., and Bassell, G.J. 2021. Mitochondrial Structure and Polarity in Dendrites and the Axon Initial Segment Are Regulated by Homeostatic Plasticity and Dysregulated in Fragile X Syndrome. *Frontiers in Cell and Developmental Biology* 9, p. 1791.

- Bulua, A.C. et al. 2011. Mitochondrial reactive oxygen species promote production of proinflammatory cytokines and are elevated in TNFR1-associated periodic syndrome (TRAPS). *Journal of Experimental Medicine* 208(3), pp. 519–533.
- Bunnell, T.M., Burbach, B.J., Shimizu, Y., and Ervasti, J.M. 2011. β -Actin specifically controls cell growth, migration, and the G-actin pool. *Molecular biology of the cell* 22(21), pp. 4047–4058.
- Burack, M.A., Silverman, M.A., and Banker, G. 2000. The role of selective transport in neuronal protein sorting. *Neuron* 26(2), pp. 465–472.
- Cajal, R. y 1888. Estructura de los centros nerviosos de las aves. *Rev. Trim. Histol. Norm. Pat.*, pp. 1–10.
- Cajal, S.R. y 1906. *The structure and connexions of neurons*.
- Cajal, S.R. y 1995. *Histology of the Nervous System of Man and Vertebrates*. Oxford Univ. Press.
- Cajigas, I.J., Tushev, G., Will, T.J., Tom Dieck, S., Fuerst, N., and Schuman, E.M. 2012. The local transcriptome in the synaptic neuropil revealed by deep sequencing and high-resolution imaging. *Neuron* 74(3), pp. 453–466.
- Calì, T., Ottolini, D., Negro, A., and Brini, M. 2012. α -Synuclein Controls Mitochondrial Calcium Homeostasis by Enhancing Endoplasmic Reticulum-Mitochondria Interactions *. *Journal of Biological Chemistry* 287(22), pp. 17914–17929.
- Calì, T., Ottolini, D., Negro, A., and Brini, M. 2013. Enhanced parkin levels favor ER-mitochondria crosstalk and guarantee Ca^{2+} transfer to sustain cell bioenergetics. *Biochimica et Biophysica Acta (BBA) - Molecular Basis of Disease* 1832(4), pp. 495–508.
- Cameron, P., Hiroi, M., Ngai, J., and Scott, K. 2010. The molecular basis for water taste in *Drosophila*. *Nature* 2010 465:7294 465(7294), pp. 91–95.
- Carafoli, E. 2007. The unusual history and unique properties of the calcium signal. *New Comprehensive Biochemistry* 41, pp. 3–22.
- Carafoli, E. and Brini, M. 2000. Calcium pumps: structural basis for and mechanism of calcium transmembrane transport. *Current opinion in chemical biology* 4(2), pp. 152–161.
- Carocho, M., Morales, P., and Ferreira, I.C.F.R. 2018. Antioxidants: Reviewing the chemistry, food applications, legislation and role as preservatives. *Trends in Food Science & Technology* 71, pp. 107–120.
- Castro, I.G. et al. 2018. A role for Mitochondrial Rho GTPase 1 (MIRO1) in motility and membrane dynamics of peroxisomes. *Traffic* 19(3), pp. 229–242.
- Cereghetti, G.M., Stangherlin, A., Martins De Brito, O., Chang, C.R., Blackstone, C., Bernardi, P., and Scorrano, L. 2008. Dephosphorylation by calcineurin regulates translocation of Drp1 to mitochondria. *Proceedings of the National Academy of Sciences of the United States of America* 105(41), pp. 15803–15808.
- Chakrabarti, R., Ji, W.K., Stan, R. V., Sanz, J. de J., Ryan, T.A., and Higgs, H.N. 2018. INF2-mediated actin polymerization at the ER stimulates mitochondrial calcium uptake, inner membrane constriction, and division. *Journal of Cell Biology* 217(1), pp. 251–268.
- Chapman, E.R. 2008. How Does Synaptotagmin Trigger Neurotransmitter

Release? *Annual review of biochemistry* 77, pp. 615–641.

- Chaturvedi, R.K. and Beal, M.F. 2013. Mitochondrial Diseases of the Brain. *Free Radical Biology and Medicine* 63, pp. 1–29.
- Chen, B.M. and Grinnell, A.D. 1995. Integrins and modulation of transmitter release from motor nerve terminals by stretch. *Science* 269(5230), pp. 1578–1580.
- Chen, Y., Harrison, J.H., and Bunting, L.D. 2018. Effects of replacement of alfalfa silage with corn silage and supplementation of methionine analog and lysine-HCl on milk production and nitrogen feed efficiency in early lactating cows. *Animal Feed Science and Technology* 242, pp. 120–126.
- Chen, Y. and Sheng, Z.H. 2013. Kinesin-1-syntrophin coupling mediates activity-dependent regulation of axonal mitochondrial transport. *Journal of Cell Biology* 202(2), pp. 351–364.
- Chen, Y.P. et al. 2013. PFN1 mutations are rare in Han Chinese populations with amyotrophic lateral sclerosis. *Neurobiology of aging* 34(7), pp. 1922.e1–1922.e5.
- Chéreau, R., Saraceno, G.E., Angibaud, J., Cattaert, D., and Nägerl, U.V. 2017. Superresolution imaging reveals activity-dependent plasticity of axon morphology linked to changes in action potential conduction velocity. *Proceedings of the National Academy of Sciences of the United States of America* 114(6), pp. 1401–1406.
- Chhabra, E.S. and Higgs, H.N. 2006. INF2 Is a WASP homology 2 motif-containing formin that severs actin filaments and accelerates both polymerization and depolymerization. *Journal of Biological Chemistry* 281(36), pp. 26754–26767.
- Chia, P.Z.C. and Gleeson, P.A. 2014. Membrane tethering. *F1000Prime Reports* 6
- Chirackal Manavalan, A.P. et al. 2019. CDK12 controls G1/S progression by regulating RNAPII processivity at core DNA replication genes. *EMBO reports* 20(9), p. e47592.
- Cichon, J. et al. 2012. Cofilin Aggregation Blocks Intracellular Trafficking and Induces Synaptic Loss in Hippocampal Neurons *. *Journal of Biological Chemistry* 287(6), pp. 3919–3929.
- Clark, I.E. et al. 2006. Drosophila pink1 is required for mitochondrial function and interacts genetically with parkin. *Nature* 2006 441:7097 441(7097), pp. 1162–1166.
- Clark, S.E., Moss, D.J., and Bray, D. 1983. Actin polymerization and synthesis in cultured neurones. *Experimental cell research* 147(2), pp. 303–314.
- Colbert, C.M. and Johnston, D. 1996. Axonal action-potential initiation and Na⁺ channel densities in the soma and axon initial segment of subicular pyramidal neurons. *Journal of neuroscience: the official journal of the Society for Neuroscience* 16(21), pp. 6676–86.
- Colbert, C.M. and Pan, E. 2002. Ion channel properties underlying axonal action potential initiation in pyramidal neurons. *Nature Neuroscience* 5(6), pp. 533–538.
- Connell-Crowley, L., Le Gall, M., Vo, D.J., and Giniger, E. 2000. The cyclin-dependent kinase Cdk5 controls multiple aspects of axon patterning in vivo. *Current biology: CB* 10(10), pp. 599–603.

- Cooper, M.L., Crish, S.D., Inman, D.M., Horner, P.J., and Calkins, D.J. 2016. Early astrocyte redistribution in the optic nerve precedes axonopathy in the DBA/2J mouse model of glaucoma. *Experimental Eye Research* 150, pp. 22–33.
- Costello, J.L. et al. 2017. ACBD5 and VAPB mediate membrane associations between peroxisomes and the ER. *Journal of Cell Biology* 216(2), pp. 331–342.
- Covill-Cooke, C., Toncheva, V.S., and Kittler, J.T. 2020. Regulation of peroxisomal trafficking and distribution. *Cellular and Molecular Life Sciences* 2020 78:5 78(5), pp. 1929–1941.
- Cozzolino, M., Pesaresi, M.G., Gerbino, V., Grosskreutz, J., and Carri, M.T. 2012. Amyotrophic Lateral Sclerosis: New Insights into Underlying Molecular Mechanisms and Opportunities for Therapeutic Intervention. <https://home.liebertpub.com/ars> 17(9), pp. 1277–1330.
- Cribbs, J.T. and Strack, S. 2007. Reversible phosphorylation of Drp1 by cyclic AMP-dependent protein kinase and calcineurin regulates mitochondrial fission and cell death. *EMBO Reports* 8(10), pp. 939–944.
- Csordás, G. et al. 2006. Structural and functional features and significance of the physical linkage between ER and mitochondria. *Journal of Cell Biology* 174(7), pp. 915–921.
- Darlington, T.K. et al. 1998. Closing the circadian loop: CLOCK-induced transcription of its own inhibitors per and tim. *Science (New York, N.Y.)* 280(5369), pp. 1599–1603.
- Davie, K. et al. 2018. A Single-Cell Transcriptome Atlas of the Aging Drosophila Brain. *Cell* 174(4), pp. 982-998.e20.
- Davis, R.C., Marsden, I.T., Maloney, M.T., Minamide, L.S., Podlisny, M., Selkoe, D.J., and Bamberg, J.R. 2011. Amyloid beta dimers/trimers potently induce cofilin-actin rods that are inhibited by maintaining cofilin-phosphorylation. *Molecular Neurodegeneration* 6(1), pp. 1–17.
- Dawson, T.M., Golde, T.E., and Lagier-Tourenne, C. 2018. Animal models of neurodegenerative diseases. *Nature Neuroscience* 2018 21:10 21(10), pp. 1370–1379.
- De Jager, P.L. et al. 2014. Alzheimer's disease: early alterations in brain DNA methylation at ANK1, BIN1, RHBDF2 and other loci. *Nature Neuroscience* 17(9), pp. 1156–1163.
- De La Cruz, E.M., Martiel, J.L., and Blanchoin, L. 2015. Mechanical Heterogeneity Favors Fragmentation of Strained Actin Filaments. *Biophysical Journal* 108(9), pp. 2270–2281.
- De Stefani, D., Raffaello, A., Teardo, E., Szabó, I., and Rizzuto, R. 2011. A forty-kilodalton protein of the inner membrane is the mitochondrial calcium uniporter. *Nature* 2011 476:7360 476(7360), pp. 336–340.
- De vos, K.J. et al. 2012. VAPB interacts with the mitochondrial protein PTPIP51 to regulate calcium homeostasis. *Human Molecular Genetics* 21(6), pp. 1299–1311.
- De Vos, K.J., Allan, V.J., Grierson, A.J., and Sheetz, M.P. 2005. Mitochondrial Function and Actin Regulate Dynamin-Related Protein 1-Dependent Mitochondrial Fission. *Current Biology* 15(7), pp. 678–683.
- De Vos, K.J. and Hafezparast, M. 2017. Neurobiology of axonal transport defects

- in motor neuron diseases: Opportunities for translational research? *Neurobiology of Disease* 105, pp. 283–299.
- Dehmelt, L. and Halpain, S. 2005. The MAP2/Tau family of microtubule-associated proteins. *Genome Biology* 6(1), pp. 1–10.
- Delbaere, L.T.J., Vandonselaar, M., Glaeske, D., Jabs, C., and Goldie, H. 1991. Crystallization of the calcium-activated phosphoenolpyruvate carboxykinase from *Escherichia coli* K12. *Journal of Molecular Biology* 219(4), pp. 593–594.
- Denk, W., Yuste, R., Svoboda, K., and Tank, D.W. 1996. Imaging calcium dynamics in dendritic spines. *Current opinion in Neurobiology* 6(3), pp. 372–378.
- Dent, E.W., Gupton, S.L., and Gertler, F.B. 2011. The growth cone cytoskeleton in axon outgrowth and guidance. *Cold Spring Harbor perspectives in biology* 3(3), pp. 1–39.
- Dimitrov, A., Quesnoit, M., Moutel, S., Cantaloube, I., Poüs, C., and Perez, F. 2008. Detection of GTP-tubulin conformation in vivo reveals a role for GTP remnants in microtubule rescues. *Science* 322(5906), pp. 1353–1356.
- Dimitrov, D., He, Y., Mutoh, H., Baker, B.J., Cohen, L., Akermann, W., and Knöpfel, T. 2007. Engineering and Characterization of an Enhanced Fluorescent Protein Voltage Sensor. *PLOS ONE* 2(5), p. e440.
- DiNubile, M.J., Cassimeris, L., Joyce, M., and Zigmond, S.H. 2017. Actin filament barbed-end capping activity in neutrophil lysates: the role of capping protein-beta 2. <https://doi.org/10.1091/mbc.6.12.1659> 6(12), pp. 1659–1671.
- Dirkx, R. et al. 2005. Absence of peroxisomes in mouse hepatocytes causes mitochondrial and ER abnormalities. *Hepatology* 41(4), pp. 868–878.
- Dooley, C.T., Dore, T.M., Hanson, G.T., Jackson, W.C., Remington, S.J., and Tsien, R.Y. 2004. Imaging dynamic redox changes in mammalian cells with green fluorescent protein indicators. *Journal of Biological Chemistry* 279(21), pp. 22284–22293.
- Drerup, C.M., Herbert, A.L., Monk, K.R., and Nechiporuk, A. V. 2017. Regulation of mitochondria-dynactin interaction and mitochondrial retrograde transport in axons. *eLife* 6
- DuBoff, B., Götz, J., and Feany, M.B. 2012. Tau promotes neurodegeneration via DRP1 mislocalization in vivo. *Neuron* 75(4), pp. 618–632.
- Dubrovsky, E.B. 2005. Hormonal cross talk in insect development. *Trends in endocrinology and metabolism: TEM* 16(1), pp. 6–11.
- Duchen, M.R. 1999. Contributions of mitochondria to animal physiology: from homeostatic sensor to calcium signalling and cell death. *Journal of Physiology* 516(Pt 1), p. 1.
- Duffy, J.B. 2002. GAL4 system in *Drosophila*: a fly geneticist's Swiss army knife. *Genesis (New York, N.Y. : 2000)* 34(1–2), pp. 1–15.
- Dumont, E.L.P., Do, C., and Hess, H. 2015. Molecular wear of microtubules propelled by surface-adhered kinesins. *Nature nanotechnology* 10(2), pp. 166–169.
- Edvardson, S., Cinnamon, Y., Jalas, C., Shaag, A., Maayan, C., Axelrod, F.B., and Elpeleg, O. 2012. Hereditary sensory autonomic neuropathy caused by a mutation in dystonin. *Annals of neurology* 71(4), pp. 569–572.

- Effertz, T., Wiek, R., and Göpfert, M.C. 2011. NompC TRP Channel Is Essential for Drosophila Sound Receptor Function. *Current Biology* 21(7), pp. 592–597.
- Egloff, S. and Murphy, S. 2008. Cracking the RNA polymerase II CTD code. *Trends in Genetics* 24(6), pp. 280–288.
- Ekumi, K.M. et al. 2015. Ovarian carcinoma CDK12 mutations misregulate expression of DNA repair genes via deficient formation and function of the Cdk12/CycK complex. *Nucleic acids research* 43(5), pp. 2575–89.
- El Idrissi, A. 2006. Taurine increases mitochondrial buffering of calcium: role in neuroprotection. *Amino Acids* 2006 34:2 34(2), pp. 321–328.
- Endo, M. 1977. Calcium release from the sarcoplasmic reticulum. *Physiological Reviews* 57(1), pp. 71–108.
- Evans, C.S. and Holzbaur, E.L.F. 2020. Quality Control in Neurons: Mitophagy and Other Selective Autophagy Mechanisms. *Journal of Molecular Biology* 432(1), pp. 240–260.
- Fabiato, A. 1983. Calcium-induced release of calcium from the cardiac sarcoplasmic reticulum. *American Journal of Physiology* 14(1)
- Fan, A., Stebbings, K.A., Llano, D.A., and Saif, T. 2015. Stretch induced hyperexcitability of mice callosal pathway. *Frontiers in Cellular Neuroscience* 9(AUGUST)
- Fan, A., Tofangchi, A., Kandel, M., Popescu, G., and Saif, T. 2017. Coupled circumferential and axial tension driven by actin and myosin influences in vivo axon diameter. *Scientific Reports* 7(1)
- Fan, J., Li, X., Issop, L., Culty, M., and Papadopoulos, V. 2016. ACBD2/EC12-mediated peroxisome-mitochondria interactions in leydig cell steroid biosynthesis. *Molecular Endocrinology* 30(7), pp. 763–782.
- Fang, E.F. et al. 2016. NAD⁺ Replenishment Improves Lifespan and Healthspan in Ataxia Telangiectasia Models via Mitophagy and DNA Repair. *Cell Metabolism* 24(4), pp. 566–581.
- Fang, Y. and Bonini, N.M. 2012. Axon degeneration and regeneration: insights from Drosophila models of nerve injury. *Annual review of cell and developmental biology* 28, pp. 575–597.
- Fang, Y. and Bonini, N.M. 2015. Hope on the (fruit) fly: the Drosophila wing paradigm of axon injury. *Neural Regeneration Research* 10(2), p. 173.
- Fang, Y., Soares, L., and Bonini, N.M. 2013. Design and implementation of in vivo imaging of neural injury responses in the adult Drosophila wing. *Nature Protocols* 2013 8:4 8(4), pp. 810–819.
- Fang, Y., Soares, L., Teng, X., Geary, M., and Bonini, N.M. 2012. A Novel Drosophila Model of Nerve Injury Reveals an Essential Role of Nmnat in Maintaining Axonal Integrity. *Current Biology* 22(7), pp. 590–595.
- Farías, G.G., Guardia, C.M., Britt, D.J., Guo, X., and Bonifacino, J.S. 2015. Sorting of Dendritic and Axonal Vesicles at the Pre-axonal Exclusion Zone. *Cell Reports* 13(6), pp. 1221–1232.
- Federico, A., Cardaioli, E., Da Pozzo, P., Formichi, P., Gallus, G.N., and Radi, E. 2012. Mitochondria, oxidative stress and neurodegeneration. *Journal of the neurological sciences* 322(1–2), pp. 254–262.
- Felleman, D.J. and Van Essen, D.C. 1991. Preface: Cerebral Cortex Has Come of

- Age. *Cerebral Cortex* 1(1), pp. 1–1.
- Fernandez-Funez, P., de Mena, L., and Rincon-Limas, D.E. 2015. Modeling the complex pathology of Alzheimer's disease in *Drosophila*. *Experimental neurology* 274(0 0), p. 58.
- Ferrari, C.K.B. 2000. Free radicals, lipid peroxidation and antioxidants in apoptosis: Implications in cancer, cardiovascular and neurological diseases. *Biologia* 55(6), pp. 581–590.
- Ferreira, M.A.R. et al. 2008. Collaborative genome-wide association analysis supports a role for ANK3 and CACNA1C in bipolar disorder. *Nature Genetics* 40(9), pp. 1056–1058.
- Fiala, A. et al. 2002. Genetically Expressed Cameleon in *Drosophila melanogaster* Is Used to Visualize Olfactory Information in Projection Neurons. *Current Biology* 12(21), pp. 1877–1884.
- Fifkov, E. 1985. *A Possible Mechanism of Morphometric Changes in Dendritic Spines Induced by Stimulation*.
- Fill, M. and Copello, J.A. 2002. Ryanodine receptor calcium release channels. *Physiological reviews* 82(4), pp. 893–922.
- Filomeni, G., Rotilio, G., and Ciriolo, M.R. 2003. Glutathione disulfide induces apoptosis in U937 cells by a redox-mediated p38 MAP kinase pathway. *FASEB journal: official publication of the Federation of American Societies for Experimental Biology* 17(1), pp. 64–66.
- Filous, A.R. and Schwab, J.M. 2018. Determinants of Axon Growth, Plasticity, and Regeneration in the Context of Spinal Cord Injury. *The American journal of pathology* 188(1), pp. 53–62.
- Fire, A., Xu, S., Montgomery, M.K., Kostas, S.A., Driver, S.E., and Mello, C.C. 1998. Potent and specific genetic interference by double-stranded RNA in *Caenorhabditis elegans*. *Nature* 391(6669), pp. 806–811.
- Fischler, W., Kong, P., Marella, S., and Scott, K. 2007. The detection of carbonation by the *Drosophila* gustatory system. *Nature* 2007 448:7157 448(7157), pp. 1054–1057.
- Flynn, K.C., Pak, C.W., Shaw, A.E., Bradke, F., and Bamberg, J.R. 2009. Growth cone-like waves transport actin and promote axonogenesis and neurite branching. *Developmental neurobiology* 69(12), pp. 761–779.
- Fortugno, P. et al. 2019. Recessive mutations in the neuronal isoforms of DST, encoding dystonin, lead to abnormal actin cytoskeleton organization and HSN type VI. *Human mutation* 40(1), pp. 106–114.
- Franco, M.C. et al. 2013. Nitration of Hsp90 induces cell death. *Proceedings of the National Academy of Sciences of the United States of America* 110(12), pp. E1102–E1111.
- Fransen, M., Lismont, C., and Walton, P. 2017. The Peroxisome-Mitochondria Connection: How and Why? *International Journal of Molecular Sciences* 18(6)
- Fransen, M., Nordgren, M., Wang, B., and Apanasets, O. 2012. Role of peroxisomes in ROS/RNS-metabolism: implications for human disease. *Biochimica et biophysica acta* 1822(9), pp. 1363–1373.
- Fransson, Å., Ruusala, A., and Aspenström, P. 2003. Atypical Rho GTPases Have Roles in Mitochondrial Homeostasis and Apoptosis. *Journal of Biological Chemistry* 278(8), pp. 6495–6502.

- Frederick, R.L., McCaffery, J.M., Cunningham, K.W., Okamoto, K., and Shaw, J.M. 2004. Yeast Miro GTPase, Gem1p, regulates mitochondrial morphology via a novel pathway. *Journal of Cell Biology* 167(1), pp. 87–98.
- Friedman, J.R., Lackner, L.L., West, M., DiBenedetto, J.R., Nunnari, J., and Voeltz, G.K. 2011. ER tubules mark sites of mitochondrial division. *Science* 334(6054), pp. 358–362.
- Fristrom, D. and Fristrom, J. 1993. *The metamorphic development of the adult epidermis*. New York: Cold Spring Harbor Press.
- Fujikawa, Y. et al. 2016. Mouse redox histology using genetically encoded probes. *Science Signaling* 9(419)
- Fujiwara, T., Ritchie, K., Murakoshi, H., Jacobson, K., and Kusumi, A. 2002. Phospholipids undergo hop diffusion in compartmentalized cell membrane. *Journal of Cell Biology* 157(6), pp. 1071–1081.
- Fung, T.S., Ji, W.-K., Higgs, H.N., and Chakrabarti, R. 2019. Two distinct actin filament populations have effects on mitochondria, with differences in stimuli and assembly factors. *bioRxiv*, p. 701771.
- Gallio, M., Ofstad, T.A., Macpherson, L.J., Wang, J.W., and Zuker, C.S. 2011. The Coding of Temperature in the Drosophila Brain. *Cell* 144(4), pp. 614–624.
- Gallo, A., Vannier, C., and Galli, T. 2016. Endoplasmic Reticulum–Plasma Membrane Associations: Structures and Functions. *Annual review of biochemistry* 32, pp. 279–301.
- Ganguly, A. et al. 2015. A dynamic formin-dependent deep F-actin network in axons. *Journal of Cell Biology* 210(3), pp. 401–417.
- Garcia-Bellido, A. and Merriam, J.R. 1971. Parameters of the wing imaginal disc development of *Drosophila melanogaster*. *Developmental biology* 24(1), pp. 61–87.
- Garofalo, T. et al. 2016. Evidence for the involvement of lipid rafts localized at the ER-mitochondria associated membranes in autophagosome formation. *Autophagy* 12(6), pp. 917–935.
- Gellerich, F.N., Gizatullina, Z., Arandarcikaite, O., Jerzembek, D., Vielhaber, S., Seppet, E., and Striggow, F. 2009. Extramitochondrial Ca²⁺ in the Nanomolar Range Regulates Glutamate-Dependent Oxidative Phosphorylation on Demand. *PLOS ONE* 4(12), p. e8181.
- Giacomello, M., Drago, I., Bortolozzi, M., Scorzeto, M., Gianelle, A., Pizzo, P., and Pozzan, T. 2010. Ca²⁺ Hot Spots on the Mitochondrial Surface Are Generated by Ca²⁺ Mobilization from Stores, but Not by Activation of Store-Operated Ca²⁺ Channels. *Molecular Cell* 38(2), pp. 280–290.
- Gilbert, C.D. and Wiesel, T.N. 1979. Morphology and intracortical projections of functionally characterised neurones in the cat visual cortex. *Nature* 1979 280:5718 280(5718), pp. 120–125.
- Glater, E.E., Megeath, L.J., Stowers, R.S., and Schwarz, T.L. 2006. Axonal transport of mitochondria requires milton to recruit kinesin heavy chain and is light chain independent. *Journal of Cell Biology* 173(4), pp. 545–557.
- Goldschmidt-Clermont, P.J., Furman, M.I., Wachstock, D., Safer, D., Nachmias, V.T., and Pollard, T.D. 2017. The control of actin nucleotide exchange by thymosin beta 4 and profilin. A potential regulatory mechanism for actin polymerization in cells. <https://doi.org/10.1091/mbc.3.9.1015> 3(9), pp. 1015–1024.

- Golic, K.G. and Lindquist, S. 1989. The FLP recombinase of yeast catalyzes site-specific recombination in the *Drosophila* genome. *Cell* 59(3), pp. 499–509.
- Gomes, A.P. et al. 2013. Declining NAD⁺ Induces a Pseudohypoxic State Disrupting Nuclear-Mitochondrial Communication during Aging. *Cell* 155(7), pp. 1624–1638.
- Gomez-Suaga, P., Paillusson, S., Stoica, R., Noble, W., Hanger, D.P., and Miller, C.C.J. 2017. The ER-Mitochondria Tethering Complex VAPB-PTPIP51 Regulates Autophagy. *Current Biology* 27(3), pp. 371–385.
- Görlach, A., Klappa, P., and Kietzmann, T. 2006. The endoplasmic reticulum: Folding, calcium homeostasis, signaling, and redox control. *Antioxidants and Redox Signaling* 8(9–10), pp. 1391–1418.
- Gray, J.J., Zommer, A.E., Bouchard, R.J., Duval, N., Blackstone, C., and Linseman, D.A. 2013. N-terminal cleavage of the mitochondrial fusion GTPase OPA1 occurs via a caspase-independent mechanism in cerebellar granule neurons exposed to oxidative or nitrosative stress. *Brain Research* 1494, pp. 28–43.
- Greene, J.C., Whitworth, A.J., Kuo, I., Andrews, L.A., Feany, M.B., and Pallanck, L.J. 2003. Mitochondrial pathology and apoptotic muscle degeneration in *Drosophila* parkin mutants. *Proceedings of the National Academy of Sciences of the United States of America* 100(7), pp. 4078–4083.
- Gross, E. et al. 2006. Generating disulfides enzymatically: Reaction products and electron acceptors of the endoplasmic reticulum thiol oxidase Ero1p. *Proceedings of the National Academy of Sciences of the United States of America* 103(2), pp. 299–304.
- Grubb, M.S. and Burrone, J. 2010. Building and maintaining the axon initial segment. *Current Opinion in Neurobiology* 20(4), pp. 481–488.
- Guardia-Laguarta, C. et al. 2014. α -Synuclein Is Localized to Mitochondria-Associated ER Membranes. *Journal of Neuroscience* 34(1), pp. 249–259.
- Gumy, L., Katrukha, E., and Grigoriev, I. 2017. MAP2 Defines a Pre-axonal Filtering Zone to Regulate KIF1- versus KIF5-Dependent Cargo Transport in Sensory Neurons. *Neuron*
- Gumy, L.F., Katrukha, E.A., Grigoriev, I., Jaarsma, D., Kapitein, L.C., Akhmanova, A., and Hoogenraad, C.C. 2018. Local mechanisms regulating selective cargo entry and long-range trafficking in axons. *Current Opinion in Neurobiology* 51, pp. 23–28.
- Guo, Y. et al. 2018. Visualizing Intracellular Organelle and Cytoskeletal Interactions at Nanoscale Resolution on Millisecond Timescales. *Cell* 175(5), pp. 1430–1442.e17.
- Guo, Y., Sirkis, D.W., and Schekman, R. 2014. Protein Sorting at the trans-Golgi Network. *Cell Biology* 30, pp. 169–206.
- Gür, B., Sporar, K., Lopez-Behling, A., and Silies, M. 2020. Distinct expression of potassium channels regulates visual response properties of lamina neurons in *Drosophila melanogaster*. *Journal of Comparative Physiology A: Neuroethology, Sensory, Neural, and Behavioral Physiology* 206(2), pp. 273–287.
- Gurel, P.S., Hatch, A.L., and Higgs, H.N. 2014. Connecting the Cytoskeleton to the Endoplasmic Reticulum and Golgi. *Current Biology* 24(14), pp. R660–R672.
- Gutschner, M. et al. 2008. Real-time imaging of the intracellular glutathione redox

- potential. *Nature Methods* 2008 5:6 5(6), pp. 553–559.
- Gutscher, M., Sobotta, M.C., Wabnitz, G.H., Ballikaya, S., Meyer, A.J., Samstag, Y., and Dick, T.P. 2009. Proximity-based Protein Thiol Oxidation by H₂O₂-scavenging Peroxidases. *Journal of Biological Chemistry* 284(46), pp. 31532–31540.
- H F Lodish, N Kong, and L Wikström 1992. Calcium is required for folding of newly made subunits of the asialoglycoprotein receptor within the endoplasmic reticulum - PubMed. *Journal of Biological Chemistry*
- Hagiwara, S. and Naka, K.I. 1964. The Initiation of Spike Potential in Barnacle Muscle Fibers under Low Intracellular Ca⁺⁺. *Journal of general physiology* 48(1), pp. 141–162.
- Hailey, D.W., Rambold, A.S., Satpute-Krishnan, P., Mitra, K., Sougrat, R., Kim, P.K., and Lippincott-Schwartz, J. 2010. Mitochondria Supply Membranes for Autophagosome Biogenesis during Starvation. *Cell* 141(4), pp. 656–667.
- Hales, K.G. and Fuller, M.T. 1997. Developmentally regulated mitochondrial fusion mediated by a conserved, novel, predicted GTPase. *Cell* 90(1), pp. 121–129.
- Hamada, F.N., Rosenzweig, M., Kang, K., Pulver, S.R., Ghezzi, A., Jegla, T.J., and Garrity, P.A. 2008. An internal thermal sensor controlling temperature preference in *Drosophila*. *Nature* 2008 454:7201 454(7201), pp. 217–220.
- Hamasaki, M. et al. 2013. Autophagosomes form at ER–mitochondria contact sites. *Nature* 2013 495:7441 495(7441), pp. 389–393.
- Hammarlund, M., Jorgensen, E.M., and Bastiani, M.J. 2007. Axons break in animals lacking β -spectrin. *Journal of Cell Biology* 176(3), pp. 269–275.
- Hammond, J.W., Huang, C.F., Kaech, S., Jacobson, C., Banker, G., and Verhey, K.J. 2010. Posttranslational modifications of tubulin and the polarized transport of kinesin-1 in neurons. *Molecular Biology of the Cell* 21(4), pp. 572–583.
- Han, B., Zhou, R., Xia, C., and Zhuang, X. 2017. Structural organization of the actin-spectrin-based membrane skeleton in dendrites and soma of neurons. *Proceedings of the National Academy of Sciences of the United States of America* 114(32), pp. E6678–E6685.
- Hanson, G.T., Aggeler, R., Oglesbee, D., Cannon, M., Capaldi, R.A., Tsien, R.Y., and Remington, S.J. 2004. Investigating mitochondrial redox potential with redox-sensitive green fluorescent protein indicators. *The Journal of biological chemistry* 279(13), pp. 13044–13053.
- Hanson, J. and Lowy, J. 1963. The structure of F-actin and of actin filaments isolated from muscle. *Journal of Molecular Biology* 6(1), pp. 46–IN5.
- Hara-Kuge, S., Kuge, O., Orci, L., Amherdt, M., Ravazzola, M., Wieland, F.T., and Rothman, J.E. 1994. En bloc incorporation of coatamer subunits during the assembly of COP-coated vesicles. *Journal of Cell Biology* 124(6), pp. 883–892.
- Harterink, M. et al. 2019. TRIM46 Organizes Microtubule Fasciculation in the Axon Initial Segment. *The Journal of neuroscience : the official journal of the Society for Neuroscience* 39(25), pp. 4864–4873.
- Hartmann, J. and Verkhatsky, A. 1998. Relations between intracellular Ca²⁺ stores and store-operated Ca²⁺ entry in primary cultured human glioblastoma cells. *The Journal of Physiology* 513(2), pp. 411–424.
- Hasan, M.T. et al. 2004. Functional fluorescent Ca²⁺ indicator proteins in

- transgenic mice under TET control. *PLoS Biology* 2(6)
- Hatch, A.L., Gurel, P.S., and Higgs, H.N. 2014. Novel roles for actin in mitochondrial fission. *Journal of Cell Science COMMENTARY* 127(Pt 21), pp. 4549–4560.
- Hatch, A.L., Ji, W.K., Merrill, R.A., Strack, S., and Higgs, H.N. 2016. Actin filaments as dynamic reservoirs for Drp1 recruitment. *Molecular Biology of the Cell* 27(20), p. 3109.
- Hay, B. a, Wolff, T., and Rubin, G.M. 1994. Expression of baculovirus P35 prevents cell death in *Drosophila*. *Development (Cambridge, England)* 120(8), pp. 2121–2129.
- He, J. et al. 2016. Prevalent presence of periodic actin-spectrin-based membrane skeleton in a broad range of neuronal cell types and animal species. *Proceedings of the National Academy of Sciences of the United States of America* 113(21), pp. 6029–6034.
- Heales, S.J.R., Bolaños, J.P., Stewart, V.C., Brookes, P.S., Land, J.M., and Clark, J.B. 1999. Nitric oxide, mitochondria and neurological disease. *Biochimica et biophysica acta* 1410(2), pp. 215–228.
- Hedstrom, K.L., Ogawa, Y., and Rasband, M.N. 2008. AnkyrinG is required for maintenance of the axon initial segment and neuronal polarity. *Journal of Cell Biology* 183(4), pp. 635–640.
- Hedstrom, K.L. and Rasband, M.N. 2006. Intrinsic and extrinsic determinants of ion channel localization in neurons. *Journal of Neurochemistry* 98(5), pp. 1345–1352.
- Hedstrom, K.L., Xu, X., Ogawa, Y., Frischknecht, R., Seidenbecher, C.I., Shrager, P., and Rasband, M.N. 2007. Neurofascin assembles a specialized extracellular matrix at the axon initial segment. *Journal of Cell Biology* 178(5), pp. 875–886.
- Heim, N. et al. 2007. Improved calcium imaging in transgenic mice expressing a troponin C-based biosensor. *Nature methods* 4(2), pp. 127–129.
- Hermann, G.J., Thatcher, J.W., Mills, J.P., Hales, K.G., Fuller, M.T., Nunnari, J., and Shaw, J.M. 1998. Mitochondrial fusion in yeast requires the transmembrane GTPase Fzo1p. *Journal of Cell Biology* 143(2), pp. 359–373.
- Hinckelmann, M.V., Zala, D., and Saudou, F. 2013. Releasing the brake: restoring fast axonal transport in neurodegenerative disorders. *Trends in Cell Biology* 23(12), pp. 634–643.
- Hirokawa, N., Noda, Y., Tanaka, Y., and Niwa, S. 2009. Kinesin superfamily motor proteins and intracellular transport. *Nature Reviews Molecular Cell Biology* 2009 10:10 10(10), pp. 682–696.
- Holmes, K.C., Popp, D., Gebhard, W., and Kabsch, W. 1990. Atomic model of the actin filament. *Nature* 347(6288), pp. 44–49.
- Hom, J.R., Gewandter, J.S., Michael, L., Sheu, S.S., and Yoon, Y. 2007. Thapsigargin induces biphasic fragmentation of mitochondria through calcium-mediated mitochondrial fission and apoptosis. *Journal of Cellular Physiology* 212(2), pp. 498–508.
- Hoppins, S., Lackner, L., and Nunnari, J. 2007. The machines that divide and fuse mitochondria. *Annual review of biochemistry* 76, pp. 751–780.
- Horga, A. et al. 2017. Genetic and clinical characteristics of NEFL-related

- Charcot-Marie-Tooth disease. *Journal of neurology, neurosurgery, and psychiatry* 88(7), pp. 575–585.
- Hortsch, M., Paisley, K.L., Tian, M.-Z., Qian, M., Bouley, M., and Chandler, R. 2002. The Axonal Localization of Large Drosophila Ankyrin2 Protein Isoforms Is Essential for Neuronal Functionality. *Molecular and Cellular Neuroscience* 20(1), pp. 43–55.
- Hsu, J.M., Kang, Y., Corty, M.M., Mathieson, D., Peters, O.M., and Freeman, M.R. 2021. Injury-induced inhibition of bystander neurons requires dSarm and signaling from glia. *Neuron* 109(3), p. 473.
- Hua, R. et al. 2017. VAPs and ACBD5 tether peroxisomes to the ER for peroxisome maintenance and lipid homeostasis. *Journal of Cell Biology* 216(2), pp. 367–377.
- Huang, C.F. and Banker, G. 2012. The translocation selectivity of the kinesins that mediate neuronal organelle transport. *Traffic* 13(4), pp. 549–564.
- Huang, C.Y.M. and Rasband, M.N. 2018. Axon initial segments: structure, function, and disease. *Annals of the New York Academy of Sciences* 1420(1), pp. 46–61.
- Huxley, H.E. 1963. Electron Microscope Studies on the Structure of Natural and Synthetic Protein Filaments from Striated Muscle. *Journal of Molecular Biology* 7(3), pp. 281–308.
- Ichimura, H., Parthasarathi, K., Quadri, S., Issekutz, A.C., and Bhattacharya, J. 2003. Mechano-oxidative coupling by mitochondria induces proinflammatory responses in lung venular capillaries. *The Journal of Clinical Investigation* 111(5), pp. 691–699.
- Imbert, N., Cognard, C., Duport, G., Guillou, C., and Raymond, G. 1995. Abnormal calcium homeostasis in Duchenne muscular dystrophy myotubes contracting in vitro. *Cell Calcium* 18(3), pp. 177–186.
- Inagaki, N., Toriyama, M., and Sakumura, Y. 2011. Systems biology of symmetry breaking during neuronal polarity formation. *Developmental Neurobiology* 71(6), pp. 584–593.
- Iqbal, K., Liu, F., Gong, C.X., del Alonso, A.C., and Grundke-Iqbal, I. 2009. Mechanisms of tau-induced neurodegeneration. *Acta neuropathologica* 118(1), pp. 53–69.
- Ishikawa-Ankerhold, H.C., Ankerhold, R., and Drummen, G.P.C. 2012. Advanced Fluorescence Microscopy Techniques—FRAP, FLIP, FLAP, FRET and FLIM. *Molecules* 17(4), p. 4047.
- Islinger, M., Grille, S., Dariush Fahimi, • H, and Schrader, M. 2012. The peroxisome: an update on mysteries. *Histochem Cell Biol* 150(5), pp. 443–471.
- Israelson, A., Abu-Hamad, S., Zaid, H., Nahon, E., and Shoshan-Barmatz, V. 2007. Localization of the voltage-dependent anion channel-1 Ca²⁺-binding sites. *Cell Calcium* 41(3), pp. 235–244.
- Iwasa, K. and Tasaki, I. 1980. Mechanical changes in squid giant axons associated with production of action potentials. *Biochemical and Biophysical Research Communications* 95(3), pp. 1328–1331.
- Izadifar, A. et al. 2021. Axon morphogenesis and maintenance require an evolutionary conserved safeguard function of Wnk kinases antagonizing Sarm and Axed. *Neuron* 109(18), pp. 2864-2883.e8.

- Jackson, G.R. et al. 1998. Polyglutamine-expanded human huntingtin transgenes induce degeneration of *Drosophila* photoreceptor neurons. *Neuron* 21(3), pp. 633–642.
- Jacobson, K., Derzko, Z., Wu, E.S., Hou, Y., and Poste, G. 1976. Measurement of the lateral mobility of cell surface components in single, living cells by fluorescence recovery after photobleaching. *Journal of supramolecular structure* 5(4), pp. 565–576.
- Jahani-Asl, A., Pilon-Larose, K., Xu, W., MacLaurin, J.G., Park, D.S., McBride, H.M., and Slack, R.S. 2011. The Mitochondrial Inner Membrane GTPase, Optic Atrophy 1 (Opa1), Restores Mitochondrial Morphology and Promotes Neuronal Survival following Excitotoxicity *. *Journal of Biological Chemistry* 286(6), pp. 4772–4782.
- Jahn, R. and Scheller, R.H. 2006. SNAREs - Engines for membrane fusion. *Nature Reviews Molecular Cell Biology* 7(9), pp. 631–643.
- Jamieson, D.J. 1998. Oxidative Stress Responses of the Yeast *Saccharomyces cerevisiae*. *Yeast* 14(16), pp. 1511–1527.
- Jegla, T. et al. 2016. Bilaterian Giant Ankyrins Have a Common Evolutionary Origin and Play a Conserved Role in Patterning the Axon Initial Segment. *PLOS Genetics* 12(12), p. e1006457.
- Jenkins, S.M. and Bennett, V. 2001. Ankyrin-G coordinates assembly of the spectrin-based membrane skeleton, voltage-gated sodium channels, and L1 CAMs at Purkinje neuron initial segments. *Journal of Cell Biology* 155(5), pp. 739–745.
- Ji, W.K., Hatch, A.L., Merrill, R.A., Strack, S., and Higgs, H.N. 2015. Actin filaments target the oligomeric maturation of the dynamin GTPase Drp1 to mitochondrial fission sites. *eLife* 4(NOVEMBER2015)
- Jin, L., Han, Z., Platasa, J., Wooltorton, J.R.A., Cohen, L.B., and Pieribone, V.A. 2012. Single Action Potentials and Subthreshold Electrical Events Imaged in Neurons with a Fluorescent Protein Voltage Probe. *Neuron* 75(5), pp. 779–785.
- John, N. et al. 2006. Brevican-containing perineuronal nets of extracellular matrix in dissociated hippocampal primary cultures. *Molecular and Cellular Neuroscience* 31(4), pp. 774–784.
- Johnson, F.H. and Shimomura, O. 1972. Preparation and Use of Aequorin for Rapid Microdetermination of Ca²⁺ in Biological Systems. *Nature New Biology* 1972 237:78 237(78), pp. 287–288.
- Johri, A. and Beal, M.F. 2012. Mitochondrial Dysfunction in Neurodegenerative Diseases. *Journal of Pharmacology and Experimental Therapeutics* 342(3), pp. 619–630.
- Jones, D.P. 2006. Redefining Oxidative Stress. *Antioxidants & Redox Signaling* 8(9–10), pp. 1865–1879.
- Jones, S.L. and Svitkina, T.M. 2016. Axon Initial Segment Cytoskeleton: Architecture, Development, and Role in Neuron Polarity. *Neural Plasticity* 2016
- Joshi, P.M., Sutor, S.L., Huntoon, C.J., and Karnitz, L.M. 2014. Ovarian cancer-associated mutations disable catalytic activity of CDK12, a kinase that promotes homologous recombination repair and resistance to cisplatin and poly(ADP-ribose) polymerase inhibitors. *Journal of Biological Chemistry* 289(13), pp. 9247–9253.

- Juan, H.C., Lin, Y., Chen, H.R., and Fann, M.J. 2016. Cdk12 is essential for embryonic development and the maintenance of genomic stability. *Cell Death and Differentiation* 23(6), pp. 1038–1048.
- Kageyama, Y. et al. 2012. Mitochondrial division ensures the survival of postmitotic neurons by suppressing oxidative damage. *Journal of Cell Biology* 197(4), pp. 535–551.
- Kalume, F., Yu, F.H., Westenbroek, R.E., Scheuer, T., and Catterall, W.A. 2007. Reduced Sodium Current in Purkinje Neurons from NaV1.1 Mutant Mice: Implications for Ataxia in Severe Myoclonic Epilepsy in Infancy. *Journal of Neuroscience* 27(41), pp. 11065–11074.
- Kamerkar, S.C., Kraus, F., Sharpe, A.J., Pucadyil, T.J., and Ryan, M.T. 2018. Dynamin-related protein 1 has membrane constricting and severing abilities sufficient for mitochondrial and peroxisomal fission. *Nature communications* 9(1)
- Kamikouchi, A., Inagaki, H.K., Effertz, T., Hendrich, O., Fiala, A., Göpfert, M.C., and Ito, K. 2009. The neural basis of *Drosophila* gravity-sensing and hearing. *Nature* 2009 458:7235 458(7235), pp. 165–171.
- Kanca, O., Caussinus, E., Denes, A.S., Percival-Smith, A., and Affolter, M. 2014. Raeppli: a whole-tissue labeling tool for live imaging of *Drosophila* development. *Development (Cambridge, England)* 141(2), pp. 472–480.
- Kandel, E., Schwartz, J., Jessell, T., Siegelbaum, S., and Hudspeth, A.J. 2012. *Principles of Neural Science*. 5th ed. McGraw-Hill Education.
- Kang, B.E. and Baker, B.J. 2016. Pado, a fluorescent protein with proton channel activity can optically monitor membrane potential, intracellular pH, and map gap junctions. *Scientific Reports* 2016 6:1 6(1), pp. 1–13.
- Kang, J.S., Tian, J.H., Pan, P.Y., Zald, P., Li, C., Deng, C., and Sheng, Z.H. 2008. Docking of axonal mitochondria by syntaphilin controls their mobility and affects short-term facilitation. *Cell* 132(1), pp. 137–148.
- Karbowski, M. and Youle, R.J. 2011. Regulating mitochondrial outer membrane proteins by ubiquitination and proteasomal degradation. *Current Opinion in Cell Biology* 23(4), pp. 476–482.
- Katayama, H., Kogure, T., Mizushima, N., Yoshimori, T., and Miyawaki, A. 2011. A sensitive and quantitative technique for detecting autophagic events based on lysosomal delivery. *Chemistry & biology* 18(8), pp. 1042–1052.
- Katsuno, H., Toriyama, M., Hosokawa, Y., Mizuno, K., Ikeda, K., Sakumura, Y., and Inagaki, N. 2015. Actin Migration Driven by Directional Assembly and Disassembly of Membrane-Anchored Actin Filaments. *Cell reports* 12(4), pp. 648–660.
- Kelly, S.M., Elchert, A., and Kahl, M. 2017. Dissection and Immunofluorescent Staining of Mushroom Body and Photoreceptor Neurons in Adult *Drosophila melanogaster* Brains. *Journal of Visualized Experiments* (129)
- Kendrick-Jones, J. and Buss, F. 2016. Editorial Overview: Myosins in Review. *Traffic* 17(8), pp. 819–821.
- Kerr, J.S., Adriaanse, B.A., Greig, N.H., Mattson, M.P., Cader, M.Z., Bohr, V.A., and Fang, E.F. 2017. Mitophagy and Alzheimer's Disease: Cellular and Molecular Mechanisms. *Trends in Neurosciences* 40(3), pp. 151–166.
- Kinosian, H.J., Newman, J., Lincoln, B., Selden, L.A., Gershman, L.C., and Estes, J.E. 1998. Ca²⁺ Regulation of Gelsolin Activity: Binding and Severing of

- F-actin. *Biophysical Journal* 75(6), pp. 3101–3109.
- Kitada, T. et al. 1998. Mutations in the parkin gene cause autosomal recessive juvenile parkinsonism. *Nature* 1998 392:6676 392(6676), pp. 605–608.
- Klarsfeld, A. and Rouyer, F. 1998. Effects of Circadian Mutations and LD Periodicity on the Life Span of *Drosophila melanogaster*. *Journal of Biological Rhythms* 13(6), pp. 471–478.
- Klinman, E. and Holzbaur, E.L.F. 2015. Stress-Induced CDK5 Activation Disrupts Axonal Transport via Lis1/Ndel1/Dynein. *Cell reports* 12(3), pp. 462–473.
- Klinman, E., Tokito, M., and Holzbaur, E.L.F.F. 2017. CDK5-dependent activation of dynein in the axon initial segment regulates polarized cargo transport in neurons. *Traffic* 18(12), p. 808.
- Ko, S.H., Choi, S.W., Ye, S.K., Cho, B.L., Kim, H.S., and Chung, M.H. 2005. Comparison of the antioxidant activities of nine different fruits in human plasma. *Journal of Medicinal Food* 8(1), pp. 41–46.
- Koch, A., Thiemann, M., Grabenbauer, M., Yoon, Y., McNiven, M.A., and Schrader, M. 2003. Dynamin-like protein 1 is involved in peroxisomal fission. *Journal of Biological Chemistry* 278(10), pp. 8597–8605.
- Koeberle, P.D. and Ball, A.K. 1999. Nitric oxide synthase inhibition delays axonal degeneration and promotes the survival of axotomized retinal ganglion cells. *Experimental Neurology* 158(2), pp. 366–381.
- Kole, M.H.P., Ilschner, S.U., Kampa, B.M., Williams, S.R., Ruben, P.C., and Stuart, G.J. 2008. Action potential generation requires a high sodium channel density in the axon initial segment. *Nature Neuroscience* 11(2), pp. 178–186.
- Kole, M.H.P. and Stuart, G.J. 2008. Is action potential threshold lowest in the axon? *Nature Neuroscience* 11(11), pp. 1253–1255.
- Konishi, Y. and Setou, M. 2009. Tubulin tyrosination navigates the kinesin-1 motor domain to axons. *Nature Neuroscience* 12(5), pp. 559–567.
- Konopka, R.J. and Benzer, S. 1971. Clock Mutants of *Drosophila melanogaster*. *Proceedings of the National Academy of Sciences* 68(9), p. 2112.
- Kordeli, E., Lambert, S., and Bennett, V. 1995. AnkyrinG: A new ankyrin gene with neural-specific isoforms localised at the axonal initial segment and node of Ranvier. *Journal of Biological Chemistry* 270(5), pp. 2352–2359.
- Korobova, F., Gauvin, T.J., and Higgs, H.N. 2014. A Role for Myosin II in Mammalian Mitochondrial Fission. *Current Biology* 24(4), pp. 409–414.
- Korobova, F., Ramabhadran, V., and Higgs, H.N. 2013. An Actin-Dependent Step in Mitochondrial Fission Mediated by the ER-Associated Formin INF2. *Science (New York, N.Y.)* 339(6118), pp. 464–467.
- Korobova, F. and Svitkina, T.M. 2010. Molecular architecture of synaptic actin cytoskeleton in hippocampal neurons reveals a mechanism of dendritic spine morphogenesis. *Molecular biology of the cell* 21(1), pp. 165–176.
- Kösel, S., Hofhaus, G., Maassen, A., Vieregge, P., and Graeber, M.B. 1999. Role of mitochondria in Parkinson disease. *Biological chemistry* 380(7–8), pp. 865–870.
- Koser, D.E. et al. 2016. Mechanosensing is critical for axon growth in the developing brain. *Nature Neuroscience* 19(12), pp. 1592–1598.

- Kovacs, G.G. et al. 2017. Plasma and cerebrospinal fluid tau and neurofilament concentrations in rapidly progressive neurological syndromes: a neuropathology-based cohort. *European journal of neurology* 24(11), pp. 1326–1377.
- Kovar, D.R. and Pollard, T.D. 2004. Insertional assembly of actin filament barbed ends in association with formins produces piconewton forces. *Proceedings of the National Academy of Sciences of the United States of America* 101(41), pp. 14725–14730.
- Kowaltowski, A.J. et al. 2019. Mitochondrial morphology regulates organellar Ca²⁺ uptake and changes cellular Ca²⁺ homeostasis. *FASEB journal : official publication of the Federation of American Societies for Experimental Biology* 33(12), pp. 13176–13188.
- Kriebel, M., Metzger, J., Trinks, S., Chugh, D., Harvey, R.J., Harvey, K., and rgen Volkmer, H. 2011. The Cell Adhesion Molecule Neurofascin Stabilizes Axo-axonic GABAergic Terminals at the Axon Initial Segment. *Journal of Biological Chemistry* 8(286), p. 27.
- Krieger, C. and Duchen, M.R. 2002. Mitochondria, Ca²⁺ and neurodegenerative disease. *European journal of pharmacology* 447(2–3), pp. 177–188.
- Krijnse-Locker, J., Parton, R.G., Fuller, S.D., Griffiths, G., and Dotti, C.G. 1995. The organisation of the endoplasmic reticulum and the intermediate compartment in cultured rat hippocampal neurons. *Molecular biology of the cell* 6(10), pp. 1315–1332.
- Kroemer, G., Galluzzi, L., and Brenner, C. 2007. Mitochondrial membrane permeabilization in cell death. *Physiological Reviews* 87(1), pp. 99–163.
- Kruppa, A.J. et al. 2018. Myosin VI-Dependent Actin Cages Encapsulate Parkin-Positive Damaged Mitochondria. *Developmental Cell* 44(4), pp. 484–499.e6.
- Kudo, M., Yamamoto, M., and Nakamura, Y. 1991. Suprachiasmatic nucleus and retinohypothalamic projections in moles. *Brain, behavior and evolution* 38(6), pp. 332–338.
- Kuijpers, M. et al. 2016. Dynein Regulator NDEL1 Controls Polarized Cargo Transport at the Axon Initial Segment. *Neuron* 89(3), pp. 461–471.
- Kukreja, R.C., Kontos, H.A., Hess, M.L., and Ellis, E.F. 1986. PGH synthase and lipoxygenase generate superoxide in the presence of NADH or NADPH. *Circulation Research* 59(6), pp. 612–619.
- Kulić, I.M. et al. 2008. The role of microtubule movement in bidirectional organelle transport. *Proceedings of the National Academy of Sciences of the United States of America* 105(29), p. 10011.
- Kural, C., Kim, H., Syed, S., Goshima, G., Gelfand, V.I., and Selvin, P.R. 2005. Kinesin and dynein move a peroxisome in vivo: a tug-of-war or coordinated movement? *Science (New York, N.Y.)* 308(5727), pp. 1469–1472.
- Kuznetsov, G., Chen, L.B., and Nigam, S.K. 1997. Multiple Molecular Chaperones Complex with Misfolded Large Oligomeric Glycoproteins in the Endoplasmic Reticulum. *Journal of Biological Chemistry* 272(5), pp. 3057–3063.
- Lai, S.-L. and Lee, T. 2006. Genetic mosaic with dual binary transcriptional systems in *Drosophila*. *Nature Neuroscience* 9(5), pp. 703–709.
- Lamoureux, P., Heidemann, S.R., Martzke, N.R., and Miller, K.E. 2010. Growth and elongation within and along the axon. *Developmental Neurobiology* 70(3),

pp. 135–149.

- Langer, T., Käser, M., Klanner, C., and Leonhard, K. 2001. AAA proteases of mitochondria: quality control of membrane proteins and regulatory functions during mitochondrial biogenesis. *Biochemical Society Transactions* 29(4), pp. 431–436.
- Larkin, A. et al. 2021. FlyBase: updates to the *Drosophila melanogaster* knowledge base. *Nucleic Acids Research* 49(D1), pp. D899–D907.
- Lassmann, H. 2014. Multiple sclerosis: Lessons from molecular neuropathology. *Experimental Neurology* 262(Part A), pp. 2–7.
- Lee, J.M. and Johnson, J.A. 2004. An important role of Nrf2-ARE pathway in the cellular defense mechanism. *Journal of Biochemistry and Molecular Biology* 37(2), pp. 139–143.
- Lee, T. and Luo, L. 1999. Mosaic Analysis with a Repressible Cell Marker for Studies of Gene Function in Neuronal Morphogenesis. *Neuron* 22(3), pp. 451–461.
- Lee, T. and Luo, L. 2001. Mosaic analysis with a repressible cell marker (MARCM) for *Drosophila* neural development. *Trends in neurosciences* 24(5), pp. 251–4.
- Lei, T. et al. 2018. Cyclin K regulates prereplicative complex assembly to promote mammalian cell proliferation. *Nature Communications* 9(1), pp. 1–15.
- Leite, S.C. et al. 2016. The Actin-Binding Protein α -Adducin Is Required for Maintaining Axon Diameter. *Cell Reports* 15(3), pp. 490–498.
- León-Espinosa, G., Defelipe, J., and Muñoz, A. 2012. Effects of amyloid- β plaque proximity on the axon initial segment of pyramidal cells. *Journal of Alzheimer's Disease* 29(4), pp. 841–852.
- Leterrier, C. 2016. The Axon Initial Segment, 50 Years Later: A Nexus for Neuronal Organization and Function. *Current Topics in Membranes* 77, pp. 185–233.
- Leterrier, C. 2018. The Axon Initial Segment: An Updated Viewpoint. *Journal of neuroscience: the official journal of the Society for Neuroscience* 38(9), pp. 2135–2145.
- Leterrier, C. and Dargent, B. 2014. No Pasaran! Role of the axon initial segment in the regulation of protein transport and the maintenance of axonal identity. *Seminars in Cell & Developmental Biology* 27, pp. 44–51.
- Leterrier, C., Potier, J., Caillol, G., Debarnot, C., Rueda Boroni, F., and Dargent, B. 2015. Nanoscale Architecture of the Axon Initial Segment Reveals an Organized and Robust Scaffold. *Cell Reports* 13(12), pp. 2781–2793.
- Lewis, S.C., Uchiyama, L.F., and Nunnari, J. 2016. ER-mitochondria contacts couple mtDNA synthesis with Mitochondrial division in human cells. *Science* 353(6296)
- Lewis, T.L., Kwon, S.K., Lee, A., Shaw, R., and Polleux, F. 2018. MFF-dependent mitochondrial fission regulates presynaptic release and axon branching by limiting axonal mitochondria size. *Nature Communications* 2018 9:1 9(1), pp. 1–15.
- Lewis, T.L., Mao, T., Svoboda, K., and Arnold, D.B. 2009. Myosin-dependent targeting of transmembrane proteins to neuronal dendrites. *Nature Neuroscience* 12(5), pp. 568–576.

- Li, G.B. et al. 2018. Mitochondrial fission and mitophagy depend on cofilin-mediated actin depolymerization activity at the mitochondrial fission site. *Oncogene* 2018 37:11 37(11), pp. 1485–1502.
- Li, S., Xu, S., Roelofs, B.A., Boyman, L., Jonathan Lederer, W., Sesaki, H., and Karbowski, M. 2015. Transient assembly of F-actin on the outer mitochondrial membrane contributes to mitochondrial fission. *Journal of Cell Biology* 208(1), pp. 109–123.
- Li, X., Chatterjee, N., Spirohn, K., Boutros, M., and Bohmann, D. 2016. Cdk12 Is A Gene-Selective RNA Polymerase II Kinase That Regulates a Subset of the Transcriptome, Including Nrf2 Target Genes OPEN. *Nature Publishing Group*
- Li, X., Kumar, Y., Zempel, H., Mandelkow, E.M., Biernat, J., and Mandelkow, E. 2011. Novel diffusion barrier for axonal retention of Tau in neurons and its failure in neurodegeneration. *EMBO Journal* 30(23), pp. 4825–4837.
- Ligon, L.A. and Steward, O. 2000. Role of Microtubules and Actin Filaments in the Movement of Mitochondria in the Axons and Dendrites of Cultured Hippocampal Neurons Indexing terms: organelle transport; axonal transport; dendritic transport. *Journal of Comparative Neurology* 427, pp. 351–361.
- Lin, T.H. et al. 2021. TSG101 negatively regulates mitochondrial biogenesis in axons. *Proceedings of the National Academy of Sciences of the United States of America* 118(20)
- Lipka, J., Kapitein, L.C., Jaworski, J., and Hoogenraad, C.C. 2016. Microtubule-binding protein doublecortin-like kinase 1 (DCLK1) guides kinesin-3-mediated cargo transport to dendrites. *The EMBO Journal* 35(3), pp. 302–318.
- Lissandron, V., Podini, P., Pizzo, P., and Pozzan, T. 2010. Unique characteristics of Ca²⁺ homeostasis of the trans-Golgi compartment. *Proceedings of the National Academy of Sciences of the United States of America* 107(20), pp. 9198–9203.
- Liu, D. et al. 2013. Nicotinamide forestalls pathology and cognitive decline in Alzheimer mice: evidence for improved neuronal bioenergetics and autophagy procession. *Neurobiology of Aging* 34(6), pp. 1564–1580.
- Liu, J.S.H., Zhao, M.L., Brosnan, C.F., and Lee, S.C. 2001. Expression of inducible nitric oxide synthase and nitrotyrosine in multiple sclerosis lesions. *The American journal of pathology* 158(6), pp. 2057–2066.
- Liu, Q., Zhang, D., Hu, D., Zhou, X., and Zhou, Y. 2018. The role of mitochondria in NLRP3 inflammasome activation. *Molecular Immunology* 103, pp. 115–124.
- Liu, X. and Davis, R.L. 2008. The GABAergic anterior paired lateral neuron suppresses and is suppressed by olfactory learning. *Nature Neuroscience* 2008 12:1 12(1), pp. 53–59.
- Liu, Z., Celotto, A.M., Romero, G., Wipf, P., and Palladino, M.J. 2012. Genetically encoded redox sensor identifies the role of ROS in degenerative and mitochondrial disease pathogenesis. *Neurobiology of disease* 45(1), p. 362.
- Lloyd, T.E. and Taylor, J.P. 2010. Flightless flies: *Drosophila* models of neuromuscular disease. *Annals of the New York Academy of Sciences* 1184
- Lobas, M.A. et al. 2019. A genetically encoded single-wavelength sensor for imaging cytosolic and cell surface ATP. *Nature Communications* 2019 10:1 10(1), pp. 1–13.

- López-Muñoz, F., Boya, J., and Alamo, C. 2006. Neuron theory, the cornerstone of neuroscience, on the centenary of the Nobel Prize award to Santiago Ramón y Cajal. *Brain Research Bulletin* 70(4–6), pp. 391–405.
- Lorincz, A. and Nusser, Z. 2010. Molecular Identity of Dendritic Voltage-Gated Sodium Channels. *Science* 328(5980), pp. 906–909.
- Lucius, R. and Sievers, J. 1996. Postnatal retinal ganglion cells in vitro: Protection against reactive oxygen species (ROS)-induced axonal degeneration by cocultured astrocytes. *Brain Research* 743(1–2), pp. 56–62.
- Lunnon, K. et al. 2014. Methylopic profiling implicates cortical deregulation of ANK1 in Alzheimer's disease. *Nature Neuroscience* 17(9), pp. 1164–1170.
- Ma, J. and Ptashne, M. 1987. The carboxy-terminal 30 amino acids of GAL4 are recognized by GAL80. *Cell* 50(1), pp. 137–42.
- Ma, T., Peng, Y., Huang, W., and Ding, J. 2017. Molecular mechanism of the allosteric regulation of the α heterodimer of human NAD-dependent isocitrate dehydrogenase. *Scientific Reports* 7(1), pp. 1–17.
- MacAskill, A.F. et al. 2009. Miro1 is a calcium sensor for glutamate receptor-dependent localization of mitochondria at synapses. *Neuron* 61(4), pp. 541–555.
- MacAskill, A.F. and Kittler, J.T. 2010. Control of mitochondrial transport and localization in neurons. *Trends in cell biology* 20(2), pp. 102–112.
- Machesky, L.M. et al. 1999. Scar, a WASp-related protein, activates nucleation of actin filaments by the Arp2/3 complex. *Proceedings of the National Academy of Sciences of the United States of America* 96(7), pp. 3739–3744.
- Malhotra, R.K. 2018. Neurodegenerative Disorders and Sleep. *Sleep Medicine Clinics* 13(1), pp. 63–70.
- Maloney, M.T. and Bamberg, J.R. 2007. Cofilin-mediated neurodegeneration in Alzheimer's disease and other amyloidopathies. *Molecular neurobiology* 35(1), pp. 21–43.
- Maloney, M.T., Minamide, L.S., Kinley, A.W., Boyle, J.A., and Bamberg, J.R. 2005. β -Secretase-Cleaved Amyloid Precursor Protein Accumulates at Actin Inclusions Induced in Neurons by Stress or Amyloid β : A Feedforward Mechanism for Alzheimer's Disease. *Journal of Neuroscience* 25(49), pp. 11313–11321.
- Mandaravally Madhavan, M. and Schneiderman, H.A. 1977. Histological analysis of the dynamics of growth of imaginal discs and histoblast nests during the larval development of *Drosophila melanogaster*. *Wilhelm Roux's archives of developmental biology* 183(4), pp. 269–305.
- Manganelli, F. et al. 2017. Novel mutations in dystonin provide clues to the pathomechanisms of HSAN-VI. *Neurology* 88(22), pp. 2132–2140.
- Marchi, S. and Pinton, P. 2014. The mitochondrial calcium uniporter complex: Molecular components, structure and physiopathological implications. *Journal of Physiology* 592(5), pp. 829–839.
- Marella, S., Fischler, W., Kong, P., Asgarian, S., Rueckert, E., and Scott, K. 2006. Imaging Taste Responses in the Fly Brain Reveals a Functional Map of Taste Category and Behavior. *Neuron* 49(2), pp. 285–295.
- Marin, M.A., Ziburkus, J., Jankowsky, J., and Rasband, M.N. 2016. Amyloid- β plaques disrupt axon initial segments. *Experimental Neurology* 281, pp. 93–

- Martorell-Riera, A. et al. 2014. Mfn2 downregulation in excitotoxicity causes mitochondrial dysfunction and delayed neuronal death. *The EMBO Journal* 33(20), pp. 2388–2407.
- Mattedi, F., Chennell, G., and Vagnoni, A. 2022. Detailed Imaging of Mitochondrial Transport and Precise Manipulation of Mitochondrial Function with Genetically Encoded Photosensitizers in Adult *Drosophila* Neurons. *Methods in molecular biology (Clifton, N.J.)* 2431, pp. 385–407.
- Mayr, E. 1982. *The growth of biological thought: diversity, evolution, and inheritance*. Harvard University Press, Cambridge.
- Mazzarello, P. 1999. A unifying concept: the history of cell theory. *Nature Cell Biology* 1999 1:1 1(1), pp. E13–E15.
- McNally, J.S. et al. 2003. Role of xanthine oxidoreductase and NAD(P)H oxidase in endothelial superoxide production in response to oscillatory shear stress. *American Journal of Physiology - Heart and Circulatory Physiology* 285(6 54-6), pp. 2290–2297.
- McWilliams, T.G. et al. 2016. mito-QC illuminates mitophagy and mitochondrial architecture in vivo. *Journal of Cell Biology* 214(3), pp. 333–345.
- McWilliams, T.G., Prescott, A.R., Villarejo-Zori, B., Ball, G., Boya, P., and Ganley, I.G. 2019. A comparative map of macroautophagy and mitophagy in the vertebrate eye. *Autophagy* 15(7), pp. 1296–1308.
- Mears, J.A., Lackner, L.L., Fang, S., Ingerman, E., Nunnari, J., and Hinshaw, J.E. 2010. Conformational changes in Dnm1 support a contractile mechanism for mitochondrial fission. *Nature Structural & Molecular Biology* 2010 18:1 18(1), pp. 20–26.
- Melissa J. Parsons and Green, D.R. 2010. Mitochondria in cell death. *Essays in Biochemistry*
- Mellström, B., Savignac, M., Gomez-Villafuertes, R., and Naranjo, J.R. 2008. Ca²⁺-operated transcriptional networks: Molecular mechanisms and in vivo models. *Physiological Reviews* 88(2), pp. 421–449.
- Menna, E., Fossati, G., Scita, G., and Matteoli, M. 2011. From filopodia to synapses: the role of actin-capping and anti-capping proteins. *European Journal of Neuroscience* 34(10), pp. 1655–1662.
- Menzies, F.M., Fleming, A., and Rubinsztein, D.C. 2015. Compromised autophagy and neurodegenerative diseases. *Nature Reviews Neuroscience* 2015 16:6 16(6), pp. 345–357.
- Micaroni, M., Perinetti, G., Di Giandomenico, D., Bianchi, K., Spaar, A., and Mironov, A.A. 2010. Synchronous intra-Golgi transport induces the release of Ca²⁺ from the Golgi apparatus. *Experimental Cell Research* 316(13), pp. 2071–2086.
- Misgeld, T. and Schwarz, T.L. 2017. Mitostasis in Neurons: Maintaining Mitochondria in an Extended Cellular Architecture. *Neuron* 96(3), pp. 651–666.
- Misko, A., Jiang, S., Wegorzewska, I., Milbrandt, J., and Baloh, R.H. 2010. Mitofusin 2 Is Necessary for Transport of Axonal Mitochondria and Interacts with the Miro/Milton Complex. *Journal of Neuroscience* 30(12), pp. 4232–4240.
- Misko, A.L., Sasaki, Y., Tuck, E., Milbrandt, J., and Baloh, R.H. 2012. Mitofusin2 Mutations Disrupt Axonal Mitochondrial Positioning and Promote Axon

- Degeneration. *Journal of Neuroscience* 32(12), pp. 4145–4155.
- Missiaen, L., Dode, L., Vanoevelen, J., Raeymaekers, L., and Wuytack, F. 2007. Calcium in the Golgi apparatus. *Cell Calcium* 41(5), pp. 405–416.
- Miyawaki, A., Llopis, J., Heim, R., Michael McCaffery, J., Adams, J.A., Ikura, M., and Tsien, R.Y. 1997. Fluorescent indicators for Ca²⁺ based on green fluorescent proteins and calmodulin. *Nature* 388(6645), pp. 882–887.
- Moore, A.S., Wong, Y.C., Simpson, C.L., and Holzbaur, E.L.F. 2016. Dynamic actin cycling through mitochondrial subpopulations locally regulates the fission–fusion balance within mitochondrial networks. *Nature Communications* 2016 7:17(1), pp. 1–13.
- Morgan, T.H. 1910. Sex limited inheritance in drosophila. *Science* 32(812), pp. 120–122.
- Mórotz, G.M., De Vos, K.J., Vagnoni, A., Ackerley, S., Shaw, C.E., and Miller, C.C.J. 2012. Amyotrophic lateral sclerosis-associated mutant VAPBP56s perturbs calcium homeostasis to disrupt axonal transport of mitochondria. *Human Molecular Genetics* 21(9), pp. 1979–1988.
- Morris, R.L. and Hollenbeck, P.J. 1993. The regulation of bidirectional mitochondrial transport is coordinated with axonal outgrowth. *Journal of Cell Science* 104(3), pp. 917–927.
- Mullins, R.D., Heuser, J.A., and Pollard, T.D. 1998. The interaction of Arp2/3 complex with actin: Nucleation, high affinity pointed end capping, and formation of branching networks of filaments. *Proceedings of the National Academy of Sciences* 95(11), pp. 6181–6186.
- Muñoz-Lasso, D.C., Romá-Mateo, C., Pallardó, F. V., and Gonzalez-Cabo, P. 2020. Much More Than a Scaffold: Cytoskeletal Proteins in Neurological Disorders. *Cells* 9(2)
- Munsie, L. et al. 2011. Mutant huntingtin causes defective actin remodeling during stress: defining a new role for transglutaminase 2 in neurodegenerative disease. *Human Molecular Genetics* 20(10), pp. 1937–1951.
- Murley, A., Lackner, L.L., Osman, C., West, M., Voeltz, G.K., Walter, P., and Nunnari, J. 2013. ER-associated mitochondrial division links the distribution of mitochondria and mitochondrial DNA in yeast. *eLife* 2013(2)
- Näbauer, M., Callewaert, G., Cleemann, L., and Morad, M. 1989. Regulation of Calcium Release Is Gated by Calcium Current, Not Gating Charge, in Cardiac Myocytes. *Science* 244(4906), pp. 800–803.
- Nagarkar-Jaiswal, S. et al. 2015. A library of MiMICs allows tagging of genes and reversible, spatial and temporal knockdown of proteins in Drosophila. *eLife* 4(4)
- Naik, E. and Dixit, V.M. 2011. Mitochondrial reactive oxygen species drive proinflammatory cytokine production. *Journal of Experimental Medicine* 208(3), pp. 417–420.
- Nakada, C. et al. 2003. Accumulation of anchored proteins forms membrane diffusion barriers during neuronal polarization. *Nature Cell Biology* 5(7), pp. 626–632.
- Nakai, J., Ohkura, M., and Imoto, K. 2001. A high signal-to-noise Ca²⁺ probe composed of a single green fluorescent protein. *Nature biotechnology* 19(2), pp. 137–141.
- Nakamura, M., Baldwin, D., Hannaford, S., Palka, J., and Montell, C. 2002.

- Defective Proboscis Extension Response (DPR), a Member of the Ig Superfamily Required for the Gustatory Response to Salt. *Journal of Neuroscience* 22(9), pp. 3463–3472.
- Nakata, T. and Hirokawa, N. 2003. Microtubules provide directional cues for polarized axonal transport through interaction with kinesin motor head. *Journal of Cell Biology* 162(6), pp. 1045–1055.
- Nakata, T., Niwa, S., Okada, Y., Perez, F., and Hirokawa, N. 2011. Preferential binding of a kinesin-1 motor to GTP-tubulin-rich microtubules underlies polarized vesicle transport. *Journal of Cell Biology* 194(2), pp. 245–255.
- Navarro, A. and Boveris, A. 2008. Mitochondrial nitric oxide synthase, mitochondrial brain dysfunction in aging, and mitochondria-targeted antioxidants. *Advanced Drug Delivery Reviews* 60(13–14), pp. 1534–1544.
- Nave, K.A. and Trapp, B.D. 2008. Axon-glia signaling and the glial support of axon function. *Annual review of neuroscience* 31, pp. 535–561.
- Neuhaus, A., Eggeling, C., Erdmann, R., and Schliebs, W. 2016. Why do peroxisomes associate with the cytoskeleton? *Biochimica et Biophysica Acta - Molecular Cell Research* 1863(5), pp. 1019–1026.
- Neukomm, L.J., Burdett, T.C., Gonzalez, M.A., Züchner, S., and Freeman, M.R. 2014. Rapid in vivo forward genetic approach for identifying axon death genes in *Drosophila*. *Proceedings of the National Academy of Sciences of the United States of America* 111(27), pp. 9965–9970.
- Nicholls, D.G., Budd, S.L., Castilho, R.F., and Ward, M.W. 1999. Glutamate excitotoxicity and neuronal energy metabolism. In: *Annals of the New York Academy of Sciences*. Ann N Y Acad Sci, pp. 1–12.
- Nieminen, A.L. 2003. Apoptosis and necrosis in health and disease: role of mitochondria. *International review of cytology* 224, pp. 29–55.
- Niethammer, M. et al. 2000. NUDEL Is a Novel Cdk5 Substrate that Associates with LIS1 and Cytoplasmic Dynein. *Neuron* 28(3), pp. 697–711.
- Niewalda, T. et al. 2011. A Combined Perceptual, Physico-Chemical, and Imaging Approach to ‘Odour-Distances’ Suggests a Categorizing Function of the *Drosophila* Antennal Lobe. *PLOS ONE* 6(9), p. e24300.
- Nishida, E., Iida, K., Yonezawa, N., Koyasu, S., Yahara, I., and Sakai, H. 1987. Cofilin is a component of intranuclear and cytoplasmic actin rods induced in cultured cells. *Proceedings of the National Academy of Sciences of the United States of America* 84(15), pp. 5262–5266.
- Nivison, M.P., Ericson, N.G., Green, V.M., Bielas, J.H., Campbell, J.S., and Horner, P.J. 2017. Age-related accumulation of phosphorylated mitofusin 2 protein in retinal ganglion cells correlates with glaucoma progression. *Experimental Neurology* 296, pp. 49–61.
- Normand, E.A. and Rasband, M.N. 2015. Subcellular Patterning: Axonal Domains with Specialized Structure and Function. *Developmental Cell* 32(4), pp. 459–468.
- O’Donnell, V.B. and Azzi, A. 1996. High rates of extracellular superoxide generation by cultured human fibroblasts: Involvement of a lipid-metabolizing enzyme. *Biochemical Journal* 318(3), pp. 805–812.
- O’Keefe, D.D., Gonzalez-Niño, E., Edgar, B.A., and Curtiss, J. 2012. Discontinuities in Rap1 activity determine epithelial cell morphology within the

- developing wing of *Drosophila*. *Developmental biology* 369(2), pp. 223–234.
- Oakley, J.C., Kalume, F., and Catterall, W.A. 2011. Insights into pathophysiology and therapy from a mouse model of Dravet syndrome. *Epilepsia* 52, pp. 59–61.
- Ogawa, Y. and Rasband, M.N. 2008. The functional organization and assembly of the axon initial segment. *Current Opinion in Neurobiology* 18(3), pp. 307–313.
- Ohta, Y., Nishidaz, E., Sakais, H., and Miyamoto, E. 1989. Dephosphorylation of Cofilin Accompanies Heat Shock-induced Nuclear Accumulation of Cofilin". *Biological Chemistry* 264(27), pp. 16143–16148.
- Okumoto, K., Ono, T., Toyama, R., Shimomura, A., Nagata, A., and Fujiki, Y. 2018. New splicing variants of mitochondrial Rho GTPase-1 (Miro1) transport peroxisomes. *Journal of Cell Biology* 217(2), pp. 619–633.
- Ori-McKenney, K.M., Jan, L.Y., and Jan, Y.N. 2012. Golgi outposts shape dendrite morphology by functioning as sites of acentrosomal microtubule nucleation in neurons. *Neuron* 76(5), p. 921.
- Otto, I.M., Raabe, T., Rennefahrt, U.E.E., Bork, P., Rapp, U.R., and Kerkhoff, E. 2000. The p150-Spir protein provides a link between c-Jun N-terminal kinase function and actin reorganization. *Current Biology* 10(6), pp. 345–348.
- Ottolini, D., Cali, T., Negro, A., and Brini, M. 2013. The Parkinson disease-related protein DJ-1 counteracts mitochondrial impairment induced by the tumour suppressor protein p53 by enhancing endoplasmic reticulum–mitochondria tethering. *Human Molecular Genetics* 22(11), pp. 2152–2168.
- Ou, C.Y. et al. 2010. Two Cyclin-Dependent Kinase Pathways Are Essential for Polarized Trafficking of Presynaptic Components. *Cell* 141(5), pp. 846–858.
- Özkan, N. et al. 2021. ER – lysosome contacts at a pre-axonal region regulate axonal lysosome availability. *Nature Communications* 12(1), pp. 1–18.
- Palay, S.L., Sotelo, C., Peters, A., and Orkand, P.M. 1968. The axon hillock and the initial segment. *Journal of Cell Biology* 38(1), pp. 193–201.
- Palmer, A.E. and Tsien, R.Y. 2006. Measuring calcium signaling using genetically targetable fluorescent indicators. *Nature Protocols* 1(3), pp. 1057–1065.
- Palop, J.J. and Mucke, L. 2009. Epilepsy and cognitive impairments in alzheimer disease. *Archives of Neurology* 66(4), pp. 435–440.
- Pan, L. et al. 2015. Heterochromatin remodeling by CDK12 contributes to learning in *Drosophila*. *Proceedings of the National Academy of Sciences of the United States of America* 112(45), pp. 13988–13993.
- Park, J. et al. 2006. Mitochondrial dysfunction in *Drosophila* PINK1 mutants is complemented by parkin. *Nature* 2006 441:7097 441(7097), pp. 1157–1161.
- Parks, A.L. et al. 2004. Systematic generation of high-resolution deletion coverage of the *Drosophila melanogaster* genome. *Nature Genetics* 2004 36:3 36(3), pp. 288–292.
- Pastore, A. et al. 2003. Actin glutathionylation increases in fibroblasts of patients with Friedreich's ataxia: a potential role in the pathogenesis of the disease. *Journal of Biological Chemistry* 278(43), pp. 42588–42595.
- Pathak, D., Sepp, K.J., and Hollenbeck, P.J. 2010. Evidence that myosin activity opposes microtubule-based axonal transport of mitochondria. *Journal of neuroscience : the official journal of the Society for Neuroscience* 30(26), pp.

8984–8992.

- Patrick, G.N., Zukerberg, L., Nikolic, M., de la Monte, S., Dikkes, P., and Tsai, L.-H. 1999. Conversion of p35 to p25 deregulates Cdk5 activity and promotes neurodegeneration. *Nature* 402(6762), pp. 615–622.
- Peeters, A. et al. 2015. Mitochondria in peroxisome-deficient hepatocytes exhibit impaired respiration, depleted DNA, and PGC-1 α independent proliferation. *Biochimica et Biophysica Acta - Molecular Cell Research* 1853(2), pp. 285–298.
- Pekkurnaz, G., Trinidad, J.C., Wang, X., Kong, D., and Schwarz, T.L. 2014. Glucose regulates mitochondrial motility via Milton modification by O-GlcNAc transferase. *Cell* 158(1), pp. 54–68.
- Pelz, D., Roeske, T., Syed, Z., De Bruyne, M., and Galizia, C.G. 2006. The molecular receptive range of an olfactory receptor in vivo (*Drosophila melanogaster* Or22a). *Journal of Neurobiology* 66(14), pp. 1544–1563.
- Perocchi, F., Gohil, V.M., Girgis, H.S., Bao, X.R., McCombs, J.E., Palmer, A.E., and Mootha, V.K. 2010. MICU1 encodes a mitochondrial EF hand protein required for Ca²⁺ uptake. *Nature* 2010 467:7313 467(7313), pp. 291–296.
- Peters, A., S Palay, and Webster, H. 1991. *The Fine Structure of the Nervous System: The Neurons and Supporting Cells*. Oxford Univ. Press.
- Petersen, J.D., Kaech, S., and Banker, G. 2014. Selective microtubule-based transport of dendritic membrane proteins arises in concert with axon specification. *Journal of neuroscience : the official journal of the Society for Neuroscience* 34(12), pp. 4135–4147.
- Petrungaro, C. and Kornmann, B. 2019. Lipid exchange at ER-mitochondria contact sites: a puzzle falling into place with quite a few pieces missing. *Current Opinion in Cell Biology* 57, pp. 71–76.
- Pfister, B.J., Bonislawski, D.P., Smith, D.H., and Cohen, A.S. 2006. Stretch-grown axons retain the ability to transmit active electrical signals. *FEBS Letters* 580(14), pp. 3525–3531.
- Pfisterer, K., Jayo, A., and Parsons, M. 2017. Control of nuclear organization by F-actin binding proteins. *Nucleus (Austin, Tex.)* 8(2), pp. 126–133.
- Pickles, S., Vigié, P., and Youle, R.J. 2018. Mitophagy and Quality Control Mechanisms in Mitochondrial Maintenance. *Current Biology* 28(4), pp. R170–R185.
- Piermarini, E. et al. 2016. Frataxin silencing alters microtubule stability in motor neurons: implications for Friedreich's ataxia. *Human molecular genetics* 25(19), pp. 4288–4301.
- Pilling, A.D., Horiuchi, D., Lively, C.M., and Saxton, W.M. 2006. Kinesin-1 and Dynein are the primary motors for fast transport of mitochondria in *Drosophila* motor axons. *Molecular biology of the cell* 17(4), pp. 2057–2068.
- Plovanich, M. et al. 2013. MICU2, a Paralog of MICU1, Resides within the Mitochondrial Uniporter Complex to Regulate Calcium Handling. *PLOS ONE* 8(2), p. e55785.
- Pollard, T.D. 2016. Actin and Actin-Binding Proteins. *Cold Spring Harbor Perspectives in Biology* 8(8), p. a018226.
- Pollard, T.D. and Borisy, G.G. 2003. Cellular Motility Driven by Assembly and Disassembly of Actin Filaments. *Cell* 112(4), pp. 453–465.

- Pollard, T.D. and Cooper, J.A. 2009. Actin, a central player in cell shape and movement. *Science* 326(5957), pp. 1208–1212.
- Polleux, F. 2020. *Cellular Migration and Formation of Axons and Dendrites*. Second. Academic Press.
- Popova, T. et al. 2016. Ovarian cancers harboring inactivating mutations in CDK12 display a distinct genomic instability pattern characterized by large tandem duplications. *Cancer Research* 76(7), pp. 1882–1891.
- Price, D.L., Sisodia, S.S., and Gandy, S.E. 1995. Amyloid beta amyloidosis in Alzheimer's disease. *Current Opinion in Neurology* 8(4), pp. 268–74.
- Prins, D. and Michalak, M. 2011. Organellar calcium buffers. *Cold Spring Harbor Perspectives in Biology* 3(3), pp. 1–16.
- Próchnicki, T. and Latz, E. 2017. Inflammasomes on the Crossroads of Innate Immune Recognition and Metabolic Control. *Cell metabolism* 26(1), pp. 71–93.
- Purice, M.D., Ray, A., Münzel, E.J., Pope, B.J., Park, D.J., Speese, S.D., and Logan, M.A. 2017. A novel Drosophila injury model reveals severed axons are cleared through a Draper/MMP-1 signaling cascade. *eLife* 6
- Purves, D., Augustine, G.J., Fitzpatrick, D., Katz, L.C., LaMantia, A.-S., McNamara, J.O., and Williams, S.M. 2001. *Neuroscience*. 2nd ed. Sinauer Associates.
- Rahim, R.S., Chen, M., Nourse, C.C., Meedeniya, A.C.B., and Crane, D.I. 2016. Mitochondrial changes and oxidative stress in a mouse model of Zellweger syndrome neuropathogenesis. *Neuroscience* 334, pp. 201–213.
- Rapaport, D., Brunner, M., Neupert, W., and Westermann, B. 1998. Fzo1p Is a Mitochondrial Outer Membrane Protein Essential for the Biogenesis of Functional Mitochondria in *Saccharomyces cerevisiae*. *Journal of Biological Chemistry* 273(32), pp. 20150–20155.
- Rasband, M.N. 2010. The axon initial segment and the maintenance of neuronal polarity. *Nature Reviews Neuroscience* 11(8), pp. 552–562.
- Rasmussen, I., Pedersen, L.H., Byg, L., Suzuki, K., Sumimoto, H., and Vilhardt, F. 2010. Effects of F/G-actin ratio and actin turn-over rate on NADPH oxidase activity in microglia. *BMC Immunology* 11(1), pp. 1–15.
- Rasola, A. and Bernardi, P. 2007. The mitochondrial permeability transition pore and its involvement in cell death and in disease pathogenesis. *Apoptosis* 12:5 12(5), pp. 815–833.
- Ravenscroft, T.A. et al. 2020. Drosophila Voltage-Gated Sodium Channels Are Only Expressed in Active Neurons and Are Localized to Distal Axonal Initial Segment-like Domains. *Journal of neuroscience : the official journal of the Society for Neuroscience* 40(42), pp. 7999–8024.
- Rego, A.C. and Oliveira, C.R. 2003. Mitochondrial dysfunction and reactive oxygen species in excitotoxicity and apoptosis: implications for the pathogenesis of neurodegenerative diseases. *Neurochemical research* 28(10), pp. 1563–1574.
- Rehklau, K. et al. 2017. Cofilin1-dependent actin dynamics control DRP1-mediated mitochondrial fission. *Cell Death & Disease* 2017 8:10 8(10), pp. e3063–e3063.
- Reiter, L.T., Potocki, L., Chien, S., Gribskov, M., and Bier, E. 2001. A systematic analysis of human disease-associated gene sequences in *Drosophila melanogaster*. *Genome research* 11(6), pp. 1114–1125.

- Ren, Z., Zhang, X., Ding, T., Zhong, Z., Hu, H., Xu, Z., and Deng, J. 2020. Mitochondrial Dynamics Imbalance: A Strategy for Promoting Viral Infection. *Frontiers in Microbiology* 11, p. 1992.
- Riddiford, L.M., Cherbas, P., and Truman, J.W. 2000. Ecdysone receptors and their biological actions. *Vitamins and hormones* 60, pp. 1–73.
- Riemensperger, T., Völler, T., Stock, P., Buchner, E., and Fiala, A. 2005. Punishment Prediction by Dopaminergic Neurons in *Drosophila*. *Current Biology* 15(21), pp. 1953–1960.
- Rink, T.J., Tsien, R.Y., and Warner, A.E. 1980. Free calcium in *Xenopus* embryos measured with ion-selective microelectrodes. *Nature* 283(5748), pp. 658–660.
- Rintoul, G.L., Filiano, A.J., Brocard, J.B., Kress, G.J., and Reynolds, I.J. 2003. Glutamate decreases mitochondrial size and movement in primary forebrain neurons. *Journal of Neuroscience* 23(21), pp. 7881–7888.
- Rogaeva, E. et al. 2004. Analysis of the PINK1 Gene in a Large Cohort of Cases With Parkinson Disease. *Archives of Neurology* 61(12), pp. 1898–1904.
- Rohatgi, R., Ma, L., Miki, H., Lopez, M., Kirchhausen, T., Takenawa, T., and Kirschner, M.W. 1999. The Interaction between N-WASP and the Arp2/3 Complex Links Cdc42-Dependent Signals to Actin Assembly. *Cell* 97(2), pp. 221–231.
- Rojo, M., Legros, F., Chateau, D., and Lombès, A. 2002. Membrane topology and mitochondrial targeting of mitofusins, ubiquitous mammalian homologs of the transmembrane GTPase Fzo. *Journal of Cell Science* 115(8), pp. 1663–1674.
- Rolls, M.M., Satoh, D., Clyne, P.J., Henner, A.L., Uemura, T., and Doe, C.Q. 2007. Polarity and intracellular compartmentalization of *Drosophila* neurons. *Neural Development* 2(1), pp. 1–15.
- Rothenfluh, A., Young, M.W., and Saez, L. 2000. A TIMELESS-independent function for PERIOD proteins in the *Drosophila* clock. *Neuron* 26(2), pp. 505–514.
- Rubin, G.M. et al. 2000. Comparative genomics of the eukaryotes. *Science* 287(5461), pp. 2204–2215.
- Russo, G.J., Louie, K., Wellington, A., Macleod, G.T., Hu, F., Panchumarthi, S., and Zinsmaier, K.E. 2009. *Drosophila* Miro Is Required for Both Anterograde and Retrograde Axonal Mitochondrial Transport. *Journal of Neuroscience* 29(17), p. 5443.
- Ruthel, G. and Banker, G. 1998. Actin-dependent anterograde movement of growth-cone-like structures along growing hippocampal axons: a novel form of axonal transport? *Cell motility and the cytoskeleton* 40(2), pp. 160–173.
- Ruthel, G. and Banker G. 1999. Role of moving growth cone-like “wave” structures in the outgrowth of cultured hippocampal axons and dendrites. *Journal of Neurobiology*
- Rutila, J.E., Suri, V., Le, M., So, W.V., Rosbash, M., and Hall, J.C. 1998. CYCLE is a second bHLH-PAS clock protein essential for circadian rhythmicity and transcription of *Drosophila* period and timeless. *Cell* 93(5), pp. 805–814.
- Sabouny, R. et al. 2017. The Keap1-Nrf2 Stress Response Pathway Promotes Mitochondrial Hyperfusion Through Degradation of the Mitochondrial Fission Protein Drp1. *Antioxidants & redox signaling* 27(18), pp. 1447–1459.

- Saheki, Y. and De Camilli, P. 2017. Endoplasmic Reticulum–Plasma Membrane Contact Sites. *Annual review of biochemistry* 86, pp. 659–681.
- Salpietro, V. et al. 2015. Zellweger syndrome and secondary mitochondrial myopathy. *European Journal of Pediatrics* 174(4), pp. 557–563.
- Saotome, M. et al. 2008. Bidirectional Ca²⁺-dependent control of mitochondrial dynamics by the Miro GTPase. *Proceedings of the National Academy of Sciences of the United States of America* 105(52), pp. 20728–20733.
- Saraste, M. 1999. Oxidative phosphorylation at the fin de siècle. *Science* 283(5407), pp. 1488–1493.
- Sargsyan, Y., Bickmeyer, U., Gibhardt, C.S., Streckfuss-Bömeke, K., Bogeski, I., and Thoms, S. 2021. Peroxisomes contribute to intracellular calcium dynamics in cardiomyocytes and non-excitable cells. *Life Science Alliance* 4(9)
- Sasaki, S., Shionoya, A., Ishida, M., Gambello, M.J., Yingling, J., Wynshaw-Boris, A., and Hirotsune, S. 2000. A LIS1/NUDEL/Cytoplasmic Dynein Heavy Chain Complex in the Developing and Adult Nervous System. *Neuron* 28(3), pp. 681–696.
- Satrústegui, J., Pardo, B., and Del Arco, A. 2007. Mitochondrial transporters as novel targets for intracellular calcium signaling. *Physiological Reviews* 87(1), pp. 29–67.
- Sawa, A. 2001. Mechanisms for neuronal cell death and dysfunction in Huntington's disease: pathological cross-talk between the nucleus and the mitochondria? *Journal of molecular medicine (Berlin, Germany)* 79(7), pp. 375–381.
- Schaedel, L., John, K., Gaillard, J., Nachury, M. V., Blanchoin, L., and Thery, M. 2015. Microtubules self-repair in response to mechanical stress. *Nature materials* 14(11), pp. 1156–1163.
- Schafer, D.P., Jha, S., Liu, F., Akella, T., McCullough, L.D., and Rasband, M.N. 2009. Disruption of the Axon Initial Segment Cytoskeleton Is a New Mechanism for Neuronal Injury. *Journal of neuroscience : the official journal of the Society for Neuroscience* 29(42), pp. 13242–13254.
- Schagen, S.B. and Wefel, J.S. 2013. Chemotherapy-related changes in cognitive functioning. *EJC supplements : EJC : official journal of EORTC, European Organization for Research and Treatment of Cancer ... [et al.]* 11(2), pp. 225–232.
- Schelski, M. and Bradke, F. 2017. Neuronal polarization: From spatiotemporal signaling to cytoskeletal dynamics. *Molecular and Cellular Neuroscience* 84, pp. 11–28.
- Schevon, C.A., Weiss, S.A., McKhann, G., Goodman, R.R., Yuste, R., Emerson, R.G., and Trevelyan, A.J. 2012. Evidence of an inhibitory restraint of seizure activity in humans. *Nature Communications* 2012 3:1 3(1), pp. 1–11.
- Schlessinger, J., Koppel, D.E., Axelrod, D., Jacobson, K., Webb, W.W., and Elson, E.L. 1976. Lateral transport on cell membranes: mobility of concanavalin A receptors on myoblasts. *Proceedings of the National Academy of Sciences of the United States of America* 73(7), pp. 2409–2413.
- Schulze, T.G. et al. 2009. Two variants in Ankyrin 3 (ANK3) are independent genetic risk factors for bipolar disorder. *Molecular Psychiatry* 14(5), pp. 487–491.
- Seeburg, D.P., Feliu-Mojer, M., Gaiottino, J., Pak, D.T.S., and Sheng, M. 2008.

- Critical Role of CDK5 and Polo-like Kinase 2 in Homeostatic Synaptic Plasticity during Elevated Activity. *Neuron* 58(4), pp. 571–583.
- Sekino, Y., Koganezawa, N., Mizui, T., and Shirao, T. 2017. Role of Drebrin in Synaptic Plasticity. *Advances in experimental medicine and biology* 1006, pp. 183–201.
- Sepulveda-Falla, D. et al. 2014. Familial Alzheimer's disease–associated presenilin-1 alters cerebellar activity and calcium homeostasis. *Journal of Clinical Investigation* 124(4), pp. 1552–1567.
- Shah, K. and Rossie, S. 2018. Tale of the Good and the Bad Cdk5: Remodeling of the Actin Cytoskeleton in the Brain. *Molecular neurobiology* 55(4), p. 3426.
- Shepherd, G.M. 1991. *Foundations of the Neurine Doctrine*. Oxford University Press.
- Sherrington, C.S. 1906. Observations on the scratch-reflex in the spinal dog. *Journal of Physiology* 34(1–2), pp. 1–50.
- Shimura, H. et al. 2000. Familial Parkinson disease gene product, parkin, is a ubiquitin-protein ligase. *Nature Genetics* 25(3), pp. 302–305.
- Shukla, V., Skuntz, S., and Pant, H.C. 2012. Deregulated Cdk5 Activity Is Involved in Inducing Alzheimer's Disease. *Archives of Medical Research* 43(8), pp. 655–662.
- Shutt, T., Geoffrion, M., Milne, R., and McBride, H.M. 2012. The intracellular redox state is a core determinant of mitochondrial fusion. *EMBO Reports* 13(10), p. 909.
- Siechen, S., Yang, S., Chiba, A., and Saif, T. 2009. Mechanical tension contributes to clustering of neurotransmitter vesicles at presynaptic terminals. *Proceedings of the National Academy of Sciences of the United States of America* 106(31), pp. 12611–12616.
- Siegel, M.S. and Isacoff, E.Y. 1997. A Genetically Encoded Optical Probe of Membrane Voltage. *Neuron* 19(4), pp. 735–741.
- Siman, R., Baudry, M., and Lynch, G. 1984. Brain fodrin: substrate for calpain I, an endogenous calcium-activated protease. *Proceedings of the National Academy of Sciences of the United States of America* 81(11), pp. 3572–6.
- Simons, M., Misgeld, T., and Kerschensteiner, M. 2014. A unified cell biological perspective on axon-myelin injury. *The Journal of cell biology* 206(3), pp. 335–345.
- Simpson, P.B. and Russell, J.T. 1998. Role of mitochondrial Ca²⁺ regulation in neuronal and glial cell signalling. *Brain research. Brain research reviews* 26(1), pp. 72–81.
- Sleigh, J.N., Rossor, A.M., Fellows, A.D., Tosolini, A.P., and Schiavo, G. 2019. Axonal transport and neurological disease. *Nature Reviews Neurology* 15(12), pp. 691–703.
- Smith, G. 2019. Unpublished.
- Smith, G.A. et al. 2019. Glutathione S-Transferase Regulates Mitochondrial Populations in Axons through Increased Glutathione Oxidation. *Neuron* 103(1), p. 52.
- Smith, K.J. and Lassmann, H. 2002. The role of nitric oxide in multiple sclerosis. *The Lancet. Neurology* 1(4), pp. 232–241.

- Soares, L., Parisi, M., and Bonini, N.M. 2014. Axon Injury and Regeneration in the Adult *Drosophila*. *Scientific Reports* 4:1 4(1), pp. 1–12.
- Sohn, P.D. et al. 2016. Acetylated tau destabilizes the cytoskeleton in the axon initial segment and is mislocalized to the somatodendritic compartment. *Molecular neurodegeneration* 11(1), p. 47.
- Song, A. hong, Wang, D., Chen, G., Li, Y., Luo, J., Duan, S., and Poo, M. ming 2009. A Selective Filter for Cytoplasmic Transport at the Axon Initial Segment. *Cell* 136(6), pp. 1148–1160.
- Song, B.J. et al. 2013. Increased nitroxidative stress promotes mitochondrial dysfunction in alcoholic and nonalcoholic fatty liver disease. *Oxidative Medicine and Cellular Longevity*
- Sood, A. et al. 2014. A Mitofusin-2-dependent inactivating cleavage of Opa1 links changes in mitochondria cristae and ER contacts in the postprandial liver. *Proceedings of the National Academy of Sciences of the United States of America* 111(45), pp. 16017–16022.
- Soubannier, V., McLelland, G.L., Zunino, R., Braschi, E., Rippstein, P., Fon, E.A., and McBride, H.M. 2012. A Vesicular Transport Pathway Shuttles Cargo from Mitochondria to Lysosomes. *Current Biology* 22(2), pp. 135–141.
- Soussain, C., Ricard, D., Fike, J.R., Mazon, J.J., Psimaras, D., and Delattre, J.Y. 2009. CNS complications of radiotherapy and chemotherapy. *Lancet (London, England)* 374(9701), pp. 1639–1651.
- Sparaco, M. et al. 2009. Friedreich's ataxia: oxidative stress and cytoskeletal abnormalities. *Journal of the neurological sciences* 287(1–2), pp. 111–118.
- Spence, E.F. and Soderling, S.H. 2015. Actin Out: Regulation of the Synaptic Cytoskeleton. *Journal of Biological Chemistry* 290(48), pp. 28613–28622.
- Spinazzi, M. et al. 2008. A novel deletion in the GTPase domain of OPA1 causes defects in mitochondrial morphology and distribution, but not in function. *Human Molecular Genetics* 17(21), pp. 3291–3302.
- Spurrier, J., Shukla, A.K., Buckley, T., Smith-Trunova, S., Kuzina, I., Gu, Q., and Giniger, E. 2019. Expression of a Fragment of Ankyrin 2 Disrupts the Structure of the Axon Initial Segment and Causes Axonal Degeneration in *Drosophila*. *Molecular neurobiology* 56(8), pp. 5689–5700.
- Stamer, K., Vogel, R., Thies, E., Mandelkow, E., and Mandelkow, E.M. 2002. Tau blocks traffic of organelles, neurofilaments, and APP vesicles in neurons and enhances oxidative stress. *Journal of Cell Biology* 156(6), pp. 1051–1063.
- Stefan, C.J. 2020. Endoplasmic reticulum–plasma membrane contacts: Principals of phosphoinositide and calcium signaling. *Current Opinion in Cell Biology* 63, pp. 125–134.
- Stevens, F.J. and Argon, Y. 1999. Protein folding in the ER. *Seminars in Cell and Developmental Biology* 10(5), pp. 443–454.
- Stocker, H. and Gallant, P. 2008. Getting started: an overview on raising and handling *Drosophila*. *Methods in molecular biology (Clifton, N.J.)* 420, pp. 27–44.
- Südhof, T.C. 1995. The synaptic vesicle cycle: a cascade of protein–protein interactions. *Nature* 1995 375:6533 375(6533), pp. 645–653.
- Südhof, T.C. 2004. THE Synaptic Vesicle Cycle. *Annual review of neuroscience* 27, pp. 509–547.

- Sugimura, K. and Ishihara, S. 2013. The mechanical anisotropy in a tissue promotes ordering in hexagonal cell packing. *Development (Cambridge, England)* 140(19), pp. 4091–4101.
- Sun, N. et al. 2015. Measuring In Vivo Mitophagy. *Molecular cell* 60(4), pp. 685–696.
- Sun, X., Wu, Y., Gu, M., Liu, Z., Ma, Y., Li, J., and Zhang, Y. 2014. Selective filtering defect at the axon initial segment in Alzheimer's disease mouse models. *Proceedings of the National Academy of Sciences of the United States of America* 111(39), pp. 14271–14276.
- Swerdlow, R.H. and Kish, S.J. 2002. Mitochondria in Alzheimer's disease. *International review of neurobiology* 53, pp. 341–385.
- Sztul, E. and Lupashin, V. 2009. Role of vesicle tethering factors in the ER-Golgi membrane traffic. *FEBS Letters* 583(23), pp. 3770–3783.
- Tabb, J.S., Molyneaux, B.J., Cohen, D.L., Kuznetsov, S.A., and Langford, G.M. 1998. Transport of ER vesicles on actin filaments in neurons by myosin V. *Journal of Cell Science* 111 (Pt 2(21), pp. 3221–3234.
- Taguchi, N., Ishihara, N., Jofuku, A., Oka, T., and Mihara, K. 2007. Mitotic phosphorylation of dynamin-related GTPase Drp1 participates in mitochondrial fission. *Journal of Biological Chemistry* 282(15), pp. 11521–11529.
- Takano, T., Xu, C., Funahashi, Y., Namba, T., and Kaibuchi, K. 2015. Neuronal polarization. *Development (Cambridge, England)* 142(12), pp. 2088–2093.
- Tamagno, E., Robino, G., Obbili, A., Bardini, P., Aragno, M., Parola, M., and Danni, O. 2003. H₂O₂ and 4-hydroxynonenal mediate amyloid β -induced neuronal apoptosis by activating JNKs and p38MAPK. *Experimental Neurology* 180(2), pp. 144–155.
- Tan, W. and Colombini, M. 2007. VDAC closure increases calcium ion flux. *Biochimica et Biophysica Acta (BBA) - Biomembranes* 1768(10), pp. 2510–2515.
- Tanabe, T., Beam, K.G., Adams, B.A., Niidome, T., and Numa, S. 1990. Regions of the skeletal muscle dihydropyridine receptor critical for excitation–contraction coupling. *Nature* 346(6284), pp. 567–569.
- Tanaka, H. et al. 2019. Peroxisomes control mitochondrial dynamics and the mitochondrion-dependent apoptosis pathway. *Journal of Cell Science* 132(11)
- Tanaka, Y., Kanai, Y., Okada, Y., Nonaka, S., Takeda, S., Harada, A., and Hirokawa, N. 1998. Targeted disruption of mouse conventional kinesin heavy chain, kif5B, results in abnormal perinuclear clustering of mitochondria. *Cell* 93(7), pp. 1147–1158.
- Tang, R. et al. 2019. Lycium barbarum polysaccharides extend the mean lifespan of *Drosophila melanogaster*. *Food & Function* 10(7), pp. 4231–4241.
- Tannock, I.F., Ahles, T.A., Ganz, P.A., and van Dam, F.S. 2004. Cognitive impairment associated with chemotherapy for cancer: report of a workshop. *Journal of clinical oncology : official journal of the American Society of Clinical Oncology* 22(11), pp. 2233–2239.
- Tapia, M., Wandosell, F., and Garrido, J.J. 2010. Impaired function of hdac6 slows down axonal growth and interferes with axon initial segment development. *PLoS ONE* 5(9), p. e12908.
- Tarasov, A.I., Griffiths, E.J., and Rutter, G.A. 2012. Regulation of ATP

- production by mitochondrial Ca²⁺. *Cell Calcium* 52(1), pp. 28–35.
- Tatton, W.G. and Olanow, C.W. 1999. Apoptosis in neurodegenerative diseases: the role of mitochondria. *Biochimica et biophysica acta* 1410(2), pp. 195–213.
- Taylor, J. and Adler, P.N. 2008. Cell rearrangement and cell division during the tissue level morphogenesis of evaginating *Drosophila* imaginal discs. *Developmental biology* 313(2), pp. 739–751.
- Terskikh, A. et al. 2000. “Fluorescent Timer”: Protein That Changes Color with Time. *Science* 290(5496), pp. 1585–1588.
- Terskikh, A. V., Fradkov, A.F., Zaraisky, A.G., Kajava, A. V., and Angres, B. 2002. Analysis of DsRed Mutants. Space around the fluorophore accelerates fluorescence development. *Journal of Biological Chemistry* 277(10), pp. 7633–7636.
- The UniProt Consortium 2021. UniProt: the universal protein knowledgebase in 2021. *Nucleic Acids Research* 49(D1), pp. D480–D489.
- Thiel, K. et al. 2013. The evolutionarily conserved protein CG9186 is associated with lipid droplets, required for their positioning and for fat storage. *Journal of Cell Science* 126(Pt 10), pp. 2198–2212.
- Tien, J.F. et al. 2017. CDK12 regulates alternative last exon mRNA splicing and promotes breast cancer cell invasion. *Nucleic acids research* 45(11), pp. 6698–6716.
- Tiloca, C. et al. 2013. Screening of the PFN1 gene in sporadic amyotrophic lateral sclerosis and in frontotemporal dementia. *Neurobiology of aging* 34(5), pp. 1517.e9-1517.e10.
- Toh, K.L. et al. 2001. An hPer2 Phosphorylation Site Mutation in Familial Advanced Sleep Phase Syndrome. *Science* 291(5506), pp. 1040–1043.
- Tour, O., Adams, S.R., Kerr, R.A., Meijer, R.M., Sejnowski, T.J., Tsien, R.W., and Tsien, R.Y. 2007. Calcium Green FAsH as a genetically targeted small-molecule calcium indicator. *Nature chemical biology* 3(7), pp. 423–431.
- Trompier, D. et al. 2014. Brain peroxisomes. *Biochimie* 98(1), pp. 102–110.
- Trunova, S., Baek, B., Giniger, E., Trunova, Baek, B., and Giniger, E. 2011. Cdk5 Regulates the Size of an Axon Initial Segment-Like Compartment in Mushroom Body Neurons of the *Drosophila* Central Brain. *Journal of Neuroscience* 31(29), pp. 10451–10462.
- Tsydzik, V. and Wright, N.J.D. 2009. Dopamine modulation of the In vivo acetylcholine response in the *Drosophila* mushroom body. *Developmental Neurobiology* 69(11), pp. 705–714.
- Tufi, R. et al. 2019. Comprehensive Genetic Characterization of Mitochondrial Ca²⁺ Uniporter Components Reveals Their Different Physiological Requirements In Vivo. *Cell reports* 27(5), pp. 1541-1550.e5.
- Vaccaro, V., Devine, M.J., Higgs, N.F., and Kittler, J.T. 2017. Miro1-dependent mitochondrial positioning drives the rescaling of presynaptic Ca²⁺ signals during homeostatic plasticity. *EMBO reports* 18(2), pp. 231–240.
- Vacher, H., Yang, J.W., Cerda, O., Autillo-Touati, A., Dargent, B., and Trimmer, J.S. 2011. Cdk-mediated phosphorylation of the Kvβ2 auxiliary subunit regulates Kv1 channel axonal targeting. *Journal of Cell Biology* 192(5), p. 813.
- Vagnoni, A. and Bullock, S.L. 2016. A simple method for imaging axonal transport in

- aging neurons using the adult *Drosophila* wing. *Nature Protocols* 2016 11:9 11(9), pp. 1711–1723.
- Vagnoni, A. and Bullock, S.L. 2018. A cAMP/PKA/Kinesin-1 Axis Promotes the Axonal Transport of Mitochondria in Aging *Drosophila* Neurons. *Current Biology* 28(8), pp. 1265-1272.e4.
- Vagnoni, A., Hoffmann, P.C., and Bullock, S.L. 2016. Reducing Lissencephaly-1 levels augments mitochondrial transport and has a protective effect in adult *Drosophila* neurons. *Journal of Cell Science* 129(1), pp. 178–190.
- Valente, E.M. et al. 2004. Hereditary early-onset Parkinson's disease caused by mutations in PINK1. *Science* 304(5674), pp. 1158–1160.
- Vallee, R.B., McKenney, R.J., and Ori-Mckenney, K.M. 2012. Multiple modes of cytoplasmic dynein regulation. *Nature Cell Biology* 2012 14:3 14(3), pp. 224–230.
- Valm, A.M. et al. 2017. Applying systems-level spectral imaging and analysis to reveal the organelle interactome. *Nature* 546(7656), pp. 162–167.
- Van Bergeijk, P., Adrian, M., Hoogenraad, C.C., and Kapitein, L.C. 2015. Optogenetic control of organelle transport and positioning. *Nature* 518(7537), pp. 111–114.
- Van Beuningen, S.F.B. et al. 2015. TRIM46 Controls Neuronal Polarity and Axon Specification by Driving the Formation of Parallel Microtubule Arrays. *Neuron* 88(6), pp. 1208–1226.
- Van Vreeswijk, C. and Sompolinsky, H. 1996. Chaos in Neuronal Networks with Balanced Excitatory and Inhibitory Activity. *Science* 274(5293), pp. 1724–1726.
- Vance, J.E. 1990. Phospholipid synthesis in a membrane fraction associated with mitochondria. *Journal of Biological Chemistry* 265(13), pp. 7248–7256.
- Vandekerckhove, J. and Weber, K. 1978. At least six different actins are expressed in a higher mammal: An analysis based on the amino acid sequence of the amino-terminal tryptic peptide. *Journal of Molecular Biology* 126(4), pp. 783–802.
- Varadi, A., Johnson-Cadwell, L.I., Cirulli, V., Yoon, Y., Allan, V.J., and Rutter, G.A. 2004. Cytoplasmic dynein regulates the subcellular distribution of mitochondria by controlling the recruitment of the fission factor dynamin-related protein-1. *Journal of cell science* 117(Pt 19), pp. 4389–4400.
- Vardy, J. and Tannock, I. 2007. Cognitive function after chemotherapy in adults with solid tumours. *Critical reviews in oncology/hematology* 63(3), pp. 183–202.
- Virbasius, J. V. and Scarpulla, R.C. 1994. Activation of the human mitochondrial transcription factor A gene by nuclear respiratory factors: a potential regulatory link between nuclear and mitochondrial gene expression in organelle biogenesis. *Proceedings of the National Academy of Sciences of the United States of America* 91(4), pp. 1309–1313.
- Von Reyn, C.R. et al. 2009. Calpain Mediates Proteolysis of the Voltage-Gated Sodium Channel α -Subunit. *Journal of Neuroscience* 29(33), p. 10350.
- Wales, P. et al. 2016. Calcium-mediated actin reset (CaAR) mediates acute cell adaptations. *eLife* 5(DECEMBER2016)
- Wallace, D.C. 2005. A Mitochondrial Paradigm of Metabolic and Degenerative

- Diseases, Aging, and Cancer: A Dawn for Evolutionary Medicine. *Annual review of genetics* 39, pp. 359–407.
- Wang, D., Malo, D., and Hekimi, S. 2010. Elevated Mitochondrial Reactive Oxygen Species Generation Affects the Immune Response via Hypoxia-Inducible Factor-1 α in Long-Lived Mcl1+/- Mouse Mutants. *The Journal of Immunology* 184(2), pp. 582–590.
- Wang, W. et al. 2008a. Superoxide Flashes in Single Mitochondria. *Cell* 134(2), pp. 279–290.
- Wang, W. et al. 2015. MFN2 couples glutamate excitotoxicity and mitochondrial dysfunction in motor neurons. *Journal of Biological Chemistry* 290(1), pp. 168–182.
- Wang, X. and Schwarz, T.L. 2009. The mechanism of Ca²⁺-dependent regulation of kinesin-mediated mitochondrial motility. *Cell* 136(1), pp. 163–174.
- Wang, Y., Guo, H.F., Pologruto, T.A., Hannan, F., Hakker, I., Svoboda, K., and Zhong, Y. 2004. Stereotyped Odor-Evoked Activity in the Mushroom Body of *Drosophila* Revealed by Green Fluorescent Protein-Based Ca²⁺ Imaging. *Journal of Neuroscience* 24(29), pp. 6507–6514.
- Wang, Y., Mamiya, A., Chiang, A.S., and Zhong, Y. 2008b. Imaging of an Early Memory Trace in the *Drosophila* Mushroom Body. *Journal of Neuroscience* 28(17), pp. 4368–4376.
- Wang, Y., Mattson, M.P., and Furukawa, K. 2002. Endoplasmic reticulum calcium release is modulated by actin polymerization. *Journal of Neurochemistry* 82(4), pp. 945–952.
- Wang, Y., Metz, J., Costello, J.L., Passmore, J., Schrader, M., Schultz, C., and Islinger, M. 2018a. Intracellular redistribution of neuronal peroxisomes in response to ACBD5 expression. *PLOS ONE* 13(12), p. e0209507.
- Wang, Y., Shan, Q., Pan, J., and Yi, S. 2018b. Actin Cytoskeleton Affects Schwann Cell Migration and Peripheral Nerve Regeneration. *Frontiers in Physiology* | www.frontiersin.org 1, p. 23.
- Warrick, J.M., Paulson, H.L., Gray-Board, G.L., Bui, Q.T., Fischbeck, K.H., Pittman, R.N., and Bonini, N.M. 1998. Expanded polyglutamine protein forms nuclear inclusions and causes neural degeneration in *Drosophila*. *Cell* 93(6), pp. 939–949.
- Watanabe, K., Al-Bassam, S., Miyazaki, Y., Wandless, T.J.J., Webster, P., and Arnold, D.B.B. 2012. Networks of Polarized Actin Filaments in the Axon Initial Segment Provide a Mechanism for Sorting Axonal and Dendritic Proteins. *Cell Reports* 2(6), pp. 1546–1553.
- Waxman, S.G. 2006. Axonal conduction and injury in multiple sclerosis: the role of sodium channels. *Nature reviews. Neuroscience* 7(12), pp. 932–941.
- Webster, C.P., Smith, E.F., Shaw, P.J., and De Vos, K.J. 2017. Protein homeostasis in amyotrophic lateral sclerosis: Therapeutic opportunities? *Frontiers in Molecular Neuroscience* 10, p. 123.
- Wellington, A., Emmons, S., James, B., Calley, J., Grover, M., Tolia, P., and Manseau, L. 1999. Spire contains actin binding domains and is related to ascidian posterior end mark-5. *Development* 126(23), pp. 5267–5274.
- Werth, J.L. and Thayer, S.A. 1994. Mitochondria buffer physiological calcium loads in cultured rat dorsal root ganglion neurons. *Journal of Neuroscience* 14(1), pp. 348–356.

- Wetmore, D.R. and Hardman, K.D. 1996. Roles of the propeptide and metal ions in the folding and stability of the catalytic domain of stromelysin (matrix metalloproteinase 3). *Biochemistry* 35(21), pp. 6549–6558.
- Whitlock, K.E. and Palka, J. 1995. Development of wing sensory axons in the central nervous system of *Drosophila* during metamorphosis. *Journal of Neurobiology* 26(2), pp. 189–204.
- Willers, I., Ressler, B., Singh, S., and Koeppen, A.H. 1993. Immunocytochemical studies on the vimentin distribution and cell proliferation of fibroblasts in patients with Friedreich's ataxia. *Journal of the neurological sciences* 117(1–2), pp. 159–163.
- Wilson, E.L. and Metzakopian, E. 2020. ER-mitochondria contact sites in neurodegeneration: genetic screening approaches to investigate novel disease mechanisms. *Cell Death & Differentiation* 2020 28:6 28(6), pp. 1804–1821.
- Winans, A.M., Collins, S.R., and Meyer, T. 2016. Waves of actin and microtubule polymerization drive microtubule-based transport and neurite growth before single axon formation. *eLife* 5(FEBRUARY2016)
- Winckler, B., Forscher, P., and Mellman, I. 1999. A diffusion barrier maintains distribution of membrane proteins in polarized neurons. *Nature* 397(6721), pp. 698–701.
- Wöllert, T., Weiss, D.G., Gerdes, H.H., and Kuznetsov, S.A. 2002. Activation of myosin V-based motility and F-actin-dependent network formation of endoplasmic reticulum during mitosis. *The Journal of Cell Biology* 159(4), p. 571.
- Wu, C.H. et al. 2012. Mutations in the profilin 1 gene cause familial amyotrophic lateral sclerosis. *Nature* 488(7412), pp. 499–503.
- Wu, C.H., Giampetruzzi, A., Tran, H., Fallini, C., Gao, F.B., and Landers, J.E. 2017a. A *Drosophila* model of ALS reveals a partial loss of function of causative human PFN1 mutants. *Human molecular genetics* 26(11), pp. 2146–2155.
- Wu, J.S. and Luo, L. 2007. A protocol for mosaic analysis with a repressible cell marker (MARCM) in *Drosophila*. *Nature Protocols* 1(6), pp. 2583–2589.
- Wu, W. et al. 2016. FUNDC1 regulates mitochondrial dynamics at the ER-mitochondrial contact site under hypoxic conditions. *The EMBO Journal* 35(13), pp. 1368–1384.
- Wu, Y., Whiteus, C., Xu, C.S., Hayworth, K.J., Weinberg, R.J., Hess, H.F., and De Camilli, P. 2017b. Contacts between the endoplasmic reticulum and other membranes in neurons. *Proceedings of the National Academy of Sciences of the United States of America* 114(24), pp. E4859–E4867.
- Xu, K., Zhong, G., and Zhuang, X. 2013. Actin, spectrin, and associated proteins form a periodic cytoskeletal structure in axons. *Science* 339(6118), pp. 452–456.
- Yagi, H., Kajiwara, N., Tanaka, H., Tsukihara, T., Kato-Yamada, Y., Yoshida, M., and Akutsu, H. 2007. Structures of the thermophilic F1-ATPase ϵ subunit suggesting ATP-regulated arm motion of its C-terminal domain in F1. *Proceedings of the National Academy of Sciences of the United States of America* 104(27), pp. 11233–11238.
- Yalçın, B. et al. 2017. Modeling of axonal endoplasmic reticulum network by spastic paraplegia proteins. *eLife* 6

- Yanagawa, A., Guigue, A.M.A., and Marion-Poll, F. 2014. Hygienic grooming is induced by contact chemicals in *Drosophila melanogaster*. *Frontiers in Behavioral Neuroscience* 8(JULY), p. 254.
- Yasuda, R., Nimchinsky, E.A., Scheuss, V., Pologruto, T.A., Oertner, T.G., Sabatini, B.L., and Svoboda, K. 2004. Imaging calcium concentration dynamics in small neuronal compartments. *Science's STKE: signal transduction knowledge environment* 2004(219)
- Yau, K.W., Schätzle, P., Tortosa, E., Pagès, S., Holtmaat, A., Kapitein, L.C., and Hoogenraad, C.C. 2016. Dendrites In Vitro and In Vivo Contain Microtubules of Opposite Polarity and Axon Formation Correlates with Uniform Plus-End-Out Microtubule Orientation. *Journal of Neuroscience* 36(4), pp. 1071–1085.
- Yoshino, J., Mills, K.F., Yoon, M.J., and Imai, S.I. 2011. Nicotinamide Mononucleotide, a Key NAD⁺ Intermediate, Treats the Pathophysiology of Diet- and Age-Induced Diabetes in Mice. *Cell Metabolism* 14(4), pp. 528–536.
- Yu, D., Baird, G.S., Tsien, R.Y., and Davis, R.L. 2003. Detection of Calcium Transients in *Drosophila* Mushroom Body Neurons with Camgaroo Reporters. *Journal of Neuroscience* 23(1), pp. 64–72.
- Yu, F.H. et al. 2006. Reduced sodium current in GABAergic interneurons in a mouse model of severe myoclonic epilepsy in infancy. *Nature Neuroscience* 9(9), pp. 1142–1149.
- Yuste, R. and Denk, W. 1995. Dendritic spines as basic functional units of neuronal integration. *Nature* 375(6533), pp. 682–684.
- Yuste, R., Majewska, A., Cash, S.S., and Denk, W. 1999. Mechanisms of calcium influx into hippocampal spines: heterogeneity among spines, coincidence detection by NMDA receptors, and optical quantal analysis. *Journal of neuroscience: the official journal of the Society for Neuroscience* 19(6), pp. 1976–1987.
- Zafar, S. et al. 2018. Cytoskeleton-Associated Risk Modifiers Involved in Early and Rapid Progression of Sporadic Creutzfeldt-Jakob Disease. *Molecular neurobiology* 55(5), pp. 4009–4029.
- Zampese, E., Fasolato, C., Kipanyula, M.J., Bortolozzi, M., Pozzan, T., and Pizzo, P. 2011. Presenilin 2 modulates endoplasmic reticulum (ER)-mitochondria interactions and Ca²⁺ cross-talk. *Proceedings of the National Academy of Sciences of the United States of America* 108(7), pp. 2777–2782.
- Zepeta-Flores, N., Valverde, M., Lopez-Saavedra, A., and Rojas, E. 2018. Glutathione depletion triggers actin cytoskeleton changes via actin-binding proteins. *Genetics and Molecular Biology* 41(2), p. 475.
- Zhang, F. et al. 2015. Posttranslational modifications of α -tubulin in alzheimer disease. *Translational neurodegeneration* 4(1)
- Zhang, H. et al. 2016a. NAD⁺ repletion improves mitochondrial and stem cell function and enhances life span in mice. *Science* 352(6292), pp. 1436–1443.
- Zhang, T. et al. 2016b. Covalent targeting of remote cysteine residues to develop CDK12 and CDK13 inhibitors. *Nature Chemical Biology* 12(10), pp. 876–884.
- Zhong, C. and Schleifenbaum, J. 2019. Genetically Encoded Calcium Indicators: A New Tool in Renal Hypertension Research. *Frontiers in Medicine* 6, p. 128.
- Zhou, D., Lambert, S., Malen, P.L., Carpenter, S., Boland, L.M., and Bennett, V.

1998. AnkyrinG is required for clustering of voltage-gated Na channels at axon initial segments and for normal action potential firing. *Journal of Cell Biology* 143(5), pp. 1295–1304.

Zhu, X.H., Lu, M., Lee, B.Y., Ugurbil, K., and Chen, W. 2015. In vivo NAD assay reveals the intracellular NAD contents and redox state in healthy human brain and their age dependences. *Proceedings of the National Academy of Sciences of the United States of America* 112(9), pp. 2876–2881.

8 Appendices

Fly Genotype	Stock number (if applicable)	Source
<i>+/+;UAS-AnkyrinG-GFP</i>	n/a	Gifted from Ronald Dubreuil (Trunova et al. 2011).
<i>OK371-Gal4, UAS-x10myr::tdTomato, UAS-mitoGFP/CyO; 3L/TM3</i>	n/a	Made by Gaynor Smith
<i>w-; BAC (27971-2-F1-M-Ch2)/(CyO); 3L/(TM3 Sb e)</i>	n/a	Plasmid constructed by P[acman] Resources, injected by Bestgene Inc.
<i>w-; OK371-Gal4, UAS-x10myr::tdTomato, Ase-FLP^{2E} /(CyO); Tubgal80,FRT2A (3L)/(TM3 Sb e)</i>	n/a	Made by Gaynor Smith
<i>w-; OK371-Gal4, UAS-x10myr::tdTomato, Ase-FLP^{2E} /(CyO); Tubgal80,FRT2A (3L)/(TM3 Sb e)</i>	n/a	Made by Gaynor Smith
<i>w-; OK371-Gal4, UAS-x10myr::tdTomato, UAS-mitoGFP Ase-FLP^{2E} /CyO; Tubgal80,FRT2A (3L)/(TM3 Sb e)</i>	n/a	Made by Gaynor Smith
<i>w-; Sp/CyO Df(3L)Exel9065, PBac{w[+mC]=RBr}Exel9065/TM6B, Tb[1]</i>	7949	BDSC
<i>w-; UAS-Cdk5 RNAi #2 /(CyO); Tubgal80,FRT2A (3L)/(TM3 Sb e)</i>	n/a	Made by Louise Townsend
<i>w-; UAS-Cdk5KA /(CyO); Tubgal80,FRT2A (3L)/(TM3 Sb e)</i>	n/a	Made by Louise Townsend
<i>w-; UAS-Cdk5KA /+; +/+</i>	n/a	Gifted by Dr Edward Giniger, as described in: (Connell-Crowley et al. 2000)

<i>w-; UAS-Cdk5-RNAi #1 /(CyO); Tubgal80,FRT2A (3L)/(TM3 Sb e)</i>	n/a	Made by Louise Townsend
<i>w-; UAS-Cdk5-RNAi #1 /+; +/+</i>	35855	VDRC
<i>w-; UAS-Cdk5-RNAi #2 /+; +/+</i>	35856	VDRC
<i>w-; UAS-Cdk5WT /(CyO); Tubgal80,FRT2A (3L)/(TM3 Sb e)</i>	n/a	Made by Louise Townsend
<i>w-; UAS-Cdk5WT /+; +/+</i>	n/a	Gifted by Dr Edward Giniger
<i>w-; UAS-x10myr::tdTomato /(CyO); Tubgal80,FRT2A (3L)/(TM3 Sb e)</i>	n/a	Made by Gaynor Smith
<i>w-;5xUAS Cdk12/(CyO); Dr/TM3 Sb e</i>	n/a	Made by Gaynor Smith
<i>w-;OK371-Gal4, UAS-x10myr::tdTomato /(CyO);Cdk12*FRT2A,FRT82B/TM3 Sb e</i>	n/a	Made by Gaynor Smith
<i>w-;OK371-Gal4, UAS-x10myrTomato, Ase-FLP^{2E} /(CyO);Dr/TM3 Sb e</i>	n/a	Made by Gaynor Smith
<i>w-;OK371-Gal4, UAS-x10myrTomato, Ase-FLP^{2E} /(CyO);Dr/TM3 Sb e</i>	n/a	Made by Gaynor Smith
<i>w-;OK371-Gal4, UAS-x10myr::tdTomato /(CyO); FRT2A,FRT82B/(TM3 Sb e)</i>	n/a	Made by Gaynor Smith
<i>w-;OK371-Gal4, UAS-x10myr::tdTomato /(CyO); FRT2A,FRT82B/(TM3 Sb e)</i>	n/a	Made by Gaynor Smith
<i>w-;OK371-Gal4, UAS-x10myr::tdTomato/(CyO);Cdk12*FRT2A,FR T82B/TM3 Sb e</i>	n/a	Made by Gaynor Smith
<i>w-;Sp/CyO; FRT2A, FRT82B /(TM3 Sb e)</i>	n/a	Made by Gaynor Smith
<i>w-;Sp/CyO;FRT2A, FRT82B, Cdk12*/TM3 Sb e</i>	n/a	Made by Gaynor Smith
<i>w-;Sp/Cyo;Tub-Gal80, FRT2A/TM3 Sb e</i>	n/a	Made by Gaynor Smith
<i>w-;UAS-Cdk12::GFP/(CyO); Dr/TM3 Sb e</i>	n/a	Made by Gaynor Smith
<i>w-;UAS-Cdk12::GFP/(CyO); Tub-Gal80, FRT2A/TM3 Sb e</i>	n/a	Made by Louise Townsend

<i>w-;UAS-cytoGrx1roGFP/(CyO);3L/TM3</i>	67662	BDSC and Louise Townsend
<i>w-;UAS-Drp1-RNAi/(CyO);3L/TM3</i>	13510	BDSC and Louise Townsend
<i>w-;UAS-GCaMP6F/(CyO);3L/TM3</i>	n/a	Made by Gaynor Smith
<i>w-;UAS-mitoGCaMP/(CyO);3L/TM3</i>	n/a	Made by Gaynor Smith
<i>w-;UAS-mitroGFP2-Grx1/(CyO);3L/TM3</i>	67664	BDSC and Louise Townsend
<i>w-;UAS-mitroGFP2-Orp1/(CyO);3L/TM3</i>	67667	BDSC and Louise Townsend
<i>w[*]; P{w[+mC]=GAL4-btl.S}2, P{w[+mC]=UASp-Act5C.T:GFP}2/CyO, P{w[+m*]=lacZ.w[+]}276</i>	8807	BDSC
<i>w[*]; P{w[+mC]=GAL4-btl.S}2, P{w[+mC]=UASp-Act5C.T:GFP}2; P{w[+mW.hs]=FRT(w[hs])}2A P{ry[+t7.2]=neoFRT}82B denuded[1520]/TM3, P{w[+mC]=tubP- GAL80}3, Sb[1]</i>	63083	BDSC
<i>w[*]; P{w[+mC]=UASp-PAGFP- alphaTub84B}F11.4</i>	32076	BDSC
<i>w[*]; P{w[+mC]=UAS-syt.eGFP}2</i>	6925	BDSC
<i>w[1118]; P{w[+mC]=UAS-DenMark}2, P{w[+mC]=UAS-syt.eGFP}2; In(3L)D, mirr[SaiD1] D[1]/TM6C, Sb[1]</i>	33064	BDSC
<i>w[1118]; P{y[+t7.7] w[+mC]=3xUAS-IVS- Syt1::smGdP-V5}su(Hw)attP5</i>	62143	BDSC
<i>w1118; P{GD13840}v35855</i>	35855	VDRC
<i>w1118; P{GD13840}v35856</i>	35856	VDRC

<i>y[1] w[*]; P{w[+mC]=UASp-GFPS65C-alphaTub84B}14-6-II/CyO, P{ry[+t7.2]=sevRas1.V12}FK1</i>	7374	BDSC
<i>y[1] w[*]; P{y[+t*] w[+mC]=UAS-Lifeact-GFP}VIE-260B</i>	35544	BDSC
<i>UAS-CG9186::GFP/+;+;+</i>	n/a	Gifted by Cahir O'Kane
<i>OK371-Gal4, UAS-x10myr::tdTomato, UAS-CG9186::GFP, ase-FLP^{2E} /CyO; FRT2A, FRT82B/TM3</i>	n/a	Daniel Maddison
<i>UAS-CG9186::GFP/CyO; Cdk12*, FRT2A, FRT82B/TM3</i>	n/a	Daniel Maddison

Appendix 1. Fly stock lines used in this chapter. Flies were either ordered from BDRC, VDRC or gifted. Stock, genotype, stock number, source and chromosomal location given.

Mammalian AIS components	<i>Drosophila</i> AIS orthologue	DIOPT score <i>Drosophila</i> >Human	Specific to the AIS?
Actin (bands and patches)	Actin5C	Human Variant and score: ActB:11/15 Actg1:11/15 Actbl2: 5/15 Acta1: 4/15 Acta2: 4/15 Actc1: 4/14 Actg2: 4/15	Excessive accumulation of actin seen as patches and filaments at the AIS
Ankyrin G	Ankyrin 1 (ubiquitously expressed) (Trunova et al. 2011) Ankyrin 2 (neuronal-specific) (Bouley et al. 2000; Hortsch et al. 2002)	<i>Drosophila</i> Ankyrin1: Ankyrin1: 9/15 Ankyrin2: 8/15 Ankyrin3: 8/15 <i>Drosophila</i> Ankyrin 2: Ankyrin1: 5/15 Ankyrin2: 7/15 Ankyrin3: 7/15	Ankyrin1 is more common at the AIS than Ankyrin 2.
Neurofascin (Nav,Kv7 channels)	(pan-neuronal) Sodium and potassium channels (Elk and Shaw lines used in previous literature to stain potassium channels (Trunova et al. 2011)	Potassium channels: Eag-like K ⁺ Elk: KCNH8: 11/15 KCNH3: 10/15 KCNH4: 9/15 Shaker cognate w (shaw) Kv3.1: Potassium voltage-gated channel subfamily C (KCNC)1 and 2: 13/15 KCNC4: 12/15 KCNC3: 11/15	Accumulation of sodium and potassium channels at the AIS (Ogawa and Rasband 2008).

α-Spectrin ($\alpha 2$)	α -Spectrin (Trunova et al. 2011)	Spectrin alpha, non-erythrocytic 1 (SPTAN1): 15/15 Spectrin alpha, erythrocytic 1 (SPTA1): 6/15	Present at the AIS, but not enriched (Trunova et al. 2011)
β-Spectrin ($\beta 2$ and 4)	β -Spectrin (Trunova et al. 2011)	Spectrin beta, non-erythrocytic (SPTBN) 1 and 2: 13/15 Spectrin beta erythrocytic (SPTB): 11/15 SPTBN4: 7/15	Present at the AIS, but not enriched (Trunova et al. 2011)

Appendix 2. AIS components.

Transgene	Function
5xUAS-Cdk12	Gal4-driven, second chromosome insertion that overexpresses <i>Drosophila</i> Cdk12.
Ase-FLP^{2E}	Asense flippase variant 2E, involved in MARCM.
BAC (27971-2-F1-M-Ch2)	Genomic BAC construct injected into the fly and inserted on the second chromosome. Expresses <i>Drosophila</i> Cdk12 ubiquitously.
Cdk12*	<i>Cdk12</i> ^{-/-} mutation. Sequence data in Appendix 4 .
CyO	Curly wings (second chromosome balancer, balances the chromosome to maintain the homozygous line)
Df3Lex^e19065	Deficiency line overlapping Cdk12 gene only. Stock generated from FLP-induced recombination between FRT transgenic insertions (Parks et al. 2004).
FRT2A	FRT site, present on the 3L arm, involved in MARCM.
FRT82B	FRT site, present on the 3R arm, involved in MARCM.
OK371-Gal4	Gal4 expressed in glutamatergic neurons
TM3 Sb^e	Short bristles present on the back of the thorax. TM3 is a third chromosome balancer and maintains the homozygous fly line. Sb;Stubble (short bristles) E;ebony (dark body)
Tub-Gal80	Expressed when tubulin is expressed (therefore everywhere). Gal80 inhibits Gal4.
UAS-β-actin-GFP	Gal4-driven GFP-tagged β-actin overexpressed on the second chromosome.
UAS-Actin#1/#2-GFP	Gal4-driven, GFP-tagged actin overexpressed on the second chromosome. Actin #1 is β-actin and actin #2 is F-actin.
UAS-Ankyrin1-GFP	Overexpression of GFP-tagged Ankyrin1, Gal4-dependent and inserted on the third chromosome.
UAS-Cdk12::GFP	GFP-tagged Cdk12, inserted on the second chromosome and driver by Gal4. Excitation and emission peak of GFP is 395nm and 475nm, respectively.
UAS-Cdk5KA	Overexpression of kinase-dead Cdk5, under UAS control.
UAS-Cdk5RNAi#1 or #2	RNAi knockdown of Cdk5, driven by Gal4 and located on the second chromosome, see Appendix 1 .

<i>UAS-Cdk5WT</i>	Overexpression of wild-type Cdk5, under UAS control.
<i>UAS-cytoGrx1roGFP</i>	Under UAS control, a glutaredoxin-based, cytoplasm-localised, fluorescent sensor of glutathione oxidation expressed on the second chromosome.
<i>UAS-Drp1-RNAi</i>	Under UAS control, RNA interference reduces Drp1 expression.
<i>UAS-GCaMP6F</i>	Expresses the GFP-tagged calcium sensor, GCaMP, under UAS control. 'F' refers to fastest decay kinetics of all the GCaMPs (Bloomington.com).
<i>UAS-LifeAct-GFP</i>	Gal4-driven, GFP-tagged F-Actin overexpressed on the second chromosome.
<i>UAS-mitoGCaMP</i>	Expresses GFP-tagged calcium sensor, mitoGCaMP, under UAS control in the mitochondria.
<i>UAS-mitoGFP</i>	GFP fused to mitochondria, overexpressed on the second chromosome and is homozygous lethal.
<i>UAS-mitoroGFP2-Grx1</i>	Under UAS control, a glutaredoxin-based, mitochondria-localised, fluorescent sensor of glutathione oxidation expressed on the second chromosome.
<i>UAS-mitoroGFP2-Orp1</i>	Under UAS control, an oxidant receptor peroxidase-based, mitochondria-localised, fluorescent sensor of hydrogen peroxide expressed on the second chromosome.
<i>UAS-SKL-GFP</i>	Gal4-driven, GFP driven expression of GFP that's tagged to the C-terminus of SKL, a peroxisomal targeting peptide.
<i>UAS-Synaptotagmin#1/#2/#3-GFP</i>	Overexpression of GFP-tagged synaptotagmin 1, Gal4-dependent and inserted on the second chromosome.
<i>UAS-x10myr::tdTomato</i>	Gal4 (<i>OK371-Gal4</i>) binds to UAS (x10 copies) (in neurons) and expresses Tomato in the glutamatergic neurons. Excitation = 554 nm. Emission = 581 nm. td; tandem dimer and increases the fluorescence of Tomato signal forming an intramolecular dimer, which is initially produced in the golgi apparatus and diffuses into the cell. UAS sites are followed by a heat shock protein (70 kilodalton) basal promoter that is fused upstream of tdTomato coding sequence. The N-terminal end is tagged with a myristoylation (myr) membrane protein localisation signal. A 67 bp intron derived from myosin heavy chain has been inserted in the 5' untranslated region (Larkin et al. 2021).

<i>UAS-Tubulin#1/#2-GFP</i>	Gal4-driven, GFP-tagged Tubulin overexpressed on the second chromosome.
<i>UAS-CG9186::GFP</i>	Gal4-driven, GFP-tagged smooth ER lipase that localises to the ER, as described in (Thiel et al. 2013) and (Yalçın et al. 2017).

Appendix 3 Transgenes used in all *Drosophila* fly lines.

>Cdk12-RB cdna:KNOWN_protein_coding_FBtr0078357

MetHASSAAATALVEYSDVSSSEDFSDQEAGDLADAGKAGAGNIKKPKPAPDNQFSKGRLDAPDKEGYDNYRRAEDSSDPVAA
GSRQTSSEATNPREEPSQASNTSKDELWGREIYMetSSDSIDTDELEAEMetKRQKRKKQKKEKHKHKSKKKSKKRKKKRAKSY
SSIDSMetSDNDINALDDRYPPTAPSKSNERTVSAAPSSFTPHNLKESSPATPPVRRPNTNSNYGESSLETANSALGSNLQ
VTVTNKQSI SNRLRSPPPSSRSGNGPRFGNSPRTPPSHYSSSGGGVVGSGSVVRDRSSRYVNSPHKEDVSAHHRSSHDH
GYQGRYSGAGSSSHDRKVKRLSPELDRYNHQPSTPPHKRRKFSDGREVGLGNFEHSRHHSGKYERYSRDRYSRRSSRSPS
VQHSRRSQSPSGGLSSGSNAFRHGGSHKHKYGTTVSSSTPSHTTTRTSKRASGTGTSGDYRSRSPRTSSRYMetESSPPSPV
GASGSHHYHRRRSPRMetRQRTRGDSRRRSPSSASSESSASRSRSPTRSRLKHKREYIKKISETSLFAELVKDRHQRKALKEIER
QEENSNSNSNGALTINDNSSVDGNTNPAADGRSAPGSGTPAAASTTNSGLQALGSKPDLDLNNIPMetPNKQNSVSVNPNASNA
DVPDSVAQLKQPLLPPFASAKNNIKPKSLTSLPLPPGMetNVLDLAGARSPSPGQKKESEDEKNVTSSGSANKSVLNLPMetPPVIP
GSEELSGDDDDVIDSPEDFDAPAVGTVHGHGGGPGTTRQRPVILNRRDRSNNVDRWGERCVDFVEMetIAQIGEGTYGQVYKAR
DHHTNDMetVALKKVRLLEHEKEGFPITAVREIKILRQLNHRNIVNLHEIVTDKQDAVEFRKDKGSFYLVFEYMetDHLMetGLLES
GMetVDFNEENNASIMetKQLLDGLNYCHKKNFLHRDIKCSNILMetNNRGRKVKLADFLGLARLYNADDRERPYTNKVITLWYRPELL
GEERYGPSIDVWSCGICILGELFVKRPLFQANAEMetAQLETISKICGSPVAVWPNVIKLPFLFHTLKQKTKHRRRLREDFEFMetPA
PALDLLKMetLDLDPDKRITAEADALRSPWLRKINPDEMetPTPQLPTWQDCHELWSKRRRQMetREQQESLPPTVIASATKYQQHG
ATMetVGDASStop

>Cdk12-RB cdna:KNOWN_protein_coding_mutation_FBtr0078357

MetHASSAAATALVEYSDVSSSEDFSDQEAGDLADAGKAGAGNIKKPKPAPDNQFSKGRLDAPDKEGYDNYRRAEDSSDPVAA
GSRQTSSEATNPREEPSQASNTSKDELWGREIYMetSSDSIDTDELEAEMetKRQKRKKQKKEKHKHKSKKKSKKRKKKRAKSY
SSIDSMetSDNDINALDDRYPPTAPSKSNERTVSAAPSSFTPHNLKESSPATPPVRRPNTNSNYGESSLETANSALGSNLQ
VTVTNKQSI SNRLRSPPPSSRSGNGPRFGNSPRTPPSHYSSSGGGVVGSGSVVRDRSSRYVNSPHKEDVSAHHRSSHDH
GYQGRYSGAGSSSHDRKVKRLSPELDRYNHQPSTPPHKRRKFSDGREVGLGNFEHSRHHSGKYERYSRDRYSRRSSRSPS
VQHSRRSQSPSGGLSSGSNAFRHGGSHKHKYGTTVSSSTPSHTTTRTSKRASGTGTSGDYRSRSPRTSSRYMetESSPPSPV
GASGSHHYHRRRSPRMetRQRTRGDSRRRSPSSASSESSASRSRSPTRSRLKHKREYIKKISETSLFAELVKDRHQRKALKEIER
QEENSNSNSNGALTINDNSSVDGNTNPAADGRSAPGSGTPAAASTTNSGLQALGSKPDLDLNNIPMetPNKQNSVSVNPNASNA
DVPDSVAQLKQPLLPPFASAKNNIKPKSLTSLPLPPGMetNVLDLAGARSPSPGQKKESEDEKNVTSSGSANKSVLNLPMetPPVIP
GSEELSGDDDDVIDSPEDFDAPAVGTVHGHGGGPGTTRQRPVILNRRDRSNNVDRWGERCVDFVEMetIAQIGEGTYGQVYKAR
DHHTNDMetVALKKVRLLEHEKEGFPITAVREIKILRQLNHRNIVNLHEIVTDKQDAVEFRKDKGSFYLVFEYMetDHLMetGLLES
GMetVDFNEENNASIMetKQLLDGLNYCHKKNFLHRDIKCSNILMetNNRGRKVKLADFLGLARLYNADDRERPYTNKVITLWYRPELL
GEERYGPSIDVWSCGICILGELFVKRPLFQANAEMetAQLETISKICGSPVAVWPNVIKLPFLFHTLKQKTKHRRRLREDFEFMetPA
PALDLLKMetLDLDPDKRITAEADALRSPWLRKINPDEMetPTPQLPTWQDCHELWSKRRRQMetREQQESLPPTVIASATKYQQHG
ATMetVGDASStop

Appendix 4 Protein sequence for Cdk12^{-/-}. Cdk12^{-/-} flies contain a frameshift mutation (red) in the Cdk12 protein sequence, induced by EMS, which resulted in a premature stop codon. The sequence in green is the resulting sequence caused by the frameshift mutation (Smith 2019).